STUDIES ON RUTHENIUM CHEMISTRY WITH HYDRAZINE BASED SCHIFF BASES

A THESIS

SUBMITTED FOR THE DEGREE OF

DOCTOR OF PHILOSOPHY

by

SATYANARAYAN PAL

SCHOOL OF CHEMISTRY

UNIVERSITY OF HYDERABAD

HYDERABAD 500 046

INDIA

JULY 2003

DEDICATED

TO

MY PARENTS

कर्मण्येवाधिकारस्ते मा फलेषु कदाचन ।
मा कर्मफलहेतुर्भूर्मा ते संगोऽस्त्वकर्मणि ॥

गीता २।४७

CONTENTS

STATEMENT

I hereby declare that the matter embodied in this thesis entitled "***Studies on Ruthenium Chemistry with Hydrazine Based Schiff Bases***" is the result of the investigations carried out by me in the School of Chemistry, University of Hyderabad, under the supervision of **Dr. Samudranil Pal**.

In keeping the general practice of reporting scientific observations, due acknowledgement has been made wherever the work is described is based on findings of other investigators. Any omission which might have occurred by oversight or error is regretted.

July 2003

Satya
Satyanarayan Pal

DR. SAMUDRANIL PAL
SCHOOL OF CHEMISTRY
UNIVERSITY OF HYDERABAD
HYDERABAD-500 046, INDIA

Phone: +91-40-2301 0500
(extn. 4756) (office)
Fax: +91-40-2301 2460
Email: spsc@uohyd.ernet.in

18th July, 2003

CERTIFICATE

Certified that the work embodied in the thesis entitled ***"Studies on Ruthenium Chemistry with Hydrazine Based Schiff Bases"*** has been carried out by **Mr. Satyanarayan Pal** under my supervision and the same has not been submitted elsewhere for any degree.

Dr. Samudranil Pal
(Thesis supervisor)

Dean
School of Chemistry
University of Hyderabad

DEAN
School of Chemistry
University of Hyd.
Hyderabad-46.

ACKNOWLEDGEMENT

I express my sincere gratitude and profound respect to my research supervisor **Dr. Samudranil Pal** for his invaluable guidance, support and constant encouragement. He has been always approachable, helpful and extremely patient throughout my research career. I am quite lucky to get such person as my supervisor. These words are not adequate to express all about him. To me he is my friend, philosopher and guide.

I would like thank the Dean, School of Chemistry, for allowing me to avail school facilities. I am extremely thankful to all faculty members of this school for their kind help and encouragement in various stages of my research work.

I gratefully acknowledge the DST funded National Single Crystal Diffractometer Facility, at School of Chemistry, University of Hyderabad for X-ray structure determination. I thank the Council of Scientific and Industrial Research, New Delhi for the research fellowship.

I express my sincere thanks to Prof. A. R. Chakravarty (IISC, Bangalore) for the variable temperature magnetic data.

I thank my senior Dr. N. R. Sangeetha for her help. I deeply acknowledge my lab mates S. S. Gupta, Sunirban, and Abhik for their help and cooperation. I thankful to all M. Phil students and M. Sc. project students in our lab for their help.

I am highly grateful to Satyen Saha for his help in various aspects.

I gratefully acknowledge Sankaran, Rana, Tin Htwe, Subbalakshmi, Sailaja, and Mangayarkarasi for their help and company.

I am thankful to Tamal, Binoy, Reddy, Sastry, Sampath, Manab, Archan, Prasun, Satish, Praveen, Sharath Chandra, Pradeep, Venugopal, and T. Praveen, for their help and providing cheerful environment.

In this occasion I would like thank my friends Satish, Manas, Indranil, Nilkamal, and Asit for their help.

All the non-teaching staffs of the school and CIL have been extremely helpful. I thank all of them. Raghavaiah, Suresh, Manjunath, Shetty, Satyanarayana, Asia Parwez, and Venkata Ramana are few to mention.

No words will be enough to thank my family members. Without their relentless support I would not have reached this stage of my life. I am indebted in each and every respect of my life to my parents who bear lot of pain for me. I am highly grateful to my younger brothers Bacchu and Basanta for their love and support. I deeply acknowledge my maternal uncle Paresh Patra and Prabhas Patra for their help, encouragement and guidance. I am thankful to my younger uncle Ramakanta Pal for his help.

I convey my regards to all my teachers who taught me throughout. I thank once again to every one who helped me to reach here.

Satyanarayan Pal

CHAPTER 1

Introduction

1.1. Abstract

In this chapter, the importance of ruthenium chemistry has been briefly discussed. The aim of the present investigation in the background of known ruthenium chemistry with Schiff bases has been stated.

1.2. Some Aspects of the Ruthenium Chemistry

Coordination chemistry came to the light after the pioneering work of Nobel laureate Alfred Werner in 1893. After that this branch of inorganic chemistry has grown vastly and expanded from small molecules to different areas such as polymers, oligomers, dendrimers, catalytic chemistry, organometallic chemistry etc. Beginning from Werner it was the turn of first transition series metals, which were studied extensively and still it is going on. Second and third transition series metals were not in much attention possibly due to the lack of knowledge to carry out the experiments in different conditions.

Ruthenium being a second transition series metal, chemistry of it was not explored much. Ruthenium chemistry is being studied extensively only in last three decades. Before this period very few ruthenium complexes were known. Some of them are ruthenium red,[1a] $[Ru(bpy)_3]^{2+}$,[1b] $[Ru(phen)_3]^{2+}$, Creutz-Taube complexes[1c] etc. Now a vast literature on ruthenium chemistry[2] is available. One of the main advantages of ruthenium chemistry is the variable oxidation state of the metal ranging from -2 to +8. Interconversion of different oxidation states are usually done by using different redox reagents. The ultimate result is the discovery of useful redox reactions where ruthenium complexes can act as

catalysts. This catalytic behavior of ruthenium complexes has been utilized for various synthetic organic reactions.

Ruthenium complexes with polypyridyl ligands have been subject of immense attention compared to any other class of ruthenium complexes. This is because of their chemical stability and photophysical, photochemical, and electrochemical properties. These complexes are being considered as promising candidates for the role of ideal photocatalysts in visible light induced decomposition of water into molecular hydrogen and oxygen.[14] These complexes are also being used to develop photomolecular devices and as probes for the elucidation of structural and electron transfer properties of proteins and DNA.[17]

Due to their unique properties and wide range of applications there is a continuous quest for new ruthenium complexes with diverse types of ligands. The goal is to tune the chemical and physical properties of the complexes by changing the coordination sphere around the metal center. The primary objective is to improve their efficiency in the above-mentioned applications and also to find out new reactivities and applications.

Some of the important applications and reactivities of ruthenium complexes are described below.

1.2.1. Catalytic properties

Ruthenium complexes with oxo, carbonyl, tertiary phosphines, cyclopentadienyl, arenes and dienes have been proved to serve as efficient catalysts.[3-6] These complexes are being utilized in C-C bond formation,[7] including metathesis and Murai coupling, oxidation[8] and isomerisation[9] reactions, nucleophilic addition to C-C and C-heteroatom multiple bonds,[10] and hydrogenation[11] reactions. At present ruthenium complexes are becoming useful for tandem catalytic[12] processes in which one catalyst supports several functions in two or more catalytic processes resulting into sequential modification of a

substrate. An example of tandem catalytic ring-opening-ring-closing metathesis reaction is shown below.

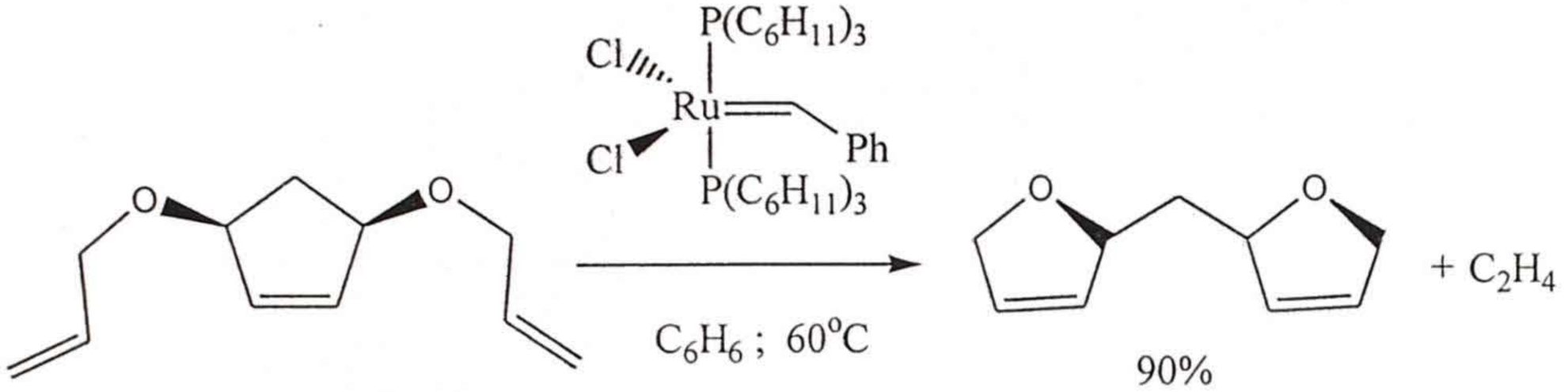

Figure 1.1

In case of water oxidation ruthenium complexes are one of the best systems. Particularly ruthenium polypyridyl and ruthenium amine complexes[13] have been proved to be very efficient. T. J. Meyer group in 1982 reported a binuclear ruthenium polypyridyl complex[14] $[(bpy)_2(H_2O)Ru(\mu\text{-}O)Ru\text{-}(H_2O)(bpy)_2]^{4+}$ capable of oxidizing water catalytically. In that same year, A. Chakravorty and co-workers reported a cationic ruthenium complex $[Ru(pap)_2(H_2O)(py)]^{2+}$ (pap = 2-phenylazopyridine, py = pyridine) that acts as homogeneous water oxidation catalyst.[14d] Ruthenium ammine complexes[15] are also good as water oxidation catalysts. Few of them are ruthenium red,[15a] $[(NH_3)_5Ru^{III}(\mu\text{-}O)Ru^{III}(NH_3)_5]^{4+}$ [15b] and $[(NH_3)_3Ru^{III}(\mu\text{-}Cl)_3Ru^{II}(NH_3)_3]^{2+}$.[15c]

1.2.2. Photochemical properties

Ruthenium polypyridyl complexes and their derivatives have very rich photochemistry. Extensive studies on this aspect have been done using $[Ru(bpy)_3]^{2+}$ and its derivatives.[16] These polypyridyl ligands provide π^* acceptor

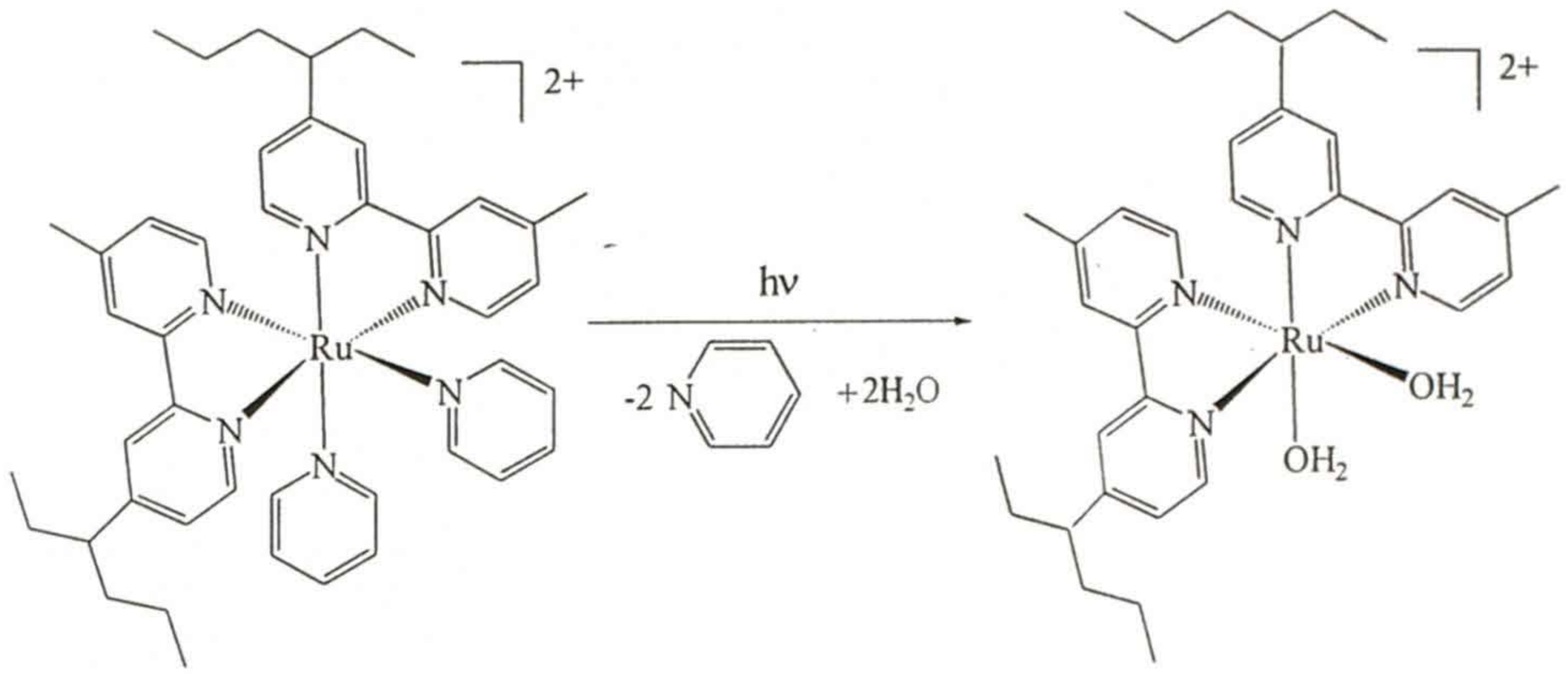

Figure 1.2

orbitals of appropriate energy and symmetry on the aromatic rings. Visible light induced dπ metal electron transition to π* ligand orbital gives rise to metal-to-ligand charge transfer (MLCT) excited state. This MLCT excited state thus formed after absorbing the visible light is of high energy and unstable species, which often shows interesting photochemical and photophysical properties. This excited species may undergo deactivation through (i) photochemical reaction (ii) emission of light (fluorescence or phosphorescence) (iii) radiationless deactivation (internal conversion or intersystem crossing) and (iv) some interaction with other species present in the medium (quenching).

When intramolecular deactivation steps are not too fast *i.e.* the life time of the excited state is sufficiently long ($>10^{-9}$ sec.), then there may have a chance for the excited molecule to collide with another molecule present in the medium. This process is called bimolecular process. The most important bimolecular processes are excited state energy transfer and electron transfer (*i e*. oxidation or reduction of the excited state). One example of photochemical reaction is given in Figure1.2.

1.2.3. DNA binding properties

Ruthenium polypyridyl complexes,[17] particularly ruthenium phenanthroline complexes and mixed ligand derivatives of ruthenium bipyridine complexes are well-known for DNA binding agents. These complexes interact with DNA through (i) intercalative interaction, in which part of the metal complex positions itself between the base pairs of DNA as sandwich like complex, (ii) non-intercalative groove binding, where metal complex binds DNA on the surface in minor or major grooves, (iii) covalent interaction, where covalent bond formation takes place between nitrogen atoms of bases and the metal complex and (iv) electrostatic interaction between the cationic metal complex and the negatively charged phosphate backbone present in DNA. The above types of ruthenium

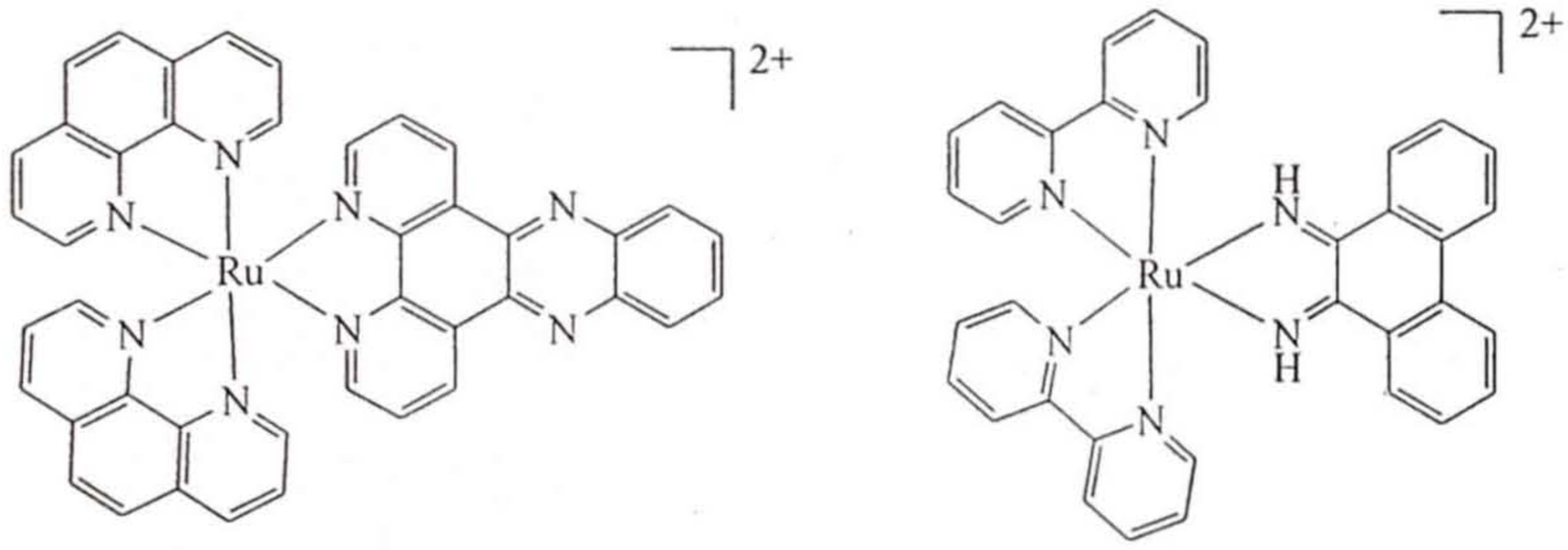

Figure 1.3

complexes are also capable of DNA cleavage on irradiation with suitable light. A couple of ruthenium complexes capable of DNA binding are shown in Figure 1.3.

1.2.4. Organometallic complexes

Ruthenium is having vast organometallic chemistry.[18] It forms a wide range of organometallic complexes with different types of ligands. The

well-known ruthenium organometallic complexes are with carbonyl, alkyl, carbene, carbyne ligands. Ruthenium metallocene complexes are also common. These complexes are having wide range of applications in homogeneous and heterogeneous catalysis. One of the most important applications of ruthenium organometallic complexes is to activate the inert C-H bond. In Figure 1.4 two examples of ruthenium organometallic complexes are shown.

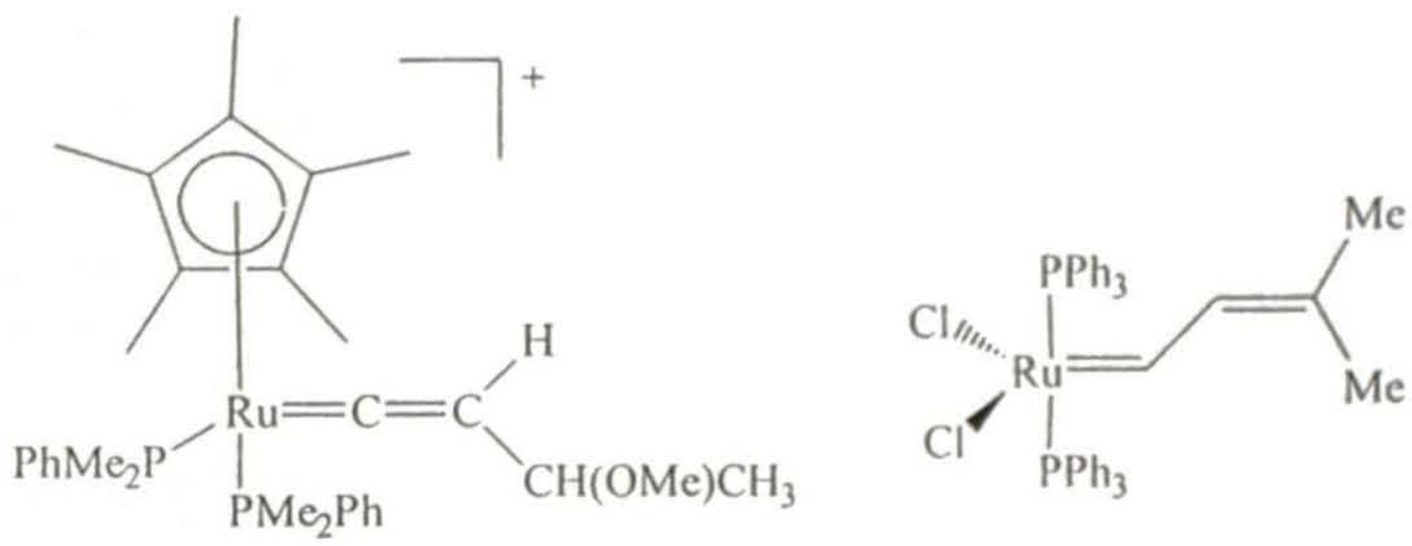

Figure 1.4

1.3. Ruthenium Schiff Base Chemistry

Considerable work has been done on ruthenium chemistry. Some selected portions have been mentioned in the earlier section. However, ruthenium Schiff base chemistry remains largely an unexplored area from beginning to till date. Presently also not much work is being reported on this area. In contrast Schiff base complexes of first transition metal ions are numerous in number and a wealth of information is available on such complexes.[19]

The first report on ruthenium Schiff base complexes, bis(N-phenylsalicylideneiminato)dicarbonylruthenium(II), and the dimeric N,N'-ethylenebis(salicylideneiminato)carbonylruthenium(II) appeared in 1969 (Calderazzo and co-workers[20]). After that only four articles were published on ruthenium Schiff base chemistry[21] in 1970's. In 1978, G. Wilkinson[21c] reported a series of ruthenium complexes with Schiff bases mostly derived from

salicylaldehyde and various diamines. The major portion of the known ruthenium Schiff base chemistry appeared in 1980's and 1990's. Application of ruthenium Schiff base complexes in (i) reversible binding of molecular oxygen and carbon monoxide, (ii) various catalytic reactions and (iii) different reactivities were also studied during this period.

In the following sections the work on ruthenium Schiff base complexes has been divided on the basis of the ligands used: (a) Schiff bases derived from salicylaldehyde and (b) Schiff bases obtained from other aldehydes/ketones.

1.3.1. Ruthenium complexes with salicylaldehyde derived Schiff bases

Schiff bases derived from salicylaldehyde and different amines constitute the major Schiff base chemistry of ruthenium. These ligands could be further divided into two groups on the basis of the types of amines used. They are (i) salicylaldehyde and various polyamine derived Schiff bases and (ii) salicylaldehyde and monoamine derived Schiff bases.

1.3.1.1. *Salicylaldehyde and polyamine derived Schiff bases and their ruthenium complexes*

These types of Schiff bases[22] are easily prepared under ambient condition by condensing proper polyamine and salicylaldehyde or substituted salicylaldehyde in 1:2 mole ratio. Condensation of salicylaldehyde and ethylenediamine produces the most familiar Schiff base in transition metal chemistry H_2salen or N,N'-ethylenebis(salicylideneimine) (Figure 1.5). Ruthenium Schiff base chemistry also started with this well-known Schiff base. Different Schiff bases[19,21,23] of this kind were synthesized using differernt polyamines. The amines used for this purpose are ethylenediamine; propylene-diamine; *o*-phenylenediamine; hexanediamine; cylcohexane-1,2-diamine; 2,2'-diamino-1,1'-binaphthyl; 3,4-diaminotoluene; α,α'-diamino-p-xylene; diethylenetriamine etc.

These Schiff bases act as tetradentate or pentadentate ligands. Deprtonation of phenolic-OH with proper base/alkali produces dinegatively charged ligand, which can bind the metal center through the phenolate oxygens, and the imine nitrogens. Coordination through imine nitrogens and phenolate oxygens to metal center produces stable six membered chelate rings. Hexa-coordinated Ru(II)/Ru(III) complexes have been isolated using these and other monodentate ancillary ligands. In these complexes, the phenolate oxygen atoms and the imine

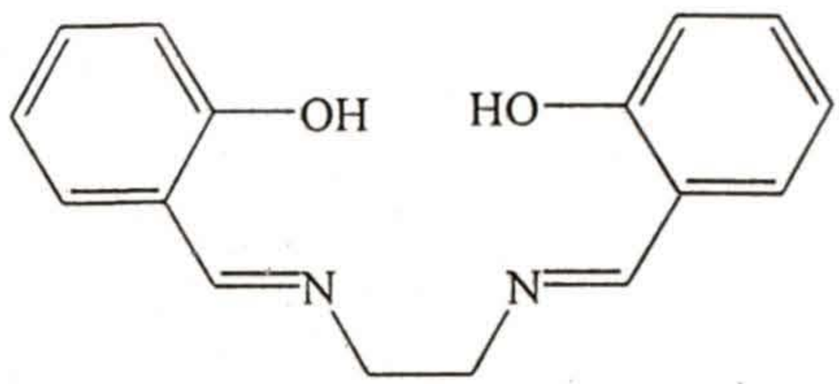

H_2salen

Figure 1.5

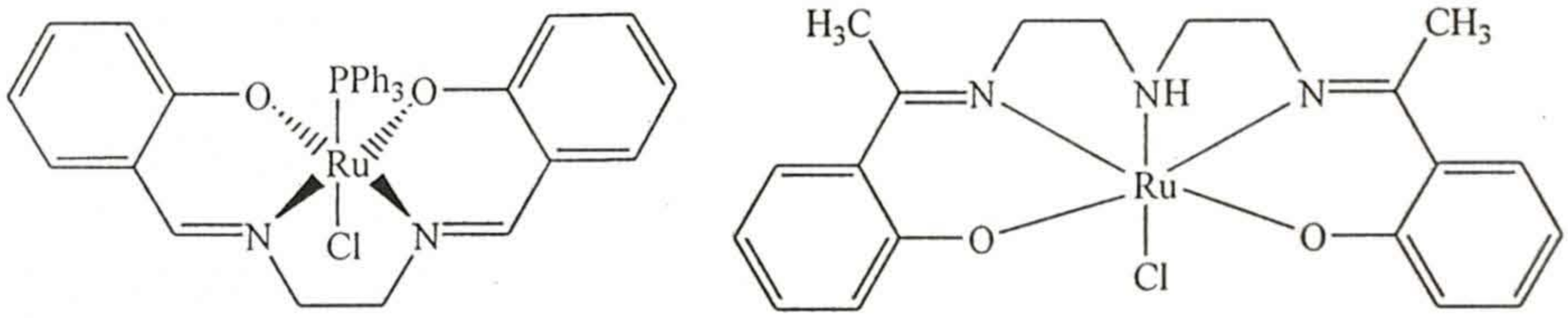

Figure 1.6

nitrogen atoms of the ligand form the square plane around the metal center and the axial positions are occupied by monodentate ligands, e.g. Cl^-, Br^-, PPh_3, py, CO, imidazole etc. For pentadentate ligand the sixth site is occupied by a monodentate ligand. Two examples are shown in Figure 1.6.

A very rare coordination mode is reported for the tetradentate Schiff base[231] obtained from substituted salicylaldehyde and 2,2'-diamino-1,1'-binaphthyl. Here the tetradentate ligand binds the ruthenium center in *cis* configuration and the square plane around the metal center is formed by the two monodentate ligands and one part of the Schiff base (Figure 1.7).

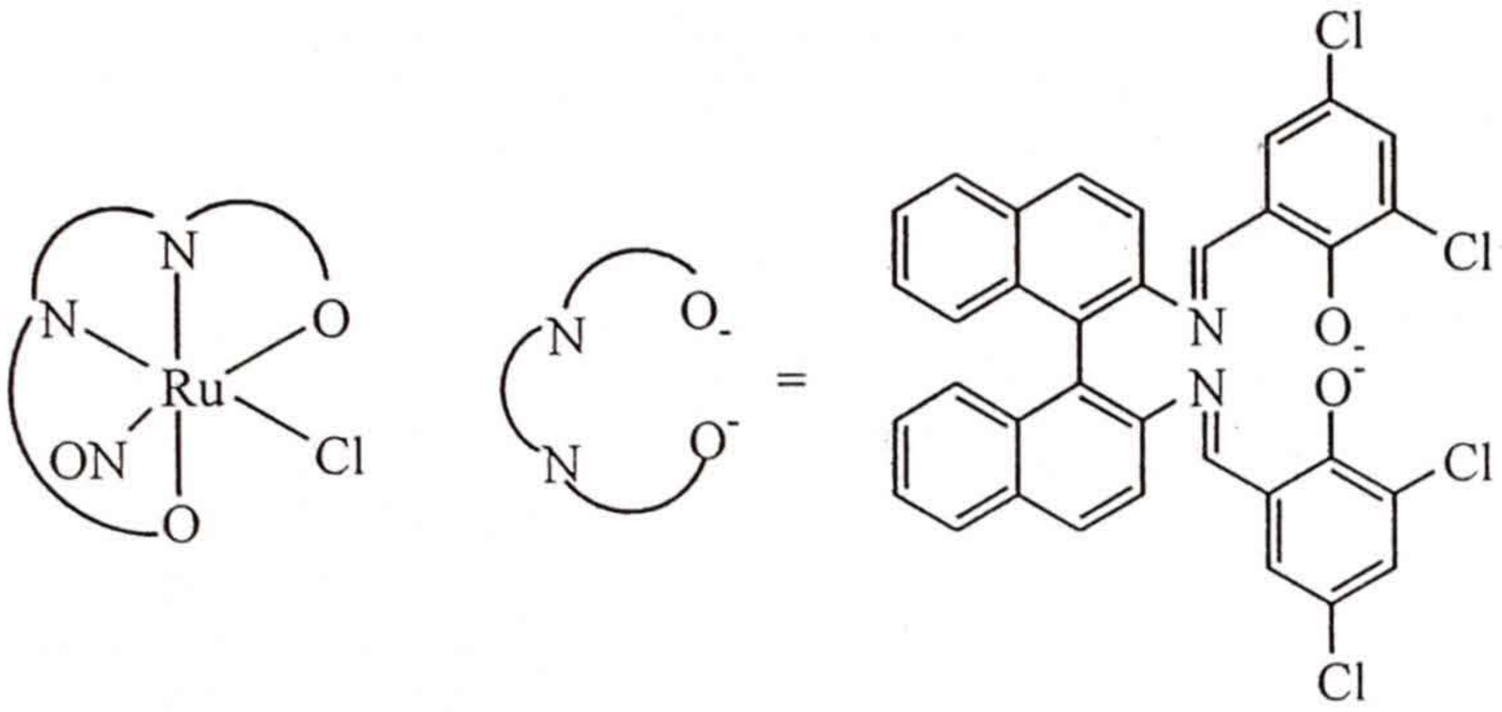

Figure 1.7

Some of the Ru(III) Schiff base complexes can bind molecular oxygen and carbon monoxide reversibly.[23e,23n-q,30b] It has been demonstrated that each of these complexes takes up one mole of molecular oxygen per mole of the complex. The reaction with respect to the molecular oxygen is reversible and coordinated oxygen can be displaced from the metal complex by bubbling nitrogen gas through solution. Oxygenation of the complex results in the oxidation of Ru(III) to a formal Ru(IV) oxidation state with the reduction of O_2 to unstable superoxide O_2^- species. Formation of Ru(IV) and superoxide were confirmed by electrochemically and IR spectrophotometry, respectively.[23e,23n-q,30b]

$$[\,Ru^{III}(L)(X)(Cl)]^{-/+/2+} + O_2 \underset{}{\overset{K_{O_2}}{\rightleftharpoons}} [\,Ru^{IV}(L)(X)(O_2^-)]^{0/2+/3+} + Cl^-$$

(L = dinegative/neutral tetradentate Schiff base ligands; X = Cl^-, imidazole, 2-methylimidazole).

Binding of cabon monoxide[23e,23n-q,30b] is also reversible. The presence of Ru(III)/Ru(II) reduction couple in the cyclic voltammograms of the CO adducts confirms that there is no reduction of the metal center due to CO binding.

1.3.1.2. *Salicylaldehyde and monoamine derived Schiff bases and their ruthenium complexes*

Condensation of salicylaldehyde or substituted salicylaldehyde with monoamines in 1:1 mole ratio produces the bidentate or tridentate ligands[23l-m,24] depending on the type of amine used. Different types of monoamines used for this purpose are aniline, m-toluidine, p-toluidine, methylamine, substituted aniline, benzylamine, L-histidine, phenylhydrazine, 4-aminobenzoic acid, ^{t}Bu-amine, anthranilic acid, α-methylbenzylamine, α-ethylbenzylamine, 2-amino-phenol, 2-diphenylphosphinoaniline, semicarbazide, thiosemicarbazide etc. Deprotonation of phenolic-OH with appropriate base/alkali produces chelating ligand, which can bind ruthenium center through the phenolate oxygen atom and the imine nitrogen atom resulting in a six-membered chelate ring. These ligands produce different types of complexes depending upon the number of ligands and ancillary ligands bound to the metal center. Mono, bis, tris chelates (Figure 1.8) and mixed ligand complexes are reported with these ligands.

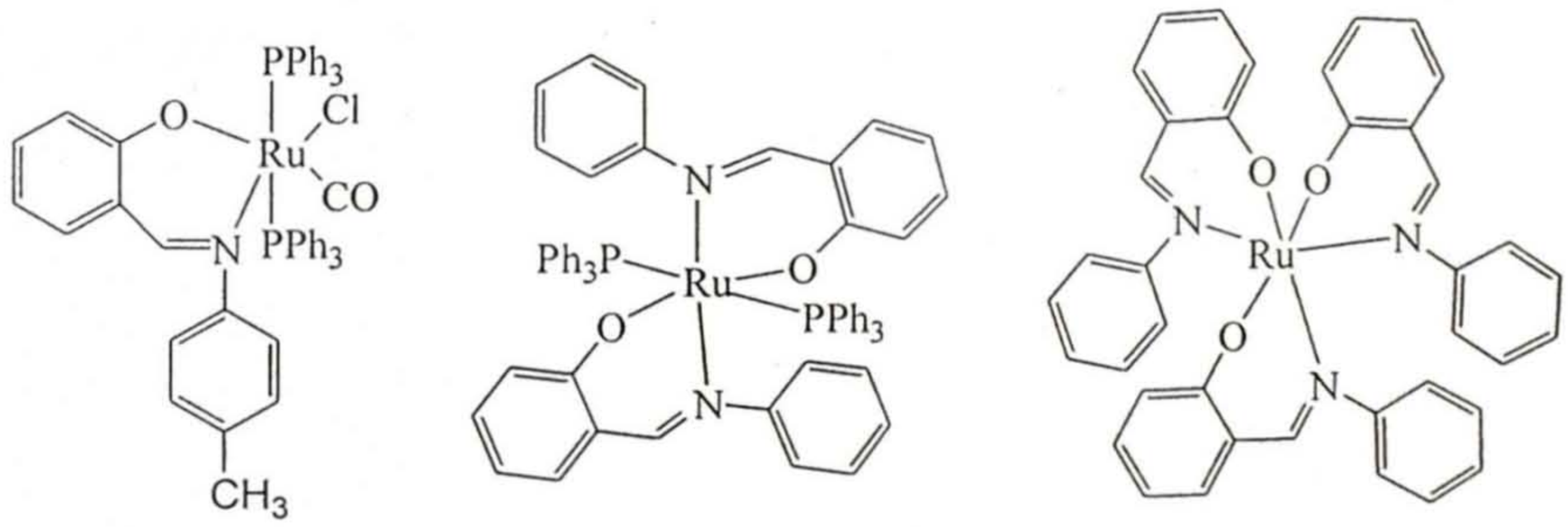

Figure 1.8

1.3.2. Other aldehyde/ketone derived Schiff bases and their ruthenium Complexes

Various types of aldehydes and ketones other than salicylaldehyde or acetophenone were used with different amines to prepare Schiff bases. This

series of ligands could be again classified in two groups: (i) Dialdehyde or diketone derived Schiff bases and (ii) monoaldehyde or monoketone derived Schiff bases.

1.3.2.1. *Dialdehyde or diketone derived Schiff bases and their ruthenium complexes*

Dialdehydes or diketones used for the synthesis of Schiff bases to explore the ruthenium chemistry are very few. They are 4-methyl-2,6-diformylphenol; 4-methyl-2,6-diketophenol; acetylacetone; glyoxal and benzil.

Different kinds of Schiff bases were synthesized from 4-methyl-2,6-diformylphenol (dfp) and its derivatives by condensing it with various amines. Numerous first transition metal complexes have been reported with various Schiff bases derived from this dialdehyde. Robson and co-worker introduced dfp[25] in 1970 for synthesis of macrocyclic oxo bridged binuclear complexes. Though it has been used extensively to synthesize first transition series metal ion complexes, very little has been reported on ruthenium chemistry. For the synthesis of ruthenium complexes, isolated or template derived Schiff bases from dfp have been employed.

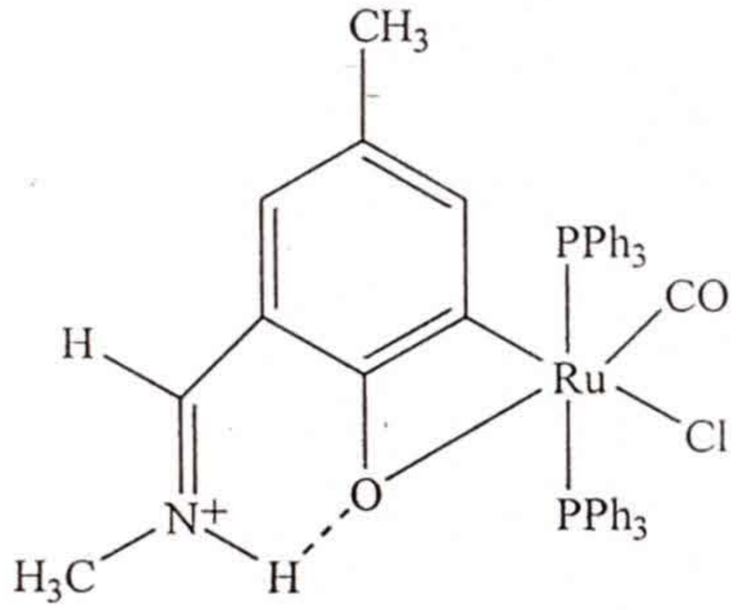

Figure 1.9

A. Chakravorty and co-worker first reported ruthenium complexes with Schiff bases obtained from dfp and different monoamines in 1:1 and 1:2 mole ratio. Reactions of $[Ru(PPh_3)_3Cl_2]$ with isolated ligands or in template method resulted in mononuclear organometallic complexes[26] as shown in Figure 1.9. The four membered rings in these

complexes undergo facile cleavage by ligands such as acetylene, phenylacetylene, etc. in boiling DCM-MeOH mixture resulting in alkyne-inserted products.

M. Schröder was successful in synthesizing a binuclear ruthenium Schiff base complex[27] from $[Ru(PPh_3)_3Cl_2]$ using the Schiff base derived from 4-methyl-2,6-diketophenol and ethylenediamine. Single crystal X-ray structure showed both the ruthenium centers are five coordinated and bridged by phenolate oxygens (Figure 1.10).

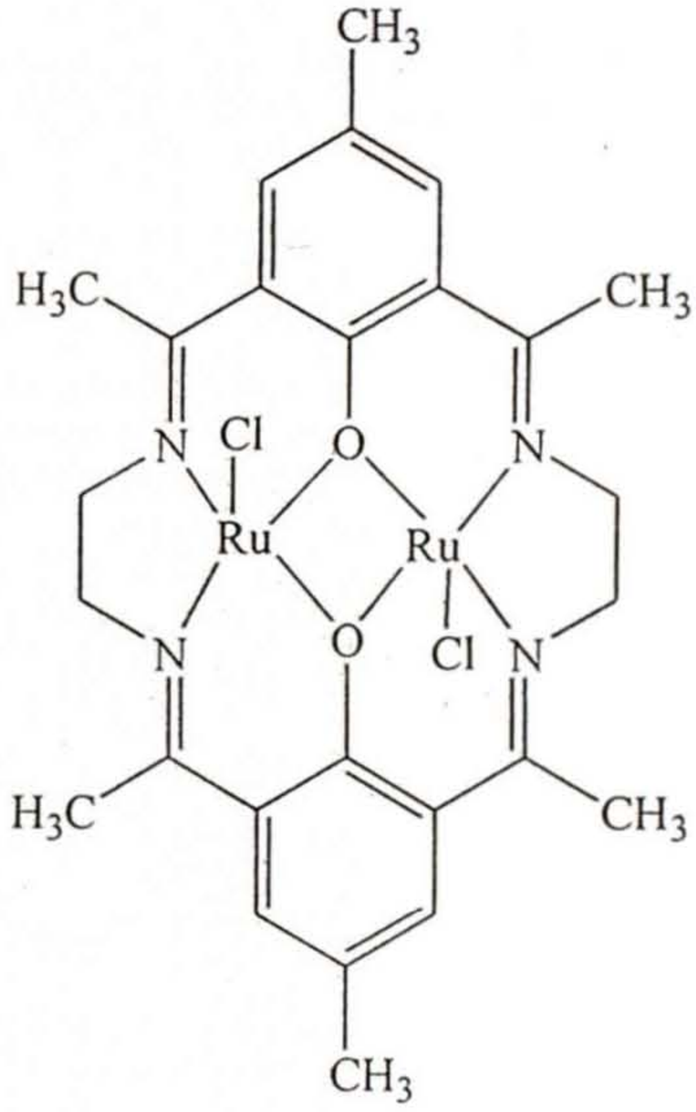

Figure 1.10

Condensation reactions of 4-methyl-2,6-diformylphenol with aliphatic diamines, $H_2N(CH_2)_nNH_2$ (n = 2, 3, 4) in the presence of $Ru(dmso)_4Cl_2$ (dmso = dimethylsulfoxide) produce acyclic dinuclear six coordinated ruthenium(II) complexes[28a] (Figure 1.11). These reactions in presence of triphenyl-phosphine produce binuclear organometallic complexes (as in Figure 1.9). Reaction of $[Ru(dmso)_4Cl_2]$ with the Schiff base obtained from dfp and tris(2-aminoethyl)-amine in 1:3 mole ratio produces a trinuclear ruthenium complex.[28b]

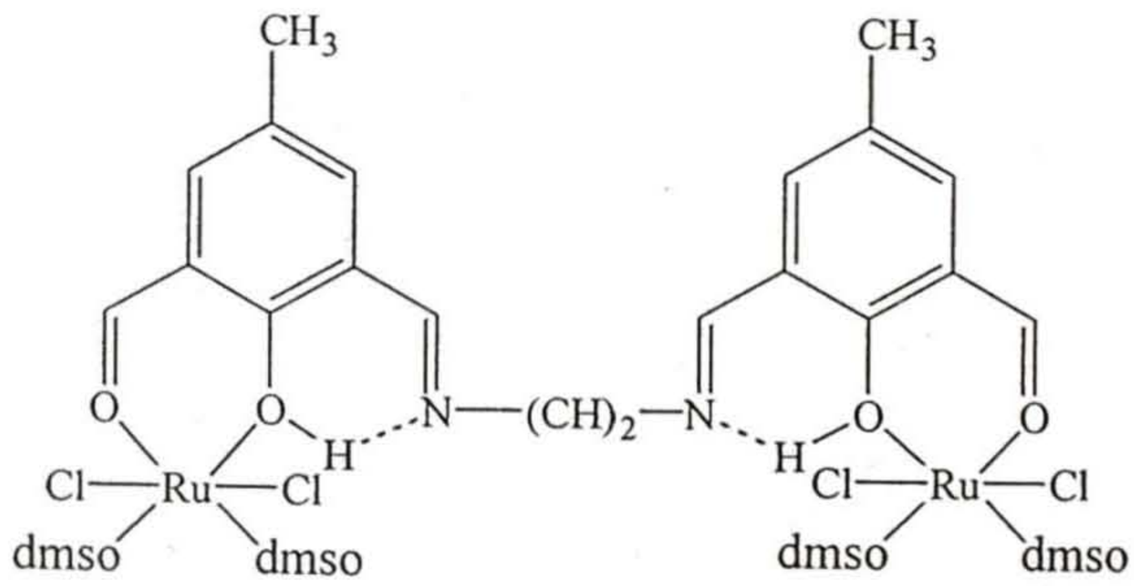

[dmso = dimethylsulphoxide]

Figure 1.11

Dioxo ruthenium(VI) complexes[23m] were isolated from Schiff bases obtained from acetylacetone and ethylenediamine or anthranilic

acid. Benzil and ethylenediamine derived Schiff base also produces a similar complex. Glyoxal and benzil were also used to derive Schiff bases from 2-aminophenol and 2-aminothiol. Isolation of Ru(III) octahedral complexes[29] are reported with these Schiff bases and other monodentate ancillary ligands (Figure 1.12).

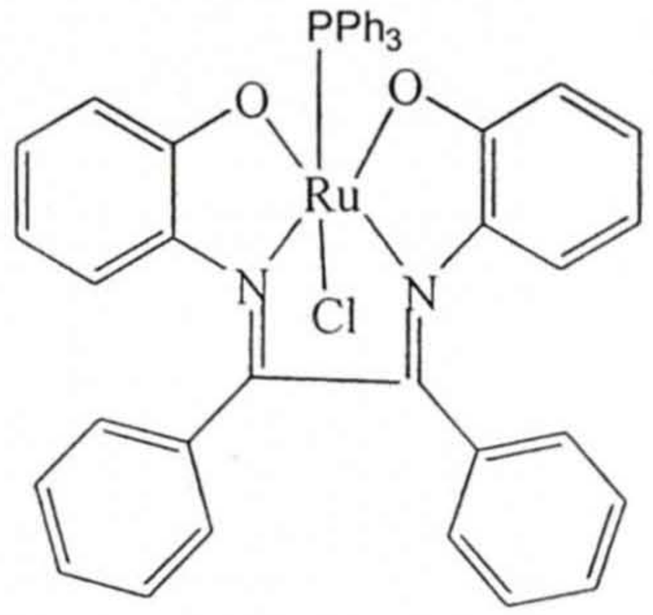

Figure 1.12

1.3.2.2. *Monoaldehyde or monoketone derived Schiff bases and their ruthenium complexes*

Different kinds of monoaldehydes and monoketones were used for preparing Schiff bases from aromatic or aliphatic monoamines and diamines. Benzaldehyde, picolinaldehyde, 2-hydroxy-1-naphthaldehyde, acetone, 1-phenyl-3-methyl-4-benzoyl-5-pyrazolone etc. are few of them.

Reaction of $K_2[RuCl_5(H_2O)]$ with Schiff bases prepared from 2-hydroxy-1-naphtaldehyde and diethylenetriamine, ethylenediamine, propylenediamine, phenylenediamine were reported to form octahedral six coordinated Ru(III) complexes[30] containing Cl^-, imidazole, 2-methylimidazole as ancillary ligand.

Reactions of $[Ru(PPh_3)_3Cl_2]$ with L-alanine, L-valine in acetone medium in presence of $NaHCO_3$ leads to formation of Schiff base complexes.[31] Structures of both the complexes were confirmed by X-ray crystallography.

$[Ru^{II}(L)_2(H_2O)]$ (L = Schiff base) type of complexes[32] were synthesized by reacting $K_2[RuCl_5(H_2O)]$ in ethanol with Schiff bases derived from 1-phenyl-3-methyl-4-benzoyl-5-pyrazolone and *p*-anisidine/ *m*-anisidine/ *m*-toluidine.

Picolinaldehyde was used to prepare tetradentate Schiff bases by condensation reactions with ethylenediamine, *o/m/p*-phenylenediamine, diethylenetriamine etc. Reaction of $K_2[RuCl_5(H_2O)]$ with these Schiff bases produce octahedral Ru(III) complexes[23n,23p-q,33] of general formula $[RuLCl_2]^+$

(Figure 1.13(a). Some of these complexes were reported to be active in reversible binding of molecular oxygen and carbon monoxide.

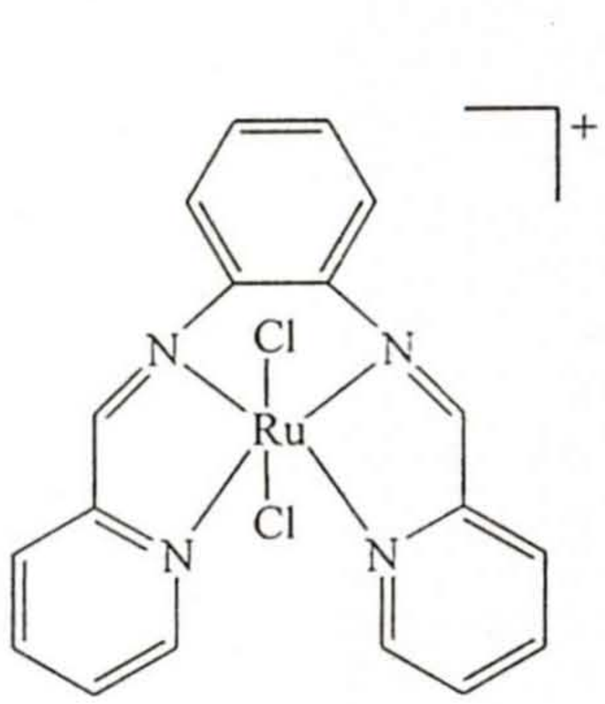

Figure 1.13(a)

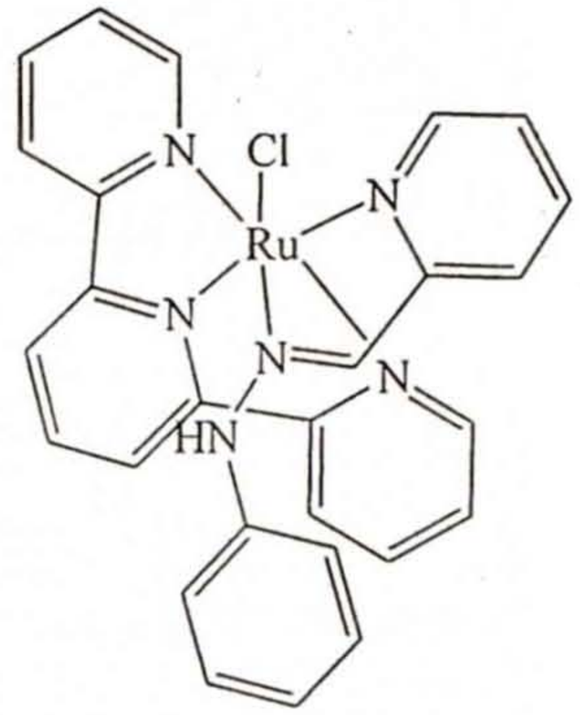

Figure 1.13(b)

Schiff base isolated from picolinaldehyde and phenylhydrazine was used for the preparation of mixed ligand complexes[34] (Figure 1.13(b)) from $Ru(tpy)Cl_3$ [tpy = terpyridine]. In one of the complexes this bidentate ligand transforms into a new class of imine-amidine based tridentate ligand. This was confirmed by X-ray crystallography.

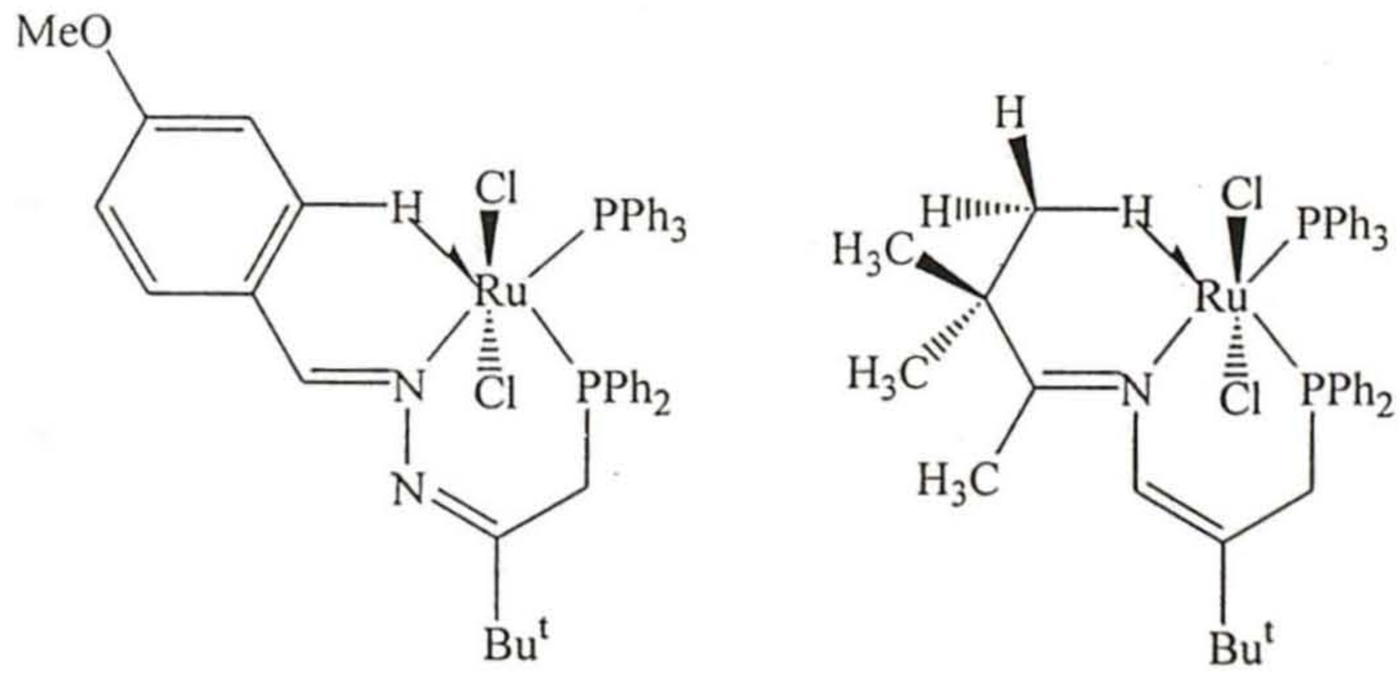

Figure 1.14

B. L. Shaw and co-workers derived Schiff bases from different types of aliphatic or aromatic aldehydes and ketones with phosphino hydrazone *Z*-$PPh_2CH_2(^tBu)=NNH_2$. These bidentate Schiff bases react with $[Ru(PPh_3)_3Cl_2]$ and $[Ru(CO)_2Cl_2]_x$ to produce five and six coordinated ruthenium complexes.[35] Most of the complexes showed agostic interaction between Ru and C-H bond (Figure 1.14).

Chiral Schiff bases derived from (1R,2R)-diaminocyclohexane with benzaldehyde, substituted benzaldehyde, 1-naphthaldehyde, 9-anthraldehyde, 2-diphenylphosphinobenzaldehyde were used to prepare ruthenium complexes.[36] These complexes were used as catalysts in hydrogen transfer reactions.

Schiff bases prepared by condensation of 2-^{t}butylthiobenzaldehyde or 2-diphenylphosphinobenzaldehyde with cyclohexanediamine, ethylenediamine, 1,2-diaminopropane and propylenediamine were reacted with $[Ru(PPh_3)_3Cl_2]$. The complexes,[37] thus obtained, showed visible light induced photosubstitution reactions.

Unsaturated aliphatic aldehydes were condensed with L-valine, and *o*-aminophenol and the resulting Schiff bases were used to synthesize a series of ruthenium complexes.[38]

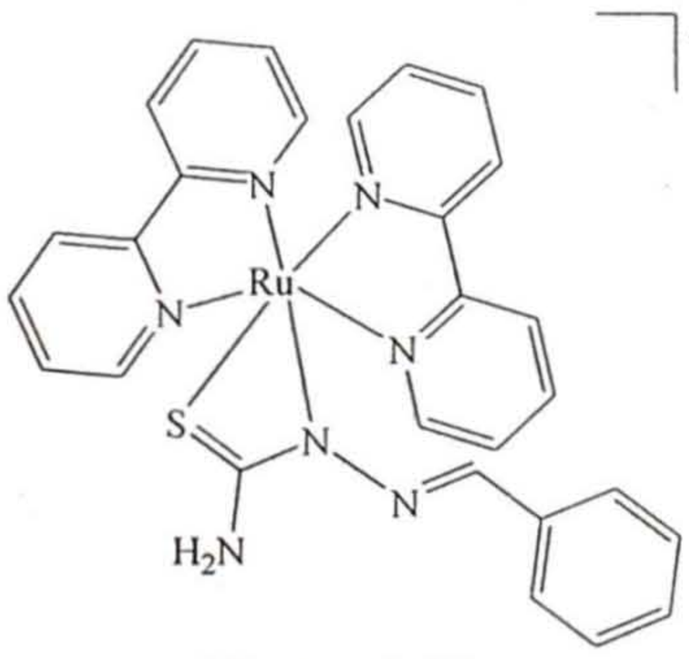

Figure 1.15

Different substituted benzaldehydes were condensed with 2-aminothiophenol to prepare bidentate Schiff bases. These compounds have been reported to form mixed tris-chelates of Ru(II/III) containing $\{Ru(bpy)_2\}$ moiety.[39]

Benzaldehyde, substituted benzaldehyde and acetone were used to get Schiff bases from semicarbazide and thiosemicarbazide.[40] Unusual coordination behavior of these ligands to ruthenium were studied (Figure 1.15) in details.

1.3.3. Catalytic properties of ruthenium Schiff base complexes

Different types of catalytic properties have been studied using ruthenium(II)/(III) Schiff base complexes. Mononuclear and polynuclear, both types of complexes are proved to be catalytically active in different organic synthetic reactions. However, the number of complexes known to act as catalyst is very few and also limited to few reactions. Different catalytic activities so far reported are as follows:

Ruthenium complexes generated in situ from $[Ru(\eta^6\text{-}C_6H_6)Cl_2]_2$ and chiral Schiff base[36] derived from (1R,2R)-diaminocyclohexane catalyze the reduction of alkyl and aryl ketones in 2-propanol to produce the corresponding alcohol.

Epoxidation of cyclohexene, norborene, *cis*–cyclooctene, styrene, *trans*-4-octene, cycloheptene, were catalyzed by Ru(III) Schiff base complexes[33b,24h,23j,23n] in presence of molecular oxygen or iodosylbenzene as oxidant.

Diels–Alder reactions between different types of dienes and dienophiles are catalyzed by a mixed ligand ruthenium complex [Ru(salen)(NO)(Cl)].[23h]

Ruthenium complexes[24m] with bidentate Schiff bases derived from salicylaldehyde and alkyl or aromatic monoamines are capable of catalyzing ring closing metathesis reactions of some selective diolefins. These systems can also catalyze Kharasch addition of carbon tetrachloride across olefins and enol ester synthesis reactions in good yields.

Ru(II)/(III) Schiff base complexes[24c,24e,24k] can act as effective catalysts for oxidation of primary alcohol to aldehyde, secondary alcohol to ketone, and 3, 5-di(tert-butyl)catechol to *o*–benzoquinone in presence of N–methyl–morpholine–N–oxide as co-oxidant.

Trimethylsilylcyanation of benzaldehyde is also reported to be catalyzed by ruthenium complexes[23l] derived from binaphthyl Schiff base ligands.

Recently C. -M. Che reported catalytic activity of Ru(II)-salen complexes[41] in amidation of silyl enol ethers and cholesteryl acetates.

1.4. Aim of the Present Investigation

In the previous section we have discussed briefly about the ruthenium Schiff base chemistry. Different types of Schiff bases were used to study ruthenium chemistry. However, there are only four reports about ruthenium complexes with hydrazine derived Schiff bases.[35]

B. L. Shaw reported first on ruthenium complexes with Schiff bases prepared from hydrazine. Two of the ligands used are shown in Figure 1.16. A series of five- and six-coordinated ruthenium complexes were synthesized and agostic interaction between C – H bond and ruthenium center in five coordinated complexes has been demonstrated.

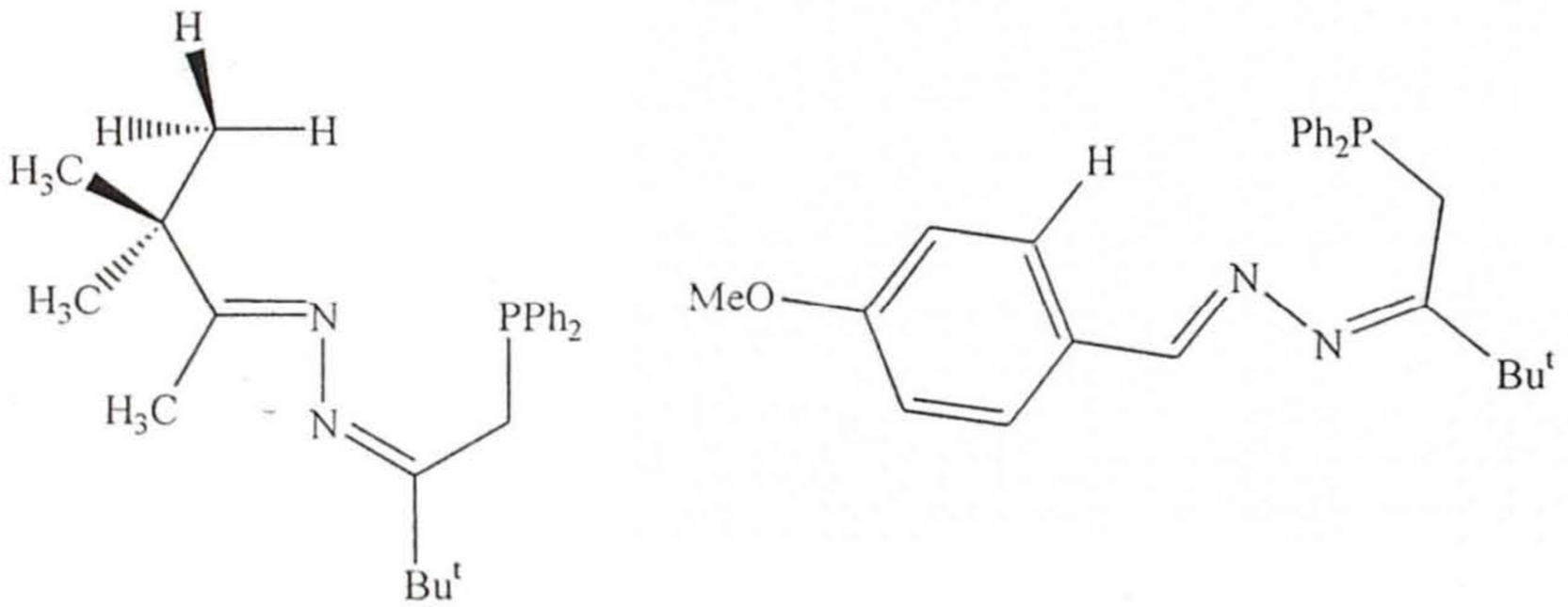

Figure 1.16

Schiff bases obtained from salicylaldehyde and hydrazine (H_2salhnR), picolinaldehyde and aroylhydrazine (HL), and salicylaldehyde and acetylhydrazine (H_2acs) have been used to study first transition metal chemistry.[42] However, there is no report on ruthenium complexes with these Schiff bases.

Condensation reactions of salicylaldehyde and substituted salicylaldehyde with hydrazine in 2:1 mole ratio produce a tetradentate Schiff base system H_2salhnR (R = H, Cl, OMe, ^{t}Bu). Crystal structure[43] of H_2salhnH shows that both the -OH groups are *trans* to each other as shown in Figure 1.17. Rotation along

N-N single bond of the diazine moiety allows the ligand to adopt *cis*, *trans*, or in between twisted configurations in complexes. Few years ago a dinuclear iron(III) complex $[Fe_2(\mu\text{-salhnH})_3]$[44a] was reported from our laboratory using this Schiff base. Other than this, two more complexes containing this ligand are known. These are a dirhodium(I) complex $[Rh_2(CO)_4(\mu\text{-salhnH})]$,[44b] and a hexanuclear cobalt(II,III) complex[44c] $[\{Co_3L\text{-}(CH_3COO)(CH_3O)_3\}_2(\mu\text{-salhnH})]$, ($H_3L$ is 2,6-bis-(salicylideneamino-methyl)-4-methyl-phenol). Recently structurally characterized dinuclear complexes of first transition metal ions are reported with similar kind of ligands N,N'-bis(picolinylidene)hydrazine or its substituted derivatives with the N-N single bond as the bridging unit. These complexes are important not only with respect to their structures but also for the influence of the structure on the interaction between the metal ions.

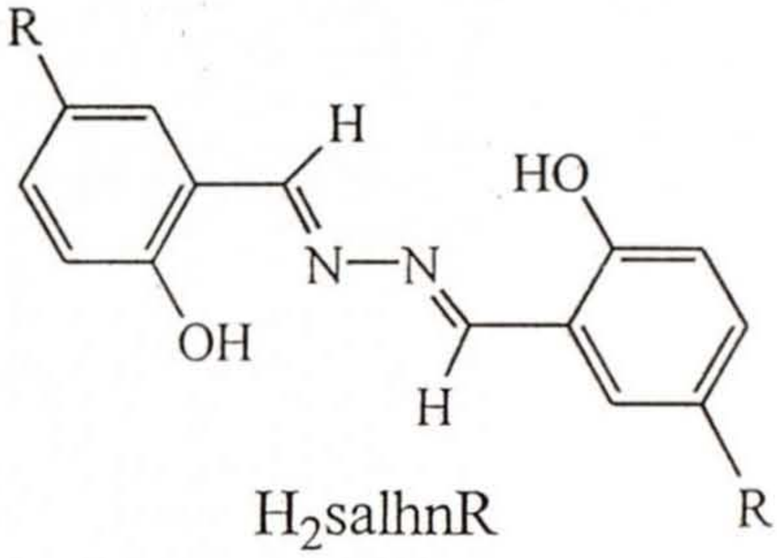

H_2salhnR

R = H, Cl, OMe, ^{t}Bu

Figure 1.17

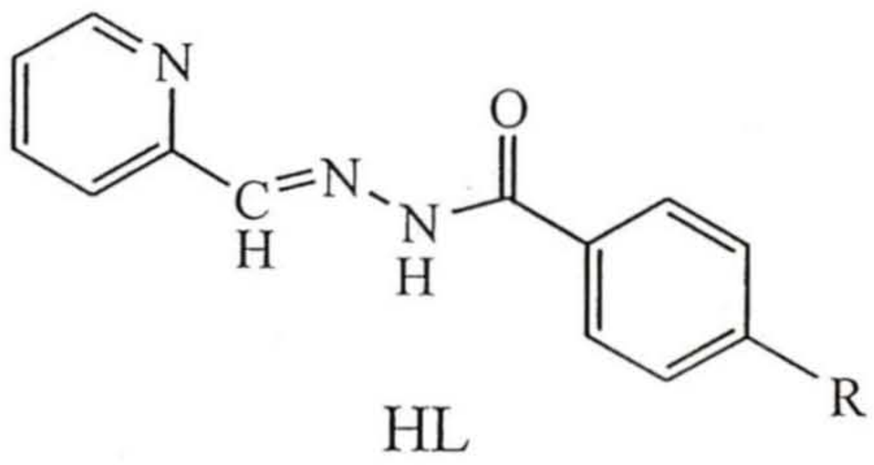

HL

R = H, Cl, OMe, Me, NMe_2

Figure 1.18

Reactions of aroylhydrazine and substituted aroylhydrazines with picolinaldehyde produce Schiff bases (HL) as shown in Figure 1.18. In deprotonated state, these Schiff bases can act as tridentate ligands. Coordination *via* the pyridine-N, the imine-N, and the amide-O to metal center forms two five membered chelate rings.

As mentioned in Section 1.2.2 ruthenium(II) complexes with α, α'-diimine ligands are very important due to the availability of low-lying π* orbitals and hence a low energy metal-to-ligand charge transfer excited state. The HL system provides this π-acidic α, α'-diimine fragment for metal coordination. In deprotonated state the third coordinating center is the amide-O atom, which is predominantly σ-basic. The σ-basicity of this coordinating atom can be varied by using different substituents at the *para* position of the aroyl moiety. Thus the electron transfer properties of the complexes can be tuned by this variation. In addition to the above, this ligand system provides the scope of studying the effect of coordinated amide protonation state on the physical properties of the complex, which is not easy for amide-N coordinated species.

Acetyl hydrazine with salicylaldehyde in 1:1 mole ratio produces the tridentate Schiff base H_2acs (Figure 1.19). Higher-valent first transition metal complexes with ligands containing amide functionality are well studied.[45] In these complexes, the N-center of the deprotonated amide functionality binds the metal ion. Very often these amide nitrogen coordinated higher-valent complexes are unstable due to self-decomposition. The reason behind this problem is the proton coupled electron transfer involving the metal ion and the hydrogen atom at the carbon α to the coordinated amide nitrogen. This leads to oxidation of the ligand and reduction of the metal center. This problem could be avoided by replacing the α H with alkyl or aryl groups.[46] Another approach is to use ligands with O-coordinating amide functionality. In deprotonated state, H_2acs can coordinate a metal center through the phenolate-O, the imine-N, and the

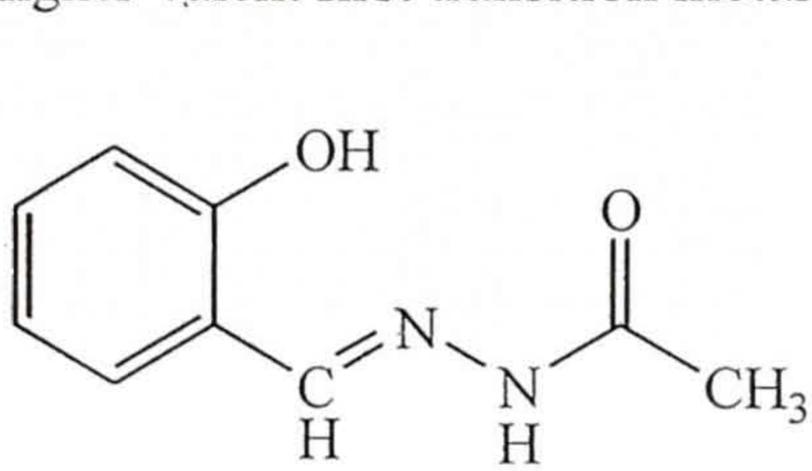

H_2acs

Figure 1.19

amide-O atoms forming a six-and a five-membered chelate ring. This ligand has not only the O-coordinating amide functionality but also another high oxidation state promoting[47] phenolate-O coordinating center. Like the HL, H_2acs also provides the opportunity of studying the influence of amide protonation state on the coordination geometry and physical properties of the complex.

In this work, we have studied the ruthenium chemistry with the above-mentioned three Schiff base systems. The main objectives are as follows:

(i) Diazine bridged dinucluer ruthenium complexes with H_2salhnR.

(ii) Mononuclear ruthenium(II) complexes with α, α'- diimine donor HL.

(iii) Higher-valent species with H_2acs.

(iv) Studies on protonation and deprotonation of the O-coordinating amide functionalities in the complexes with HL and H_2acs.

The results obtained are described in the following chapters with special reference to (i) synthesis and characterization, (ii) structure and bonding, and (iii) chemical, spectroscopic and electrochemical properties.

1.5. References

1. (a) A. Joly, *C. R. Acad. Sci.*, **1892**, *115*, 1299. (b) F. H. Burstall, *J. Chem. Soc.*, **1936**, 173. (c) C. Creutz, H. Taube, *J. Am. Chem. Soc.*, **1973**, *95*, 1086.
2. (a) E. Tfouni, *Coord. Chem. Rev.*, **2000**, *196*, 281. (b) H. E. Toma, K. Araki *Coord. Chem. Rev.*, **2000**, *196*, 307. (c) A. B. P. Lever, S. I. Gorelsky, *Coord. Chem. Rev.*, **2000**, *208*, 153. (d) Md. K. Nazeeruddin, S. M. Zakeeruddin, R. Humpry-Baker, S. I. Gorelsky, A. B. P. Lever, M. Gratzel, *Coord. Chem. Rev.*, **2000**, *208*, 213. (e) K. Szacilowski, W. Macyk, G. Stochel, Z. Stasicka, S. Sostero, O. Traverso, *Coord. Chem. Rev.*, **2000**, *208*, 277. (f) B. -Z. Shan, Q. Zhao, N. Goswami, D. M. Eichhorn, D. P. Rillema, *Coord. Chem. Rev.*, **2001**, *211*, 117. (g) V. Balzani, A. Juris, *Coord. Chem. Rev.*, **2001**, *211*, 97. (h) H. E. Toma, K. A. Anamaria, D. P. Alexiou, S. Nikolaou, S. Dovidauskas, *Coord. Chem. Rev.*, **2001**, *219-221*, 187. (i) S. I. Gorelsky, A. B. P. Lever, M. Ebadi, *Coord. Chem. Rev.*, **2002**, *230*, 97. (j) M. J. Clarke, *Coord. Chem. Rev.*, **2002**, *232*, 69. (k) E. Tfouni, M. Krieger, B. R. McGarvey, D. W. Franco, *Coord. Chem. Rev.*, **2003**, *236*, 57. (l) H. Yersin, C. Kratzer, *Coord. Chem. Rev.*, **2002**, *229*, 75. (m) I. Ortmans, C. Moucheron, A. K.-De. Mesmaeker, *Coord. Chem. Rev.*, **1998**, *168*, 233. (n) A. Islam, N. Ikeda, K. Nozaki, Y. Okamoto, B. Gholamkhass, A. Yoshimura, T. Ohno, *Coord. Chem. Rev.*, **1998**, *171*, 355. (o) P. J. Dyson, B. F. G. Jonson, C. M. Martin, *Coord. Chem. Rev.*, **1998**, *175*, 59. (p) M. J. Clarke, *Coord. Chem. Rev.*, **2003**, *236*, 209. (q) J. Wing-Sze Hui, Wing-Tak Wong, *Coord. Chem. Rev.*, **1998**, *172*, 389. (r) Siu-Ming Lee, Wing-Tak Wong, *Coord. Chem. Rev.*, **1997**, *164*, 415. (s) C. Dietrich-Buchecker, G. Rapenne, J.-P. Sauvage, *Coord. Chem. Rev.*, **1999**, *185-186*, 167. (t) C. Slugovc, R. Schmid, K. Kirchner, *Coord. Chem. Rev.*, **1999**, *185-186*, 109. (u) S. Sabo-Etienne, B. Chaudret, *Coord. Chem. Rev.*, **1998**, *178-180*, 381.

(v) Luisa De Cola, P. Besler, *Coord. Chem. Rev.*, **1998**, *177*, 301. (w) D. J. Stufkens, A. Vlček Jr., *Coord. Chem. Rev.*, **1998**, *177*, 127.

3. T. Naota, H. Takaya, S. I. Murahashi, *Chem. Rev.*, **1998**, *98*, 2599.
4. B. M. Trost, F. D. Toste, A. B. Pinkerton, *Chem. Rev.*, **2001**, *101*, 2067.
5. M. Bresson, N. d'Allessandro, L. Liberatore A. Morvillo, *Coord. Chem. Rev.*, **1999**, *185-186*, 385.
6. S. Murai, N. Chatani, F. Kakiuchi, *Pure Appl. Chem.*, **1997**, *69*, 589.
7. (a) T. Mirsudo, S. -W. Zhang, M. Nagao, Y. Watanabe, *J. Chem. Soc., Chem. Commun.*, **1991**, 598. (b) N. Chatani, H. Inoue, T. Ikeda, S. Murai, *J. Org. Chem.*, **2000**, *65*, 4913. (c) C. S. Yi, N. Liu, *J. Organomet. Chem.*, **1998**, *553*, 157. (d) E. Galardon, P. Le Maux, G. Simonneaux, *Tetrahedron*, **2000**, *56*, 615. (e) J. W. Faller, J. Parr, *Organometallics*, **2000**, *19*, 1820. (f) T. Midsudo, M. Takagi, S. -W. Zhang, Y. Watanabe, *J. Organomet. Chem.*, **1992**, *423*, 405. (g) M. Yamaguchi, Y. Kido, K. Omata, M. Hirama, *Synlett.*, **1995**, 1181. (h) S. Murai, F. Kakiuchi, S. Sekine, Y. Tanaka, A. Kamatani, M. Sonoda, N. Chatani, *Nature*, **1993**, *366*, 529. (i) F. Kakiuchi, Y. Yamamoto, N. Chatani, S. Murai, *Chem. Lett.*, **1996**, 111. (j) R. Grigg, V. Savig, *Tetrahedon Lett.*, **1997**, *38*, 5737. (k) T. Takemori, H. Suzuki, M. Tanaka, *Organometallics*, **1996**, *15*, 4346. (l) S. Cenini, F. Ragaini, S. Tollari, D. Paone, *J. Am. Chem. Soc.*, **1996**, *118*, 11964. (m) W. A. Hermann, W. C. Schattenmann, O. Nuyken, S. C. Glander, *Angew. Chem., Int. Ed.*, **1997**, *36*, 2121. (n) Y. -S. Shon, T. R. Lee, *Tetrahedon Lett.*, **1997**, 38, 1283. (o) M. J. Marsella, H. D. Maynard, R. H. Grubbs, *Angew. Chem. Int. Ed.*, **1997**, *36*, 1101. (p) S. –H. Kim, N. Bowden, R. H. Grubbs, *J. Am. Chem. Soc.*, **1994**, *116*, 10801. (q) A. Demonceau, C. A. Lemoine, A. F. Noels, I. T. Chizhevsky, P. V. Sorokin, *Tetrahedron Lett.*, **1995**, *36*, 8419. (r) T. Kondo, N. Suzuki, T. Okada, T. Mitsudo, *J. Am. Chem. Soc.*, **1997**, *119*, 6187. (s) J. W. Steed, D. A. Tocher, R. D. Rogers, *J. Chem. Soc., Chem. Commun.*, **1996**,

1589. (t) H. Nakamatsu, S. Blechert, *Angew. Chem., Int. Ed.*, **2002**, *41*, 794. (u) J. C. Sworen, J. H. Pawlow, W. Case, J. Lever, K. B. Wagener, *J. Mol. Catal., A: Chem.*, **2003**, *194*, 69.

8. (a) S. -I. Murahashi, T. Naota, Y. Oda, N. Hirai, *Synlett.*, **1995**, 733. (b) G. Barak, J. Dakka, Y. Sasson, *J. Org. Chem.*, **1988**, *53*, 3553. (c) M. Matsumoto, S. J. Ito, *J. Chem. Soc., Chem. Commun.*, **1981**, 907. (d) M. Matsumoto, S. J. Ito, *Synth. Commun.*, **1984**, *14*, 697.
9. (a) T. N. Mitchell, F. Giesselmann, *Synlett.*, **1996**, 475. (b) T. Mitsudo, S.-W. Zhang, N. Satake, T. Kondo, Y. Watanabe, *Tetrahedron Lett.*, **1992**, *33*, 5533.
10. (a) C. Ruppin, P. H. Dixneuf, S. Lecolier, *Tetrahedron Lett.*, **1998**, *29*, 5365. (b) J. Fournier, C. Bruneau, P. H. Dixneuf, S. Licolier, *J. Org. Chem.*, **1991**, *56*, 4456. (c) S. -I. Murahashi, T. Naota, E. Saito, *J. Am. Chem. Soc.*, **1986**, *108*, 7846.
11. (a) J. F. Knifton, *J. Org. Chem.*, **1976**, *41*, 1200. (b) T. Ohta, T. Miyake, H. Takaya, *J. Chem. Soc., Chem. Commun.*, **1992**, 1725. (c) H. Takaya, T. Ohta, R. Noyori, *Tetrahedron Lett.*, **1990**, *31*, 7189. (d) T. Ohkuma, H. Ikehira, T. Ikariya, R. Noyori, *Synlett.*, **1997**, 467.
12. (a) W. J. Zuercher, M. Hashimoto, R. H. Grubbs, *J. Am. Chem. Soc.*, **1996**, *118*, 6634. (b) D. E. Fogg, D. Amoroso, S. D. Drouin, J. Snelgrove, J. Conrad, F. Zamanian, *J. Mol. Catal.*, **2002**, *190A*, 177.
13. (a) W. Rűttinger, G. C. Dismukes, *Chem. Rev.*, **1997**, *97*, 1. (b) M. Yagi, M. Kaneko, *Chem. Rev.*, **2001**, *101*, 21.
14. (a) S. W. Gersten, G. J. Samuels, T. J. Meyer, *J. Am. Chem. Soc.*, **1982**, *104*, 4029. (b) J. A. Gilbert, D. S. Eggleston, W. R. Murphy Jr., D. A. Geselowitz, S. W. Gersten, D. J. Hodgson, T. J. Meyer, *J. Am. Chem. Soc.*, **1985**, *107*, 3855. (c) J. R. Schoonover, J. F. Ni, L. Roecker, P. S. White, T. J. Meyer, *Inorg. Chem.*, **1996**, *35*, 5885. (d) S. Goswami, A. R. Chakravarty, A. Chakravorty, *J. Chem. Soc., Chem. Commun.*, **1982**. 1288.

15. (a) M. Yagi, S. Tokita, K. Nagoshi, I. Ogino, M. Kaneko, *J. Chem. Soc., Faraday Trans.*, **1996**, *92*, 2457. (b) K. Nagoshi, M. Yagi, M. Kaneko, *Bull. Chem. Soc. Jpn.*, **2000**, *73*, 2193. (c) M. Yagi, Y. Osawa, N. Sukegawa, M. Kaneko, *Langmuir*, **1999**, *15*, 7406.

16. (a) A. Juris, V. Balzani, F. Barigelletti, S. Campagna, P. Belser, A. Von Zelewsky, *Coord. Chem. Rev.*, **1988**, *84*, 85. (b) V. Balzani, A. Juris, M. Venturi, S. Campagna, S. Seroni, *Chem. Rev.*, **1996**, *96*, 759. (c) C. A. Bignozzi, R. Argazzi, C. Chiorboli, S. Roffia, F. Scandola, *Coord. Chem. Rev.*, **1991**, *111*, 261. (d) F. Scandola, M. T. Indelli, C. Chiorboli, C. A. Bignozzi, *Top. Curr. Chem.*, **1990**, *58*, 73. (e) J. R. Schoonover, C. A. Bognozzi, T. J. Meyer, *Coord. Chem. Rev.*, **1997**, *165*, 239. (f) H. Dürr, S. Bossmann, *Acc. Chem. Res.*, **2001**, *34*, 905. (g) M. Osawa, M. Hoshino, Y. Wakatsuki, *Angew. Chem., Int. Ed.*, **2001**, *40*, 3472. (h) J. F. Endicott, H. B. Schlegel, Md. J. Uddin, D. S. Seniveratne, *Coord. Chem. Rev.*, **2002**, *229*, 95.

17. (a) Y. Xiong, L. -N. Ji, *Coord. Chem. Rev.*, **1999**, *185-186*, 711. (b) A. Ambroise, B. G. Maiya, *Inorg. Chem.*, **2000**, *39*, 4264. (c) J. K. Barton, A. T. Danishefsky, J. M. Goldberg, *J. Am. Chem. Soc.*, **1984**, *106*, 2172. (d) C. V. Kumar, J. K. Barton, N. J. Turro, *J. Am. Chem. Soc.*, **1985**, *107*, 5518. (e) A. M. Pyle, J. P. Rehman, R. Meshoyrer, C. V. Kumar, N. J. Turro, J. K. Barton, *J. Am. Chem. Soc.*, **1989**, *111*, 3051. (f) H. Y. Mei, J. K. Barton, *Proc. Natl. Acad. Sci.*, **1988**, *85*, 1339. (g) E. Amouyal, A. Homsi, J. C. Chambron, J. P. Souvage, *J. Chem. Soc., Dalton Trans.*, **1990**, 1841. (h) P. Lincoln, B. Norden, *J. Chem. Soc., Chem. Commun.*, **1996**, 2145. (i) T. K. Schoch, J. L. Hubbard, C. R. Zoch, G. B. Yi, M. Sorile, *Inorg. Chem.*, **1996**, *35*, 4383. (j) D. R. Frasca, M. J. Clarke, J. *Am. Chem. Soc.*, **1999**, *121*, 8523. (k) P. J. Carter, C. C. Cheng, H. H. Thorp, *J. Am. Chem. Soc.*, **1998**, *120*, 632.

18. (a) D. Touchard, P. H. Dixneuf, *Coord. Chem. Rev.*, **1998**, *178-180*, 409. (b) M. I. Bruce, *Chem. Rev.*, **1991**, *91*, 197. (c) R. Wiedemann, P. Steinert,

O. Gevert, H. Werner, *J. Am. Chem. Soc.*, **1996**, *118*, 2495. (d) H. Werner, M. Laubender, R. Wiedemann, W. Windmfler, *Angew. Chem.*, *Int. Ed.*, **1996**, *35*, 1237. (e) M. A. Bannett, G. A. Heath, D. C. R. Hockless, I. Kovacik, A. C. Willis, *Organometallics*, **1998**, *17*, 5867. (f) H. P. Xia, R. C. Y. Yeung, G. Jia, *Organometallics*, **1998**, *17*, 4762. (g) A. A. Koridze, V. I. Zdanovich, A. M. Sheloumov, V. Yu, L. Pavel, V. Petrovskii, A. S. Peregudov, F. M. Dolgushin, A. I. Yanavsky, *Organometallics*, **1997**, *16*, 2285. (h) M. I. Bruce, B. C. Hall, B. D. Kelly, P. J. Low, B. W. Skelton, A. H. White, *J. Chem. Soc.*, *Dalton*, *Trans.*, **1999**, 3719.

19. (a) M. D. Hobday, T. D. Smith, *Coord. Chem. Rev.*, **1973**, *9*, 311. (b) M. Caligaris, *Ibid.*, **1972**, *7*, 385. (c) R. D. Jones, D. A. Summerville, F. Basolo, *Chem. Rev.*, **1979**, *79*, 139. (d) E. C. Niederhoffer, J. H. Timmons, A. E. Martell, *Chem. Rev.*, **1984**, *84*, 137.
20. F. Calderazzo, C. Floriani, R. Henzi, F. L. Eplattenier, *J. Chem. Soc.*, *A*, **1969**, 1378.
21. (a) K. S. Finney, G. W. Everett, *Inorg. Chim. Acta*, **1974**, *11*, 185. (b) G. Henrich-Olive, S. Olive, *J. Mol. Catal.*, **1976**, *1*, 121. (c) J. R. Thornback, G. Wilkinson, *J. Chem. Soc.*, *Dalton Trans.*, **1978**, 110. (d) K. S. Murray, A. M. van den Bergen, B. O. West, *Aust. J. Chem.*, **1978**, *31*, 203.
22. C. S. Marvel, S. A. Aspey, E. A. Dudley, *J. Am. Chem. Soc.*, **1956**, *78*, 4905.
23. (a) N. Farrel, M. N. D. O. Bastos, A. A. Neves, *Polyhedron*, **1983**, *2*, 1243. (b) H. Doine, F. F. Stephens, R. D. Cannon, *Bull. Chem. Soc. Jpn.*, **1985**, *58*, 1327. (c) M. M. Taqui Khan, C. Sreelatha, S. A. Mirza, G. Ramachandraiah, S. H. R. Abdi, *Inorg. Chim. Acta*, **1988**, *154*, 103. (d) M. M. Taqui Khan, N. H. Khan, R. I. Kureshy, A. B. Boricha, Z. A. Shaikh, *Inorg. Chim. Acta*, **1990**, *170*, 213. (e) M. M. Taqui Khan, S. B. Halligudi, S. Shukla, Z. A. Shaikh, *J. Mol. Catal.*, **1990**, *57*, 301. (f) M. M. Taqui Khan, S. B. Halligudi, S. Shukla, Z. A. Shaikh, *J. Mol. Catal.*, **1990**, *57*, 307. (g) W. Odenkirk, A.

L. Rheingold, B. Bosnich, *J. Am. Chem. Soc.*, **1992**, *114*, 6392. (h) K. Inoue, N. Matsumoto, H. Okawa, *Chem. Lett.*, **1993**, 1433. (i) D. D. Agarwal, R. Rastogi, *Indian J. Chem.*, **1994**, *33B*, 787. (j) W.-H. Leung, E. Y. Y. Chan, E. K. F. Chow, I. D. Williams, S. -M. Peng, *J. Chem. Soc., Dalton Trans.*, **1996**, 1229. (k) S. Chakraborty, M. G. Walawalkar, G. K. Lahiri, *Polyhedron*, **2001**, *20*, 1851. (l) X. -G. Zhou, J. -S. Huang, P. -H. Ko, K. -K. Cheung, C. -M. Che, *J. Chem. Soc., Dalton Trans.*, **1999**, 3303. (m) D. D. Agarwal, R. Rastogi, *Indian J. Chem.*, **1995**, *34A*, 661. (n) M. M. Taqui Khan, D. Srinivas, R. I. Kureshy, N. H. Khan, *Inorg. Chem.*, **1990**, *29*, 2320. (o) M. M. Taqui Khan, S. A. Mirza, A. P. Rao, C. Sreelatha, *J. Mol. Catal.*, **1988**, *44*, 107. (p) M. M. Taqui Khan, Z. A. Shaikh, R. I. Kureshy, A. B. Boricha, *Polyhedron*, **1992**, *11*, 91. (q) M. M. Taqui Khan, S. A. Mirza, Z. A. Shaikh, C. Sreelatha, P. Paul, R. S. Shukla, D. Srinivas, A. P. Rao, S. H. R. Abdi, S. D. Bhatt, G. Ramachandraiah, *Polyhedron*, **1992**, 1821. (r) M. M. Taqui Khan, R. I. Kureshy, N. H. Khan, *Inorg. Chim. Acta*, **1991**, *181*, 119.

24. (a) V. Alteparmakian, S. D. Robinson, *Inorg. Chim. Acta*, **1986**, *116*, L37. (b) G. K. Lahiri, S. Bhattacharya, B. K. Ghosh, A. Chakravorty, *Inorg. Chem.*, **1987**, *26*, 4324. (c) A. M. El-Hendawy, A. E. -G. El -Kourashy, M. M. Shanab, *Polyhedron*, **1992**, *11*, 523. (d) S. K. Mandal, A. R. Chakravarty, *J. Chem. Soc., Dalton Trans.*, **1992**, 1627. (e) A. M. El -Hendawy, A. H. Alkubaisi, A. E. -G. El -Kourashy, M. M. Sanab, *Polyhedron*, **1993**, *12*, 2343. (f) R. I. Kureshy, N. H. Khan, *Polyhedron*, **1993**, *12*, 195. (g) S. K. Mandal, A. R. Chakravarty, *Inorg. Chem.*, **1993**, *32*, 3851. (h) R. I. Kureshy, N. H. Khan, S. H. R. Abdi, *J. Mol. Catal., A: Chem.*, **1995**, *96*, 117. (i) F. Basuli, S. -M. Peng, S. Bhattacharya, *Inorg. Chem.*, **1997**, *36*, 5645. (j) K. D. Keerthi, B. K. Santra, G. K. Lahiri, *Polyhedron*, **1998**, *17*, 1387. (k) M. G. Bhowon, H. L. K. Wah, R. Narain, *Polyhedron*, **1999**, *18*, 341. (l) R. Ramesh, N. Dharmaraj, R. Karvembu, K. Natarajan, *Indian J. Chem.*, **2000**, *39A*, 1079.

(m) B. D. Clercq, F. Verpoort, *Tetrahedron Lett.*, **2001**, *42*, 8959. (n) B. D. Clercq, F. Verpoort, *Tetrahedron Lett.*, **2001**, *43*, 4687.

25. N. H. Pilkington, R. Robson, *Aus. J. Chem.*, **1970**, *23*, 2225.
26. (a) N. Bag, S. B. Choudhury, G. K. Lahiri, A. Chakravorty, *J. Chem. Soc., Chem. Commun.*, **1990**, 1626. (b) N. Bag, S. B. Choudhury, A. Pramanik, G. K. Lahiri, A. Chakravorty, *Inorg. Chem.*, **1990**, *29*, 5013. (c) P. Ghosh, N. Bag, A. Chakravorty, *Organometallics*, **1996**, *15*, 3042. (d) B. K. Panda, S. Chattopadhyay, K. Ghosh, A. Chakravorty, *Polyhedron*, **2002**, *21*, 899. (e) S. Chattopadhyay, K. Ghosh, S. Pattanayak, A. Chakravorty, *Indian J. Chem.*, **2001**, *40A*, 1. (f) K. Ghosh, S. Chattopadhyay, S. Pattanayak, A. Chakravorty, *Organometallics*, **2001**, *20*, 1419. (g) S. Chattopadhyay, K. Ghosh, S. Pattanayak, A. Chakravorty, *J. Chem. Soc., Dalton Trans.*, **2001**, 54. (h) A. Chakravorty, *Proc. Indian Acad. Sci. (Chem. Sci.)*, **1999**, *111*, 469. (i) P. Ghosh, A. Chakravorty, *Inorg. Chem.*, **1997**, *36*, 64. (j) K. Ghosh, S. Pattanayak A. Chakravorty, *Organometallics*, **1998**, *17*, 1956.
27. A. J. Atkins, D. Black, A. J. Blacke, A. M. -Becerra, S. Parsons, L. R. Ramirez, M. Schröder, *J. Chem. Soc., Dalton Trans.*, **1996**, 35.
28. (a) H. Aneetha, C. R. K. Rao, K. M. Rao, P. S. Zacharias, X. Feng, T. C. W. Mak, B. Srinivas, M. Y. Chiang, *J. Chem. Soc., Dalton Trans.*, **1997**, 38. (b) N. Mangayarkarasi, S. R. Korupoju, H. Aneetha, P. S. Zacharias, *Indian J. Chem.*, **2001**, *40A*, 442.
29. P. Viswanathamurthi, K. Natarajan, *Indian J. Chem.*, **1999**, *38A*, 797.
30. (a) M. M. Taqui Khan, D. Srinivas, R. I. Kureshy, N. H. Khan, *Polyhedron*, **1991**, *10*, 2559. (b) M. M. Taqui Khan, N. H. Khan, R. I. Kureshy, A. B. Boricha, *Inorg. Chim. Acta*, **1990**, *174*, 175. (c) D. D. Agarwal, R. Rastogi, *Indian J. Chem.*, **1999**, *38A*, 377.
31. W. S. Sheldrick, R. Exner, *Inorg. Chim. Acta*, **1990**, *175*, 261.

32. R. C. Maurya, D. D. Mishra, N. S. Rao, N. N. Rao, *Polyhedron*, **1992**, *11*, 2837.
33. M. J. Upadhyay, P. K. Bhattacharya, P. A. Ganeshpure, S. Satish, *J. Mol. Catal.*, **1992**, *73*, 277.
34. B. Mondal, V. G. Puranik, G. K. Lahiri, *Inorg. Chem.*, **2002**, *41*, 5831.
35. (a) S. D. Perera, B. L. Shaw, *J. Chem. Soc., Chem. Commun.*, **1994**, 1201. (b) S. D. Perera, B. L. Shaw, *J. Chem. Soc., Dalton Trans.*, **1995**, 3861. (c) B. L. Shaw, U. U. Ike, S. D. Perera, M. Thornton-Pett, *Inorg. Chim. Acta*, **1998**, *279*, 95. (d) S. D. Perera, B. L. Shaw, M. Thornton-Pett, *Inorg. Chim. Acta*, **2001**, *325*, 151.
36. (a) P. Krasik, H. Alper, *Tetrahedron*, **1994**, *50*, 4347. (b) J. -X. Gao, T. Ikariya, R. Noyori, *Organometallics*, **1996**, *15*, 1087.
37. K. Nakajima, Y. Ando, H. Mano, M. Kojima, *Inorg. Chim. Acta*, **1998**, *274*, 184.
38. O. Briel, A. Fehn, K. Polborn, W. Beck, *Polyhedron*, **1998**, *18*, 225.
39. D. Bhattacharya, S. Chakraborty, P. Munsi, G. K. Lahiri, *Polyhedron*, **1999**, *18*, 2951.
40. (a) F. Basuli, M. Ruf, C. G. Pierpont, S. Bhattacharya, *Inorg. Chem.*, **1998**, *37*, 6113. (b) F. Basuli, S. -M. Peng, S. Bhattacharya, *Inorg. Chem.*, **2000**, *39*, 1120. (c) F. Basuli, S. -M. Peng, S. Bhattacharya, *Inorg. Chem.*, **2001**, *40*, 1126.
41. J. -L. Liang, X. -Q Yu, C. -M. Che, *J. Chem. Soc., Chem. Commun.*, **2002**, 124.
42. (a) A. Choudhury, B. Geetha, N. R. Sangeetha, V. Kavita, V. Susila, S. Pal, *J. Coord. Chem.*, **1999**, *48*, 87. (b) G. V. Karunakar, N. R. Sangeetha, V. Susila, S. Pal, *J. Coord. Chem.*, **2000**, *50*, 51. (c) S. N. Pal, J. Pushparaju, N. R. Sangeetha, S. Pal, *Trans. Met. Chem.*, **2000**, *25*, 528. (d) N. R. Sangeetha,

S. N. Pal, S. Pal, *Polyhedron*, **2000**, *19*, 2713. (e) S. C. Chan, L. L. Koh, P. -H. Leung, J. D. Ranford, K. Y. Sim, *Inorg. Chim. Acta*, **1995**, *236*, 101.

43. (a) G. Arcovito, M. Bonamico, A. Domenicano, A. Vaciago, *J. Chem. Soc., B*, **1969**, 733. (b) X. -X. Xu, X. -Z. You, Z. -F. Sun, X. Wang, H. -X. Liu, *Acta Crystallogr., Sect. C*, **1994**, *50*, 1169.
44. (a) J. Saroja, V. Manivannan, P. Chakraborty, S. Pal, *Inorg. Chem.*, **1995**, *34*, 3099. (b) S. Gopinathan, S. A. Pardhy, C. Gopinathan, V. G. Puranik, S. S. Tavale, T. N. G. Row, *Inorg. Chim. Acta*, **1986**, *111*, 133. (c) M. Mikuriya, M. Fukuya, *Chem. Lett.*, **1998**, 421.
45. D. W. Margerum, *Pure Appl. Chem.*, **1983**, *55*, 23.
46. (a) K. L. Kosta, B. G. Fox, M. P. Hendrich, T. J. Collins, C. E. Rickard, L. J. Wright, E. Münck, *J. Am. Chem. Soc.*, **1993**, *115*, 6746. (b) S. K. Chandra, A. Chakravorty, *Inorg. Chem.*, **1992**, *31*, 760.
47. (a) N. R. Sangeetha, S. Pal, *Bull. Chem. Soc. Jpn.*, **2000**, *73*, 357. (b) M. Mikuriya, D. Jie, Y. Kakuta, T. Tokii, *Bull. Chem. Soc. Jpn.*, **1993**, *66*, 1132.

CHAPTER 2

Diazine and Dichloro Bridged Diruthenium(III) Complexes*

2.1. Abstract

A series of dinuclear ruthenium(III) complexes with N,N' bis(salicylidene)hydrazine and its substituted derivatives (H_2salhnR; R = H, Cl, OMe, ^{t}Bu; two H stand for the dissociable protons of the phenolic-OH functionalities) having the general formula $[Ru_2^{III}Cl_2(PPh_3)_2(\mu\text{-}Cl)_2(\mu\text{-salhnR})]$ has been synthesized. Reactions of two mole equivalents of $[Ru^{II}(PPh_3)_3Cl_2]$ with one mole equivalent of ligands in $CHCl_3$ under aerobic condition produce the complexes in reasonable yields. All the complexes have been characterized by using analytical, spectroscopic and electrochemical techniques. $[Ru_2Cl_2(PPh_3)_2(\mu\text{-}Cl)_2(\mu\text{-salhnH})]$ crystallizes from $CHCl_3$-hexane with one molecule of $CHCl_3$ in the monoclinic space group $P2_1/n$ with a = 17.857(3) Å, b = 16.709(2) Å, c = 18.236(2) Å, β = 91.32(12)°, V = 5439.5(13) Å^3 and Z = 4. The metal ions are bridged by the diazine (=N-N=) moiety of salhnH^{2-} and two chloride ligands. Bond parameters are consistent with Ru_2^{III} oxidation state assignment. Both the $RuNOPCl_3$ octahedra are distorted. The electronic absorption spectra of the complexes in $CHCl_3$ solutions display one broad absorption in the range 705 – 799 nm and a shoulder in the range 351-373 nm due to ligand-to-metal charge transfer and intraligand transitions, respectively. The axial EPR spectra ($g_\perp$ ~2.41, $g_\parallel$ ~1.75) displayed by the complexes in frozen (108 K) $CHCl_3$-toluene (1:1) solutions are consistent with two weakly coupled low-spin Ru(III) centers. In the cyclic voltammograms, complexes show two reduction responses in the ranges 0.24 to -0.18 V and 0.01 to -0.30 V (vs. SCE). The first response is

*Part of this work has been published in *Inorg. Chem.*, **2001**, *40*, 4807.

assigned to the $Ru_2^{III}/Ru^{III}Ru^{II}$ and the second response is assigned to the $Ru^{III}Ru^{II}/Ru_2^{II}$ couples. Variable temperature (20-296 K) magnetic susceptibility data, for a powdered sample of $[Ru_2Cl_2(PPh_3)_2(\mu\text{-}Cl)_2(\mu\text{-salhnH})]$ collected at a constant magnetic field of 5 kG, were fitted with the χ_M vs. T expression generated from the isotropic spin Hamiltonian $H = -2JS_1 \cdot S_2$ ($S_1 = S_2 = 1/2$). The J value (-9.0(1) cm^{-1}) obtained suggests a weak antiferromagnetic interaction between the two Ru(III) centers.

2.2. Introduction

In the previous chapter, we have discussed the known ruthenium Schiff base chemistry. Very little is reported on the complexes of ruthenium with hydrazine derived Schiff bases. Only four reports are known in the literature.[1] We have chosen a potentially dinucleating tetradentate hydrazine based Schiff base system (H_2salhnR, Figure 2.1) to study the ruthenium chemistry.

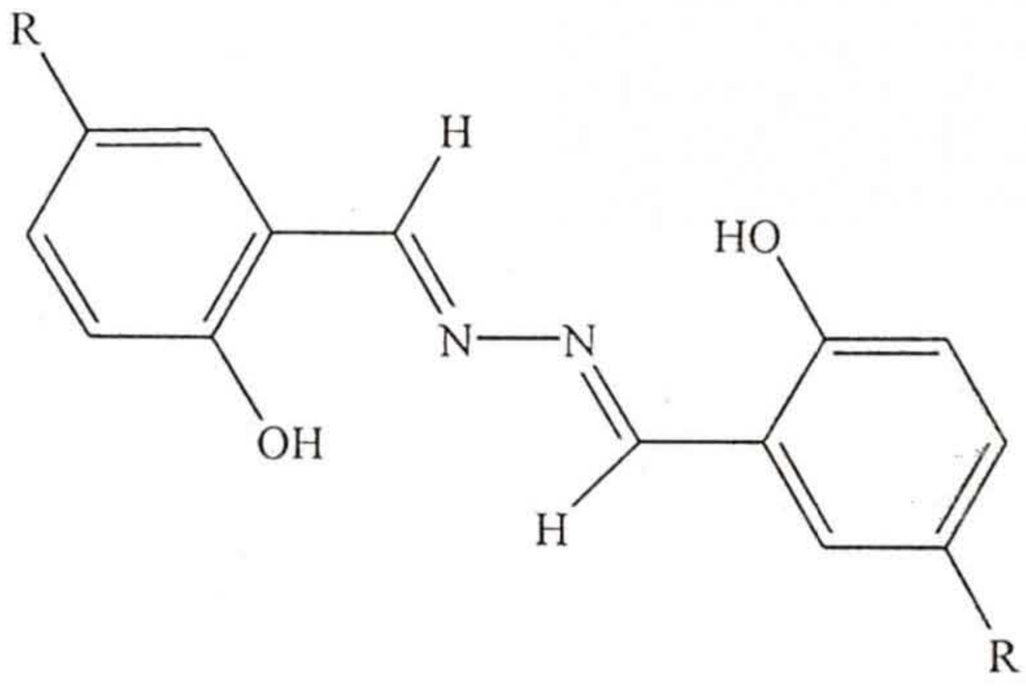

H_2salhnH (R = H)
H_2salhnCl (R = Cl)
H_2salhn^{t}Bu (R = ^{t}Bu)
H_2salhnOMe (R = OMe)

Figure 2.1

These Schiff bases are easily obtained from condensation of salicylaldehyde or substituted salicylaldehyde with hydrazine hydrate under ambient conditions. In deprotonated state, it can coordinate the metal center

through the phenolate-O, and the imine-N centers. Crystal structure[2] of H_2salhnH shows the *trans* configuration of the ligand in solid state as shown in Figure 2.1.

Diazine moiety (=N-N=) is one of the important features of this system. Free rotation along the N-N bond allows the ligands to adopt *cis*, *trans*, or in between configurations. There are only three reports on transition metal complexes with this Schiff base system. Few years ago a dinuclear iron(III) complex[3a] [$Fe_2(\mu$-salhnH$)_3$] was reported from our laboratory. A dinuclear rhodium(I)[3b] complex [$Rh_2(CO)_4(\mu$-salhnH)] and a hexanuclear cobalt (II,III)[3c] complex [$\{Co_3L$-$(CH_3COO)(CH_3O)_3\}_2(\mu$-salhnH)], ($H_3L$ is 2,6-bis-(salicylideneamino-methyl)-4-methyl-phenol) were also reported with this Schiff base. In each of these complexes, the diazine moiety of the ligand acts as the bridging unit between the metal ions. In the Fe(III) complex, the configurations of the ligands are in between *cis* and *trans*. On the other hand, salhnH^{2-} is in *trans* configuration in both Rh(I) and the Co(III) complexes. Structurally characterized dinuclear first transition metal ion complexes are reported with a similar diazine ligand system N,N'-bis(picolinylidene)hydrazine and its derivatives.[4] In all these complexes, N-N single bond acts as the bridging unit. Dinuclear complexes of this class are of interest not only with respect to their structures but also for the influence of the structure on the interaction between the two metal ions.[4]

Another important feature of this ligand system (H_2salhnR) is the phenolic-OH groups as the coordinating sites. The phenolate-O center is primarily σ basic and known to stabilize higher oxidation[5] states of metal. This σ basicity can be tuned by varying the substituent at *para* position. Thus electron withdrawing to electron donating substituents on the aromatic ring can influence the redox properties of the complexes.

Considering the above facts we have used H_2salhnH and its derivatives to prepare new ruthenium complexes and explore their structural and physical properties.

2.3. Experimental Section

2.3.1. Materials

The Schiff bases, H_2salhnR were obtained in ~95% yield by reacting 2 mole equivalents of salicylaldehyde or substituted salicylaldehyde with 1 mole equivalent of hydrazine in methanol followed by recrystallization from the same solvent. $[Ru(PPh_3)_3Cl_2]$ was prepared by following a reported procedure.[6] All other chemicals and solvents used were of analytical grade available commercially and were used without further purification.

2.3.2. Physical measurements

Elemental (C, H, N) analysis data were obtained with a Perkin-Elmer Model 240C elemental analyzer. Infrared spectra were collected by using KBr pellets on a Jasco-5300 FT-IR spectrophotometer. A Shimadzu 3101-PC UV/vis/NIR spectrophotometer was used to record the electronic spectra. Room temperature solid state magnetic susceptibilities were measured by using a Sherwood Scientific magnetic susceptibility balance. Diamagnetic corrections calculated from Pascal's constants[7] were used to obtain the molar paramagnetic susceptibilities. The variable temperature (20-296 K) magnetic susceptibility measurements were performed with a powdered sample of $[Ru_2Cl_2(PPh_3)_2(\mu\text{-}Cl)_2(\mu\text{-salhnH})]$ using the Faraday technique with a set-up comprising a George Associates Lewis coil force magnetometer, a CAHN microbalance and an Air Products cryostat. $Hg[Co(NCS)_4]$ was used as the standard. EPR spectra were recorded on a Jeol JES-FA200 spectrometer. Solution electrical conductivities were measured with a Digisun DI-909 conductivity meter. A CH-Instruments model 620A electrochemical analyzer was used for cyclic voltammetric experiments with acetonitrile solutions of the complexes containing $[(n\text{-}C_4H_9)_4N]ClO_4$ (TBAP) as supporting electrolyte. The three electrode measurements were carried out at 298 K under a dinitrogen atmosphere with a platinum disk working electrode, a platinum wire auxiliary electrode and a

saturated calomel reference electrode (SCE). The potentials reported in this work are uncorrected for junction contributions.

2.3.3. Synthesis of complexes

All the complexes were prepared by following the same procedure. Details are given for a representative case.

$[Ru_2Cl_2(PPh_3)_2(\mu\text{-}Cl)_2(\mu\text{-}salhnH)]$

Solid $[Ru(PPh_3)_3Cl_2]$ (364 mg, 0.38 mmol) was added to a light yellow solution of H_2salhnH (45 mg, 0.19 mmol) in 50 ml of $CHCl_3$. The brown mixture was stirred in air at room temperature for 24 h. The resulting dark green solution was filtered to remove any unreacted solid starting materials followed by the addition of excess hexane with stirring. The green solid precipitated was collected by filtration. This solid was redissolved in $CHCl_3$ and precipitated by slow addition of hexane with stirring. The process of dissolution in $CHCl_3$ and precipitation by hexane was repeated for two more times and the solid obtained was dried in vacuum. This procedure provided 130 mg (yield 62%) of the complex in high purity. $[Ru_2Cl_2(PPh_3)_3(\mu\text{-}Cl)_2(\mu\text{-}salhnOMe)]$ was prepared in similar yield (60%), whereas $[Ru_2Cl_2(PPh_3)_2(\mu\text{-}Cl)_2(\mu\text{-}salhnCl)]$ and $[Ru_2Cl_2(PPh_3)_2(\mu\text{-}Cl)_2(\mu\text{-}salhn^tBu)]$ were prepared in low yields (~20%).

Selected infrared bands[8] (cm^{-1}):

$[Ru_2Cl_2(PPh_3)_2(\mu\text{-}Cl)_2(\mu\text{-}salhnH)]$: 1595(s), 1533(m), 1481(w), 1433(s), 1279(m), 1188(m), 1092(s), 978(m), 905(w), 745(s), 694(s), 525(s), 451(m).

$[Ru_2Cl_2(PPh_3)_2(\mu\text{-}Cl)_2(\mu\text{-}salhnOME)]$: 1585(m), 1521(m), 1481(m), 1435(s), 1269(m), 1159(w), 744(s), 692(s), 524(s).

$[Ru_2Cl_2(PPh_3)_2(\mu\text{-}Cl)_2(\mu\text{-}salhn^tBu)]$: 1570(m), 1522(m), 1481(m), 1433(s), 1255(m), 1188(m), 1091(s), 835(m), 744(s), 692(s), 522(s).

$[Ru_2Cl_2(PPh_3)_2(\mu\text{-}Cl)_2(\mu\text{-}salhnCl)]$: 1572(m), 1518(m), 1481(m), 1433(s), 1280(m), 1170(m), 1091(s), 823(m), 742(s), 692(s), 524(s).

2.3.4. Single crystal X-ray structure determination

Single crystals of $[Ru_2Cl_2(PPh_3)_2(\mu\text{-}Cl)_2(\mu\text{-}salhnH)]$ were grown by slow diffusion of a $CHCl_3$ solution of the complex into an overlying layer of hexane. A crystal of dimension 0.38 x 0.36 x 0.25 mm was mounted at the end of a glass fibre and covered with a thin layer of epoxy. The data were collected on an Enraf-Nonius Mach-3 single crystal diffractometer using graphite monochromated Mo $K\alpha$ radiation (λ = 0.71073 Å) by ω-scan method at 298 K. Unit cell parameters were determined by least-squares fit of 25 reflections having θ value in the range 9-11°. Intensities of 3 check reflections were measured after every 1.5 h during the data collection to monitor the crystal stability. No decay was observed in 99 h of exposure to X-ray. Data were corrected for Lorentz-polarization effects. The ψ-scans[9] of 4 reflections with 2θ in the range 10-27° and χ within 84-88° were used for an empirical absorption correction with the help of Datcor program.[10] The structure was solved by direct methods and refined on F^2 by full-matrix least-squares procedures. The asymmetric unit contains a molecule of $[Ru_2Cl_2(PPh_3)_2(\mu\text{-}Cl)_2(\mu\text{-}salhnH)]$ with a disordered $CHCl_3$ molecule. The carbon of $CHCl_3$ is found in two positions and three chlorine atoms are found in 6 positions in between the carbon positions. These partial occupancy atoms are refined with geometrical restraints in such a way that a 6-fold axis is passing through the two carbon positions and six chlorine sites are around this 6-fold axis. All non-hydrogen atoms having full occupancies were refined using anisotropic thermal parameters. Hydrogen atoms were included in the structure factor calculation at idealized positions, but not refined. The calculations were performed using Xtal3.4 software[11] for data reduction, and SHELX-97 programs[12] for structure solution and refinement. The ORTEX6a and Platon packages were used for molecular graphics.[13] Significant crystal data are listed in Table 2.1 and final atomic coordinates and equivalent isotropic thermal parameters are given in Table 2.2.

Table 2.1. Crystal and structure refinement data for $[Ru_2Cl_2(PPh_3)_2(\mu\text{-}Cl)_2(\mu\text{-}salhnH)]\cdot CHCl_3$

Chemical formula	$C_{51}H_{41}Cl_7N_2O_2P_2Ru_2$
Formula weight	1226.09
Space group	Monoclinic, $P2_1/n$
a, Å	17.857(3)
b, Å	16.709(2)
c, Å	18.236(2)
β, deg.	91.32(12)
V, Å^3	5439.5(13)
Z	4
ρ_{calcd}, g cm^{-3}	1.497
μ mm^{-1}	0.997
Reflections collected/unique	8929/8455
Reflections $I > 2\sigma(I)$/parameters	4654/591
R1[a], wR2[b] $[(I > 2\sigma(I)]$	0.0762, 0.1922
R1, wR2 (all data)	0.1546, 0.2333
GOF[c] on F^2	1.067
$\Delta\rho_{max/min}$ e Å^{-3}	1.279, -0.917

[a] $R1 = \sum||F_o| - |F_c||/\sum|F_o|$. [b] $wR2 = \{\sum[(F_o^2 - F_c^2)^2]/\sum[w(F_o^2)^2]\}^{1/2}$.
[c] $GOF = \{\sum[w(F_o^2 - F_c^2)^2]/(n - p)\}^{1/2}$ where n is the number of reflections and p is the number of parameters refined; $w = 1/[\sigma^2(F_o^2) + (aP)^2 + bP]$ where $a = 0.1202$ and $b = 0$.

Table 2.2. Atomic coordinates (x 10^4) and equivalent isotropic displacement parameters[a] (Å^2 x 10^3) for $[Ru_2Cl_4(PPh_3)_2(salhnH)]\cdot CHCl_3$

Atom	x	y	z	U(eq)
Ru(1)	4293(1)	9740(1)	1902(1)	40(1)
Ru(2)	2521(1)	9994(1)	1315(1)	39(1)
Cl(1)	3437(2)	10869(2)	1874(2)	49(1)
Cl(2)	3162(2)	9035(2)	2091(2)	48(1)
Cl(3)	5287(2)	10565(2)	1564(2)	60(1)
Cl(4)	1836(2)	8990(2)	731(2)	53(1)
P(1)	4601(2)	9821(2)	3174(2)	43(1)
P(2)	1532(2)	10193(2)	2153(2)	48(1)
O(1)	4922(5)	8783(5)	1912(4)	54(2)
O(2)	2048(5)	10835(4)	707(4)	50(2)
N(1)	4024(5)	9523(6)	805(5)	44(2)
N(2)	3356(5)	9881(5)	546(5)	40(2)
C(1)	5234(8)	8443(8)	1353(8)	61(4)
C(2)	5840(9)	7942(10)	1481(8)	86(5)
C(3)	6189(12)	7538(13)	932(10)	136(9)
C(4)	5946(12)	7642(14)	189(9)	142(10)
C(5)	5328(9)	8096(11)	48(8)	95(6)
C(6)	4998(8)	8550(9)	603(7)	64(4)
C(7)	4345(7)	9015(8)	395(6)	53(3)
C(8)	3338(7)	10190(7)	-95(7)	52(3)
C(9)	2691(8)	10596(8)	-415(7)	63(4)
C(10)	2677(11)	10738(11)	-1165(8)	100(6)
C(11)	2097(12)	11113(13)	-1516(9)	123(8)
C(12)	1505(11)	11370(11)	-1121(8)	111(7)
C(13)	1527(8)	11287(7)	-389(7)	66(4)
C(14)	2114(7)	10894(7)	-8(6)	47(3)
C(15)	5500(7)	9366(8)	3446(7)	52(3)
C(16)	6104(9)	9497(12)	3012(8)	100(6)
C(17)	6800(10)	9213(15)	3256(10)	128(9)
C(18)	6869(11)	8787(12)	3900(11)	111(8)
C(19)	6264(11)	8673(10)	4325(10)	84(5)
C(20)	5590(8)	8949(8)	4074(7)	61(4)
C(21)	4678(7)	10809(7)	3586(6)	47(3)
C(22)	5330(8)	11067(8)	3925(8)	67(4)
C(23)	5352(9)	11835(10)	4244(9)	82(5)

C(24)	4782(9)	12354(8)	4165(7)	66(4)
C(25)	4128(8)	12116(8)	3818(7)	64(4)
C(26)	4084(8)	11351(8)	3530(7)	63(4)
C(27)	3948(7)	9266(7)	3742(7)	44(3)
C(28)	3535(7)	9698(9)	4269(7)	60(4)
C(29)	3044(9)	9163(12)	4668(9)	89(5)
C(30)	2959(9)	8353(12)	4524(9)	85(6)
C(31)	3397(9)	7994(9)	3989(8)	70(4)
C(32)	3867(8)	8458(8)	3607(7)	59(4)
C(33)	1765(7)	10797(8)	2957(6)	49(3)
C(34)	2048(8)	11565(8)	2828(8)	61(4)
C(35)	2210(10)	12078(9)	3400(9)	86(5)
C(36)	2089(11)	11830(11)	4085(11)	97(6)
C(37)	1833(13)	11104(13)	4229(10)	126(8)
C(38)	1678(10)	10572(10)	3650(8)	92(5)
C(39)	1129(7)	9276(8)	2516(6)	51(3)
C(40)	1567(9)	8749(9)	2926(8)	70(4)
C(41)	1294(10)	8019(9)	3194(9)	78(5)
C(42)	585(11)	7837(10)	3038(8)	85(5)
C(43)	135(12)	8327(12)	2663(12)	130(9)
C(44)	405(10)	9056(10)	2348(10)	96(6)
C(45)	723(7)	10693(8)	1739(7)	53(3)
C(46)	399(8)	11365(9)	2041(8)	76(5)
C(47)	-238(10)	11711(11)	1691(11)	106(7)
C(48)	-520(9)	11418(11)	1060(9)	87(5)
C(49)	-211(9)	10784(11)	788(9)	83(5)
C(50)	418(8)	10441(9)	1083(7)	71(4
C(51A)	-2531(11)	12309(12)	1727(12)	510(17)
C(51B)	-3228(12)	11460(12)	1823(12)	320(3)
Cl(5)	-2646(7)	11532(7)	1013(6)	192(4)
Cl(5A)	-2234(15)	11278(17)	1780(2)	270(2)
Cl(6)	-2444(14)	11598(16)	2469(13)	325(14)
Cl(6A)	-3109(13)	12167(14)	2537(10)	281(11)
Cl(7)	-3528(9)	12521(11)	1716(12)	214(7)
Cl(7A)	-3315(17)	12185(19)	1093(15)	580(3)

[a] Equivalent isotropic U defined as one third of the trace of the orthogonalized U(ij) tensor.

2.4. Results and Discussion

2.4.1. Synthesis and some properties

The complexes were synthesized by reacting one mole equivalent of H_2salhnR (R = H, Cl, OMe, ^{t}Bu) with two mole equivalents of $[Ru(PPh_3)_3Cl_2]$ in $CHCl_3$ in air. The elemental analysis data (Table 2.3) are satisfactory with the molecular formula, $[Ru_2Cl_4(PPh_3)_2$(salhnR)]. In solution, all the complexes are electrically non-conducting. The room temperature magnetic moments (2.23 - 2.79 μ_B) suggest two unpaired electrons and hence the +3 oxidation state and low-spin nature of both metal ions. During the formation of the complexes aerial oxygen is the most likely oxidizing agent in the oxidation of the metal ions. The low reduction potentials (*vide infra*) observed for the complexes are consistent with such oxidation process.

Table 2.3. Elemental analysis data[a]

Complex	%C	%H	%N
$[Ru_2Cl_2(PPh_3)_2(\mu\text{-}Cl)_2(\mu\text{-salhnOMe})]$	52.15(53.53)	3.68(3.80)	2.15(2.40)
$[Ru_2Cl_2(PPh_3)_2(\mu\text{-}Cl)_2(\mu\text{-salhn}^t\text{Bu})]$	56.71(57.15)	4.37(4.63)	2.11(2.30)
$[Ru_2Cl_2(PPh_3)_2(\mu\text{-}Cl)_2(\mu\text{-salhnH})]$	53.84(54.26)	3.31(3.64)	2.31(2.53)
$[Ru_2Cl_2(PPh_3)_2(\mu\text{-}Cl)_2(\mu\text{-salhnCl})]$	50.68(51.08)	3.04(3.26)	2.14(2.38)

[a] Calculated values are in parentheses

2.4.2. Infrared spectral properties

The infrared spectra of the complexes were collected in the range of 4000-400 cm^{-1}. A representative spectrum is depicted in Figure 2.2. As expected the free Schiff base phenolic-OH stretching[14] (~3600 cm^{-1}) is not observed in the

infrared spectra of the complexes. The C=N stretching[3a,15] is observed in the range 1570-1595 cm^{-1}, which is substantially lower than that displayed by H_2salhnR at ~1622 cm^{-1}. The strong bands in the region 1433-1527 cm^{-1} are assigned to the C=C stretching vibrations of the aromatic rings.[16] A weak peak observed just above 3000 cm^{-1} for each complex is likely to be due to the aromatic C–H bonds.[16]

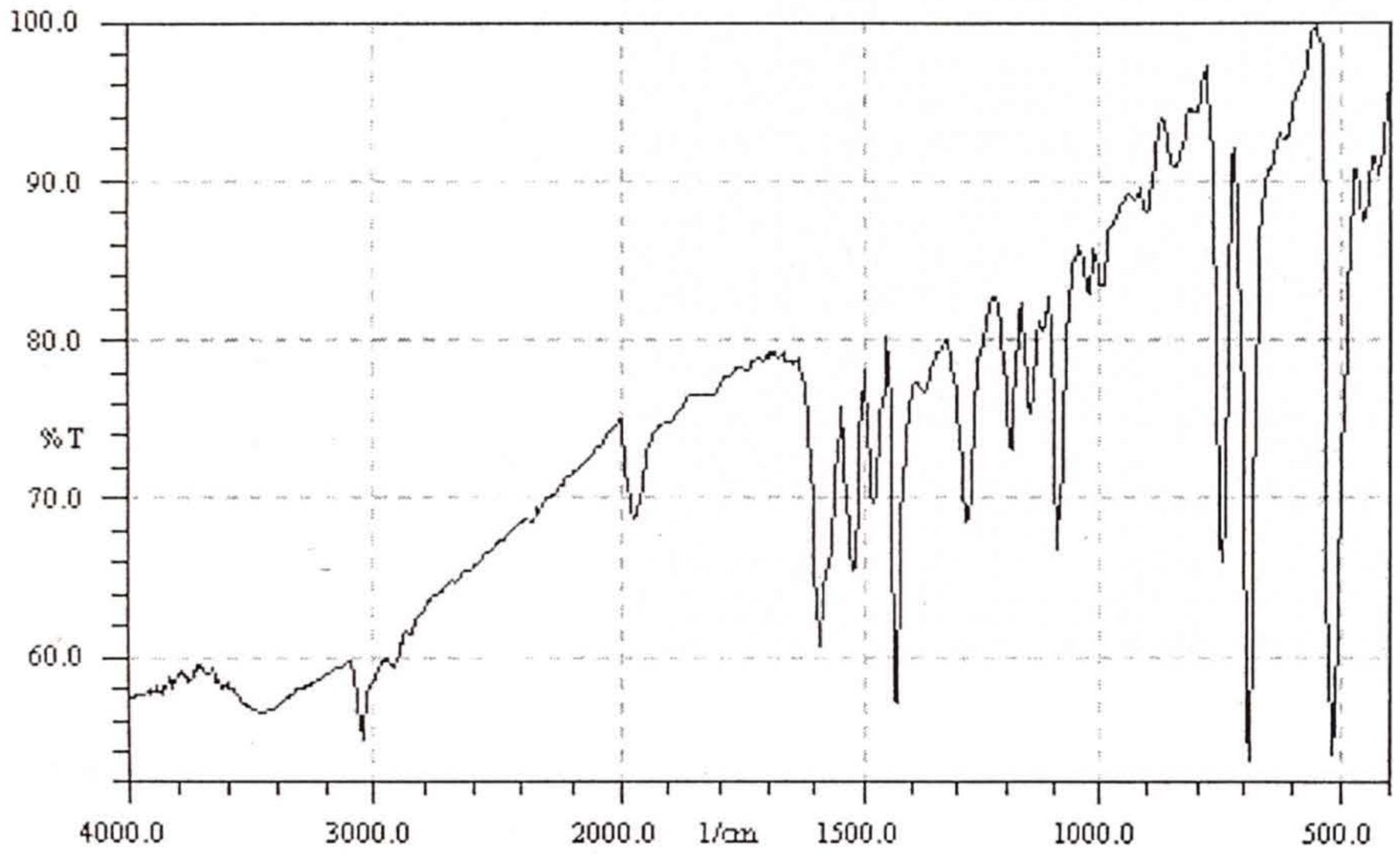

Figure 2.2. Infrared spectrum of $[Ru_2Cl_2(PPh_3)_2(\mu\text{-}Cl)_2(\mu\text{-salhnH})]$ in KBr disk.

2.4.3. Electronic spectral properties

The electronic spectral profiles of the complexes in $CHCl_3$ are very similar (Table 2.4). All the complexes display two absorptions in the ranges 705 - 799 nm and 351 – 373 nm. A representative spectrum is shown in Figure 2.3. For each complex the absorption in the visible region is broad and the origin of this

absorption is most probably ligand-to-metal charge transfer transition. The absorption in the ultraviolet region appears as a shoulder. This high energy absorption is assigned to the intraligand transition. Red shift of ligand-to-metal charge transfer band positions with the increasing electron releasing nature of the ligand substituent for some Fe, Cu, Mn, and Ni complexes has been reported before.[17] In the present series of complexes the ligand-to-metal charge transfer band position shifts to lower energy as the R is changing from Cl to ^{t}Bu to OMe (Table 2.4). However, the complex of salhnH^{2-} does not follow this trend. At present we do not have any suitable explanation for this anomalous behavior of this complex with the unsubstituted ligand.

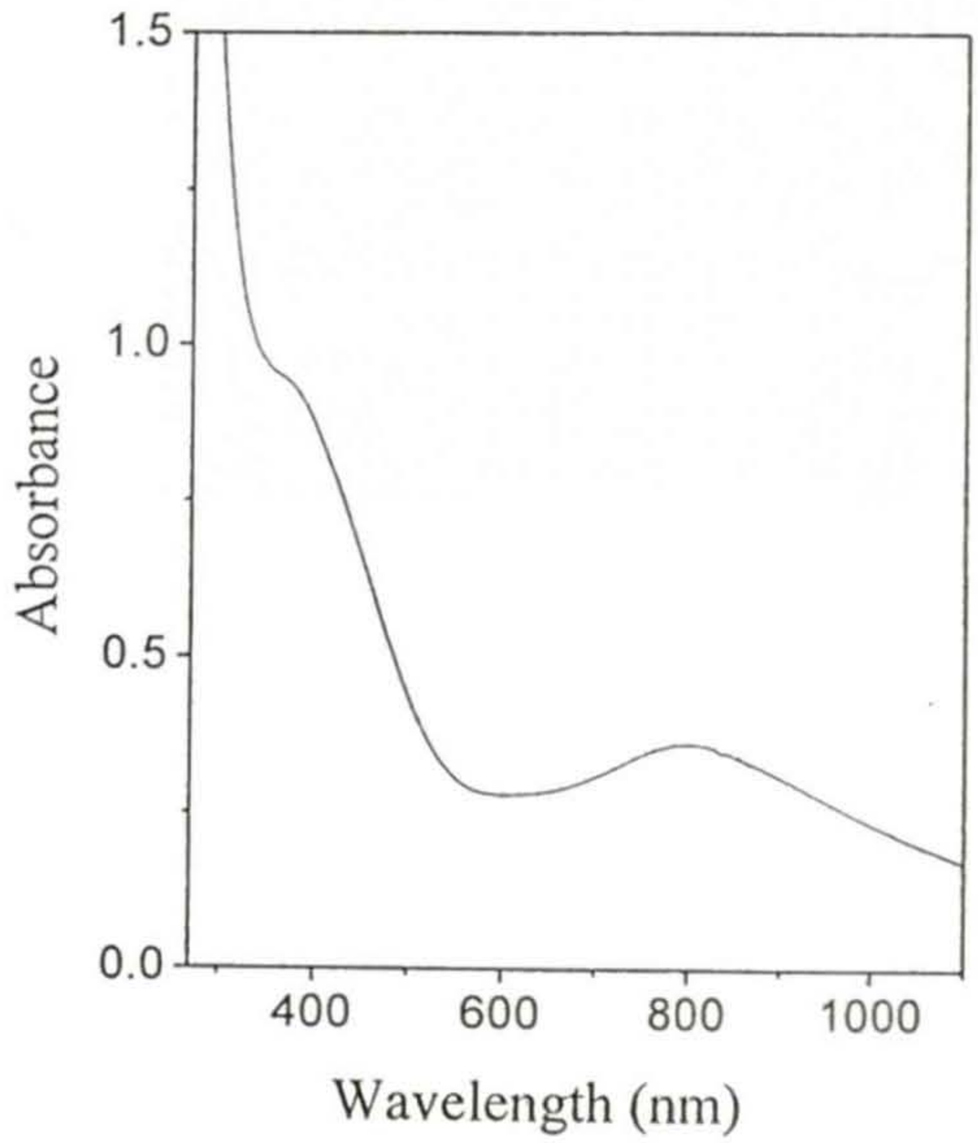

Figure 2.3. Electronic spectrum of $[Ru_2Cl_2(PPh_3)_2(\mu\text{-}Cl)_2(\mu\text{-}salhnOMe)]$ in chloroform.

Table 2.4. Electronic spectral data in chloroform solution

Complex	λ_{max} (nm) (ε ($M^{-1}cm^{-1}$))
$[Ru_2Cl_2(PPh_3)_2(\mu\text{-}Cl)_2(\mu\text{-}salhnOMe)]$	799 (4600), 373^{sh} (11900)
$[Ru_2Cl_2(PPh_3)_2(\mu\text{-}Cl)_2(\mu\text{-}salhn^tBu)]$	776 (3780), 360^{sh} (9900)
$[Ru_2Cl_2(PPh_3)_2(\mu\text{-}Cl)_2(\mu\text{-}salhnH)]$	705 (3550), 351^{sh} (12404)
$[Ru_2Cl_2(PPh_3)_2(\mu\text{-}Cl)_2(\mu\text{-}salhnCl)]$	748 (3430), 362^{sh} (10270)

sh = Shoulder

2.4.4. EPR spectral properties

The EPR spectra of the complexes in frozen (108 K) $CHCl_3$-$C_6H_5CH_3$ (1:1) solutions showed the axial pattern, which is very common for low-spin Ru(III) complexes.[18] In addition to $g_\perp$ and $g_\parallel$ signals, some weak resonances were observed in each spectrum most likely due to the hyperfine interaction with the ^{101}Ru and ^{99}Ru nuclei. g values are collected in Table 2.5. A representative spectrum is shown in Figure 2.4. The room temperature magnetic moments of

Table 2.5. EPR g values[a] and magnetic moments[b]

Complex	$g_\perp$	$g_\parallel$	μ_{eff}/μ_B
$[Ru_2Cl_2(PPh_3)_2(\mu\text{-}Cl)_2(\mu\text{-}salhnOMe)]$	2.40	1.75	2.79
$[Ru_2Cl_2(PPh_3)_2(\mu\text{-}Cl)_2(\mu\text{-}salhn^tBu)]$	2.41	1.75	2.23
$[Ru_2Cl_2(PPh_3)_2(\mu\text{-}Cl)_2(\mu\text{-}salhnH)]$	2.41	1.75	2.45
$[Ru_2Cl_2(PPh_3)_2(\mu\text{-}Cl)_2(\mu\text{-}salhnCl]$	2.42	1.74	2.45

[a] In chloroform and toluene (1:1); [b] At room temperature(298 K) in powder phase.

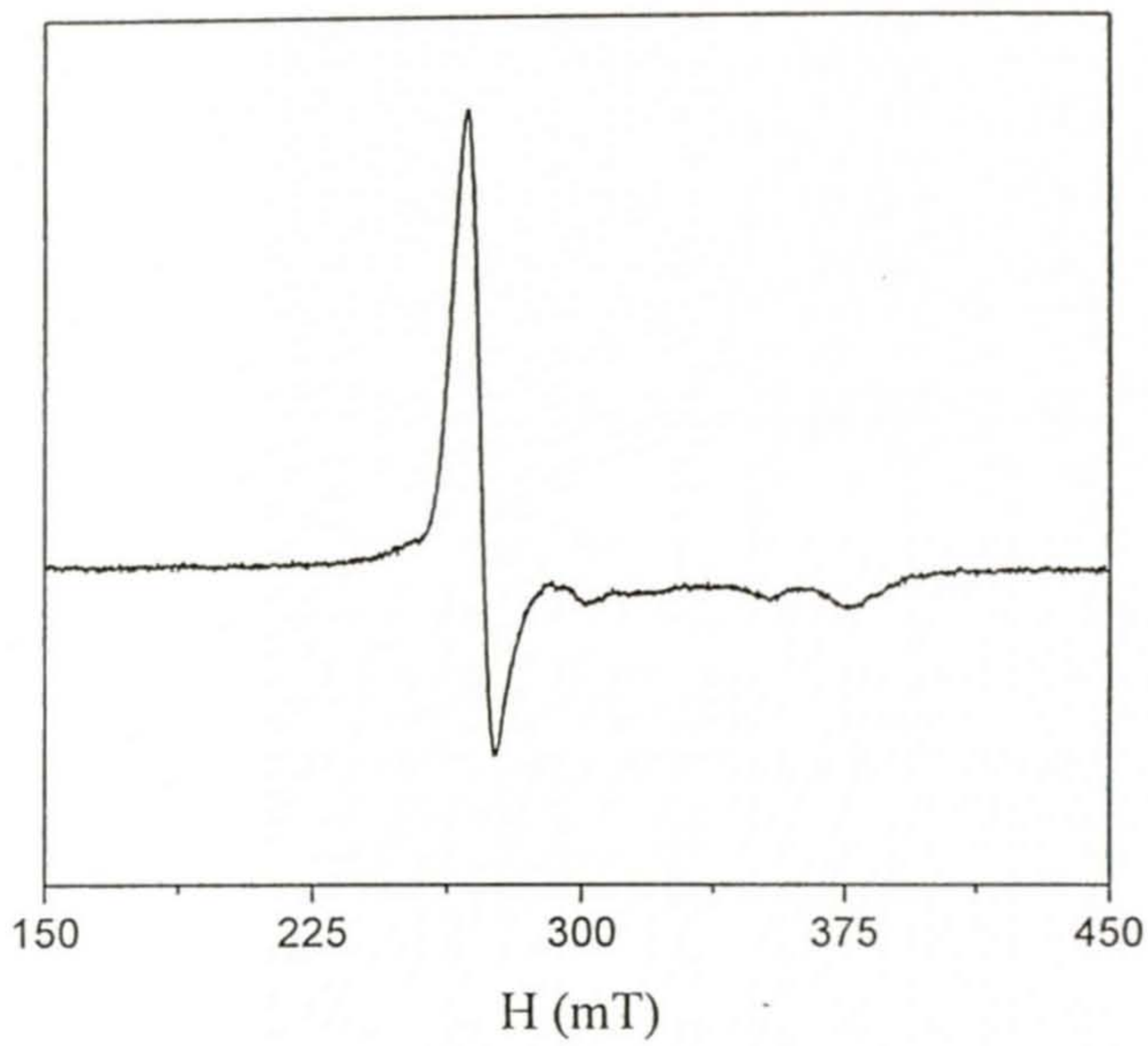

Figure 2.4. X-band EPR spectrum of $[Ru_2Cl_2(PPh_3)_2(\mu\text{-}Cl)_2(\mu\text{-}salhn^tBu)]$ in frozen $CHCl_3$ - toluene (1:1) solution.

these complexes are in the range 2.45 - 2.79 μ_B. These values suggest that at this temperature there is practically no spin coupling between the two low spin Ru(III) centers in any of the four complexes. Variable temperature magnetic susceptibility measurements for $[Ru_2Cl_2(PPh_3)_2(\mu\text{-}Cl)_2(\mu\text{-}salhnH)]$ show a very weak antiferromagnetic spin-coupling (*vide infra*) between the two metal centers. The magnetic moment of this complex at 108K is 2.32 μ_B (Figure 2.6). This corresponds to 1.64 μ_B/Ru center, which is slightly lower than the spin-only moment for one unpaired electron. A similar situation is expected for the other three complexes. Thus the axial spectra observed for these complexes are consistent for dinuclear species containing two weakly coupled low-spin Ru(III) centers.

2.4.5. Redox properties

Electron transfer properties of all the complexes have been studied by cyclic voltammetry in acetonitrile solutions. The complexes display two reduction responses (Table 2.6). The current heights observed for all the responses are comparable with known one electron redox processes under identical conditions.[19] Considering the dinuclear structure of the molecules, the weak antiferromagnetic spin-coupling and reasonably well separated two reduction responses,[20] we assign the first reduction to Ru(III)Ru(III) → Ru(III)Ru(II) process and the second reduction to Ru(III)Ru(II) → Ru(II)Ru(II) process. A representative cyclic voltammogram is shown in Figure 2.5.

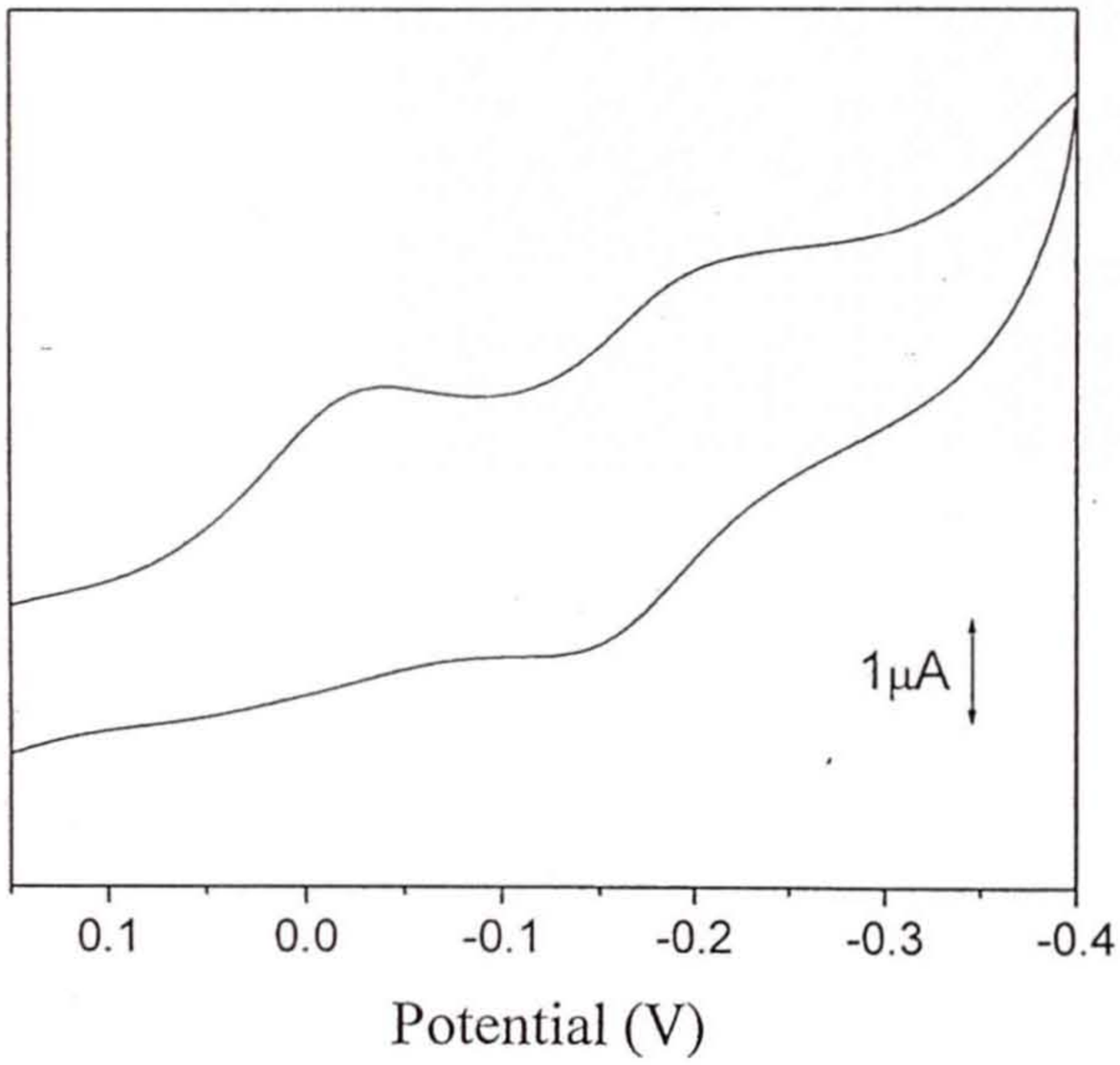

Figure 2.5. Cyclic voltammogram of $[Ru_2Cl_2(PPh_3)_2(\mu\text{-}Cl)_2(\mu\text{-}salhnH)]$ (scan rate 50 mVs^{-1}) in acetonitrile (0.1M TBAP) at a platinum electrode (298 K).

Table 2.6. Cyclic voltammetric data

Complex	$Ru_2^{III}/Ru^{III}Ru^{II}$	$Ru^{III}Ru^{II}/Ru_2^{II}$
$[Ru_2Cl_2(PPh_3)_2(\mu\text{-}Cl)_2(\mu\text{-}salhnOMe)]$	-0.04[a]	-0.30[a]
$[Ru_2Cl_2(PPh_3)_2(\mu\text{-}Cl)_2(\mu\text{-}salhn^tBu)]$	-0.05[a]	-0.30[a]
$[Ru_2Cl_2(PPh_3)_2(\mu\text{-}Cl)_2(\mu\text{-}salhnH)]$	-0.18[b] (80)[c]	-0.03[a]
$[Ru_2Cl_2(PPh_3)_2(\mu\text{-}Cl)_2(\mu\text{-}salhnCl)]$	0.24[b] (80)[c]	0.01[b] (120)[c]

[a] E_{pc} values; [b] $E_{1/2}$ values, [c] ΔE_p values, E_{pa} = anodic peak potential, E_{pc} = cathodic peak potential, $E_{1/2} = (E_{pa} + E_{pc})/2$, $\Delta E_p = E_{pa} - E_{pc}$.

2.4.6. Magnetic susceptibility

Magnetic susceptibility measurements with a powdered sample of $[Ru_2Cl_2(PPh_3)_2(\mu\text{-}Cl)_2(\mu\text{-}salhnH)]$ were conducted in the temperature range 20-296 K at a constant magnetic field of 5 kG. The effective magnetic moment (2.45 μ_B) at 296 K is essentially the spin-only moment for a dimer containing two metal ions having S = 1/2 spin states. The moment gradually decreases to 1.87 μ_B at 20 K (Figure 2.6) indicating an antiferromagnetic interaction between the two Ru(III) centers. The data were fitted using an expression[21] for χ_M vs. T derived from the isotropic spin exchange Hamiltonian $H = -2JS_1 \cdot S_2$, where $S_1 = S_2 = 1/2$. The best least-squares fit was obtained with J = -9.0(1) cm^{-1}, g = 1.915(1), p = 1.33%, and TIP = 2.31 x 10^{-4} emu/mol, where J is the antiferromagnetic coupling constant, p is the mononuclear low-spin Ru(III) impurity, and TIP is the temperature independent paramagnetism.[22] Dicopper(II) complexes containing the =N-N= bridge are known to exhibit very weak to strong intramolecular antiferromagnetic spin-coupling.[4a-c,e] In these complexes, the extent of interaction is determined mainly by the twist along the N-N single bond.[4b,c,e] Dinuclear

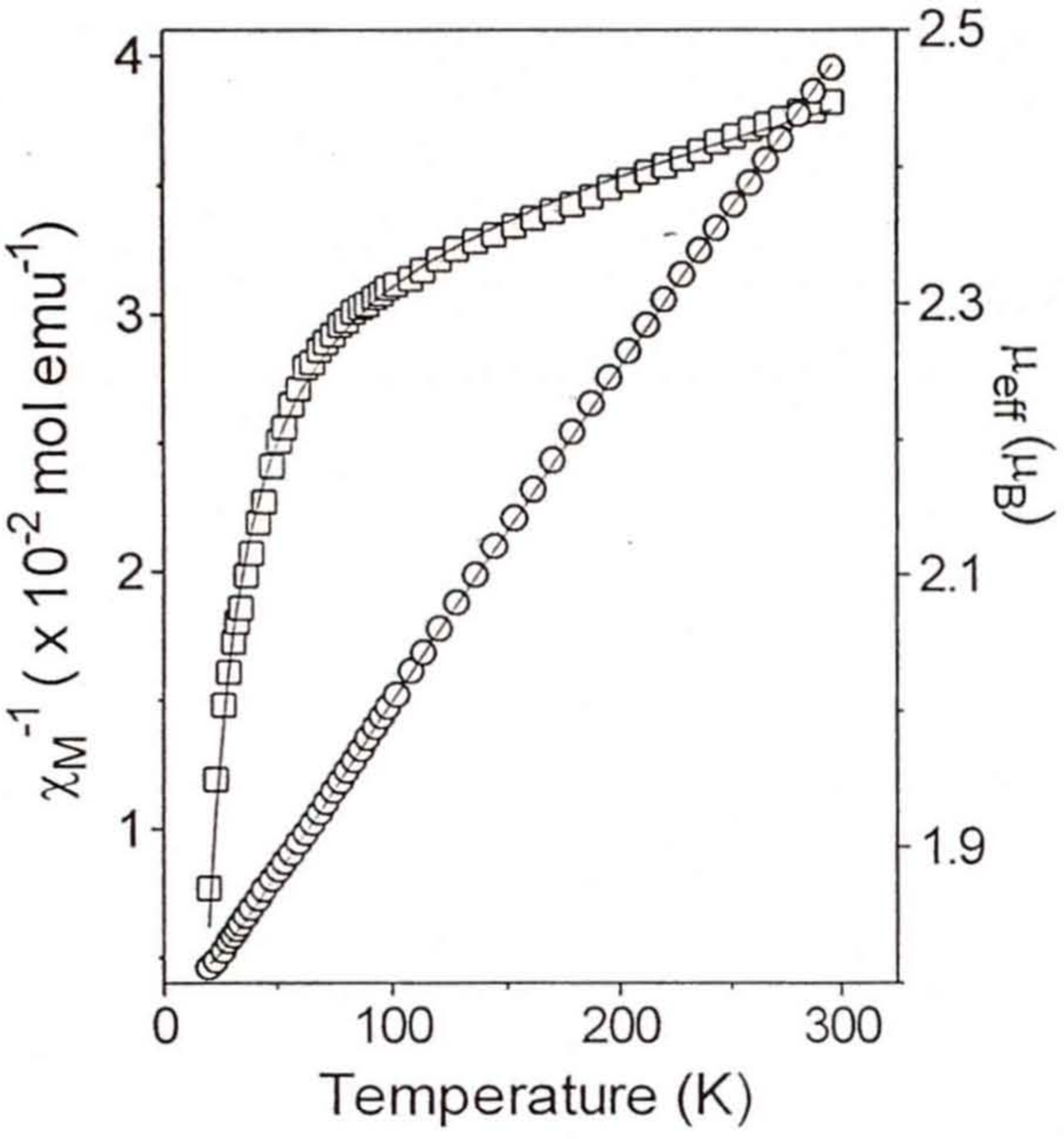

Figure 2.6. Inverse molar magnetic susceptibility (O) and effective magnetic moment (□) of $[Ru_2Cl_2(PPh_3)_2(\mu\text{-}Cl)_2(\mu\text{-salhnH})]$ as a function of temperature. The solid lines were generated from the best least-squares fit parameters given in the text.

complexes of other 3d metal ions having the same linkage between the metal centers[4d,2a,23] display no coupling or very weak intramolecular spin-coupling as observed in the present complex. In addition to the diazine bridge there are two chloride bridges between the Ru(III) centers in the present complex. The folding of the $Ru_2(\mu\text{-}Cl)_2$ core[24] along the Cl, Cl line (*vide infra*) and the nearly orthogonal Ru-Cl-Ru bridge angles[25] (87.62(10) and 88.82(11)°) are most likely not conducive for an effective antiferromagnetic super exchange interaction *via* the chloride bridges. Thus a small *J* value (-9.0(1) cm^{-1}) is observed.

2.4.7. Structure of $[Ru_2Cl_2(PPh_3)_2(\mu\text{-}Cl)_2(\mu\text{-}salhnH)]$

The molecular structure of $[Ru_2Cl_2(PPh_3)_2(\mu\text{-}Cl)_2(\mu\text{-}salhnH)]$ is shown in Figure 2.7. Bond parameters associated with the metal ions are listed in Table 2.7. The metal ions are in distorted octahedral $NOCl_3P$ coordination spheres. The pair of salicylaldimine moieties in $salhnH^{2-}$ binds the Ru centers through the phenolate-O and the imine-N atoms to form two six-membered chelate rings and provide the N-N bridge between them. In addition, the metal ions are bridged by

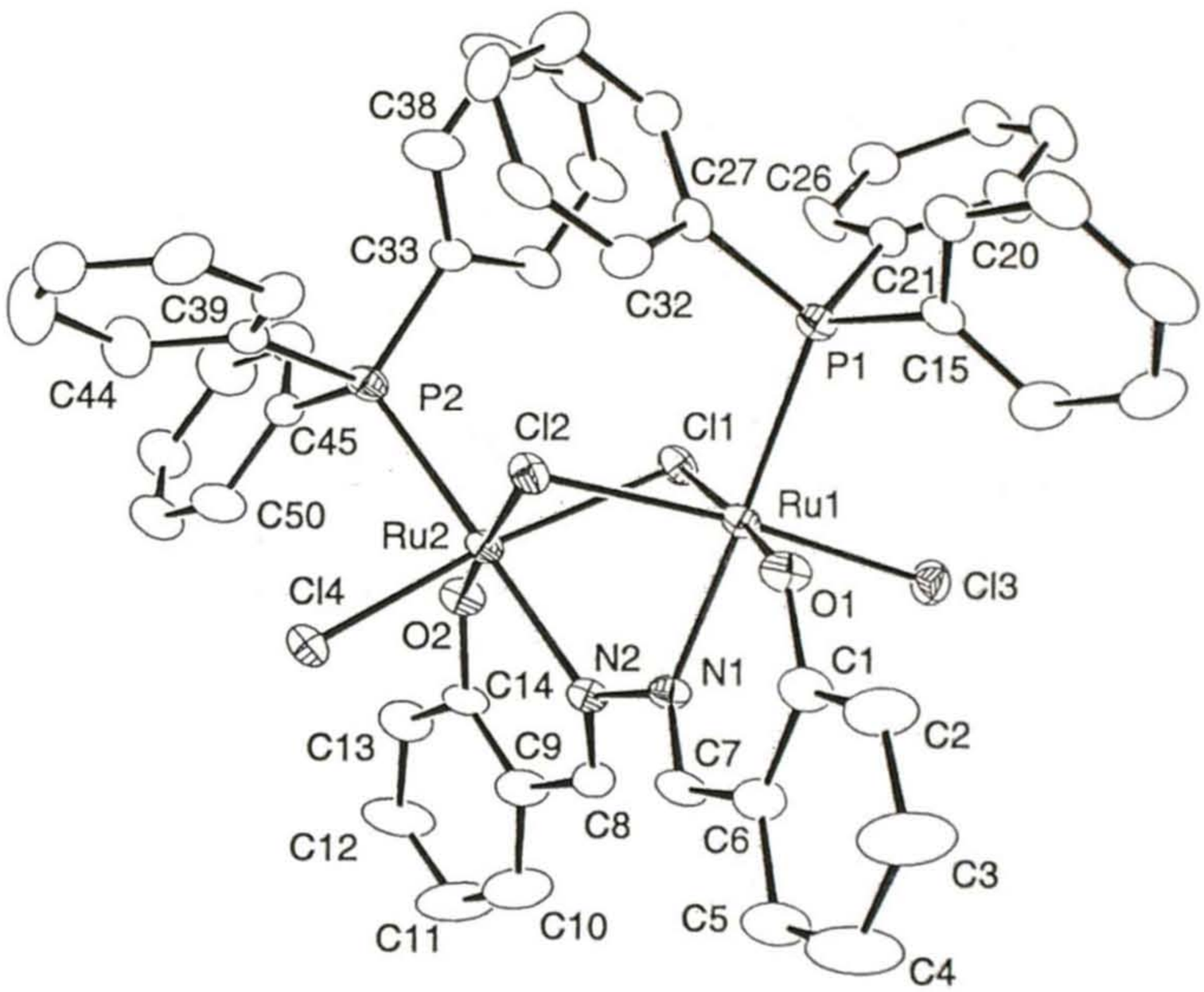

Figure 2.7. Structure of $[Ru_2Cl_2(PPh_3)_2(\mu\text{-}Cl)_2(\mu\text{-}salhnH)]$ with the atom-labeling scheme. All atoms are represented by their 20% probability thermal ellipsoids. Hydrogen atoms are omitted and selected carbon atoms are labeled for clarity.

two of the four chloride ligands. As expected the $Ru_2(\mu\text{-}Cl)_2$ unit is not planar due to the presence of the third diazine bridge. The angle between the planes containing Ru1, Cl1, Cl2 and Ru2, Cl1, Cl2 is 47.0(1)°. The Ru---Ru distance is 3.344(2) Å. The terminal chlorine atoms are *trans* to the bridging chlorine atoms and the PPh_3 molecules coordinate through P atoms at the *trans* sites of the imine-N atoms. The Ru-O(phenolate) and Ru-N(imine) distances (Table 2.7) are similar to those reported for Ru(III) complexes containing the same coordinating atoms.[26,27] The Ru(III)-P distances are unexceptional.[27] The Ru-Cl(bridging) distances, not surprisingly, are longer than the Ru-Cl(terminal) distances. These distances are comparable with the distances reported for other structurally characterized diruthenium(III) complexes containing bridging and terminal

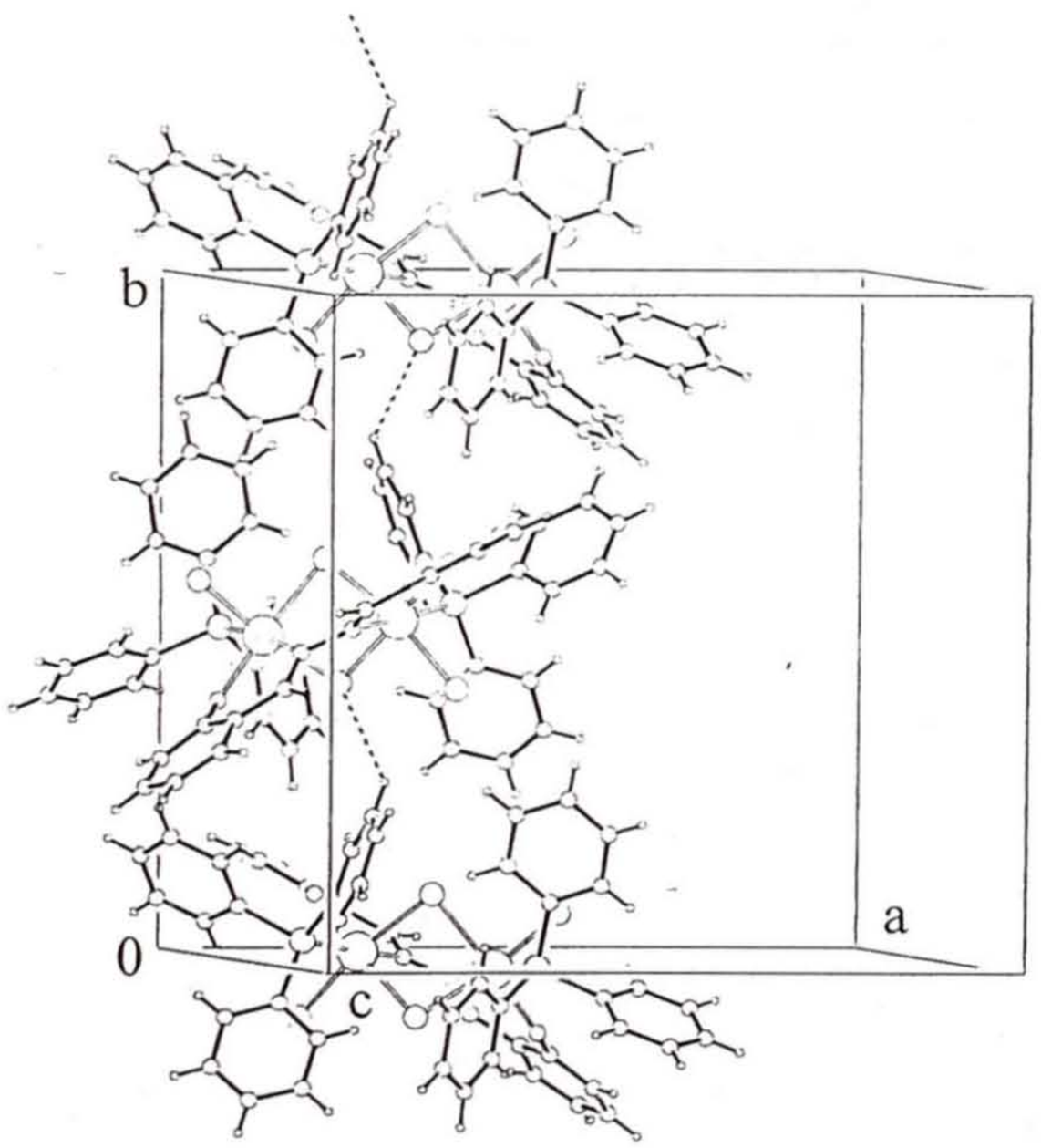

Figure 2.8. Hydrogen bonded one-dimensional chain.

chlorides.[28] Both salicylaldimine fragments are satisfactorily planar. The mean deviations are 0.05 and 0.08 Å for the first (O1, C1-C7, N1) and the second (N2, C8-C14, O2) fragments, respectively. The corresponding Ru centers, Ru1 and Ru2 are displaced from these planes by 0.45(1) and 0.57(1) Å, respectively. Thus the six-membered chelate rings are folded along the O, N line. The fold angles are 17.7(5) and 22.1(5)° for the first and the second chelate ring, respectively. Similar folding has been also observed for $[Fe_2(\mu\text{-salhn})_3]$.[3a] A weak intermolecular C-H···Cl interaction between the bridging chloride Cl2 and H35 leads to a one-dimensional chain (Figure 2.8). The distances between Cl2 and C35, and Cl2 and H35 are 3.451 and 2.715 Å, respectively. The C35-H35···Cl2 angle is 136.63°. This type of aromatic C-H···Cl interactions have been reported before.[29]

The solid state structure of the uncomplexed H_2salhnH is known.[2] The compound is in usual *trans* configuration (Figure 2.1). As mentioned before there are three structurally characterized complexes containing bridging $salhnH^{2-}$. In two of them, $[(CO)_2Rh(\mu\text{-salhnH})(CO)_2Rh]$[3b] and $[\{Co_3L(CH_3COO)(CH_3O)_3\}_2(\mu\text{-salhnH})]$,[3c] only the diazine fragment of $salhnH^{2-}$ is bridging two metal ions and the ligand is in *trans* configuration. In the third complex, $[Fe_2(\mu\text{-salhnH})_3]$,[3a] the diazine fragments of three $salhnH^{2-}$ bridge the two metal ions and all the three ligands are twisted along the N-N bond. However, the extent of twisting is different for the three ligands. The maximum is 56.8° and the minimum is 26.6°. In the present complex, the $salhnH^{2-}$ is also in twisted configuration but to a much lesser extent. The dihedral angle between the salicylaldimine moieties is 17.1(4)°. In this complex, the additional two chloride bridges and the *trans* arrangement of the terminal chlorides are most likely responsible for the near *cis* configuration of $salhnH^{2-}$.

Table 2.7. Selected bond distances (Å) and angles (deg.) for $[Ru_2Cl_2(PPh_3)_2(\mu\text{-}Cl)_2(\mu\text{-}salhnH)]\cdot CHCl_3$

Ru(1)-O(1)	1.953(8)	Ru(2)-O(2)	1.969(7)
Ru(1)-N(1)	2.078(9)	Ru(2)-N(2)	2.078(10)
Ru(1)-Cl(3)	2.341(3)	Ru(2)-Cl(4)	2.320(3)
Ru(1)-Cl(2)	2.369(3)	Ru(2)-P(2)	2.385(4)
Ru(1)-P(1)	2.377(3)	Ru(2)-Cl(1)	2.403(3)
Ru(1)-Cl(1)	2.428(3)	Ru(2)-Cl(2)	2.410(3)
O(1)-Ru(1)-N(1)	89.2(4)	O(2)-Ru(2)-N(2)	89.4(3)
O(1)-Ru(1)-Cl(3)	92.6(3)	O(2)-Ru(2)-Cl(4)	92.5(3)
N(1)-Ru(1)-Cl(3)	90.5(3)	N(2)-Ru(2)-Cl(4)	90.2(3)
O(1)-Ru(1)-Cl(2)	94.8(3)	O(2)-Ru(2)-P(2)	87.0(3)
N(1)-Ru(1)-Cl(2)	82.8(3)	N(2)-Ru(2)-P(2)	176.4(2)
Cl(3)-Ru(1)-Cl(2)	169.97(11)	Cl(4)-Ru(2)-P(2)	90.29(12)
O(1)-Ru(1)-P(1)	85.3(3)	O(2)-Ru(2)-Cl(1)	94.8(3)
N(1)-Ru(1)-P(1)	173.2(3)	N(2)-Ru(2)-Cl(1)	81.3(3)
Cl(3)-Ru(1)-P(1)	93.63(14)	Cl(4)-Ru(2)-Cl(1)	168.79(12)
Cl(2)-Ru(1)-P(1)	93.73(15)	P(2)-Ru(2)-Cl(1)	98.60(11)
O(1)-Ru(1)-Cl(1)	176.0(3)	O(2)-Ru(2)-Cl(2)	175.9(2)
N(1)-Ru(1)-Cl(1)	89.1(3)	N(2)-Ru(2)-Cl(2)	89.8(2)
Cl(3)-Ru(1)-Cl(1)	91.01(12)	Cl(4)-Ru(2)-Cl(2)	91.56(12)
Cl(2)-Ru(1)-Cl(1)	81.42(11)	P(2)-Ru(2)-Cl(2)	93.73(11)
P(1)-Ru(1)-Cl(1)	96.18(13)	Cl(1)-Ru(2)-Cl(2)	81.11(12)
Ru(2)-Cl(1)-Ru(1)	87.62(10)	Ru(1)-Cl(2)-Ru(2)	88.82(11)

2.5. Conclusion

Diazine bridged diruthenium(III) complexes of general formula $[Ru_2Cl_2(PPh_3)_2(\mu\text{-}Cl)_2(\mu\text{-salhnR})]$ with H_2salhnR have been synthesized. In these complexes, the two ruthenium centers are bridged by =N-N= moiety along with two chlorides ligands. All the complexes have been characterized by elemental analysis, different spectroscopic and electrochemical methods. Both ruthenium centers are in low spin state. *J* value obtained from variable temperature magnetic susceptibility data of $[Ru_2Cl_2(PPh_3)_2(\mu\text{-}Cl)_2(\mu\text{-salhnH})]$, suggests a very weak antiferromagnetic spin coupling between the two ruthenium centers. The molecular structure of one of the complex, $[Ru_2Cl_2(PPh_3)_2(\mu\text{-}Cl)_2(\mu\text{-salhnH})]$ has been determined by single crystal X-ray crystallography. The ligand is in near *cis* configuration in this molecule. The additional two chloride bridges and the terminal *trans* chlorides force this configuration. If only the diazine moiety acts as the bridging unit between the metal centers, a *trans* configuration of $salhnH^{2-}$ will possibly be the preferred arrangement as observed in the previously reported Rh(I) and Co(II,III) complexes. For such a molecule the remaining four coordination sites of each metal ion has to be satisfied by other non bridging ancillary ligands. In the following chapter, we have described the results obtained in our attempts to synthesize such a species using *cis*-$[Ru(bpy)_2Cl_2]$ as the starting material.

2.6. References

1. (a) S. D. Perera, B. L. Shaw, *J. Chem. Soc., Chem. Commun.*, **1994**, 1201. (b) S. D. Perera, B. L. Shaw, *J. Chem. Soc., Dalton Trans.*, **1995**, 3861. (c) B. L. Shaw, U. U. Ike, S. D. Perera, M. Thornton-Pett, *Inorg. Chim. Acta*, **1998**, *279*, 95. (d) S. D. Perera, B. L. Shaw, M. Thornton-Pett, *Inorg. Chim. Acta*, **2001**, *325*, 151.

2. (a) G. Arcovito, M. Bonamico, A. Domenicano, A. Vaciago, *J. Chem. Soc., B*, **1969**, 733. (b) X. -X. Xu, X. -Z. You, Z. -F. Sun, X. Wang, H. -X. Liu, *Acta Crystallogr., Sect. C*, **1994**, *50*, 1169.
3. (a) J. Saroja, V. Manivannan, P. Chakraborty, S. Pal, *Inorg. Chem.*, **1995**, *34*, 3099. (b) S. Gopinathan, S. A. Pardhy, C. Gopinathan, V. G. Puranik, S. S. Tavale, T. N. G. Row, *Inorg. Chim. Acta*, **1986**, *111*, 133. (c) M. Mikuriya, M. Fukuya, *Chem. Lett.*, **1998**, 421.
4. (a) C. J. O'Connor, R. J. Romananch, D. M. Robertson, E. E. Eduok, F. R. Fronczek, *Inorg. Chem.*, **1983**, *22*, 449. (b) Z. Xu, L. K. Thompson, D. O. Miller, *Inorg. Chem.*, **1997**, *36*, 3985. (c) L. K. Thompson, Z. Xu, A. E. Goeta, J. A. K. Howard, H. J. Clase, D. O. Miller, *Inorg. Chem.*, **1998**, *37*, 3217. (d) Z. Xu, L. K. Thompson, D. O. Miller, H. J. Clase, J. A. K. Howard, A. E. Goeta, *Inorg. Chem.*, **1998**, *37*, 3620. (e) Z. Xu, L. K. Thompson, C. J. Matthews, D. O. Miller, A. E. Goeta, C. Wilson, J. A. K. Howard, M. Ohba, H. Okawa, *J. Chem. Soc., Dalton Trans.*, **2000**, 69.
5. (a) N. R. Sangeetha, S. Pal, *Bull. Chem. Soc. Jpn.*, **2000**, *73*, 357. (b) M. Mikuriya, D. Jie, Y. Kakuta, T. Tokii, *Bull. Chem. Soc. Jpn.*, **1993**, *66*, 1132.
6. T. A. Stephenson, G. Wilkinson, *J. Inorg. Nucl. Chem.*, **1966**, *28*, 945.
7. W. E. Hatfield, In *Theory and Applications of Molecular Paramagnetism*: Boudreaux, E. A., Mulay, L. N., Eds.; Wiley: New York 1976, p 491.
8. w, weak; m, medium; s, strong; vs, very strong.
9. A. C. T. North, D. C. Philips, F. S. Mathews, *Acta Crystallogr., Sect. A*, **1968**, *24*, 351.
10. J. Riebenspies, *Q & D Crystallographic Program Package*; Texas A & M University: College Station, Texas, USA, 1989.
11. *Xtal3.4 User's Manual*, S. R. Hall, G. S. D. King, J. M. Stewart, Eds.; University of Western Australia: Perth, Australia, 1995.

12. G. M. Sheldrick, *SHELX-97 Structure Determination Software*; University of Göttingen: Göttingen, Germany, 1997.
13. (a) P. J. McArdle, *Appl. Crystallogr.*, **1995**, *28*, 65. (b) A. L. Spek, *Platon (Version 150401), Molecular Graphics Software*, University of Glasgow, UK 2001.
14. M. St. C. Flett, *Spectrochim. Acta*, **1957**, *10*, 21.
15. S. Choudhury, M. Kakoti, A. K. Deb, S. Goswami, *Polyhedron*, **1992**, *11*, 3183.
16. R. M. Silverstein, F. X. Webster, "*Spectrometric Identification of Organic Compounds*" (John Wiley & Sons, Inc. New York, 1998). P - 87.
17. (a) B. P. Gaber, W. Miskowski, T. G. Spiro, *J. Am. Chem. Soc.*, **1974**, *96*, 6868. (b) E. W. Ainscough, A. M. Brodie, J. E. Plowman, K. L. Brown, A. W. Addision, A. R. Gainsford, *Inorg. Chem.*, **1980**, *19*, 3655. (c) C. J. Carrano, M. W. Carrano, K. Sharma, G. Backes, J. Sanders-Loehr, *Inorg. Chem.*, **1970**, *29*, 1865. (d) C. K. Jorgenesen, *Prog. Inorg. Chem.*, **1970**, *12*, 101.
18. A. K. Mahapatra, S. Datta, S. Goswami, M. Mukherjee, A. K. Mukherjee, A. Chakravorty, *Inorg. Chem.*, **1986**, *25*, 1715.
19. S. Pal, D. Bandyopadhyay, D. Datta, A. Chakravorty, *J. Chem. Soc., Dalton Trans.*, **1985**, 159.
20. (a) J. E. Sutton, H. Taube, *Inorg. Chem.*, **1981**, *20*, 3125. (b) M. Ciampolini, L. Fabbrizzi, A. Perotti, A. Poggi, B. Seghi, F. Zanobini, *Inorg. Chem.*, **1987**, *26*, 3527.
21. C. J. O'Connor, *Prog. Inorg. Chem.*, **1982**, *29*, 203.
22. M. P. Cifuentes, M. G. Humphrey, J. E. McGrady, P. J. Smith, R. Stranger, K. S. Murray, B. Moubaraki, *J. Am. Chem. Soc.*, **1997**, *119*, 2647.
23. P. W. Ball, A. B. Blake, *J. Chem. Soc., A*, **1969**, 1415.

24. D. R. Gamelin, M. L. Kirk, T. L. Stemmler, S. Pal, W. H. Armstrong, J. E. Penner-Hahn, E. I. Solomon, *J. Am. Chem. Soc.*, **1994**, *116*, 2392.
25. J. Kanamori, *J. Phys. Chem. Solids*, **1959**, *10*, 87.
26. P. Bhattacharyya, M. L. Loza, J. Parr, A. M. Z. Slawin, *J. Chem. Soc., Dalton Trans.*, **1999**, 2917.
27. K. Nakajima, Y. Ando, H. Mano, M. Kojima, *Inorg. Chim. Acta*, **1998**, *274*, 184.
28. (a) F. A. Cotton, M. Matusz, R. C. Torralba, *Inorg. Chem.*, **1989**, *28*, 1516. (b) F. A. Cotton, R. C. Torralba, *Inorg. Chem.*, **1991**, *30*, 2196.
29. (a) A. Nangia, *CrystEngComm*, **2002**, *4*, 93. (b) C. B. Akeröy, T. A. Evans, K. R. Seddon, I. Pálinkó, *New J. Chem.*, **1999**, *23*, 145.

CHAPTER 3

Complexes of Bis(2,2'-bipyridine)ruthenium(II) with Salicylaldehyde and its Derivatives*

3.1. Abstract

Ruthenium(II) mixed-ligand complexes having the general formula $[Ru(bpy)_2(salR)]PF_6$ derived from 2,2'-bipyridine and salicylaldehyde or its 5-substituted derivatives (HsalR, H stands for the dissociable phenolic-OH proton; R = H, OMe, ^tBu, Cl, NO_2) are described. Characterization of the complexes were performed by using microanalysis, cyclic voltammetry and various spectroscopic methods such as infrared, UV-vis, one and two-dimensional ^1H NMR. Diamagnetic character of the complexes is consistent with low-spin ruthenium(II) system. In solution, each of them behaves as 1:1 electrolyte. Crystal structures of $[Ru(bpy)_2(salH)]PF_6$ and $[Ru(bpy)_2(salCl)]PF_6$ have been determined. In solid state, $salR^-$ ligand exists as the intermediate of the normal phenolate structure and a quinonoid structure. Electronic spectral profiles of all the complexes are very similar. The complexes display the Ru(III)-Ru(II) couple in the potential range 0.61-0.84 V (vs. Ag/AgCl) in acetonitrile solutions. The potential of this couple is linearly related to the Hammett constant of the substituent R. ^1H NMR spectra for all the complexes were recorded in CD_3CN and aromatic protons were assigned with the help of ^1H-^1H correlation spectroscopy (COSY).

*This work has been published in *Z. Anorg. Allg. Chem.*, **2002**, *628*, 2091.

3.2. Introduction

The ruthenium(II) complexes containing polypyridyl ligands are always interesting for their electronic and redox properties. The fine tuning of these properties by alteration of the coordination sphere around the metal center affects the photophysical and photochemical phenomena exhibited by such complexes.[1-3] In this respect, new ruthenium(II) polypyridine complexes with different types of coligands are of significant importance. A large number of mononuclear ruthenium(II) complexes containing the $\{Ru(bpy)_2\}$ (bpy = 2,2'-bipyridine) moiety with a variety of ancillary monodentate, and bidentate ligands have been reported.[1-7] Recently considerable effort has been devoted to synthesize binuclear

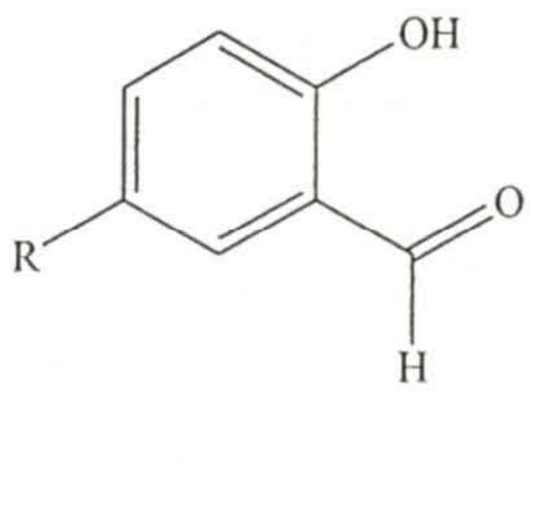

HsalH (R = H)
HsalCl (R = Cl)
HsalOMe (R = OMe)
Hsal^{t}Bu ($R = {}^t$Bu)
HsalNO_2 ($R = NO_2$)

Figure 3.1

to polynuclear ruthenium(II) polypyridine complexes using various bridging ligands. The primary goal is to obtain supramolecular multicomponent systems that can function as photomolecular devices.[8]

In the previous chapter, we have used H_2salhnR to prepare dinuclear ruthenium complexes from $Ru(PPh_3)_3Cl_2$. In these complexes, both the ruthenium atoms are in +3 oxidation state and the metal ions are bridged by the diazine moiety (=N-N=) of salhnR^{2-} as well as by two chloride ligands. In search of new binuclear ruthenium(II) complexes, we have chosen *cis*-$[Ru(bpy)_2Cl_2]\cdot 2H_2O$ as

the starting material and salhnR^{2-} as the bridging ligand that can replace the two chloride ligands and form diazine bridged diruthenium(II) species.

In our attempt to prepare such complexes using *cis*-$[Ru(bpy)_2Cl_2]\cdot 2H_2O$ and H_2salhnR in alkaline medium, we have isolated mononuclear Ru(II) species of general formula $[Ru(bpy)_2(salR)]^+$. This is because of the hydrolysis of the Schiff bases in the reaction media. In these complexes, deprotonated salicylaldehyde and substituted salicylaldehyde moieties bind the metal center through the phenolate-O and the aldehydic-O replacing two chlorides in *cis*-$Ru(bpy)_2Cl_2$. Our all efforts failed to prevent this hydrolysis of H_2salhnR and isolation of the targeted dimeric complexes. These complexes can also be synthesized in good yields directly from *cis*-$[Ru(bpy)_2Cl_2]\cdot 2H_2O$, HsalR, and NaOH (1:1:1 mole ratio) in methanolic media.

Recently there is a report on the quinonoid behavior of the bidentate O,O-donor salicylate(L^{2-}) in the complex, $[Ru(bpy)_2L]$.[6] Complexes with quinonoid ligands are of particular interest as these ligands can play important roles in deciding the physical properties of the complexes due to the possibility of redox electron delocalization between the metal ion and the ligand. The complexes we have isolated contain deprotonated salicylaldehyde, which is closely related to salicylate. Thus we have performed an elaborate investigation on this series of complexes having the general formula $[Ru(bpy)_2(salR)]PF_6$.

3.3. Experimental Section

3.3.1. Materials

cis-$[Ru(bpy)_2Cl_2]\cdot 2H_2O$ was prepared by using a reported procedure.[9] Acetonitrile used for electrochemical and spectral studies was purified and dried according to a reported method.[10] All other chemicals and solvents were of analytical grade available commercially and were used as received.

3.3.2. Physical measurements

Proton NMR spectra of the complexes in CD_3CN solutions were recorded on a Bruker 200 MHz spectrometer using $Si(CH_3)_4$ as an internal standard. All other measurements were performed as described in chapter 1.

3.3.3. Synthesis of complexes

All the five complexes $[Ru(bpy)_2(salOMe)]PF_6$ (**1**), $[Ru(bpy)_2(sal^tBu)]PF_6$ (**2**), $[Ru(bpy)_2(salH)]PF_6$ (**3**), $[Ru(bpy)_2(salCl)]PF_6$ (**4**), and $[Ru(bpy)_2(sal\text{-}NO_2)]PF_6$ (**5**) reported in this chapter were synthesized from *cis*-$[Ru(bpy)_2Cl_2]\cdot 2H_2O$ and salicylaldehyde or its 5-substituted derivatives in comparable yields by following similar procedures. Details are given for a representative case.

$[Ru(bpy)_2(salH)]PF_6$ (3)

cis-$[Ru(bpy)_2Cl_2]\cdot 2H_2O$ (221 mg, 0.425 mmol) was added to a methanol solution (30 ml) of salicylaldehyde (52 mg, 0.426 mmol) and NaOH (17 mg, 0.425 mmol). The mixture was refluxed for 12 h. The resulting brown solution was evaporated to dryness and the solid obtained was dissolved in 15 ml of water. To this water solution excess NH_4PF_6 was added and a brown solid was precipitated. This solid was collected by filtration, washed thoroughly with water and dried in vacuum over anhydrous $CaCl_2$. The purification of the complex was performed on a neutral aluminium oxide column (15 cm long). The first moving brown band was eluted with dichloromethane containing 5% acetone. This was collected and evaporated. The solid thus obtained was recrystallized from acetone-diethylether (2:1). The yield was 180 mg (62%).

Selected IR bands[11] (cm^{-1}): 1605(s), 1580(s), 1508(s), 1441(s), 1341(w), 1263(m), 1240(w), 1182(m), 1148(m), 1130(w), 1020(s), 901(m), 839(vs), 760(s), 727(s), 658(m), 556(s).

Selected IR bands[11] (cm^{-1}) for the other four complexes are as follows:
$[Ru(bpy)_2(salOMe)]PF_6$ (1): 1600(m), 1578(s), 1508(s), 1458(s), 1321(m), 1265(w), 1242(m), 1209(m), 1146(s), 1022(s), 839(vs), 762(s), 727(s), 658(w), 556(s).
$[Ru(bpy)_2(sal^tBu)]PF_6$ (2): 1622(s), 1580(s), 1512(s), 1445(s), 1420(m), 1364(m), 1327(m), 1263(s), 1167(s), 1020(s), 841(vs), 762(s), 731(m), 658(m), 557(s).
$[Ru(bpy)_2(salCl)]PF_6$ (4): 1605(s), 1580(s), 1501(s), 1445(s), 1325(m), 1265(m), 1235(w), 1155(s), 1024(m), 841(vs), 762(s), 729(s), 658(w), 556(s).
$[Ru(bpy)_2(salNO_2)]PF_6$ (5): 1602(s), 1589(s), 1539(s), 1487(m), 1449(s), 1418(m), 1331(s), 1267(w), 1242(m), 1175(w), 1099(s), 1024(w), 939(w), 841(vs), 762(s), 729(s), 662(w), 557(s).

3.3.4. Single crystal X-ray structure determination

Single crystals of $[Ru(bpy)_2(salH)]PF_6$ (**3**) were grown by slow evaporation of a dichloromethane-diethylether (1:1) solution of the complex and that of $[Ru(bpy)_2(salCl)]PF_6$ (**4**) were grown by slow evaporation of an acetone-diethylether (1:1) solution of the complex. In each case, data were collected on an Enraf-Nonius Mach-3 single crystal diffractometer using graphite monochromated Mo *Kα* radiation (λ = 0.71073 Å) by ω-scan method at 298 K. Unit cell parameters were determined by least-squares fit of 25 reflections having 2θ values in the range 18-22°. Intensities of 3 check reflections were measured after every 1.5 h during the data collection to monitor the crystal stability. In both cases, there is no significant change in the intensities of the check reflections. Data were corrected for Lorentz-polarization effects. Empirical absorption corrections were applied to both data sets based on the Ψ-scans[12] of 6 reflections in each case. These reflections have 2θ in the range 7-42° and χ within 81-89° for $[Ru(bpy)_2(salH)]PF_6$ (**3**) and 2θ in the range 3-31° and χ within 84-88° for $[Ru(bpy)_2(salCl)]PF_6$ (**4**). The structures were solved by direct methods and

refined on F^2 by full-matrix least-squares procedures. The asymmetric unit of $[Ru(bpy)_2(salH)]PF_6$ contains a molecule of the complex and a dichloromethane molecule and that of $[Ru(bpy)_2(salCl)]PF_6$ contains a molecule of the complex and one molecule of acetone. All non-hydrogen atoms were refined using anisotropic thermal parameters. Hydrogen atoms were included in the structure factor calculation at idealized positions by using riding model, but not refined. In the case of $[Ru(bpy)_2(salH)]PF_6 \cdot CH_2Cl_2$, the programs of WinGX[13] were used for data reduction and absorption correction. For the dataset of $[Ru(bpy)_2(salCl)]PF_6 \cdot (CH_3)_2CO$, the Xtal3.4 software[14] and Datcor program[15] were used for data reduction and absorption correction, respectively. Structure solution and refinement were performed with the SHELX-97 programs.[16] The Platon and Ortep-3 programs were used for molecular graphics.[17] Selected crystal and refinement data are listed in Table 3.1.

Further details are available from the Cambridge Crystallographic Data Centre, 12 Union Road, Cambridge CB2 1EZ, UK on request, quoting the deposition nos. CCDC 185005 and 185006.

Table 3.1. Crystal and structure refinement data for $[Ru(bpy)_2(salH)]PF_6 \cdot CH_2Cl_2$ (**3**$\cdot CH_2Cl_2$) and $[Ru(bpy)_2(salCl)]PF_6 \cdot (CH_3)_2CO$ (**4**$\cdot (CH_3)_2CO$)

Complex	3·CH_2Cl_2	4·$(CH_3)_2CO$
Chemical formula	$C_{28}H_{23}N_4O_2F_6Cl_2PRu$	$C_{30}H_{26}N_4O_3F_6ClPRu$
Crystal size, mm	0.50 x 0.47 x 0.35	0.48 x 0.45 x 0.38
Formula weight	764.44	772.04
Space group	Monoclinic, $P2_1/n$	Triclinic, $P\bar{1}$
a, Å	9.289(2)	10.3637(15)
b, Å	20.099(5)	12.973(2)
c, Å	16.388(4)	13.361(3)
α, deg.	90	110.22(2)
β, deg.	90.27(2)	106.753(18)
γ, deg.	90	91.491(13)
V, $Å^3$	3059.4(12)	1598.3(5)
Z	4	2
ρ_{calcd}, g cm^{-3}	1.660	1.604
μ mm^{-1}	0.810	0.698
Reflections collected/unique	7229/7014	5611/5611
Reflections $I > 2\sigma(I)$/parameters	4811/397	4389/415
R1[a], wR2[b] [$(I > 2\sigma(I)$]	0.0510, 0.1372	0.0493, 0.1429
R1, wR2 (all data)	0.0818, 0.1566	0.0694, 0.1544
Goodness-of-fit[c]	1.020	1.176
$\Delta\rho_{max/min}$ e $Å^{-3}$	1.104, -0.824	0.946, -0.491

[a] $R1 = \sum||F_o| - |F_c||/\sum|F_o|$. [b] $wR2 = \{\sum[(F_o^2 - F_c^2)^2]/\sum[w(F_o^2)^2]\}^{1/2}$.

[c] $GOF = \{\sum[w(F_o^2 - F_c^2)^2]/(n - p)\}^{1/2}$ where 'n' is the number of reflections and 'p' is the number of parameters refined; $w = 1/[\sigma^2(F_o^2) + (aP)^2 + bP]$ where a = 0.08 and b = 3.1739 for **3**$\cdot CH_2Cl_2$; and 0.0927 and b = 0 for **4**$\cdot (CH_3)_2CO$

Table 3.2. Atomic coordinates ($x10^4$) and equivalent isotropic displacement parameters[a] ($Å^2x10^3$) for $[Ru(bpy)_2(salH)]PF_6 \cdot CH_2Cl_2$

Atom	x	y	z	U(eq)
Ru	4598(1)	7769(1)	4778(1)	48(1)
P	6482(2)	9634(1)	1705(1)	64(1)
Cl(1)	3744(4)	6578(2)	2174(2)	157(1)
Cl(2)	5868(4)	6103(2)	1089(2)	196(2)
F(1)	5999(5)	8889(2)	1532(3)	111(1)
F(2)	4914(4)	9788(3)	1986(3)	134(2)
F(3)	6977(6)	10379(2)	1822(3)	134(2)
F(4)	8049(4)	9478(2)	1399(3)	131(2)
F(5)	6076(5)	9810(2)	798(2)	108(1)
F(6)	6878(6)	9439(3)	2589(3)	167(2)
O(1)	2636(3)	8223(2)	4594(2)	62(1)
O(2)	5123(4)	7847(2)	3562(2)	64(1)
N(1)	4168(4)	7786(2)	5995(2)	55(1)
N(2)	5491(4)	8665(2)	5095(3)	61(1)
N(3)	6400(4)	7217(2)	4940(2)	56(1)
N(4)	3824(4)	6838(2)	4506(2)	56(1)
C(1)	2153(5)	8429(2)	3891(3)	60(1)
C(2)	764(6)	8720(3)	3875(4)	78(2)
C(3)	187(7)	8955(4)	3173(5)	99(2)
C(4)	928(8)	8919(4)	2437(5)	110(3)
C(5)	2258(7)	8640(4)	2424(4)	94(2)
C(6)	2915(5)	8382(2)	3139(3)	64(1)
C(7)	4311(6)	8105(3)	3041(3)	69(1)
C(8)	3461(6)	7316(3)	6411(3)	65(1)
C(9)	3166(7)	7377(4)	7226(4)	88(2)
C(10)	3604(9)	7937(4)	7630(4)	106(2)
C(11)	4317(8)	8422(4)	7210(4)	98(2)
C(12)	4607(6)	8347(2)	6387(3)	65(1)
C(13)	5365(5)	8833(2)	5879(4)	66(1)
C(14)	5950(8)	9430(3)	6175(5)	96(2)
C(15)	6701(8)	9835(3)	5637(7)	115(3)

C(16)	6844(8)	9650(3)	4844(6)	110(3)
C(17)	6221(6)	9073(3)	4587(4)	82(2)
C(18)	7676(6)	7437(3)	5202(3)	72(1)
C(19)	8854(7)	7019(4)	5302(4)	93(2)
C(20)	8692(8)	6356(4)	5120(4)	94(2)
C(21)	7407(7)	6124(3)	4849(4)	83(2)
C(22)	6265(6)	6553(2)	4765(3)	63(1)
C(23)	4820(6)	6345(2)	4494(3)	62(1)
C(24)	4448(8)	5700(3)	4241(4)	85(2)
C(25)	3079(9)	5560(3)	4020(4)	95(2)
C(26)	2061(8)	6055(3)	4050(4)	85(2)
C(27)	2455(6)	6687(3)	4286(3)	67(1)
C(28)	5095(12)	5938(8)	1968(8)	224(8)

[a] Equivalent isotropic U defined as one third of the trace of the orthogonalized U(ij) tensor.

Table 3.3. Atomic coordinates ($x10^4$) and equivalent isotropic displacement parameters[a] ($Å^2x10^3$) for $[Ru(bpy)_2(salCl)]PF_6 \cdot (CH_3)_2CO$

Atom	x	y	z	U(eq)
Ru	3578(1)	6871(1)	2379(1)	45(1)
P	13095(2)	1654(2)	1940(2)	81(1)
Cl	9669(2)	4116(2)	2888(2)	94(1)
F(1)	11838(6)	2296(5)	2008(4)	134(2)
F(2)	12297(6)	568(4)	1890(5)	130(2)
F(3)	12579(6)	1232(5)	620(4)	127(2)
F(4)	14377(6)	1049(5)	1905(5)	145(2)
F(5)	13919(7)	2734(4)	2011(5)	146(2)
F(6)	13614(5)	2068(4)	3266(4)	113(2)
O(1)	5621(3)	7167(3)	3247(3)	57(1)
O(2)	3818(3)	5386(3)	1255(3)	56(1)
O(3)	2274(13)	9845(17)	7677(9)	331(10)
N(1)	3380(4)	8264(3)	3589(3)	47(1)
N(2)	3352(4)	6240(3)	3541(3)	49(1)

N(3)	1590(4)	6682(3)	1446(3)	48(1)
N(4)	3738(4)	7589(3)	1274(3)	52(1)
C(1)	6461(5)	6444(4)	3098(4)	53(1)
C(2)	7803(6)	6746(5)	3868(5)	71(2)
C(3)	8754(6)	6041(5)	3798(6)	75(2)
C(4)	8423(6)	5000(5)	2927(5)	66(2)
C(5)	7196(6)	4676(5)	2168(5)	62(1)
C(6)	6152(5)	5386(4)	2211(4)	52(1)
C(7)	4893(6)	4965(5)	1366(5)	59(1)
C(8)	3320(5)	9280(4)	3534(5)	56(1)
C(9)	3283(6)	10188(5)	4422(5)	65(2)
C(10)	3317(6)	10083(5)	5407(5)	68(2)
C(11)	3369(6)	9055(5)	5487(5)	64(1)
C(12)	3387(5)	8154(4)	4570(4)	51(1)
C(13)	3377(5)	7005(4)	4530(4)	52(1)
C(14)	3346(6)	6705(5)	5430(5)	65(1)
C(15)	3292(6)	5602(6)	5291(6)	73(2)
C(16)	3245(6)	4834(5)	4286(6)	69(2)
C(17)	3280(5)	5160(4)	3422(5)	58(1)
C(18)	539(5)	6168(5)	1572(5)	61(1)
C(19)	-789(6)	6094(6)	914(6)	77(2)
C(20)	-1040(6)	6574(6)	127(6)	81(2)
C(21)	25(6)	7104(5)	2(5)	72(2)
C(22)	1324(5)	7142(4)	653(4)	54(1)
C(23)	2546(5)	7660(4)	555(4)	54(1)
C(24)	2522(7)	8159(5)	-218(5)	71(2)
C(25)	3726(8)	8558(6)	-266(6)	84(2)
C(26)	4928(8)	8474(6)	442(6)	83(2)
C(27)	4891(6)	7995(5)	1194(5)	67(2)
C(28)	283(16)	8945(16)	6500(2)	329(15)
C(29)	1082(13)	9840(3)	7311(13)	273(15)
C(30)	489(18)	10857(17)	7300(2)	410(2)

[a] Equivalent isotropic U defined as one third of the trace of the orthogonalized U(ij) tensor.

3.4. Results and Discussion

3.4.1. Synthesis and some properties

The syntheses of all the five complexes were performed by using a general method. Reactions of stoichiometric quantities of *cis*-$[Ru(bpy)_2Cl_2]\cdot 2H_2O$, HsalR and NaOH in boiling methanol afford the complexes in good yields. The cationic complexes were precipitated as their hexafluorophosphate salts. However, chromatographic purification was necessary on a neutral aluminium oxide column. Elemental analysis data (Table 3.4) are satisfactory with the general formula $[Ru(bpy)_2(salR)]PF_6$. Molar conductivity values (Table 3.5) of all the complexes in acetonitrile solutions are consistent with 1:1 electrolytic behavior.[18] The complexes are diamagnetic and NMR active. Thus the ruthenium centers in these complexes are in +2 oxidation state and low-spin in character.

Table 3.4. Elemental analysis data[a]

Complex	%C	%H	%N
$[Ru(bpy)_2(salOMe)]PF_6$	47.28 (47.40)	3.12 (3.27)	7.69 (7.90)
$[Ru(bpy)_2(sal^tBu)]PF_6$	50.81 (50.61)	3.55 (3.97)	7.43 (7.62)
$[Ru(bpy)_2(salH)]PF_6$	47.56 (47.72)	2.98 (3.11)	7.94 (8.24)
$[Ru(bpy)_2(salCl)]PF_6$	45.32 (45.42)	2.71 (2.82)	7.68 (7.85)
$[Ru(bpy)_2(salNO_2)]PF_6$	44.43 (44.76)	2.49 (2.78)	9.46 (9.67)

[a] Calculated values are in parentheses.

3.4.2. Infrared spectral properties

Infrared spectra of the complexes do not display any band near 3300 cm^{-1} suggesting deprotonation of the phenolic-OH of HsalR in the complexes. The

free aldehydes (HsalR) display a peak near 1650 cm^{-1} due to the C=O group. A medium to strong peak is observed in the range 1600-1622 cm^{-1} for all the five complexes. The origin of this peak[19] might involve the metal coordinated C=O group of $salR^-$. The strong and sharp peak displayed by the complexes in the range 1578-1589 cm^{-1} is likely to be associated with the C=N fragments of the bpy ligands.[7c] The presence of PF_6^- in each complex is indicated by a strong peak[19] at ~840 cm^{-1}. A representative spectrum is shown below.

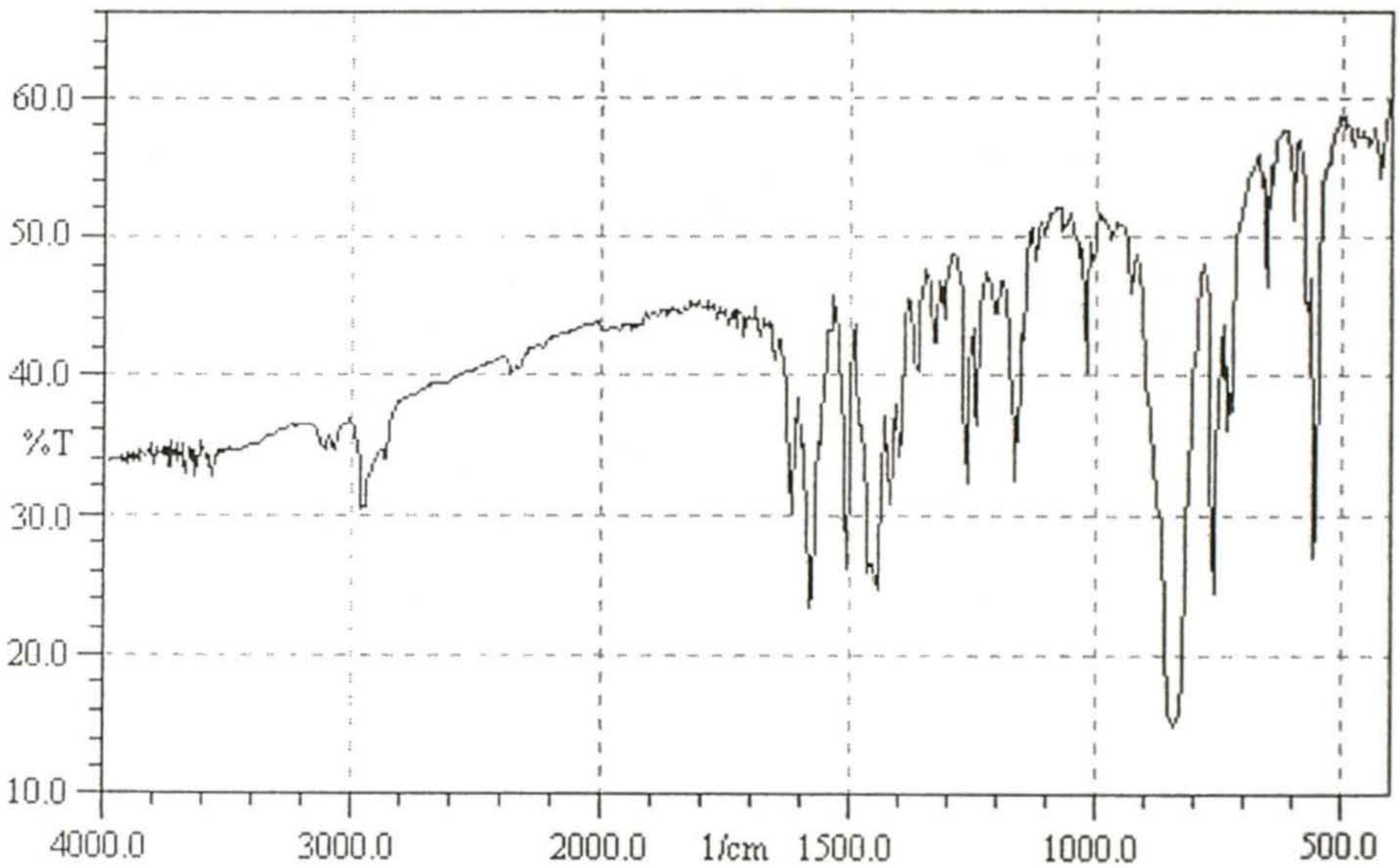

Figure 3.2. Infrared spectrum of $[Ru(bpy)_2(sal^tBu)]PF_6$ in KBr disc.

3.4.3. Electronic spectral properties

Electronic spectral data of the complexes in acetonitrile solutions are listed in Table 3.5. A representative spectrum is shown in Figure 3.3. Except for the $[Ru(bpy)_2(salNO_2)]PF_6$, the spectral profiles of the other four complexes are very

similar. $[Ru(bpy)_2(salNO_2)]PF_6$ differs only in the relative intensities of the absorption bands when compared with the rest. In the visible region, all the complexes display four absorptions in the ranges 537-557 nm, 476-489 nm, 402-415 nm and 341-368 nm. These absorptions for $[Ru(bpy)_2(salNO_2)]PF_6$ are

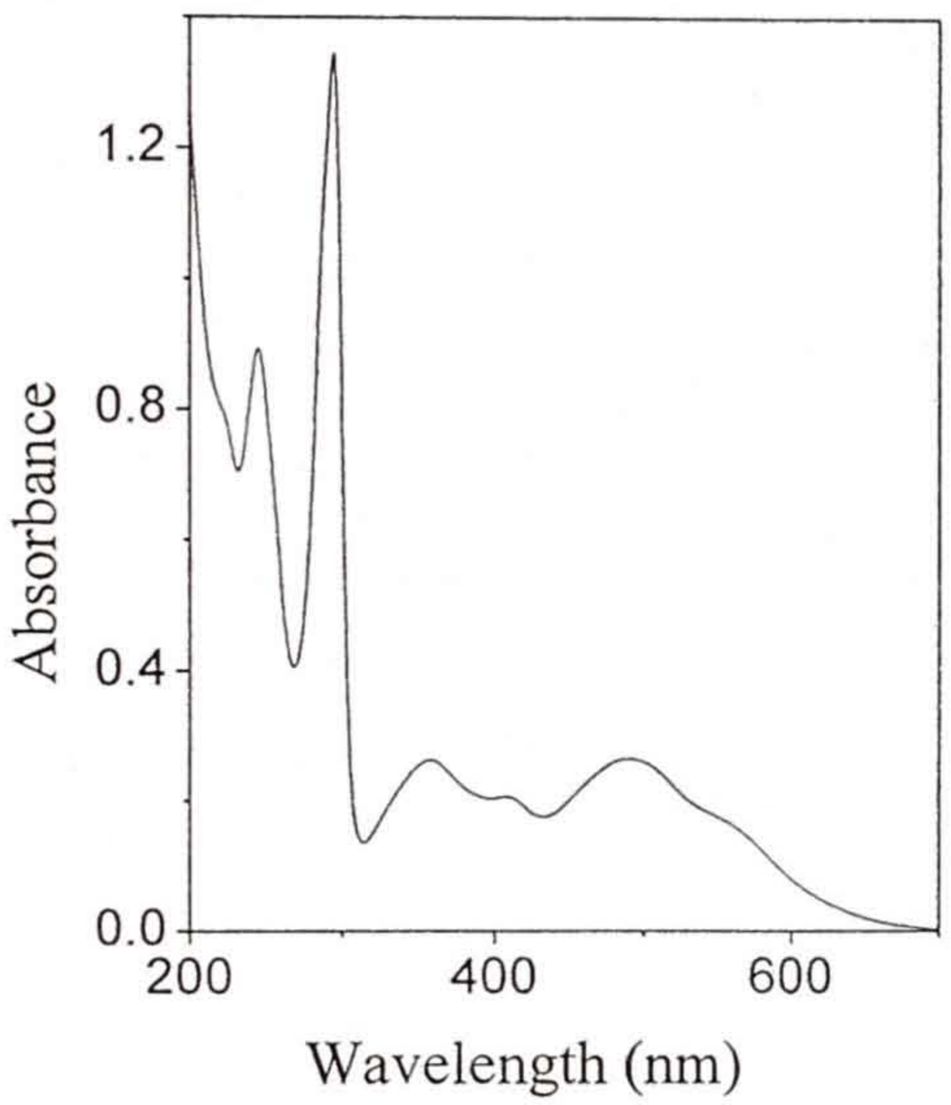

Figure 3.3. Electronic spectrum of $[Ru(bpy)_2(salH)]PF_6$ in acetonitrile.

significantly blue shifted compared to the other four complexes (Table 3.5). Multiple transitions in the visible region in this type of complexes are common due to presence of several closely spaced acceptor levels.[4-7] The lowest energy $d\pi$ $(Ru^{II}) \rightarrow \pi^*(bpy)$ band for $[Ru(bpy)_3]^{2+}$ is observed at 450 nm.[20] In the present series of complexes, this MLCT band appears in the range 476-491 nm with a shoulder within 537-557 nm. This red shift is consistent with the replacement of

one π-accepting bpy ligand with the σ-donating asymmetric salR$^-$ having reduced ligand-field strength and lowering of the molecular symmetry due to the replacement. An interesting observation is the trend of this band position within this series of $[Ru(bpy)_2(salR)]PF_6$ complexes. When R = OMe, ^tBu and H it appears at 490 ± 1 nm. On the other hand, for R = Cl and NO_2 the peak is observed at 485 and 476 nm, respectively. A possible rationale for the above shift is as follows. Electron withdrawing substituents such as Cl and NO_2 at the *para*

Table 3.5. Electronic spectral[a] and molar conductivity[a] data

Complex	λ_{max} (nm) (ε (M^{-1} cm^{-1}))	Λ_M (Ω^{-1} cm^2 mol^{-1})
$[Ru(bpy)_2(salOMe)]PF_6$	557[b] (6700), 489 (10300), 411[b] (7900), 368 (10800), 295 (45500), 243 (32400)	138
$[Ru(bpy)_2(sal^tBu)]PF_6$	560[b] (7900), 491 (12400), 404 (10200), 362 (12800), 295 (60900), 245 (43500)	150
$[Ru(bpy)_2(salH)]PF_6$	556[b] (8200), 489 (12800), 408 (9900), 358 (12700), 295 (65300), 245 (43400)	152
$[Ru(bpy)_2(salCl)]PF_6$	556[b] (3600), 485 (6700), 415 (4100), 361 (6100), 294 (30100), 244 (20400)	142
$[Ru(bpy)_2(salNO_2)]PF_6$	537[b] (7900), 476 (17300), 402 (16700), 341 (14400), 293 (64800), 245 (42000)	147

[a] In acetonitrile, [b] Shoulder.

position of the phenolate-O will reduce the σ-donating ability of the coordinating atom. However, the energy of the phenolate-pπ levels are expected to be lower due to the presence of an electron withdrawing group at *para* to the phenolate-O compared to the energy of the phenolate-pπ levels in presence of an electron releasing group at the same position. In the latter case, the interaction of Ru^{II}-dπ with phenolate-pπ will increase the energy of the former and hence Ru^{II}-dπ will be nearer to the bpy-π* levels. The opposite is expected for the electron-withdrawing group. Thus there is a high energy shift of the lowest energy MLCT band for these two complexes compared to the rest. The shoulder in the range 537-557 nm possibly involves charge transfer from both Ru(II) and $salR^-$ to bpy.[6a] Here also the absorption for $salNO_2^-$ complex is blue shifted compared to the rest. In the UV region, all the complexes display two intense peaks. The positions of these two peaks are essentially same (294 ± 1 and 244 ± 1 nm). In similar ruthenium(II) bipyridine heterochelates, absorptions in this region are assigned to bipyridine $\pi \rightarrow \pi^*$ transitions.[4-7]

3.4.4. NMR spectral properties

The proton NMR spectra of all the complexes were recorded in CD_3CN. A representative spectrum is shown in Figure 3.4. The absence of free HsalR -OH proton (δ > 10) in all the spectra[21] confirm the complexation through the phenolate-O. The -CHO proton is observed in the range 8.99-9.31 δ (Table 3.6). There is an upfield shift for this signal with the increasing electron releasing nature of R. A similar substituent effect on the chemical shift of -CH=N- proton is noted for some ruthenium(II) Schiff base complexes described in the following chapter. The methyl protons of $[Ru(bpy)_2(salOMe)]PF_6$ and $[Ru(bpy)_2(sal^tBu)]PF_6$ appear as singlet at 3.66 and 1.22 δ, respectively.

The aromatic region of each spectrum is very complicated. In each complex, the equatorial plane contains two pyridine rings (b, d) from two bpy

ligands and the salR$^-$ (ring p) moiety. The remaining two pyridine rings (a, c) occupy the axial positions (Scheme 1). Thus the four pyridine rings from

Table 3.6. ^{1}H NMR data[a] (δ) in CD_3CN

$[Ru(bpy)_2(salOMe)]PF_6$	3.66 (3 H, s), 6.46 (1 H, d, J = 10), 6.70 (1 H, d, J = 3.8), 6.93-6.99 (1 H, q), 7.09-7.19 (2 H, m), 7.52-7.63 (2 H, q), 7.74-7.88 (4 H, m), 8.02-8.13 (2 H, q), 8.36 (2 H, d, J = 6.4), 8.48 (2 H, d, J = 8.4), 8.67-8.74 (2 H, t), 8.99 (1 H, s).
$[Ru(bpy)_2(sal^tBu)]PF_6$	1.22 (9 H, s), 6.49 (1 H, d, J = 9), 7.01-7.19 (2 H, m), 7.23 (1 H, d, J = 2.9), 7.36 (1 H, dd, J = 9.7, 2.9), 7.52-7.63 (2 H, q), 7.74-7.87 (4 H, m), 8.01-8.13 (2 H, q), 8.36 (2 H, dd, J = 9.8, 2), 8.48 (2 H, dd, J = 8.8, 2), 8.66-8.74 (2 H, q), 9.03 (1 H, s).
$[Ru(bpy)_2(salH)]PF_6$	6.43-6.53 (2 H, m), 7.10-7.19 (2 H, m), 7.22-7.27 (1 H, m), 7.32 (1 H, dd, J = 7.8, 2), 7.52-7.63 (2 H, q), 7.75-7.88 (4 H, m), 8.02-8.14 (2 H, q), 8.36 (2 H, d, J = 6.4), 8.48 (2 H, d, J = 8.4), 8.67-8.76 (2 H, q), 9.06 (1 H, s).
$[Ru(bpy)_2(salCl)]PF_6$	6.49 (1 H, d, J = 9.2), 7.11 - 7.19 (3 H, m), 7.32 (1 H d, J = 3), 7.53 - 7.65 (2 H, m), 7.74 - 7.86 (4 H, m), 8.03 - 8.15 (2 H, m), 8.36 (2 H, dd, J = 7.8, 3), 8.49 (2 H, d, J = 8), 8.66 - 8.73 (2 H, m), 9.05 (1 H, s).
$[Ru(bpy)_2(salNO_2)]PF_6$	6.54 (1 H, d, J = 10), 7.15 - 7.21 (2 H, m), 7.57 - 7.66 (2 H, q), 7.76 - 7.85 (4 H, m), 7.88 (1 H, t), 7.97 (1 H, dd, J = 9.7, 4), 8.08 - 8.19 (2 H, m), 8.38 (2 H, dd, J = 7.2, 1.6), 8.45 - 8.53 (2 H, q), 8.66 - 8.72 (2 H, m), 9.31 (1 H, s).

[a] s, singlet; d, doublet; t, triplet; q, quartet; m, multiplet.

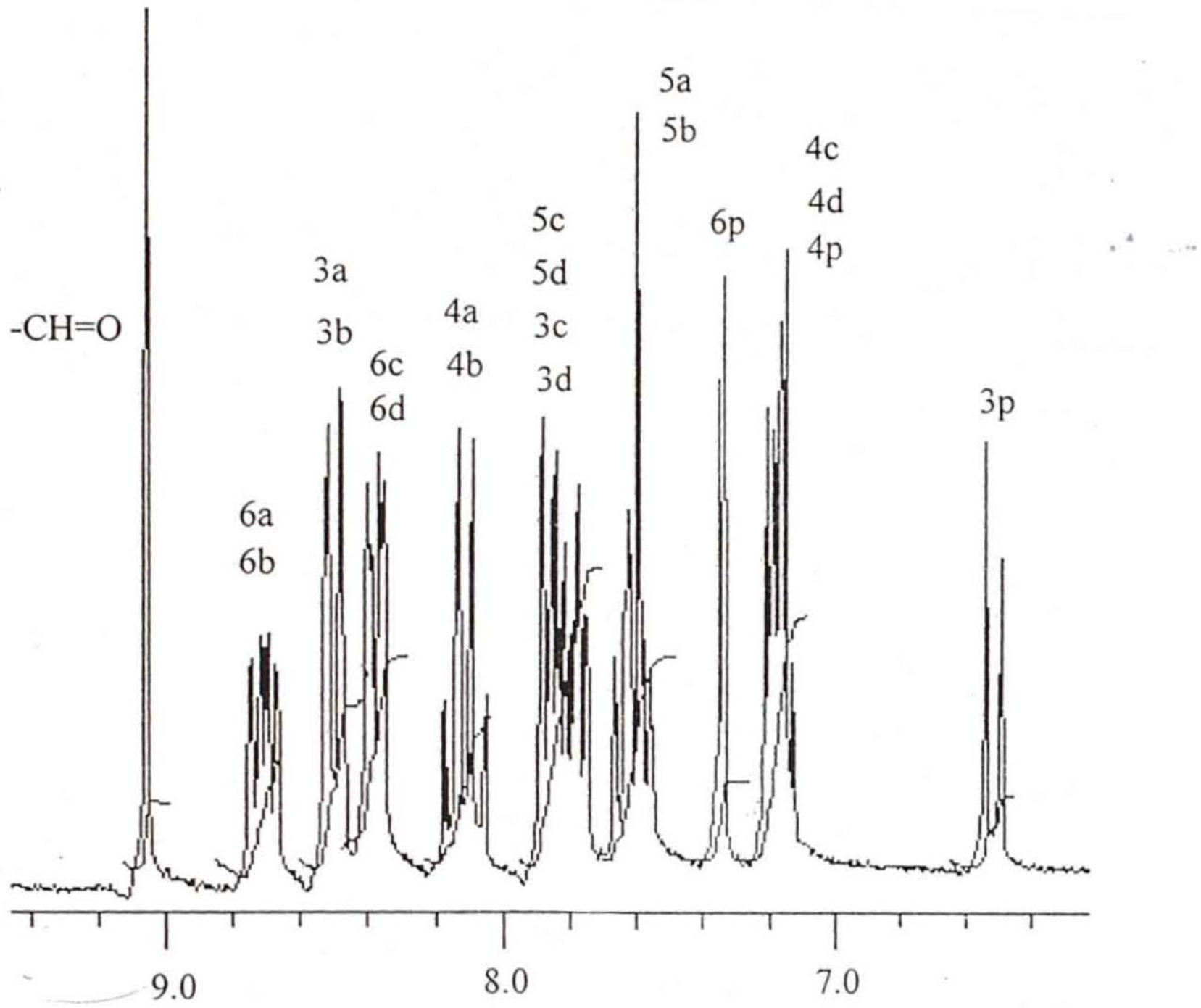

Figure 3.4. ^{1}H NMR spectrum of $[Ru(bpy)_2(salCl)]PF_6$ in CD_3CN.

two bpy ligands are non-equivalent due to chelation of the asymmetric $salR^-$. Although all the aromatic protons are non-equivalent, many of them are in similar electronic environment. Thus the assignment of the signals becomes difficult due to their appearance in a narrow chemical shift range causing partial overlapping of the signals. However, the aromatic protons can be separated in different groups with the help of two-dimensional ^{1}H-^{1}H correlation spectroscopy (COSY). The twenty aromatic protons in $[Ru(bpy)_2(salH)]PF_6$ separate into five groups of four, each corresponding to H^3, H^4, H^5 and H^6 (usual numbering scheme). For each of the rest four complexes, nineteen aromatic protons are separated into four groups

of four protons and one group of three protons. The positions of the complexed salR$^-$ ring protons are influenced by the electronic nature of R at *para* to the phenolate-O. The order of the salR$^-$ ring protons in increasing chemical shift is 6 > 4 > 3 when R is electron withdrawing group (Cl and NO_2) and that is 4 > 6 > 3 for electron releasing groups (R = OMe and CMe_3). For the complex with the unsubstituted deprotonated salicylaldehyde (salH$^-$) the order is 6 > 4 > 3,5. The protons of the pyridine ring (d), which is at *trans* to the phenolate-O, are expected to be at lower chemical shift compared to the other pyridine ring protons due to the *trans* effect. In addition, the effect of the electron withdrawing or releasing property of the substituent R at *para* to the phenolate-O is reflected in the relative chemical shifts of the protons on the ring 'd'. Assignments of the other sets of protons to specific pyridine rings cannot be done unambiguously. In all the complexes, the order of the pyridine ring protons with respect to increasing chemical shift is 6 > 3 > 4 > 5 for rings 'a' and 'b' and that for pyridine rings 'c' and 'd' is 6 > 3,5 > 4. Similar distributions of pyridine protons in the NMR spectra have been observed before for other bis(bipyridine)ruthenium(II) complexes with asymmetric bidentate chelating ligands.[4b,d]

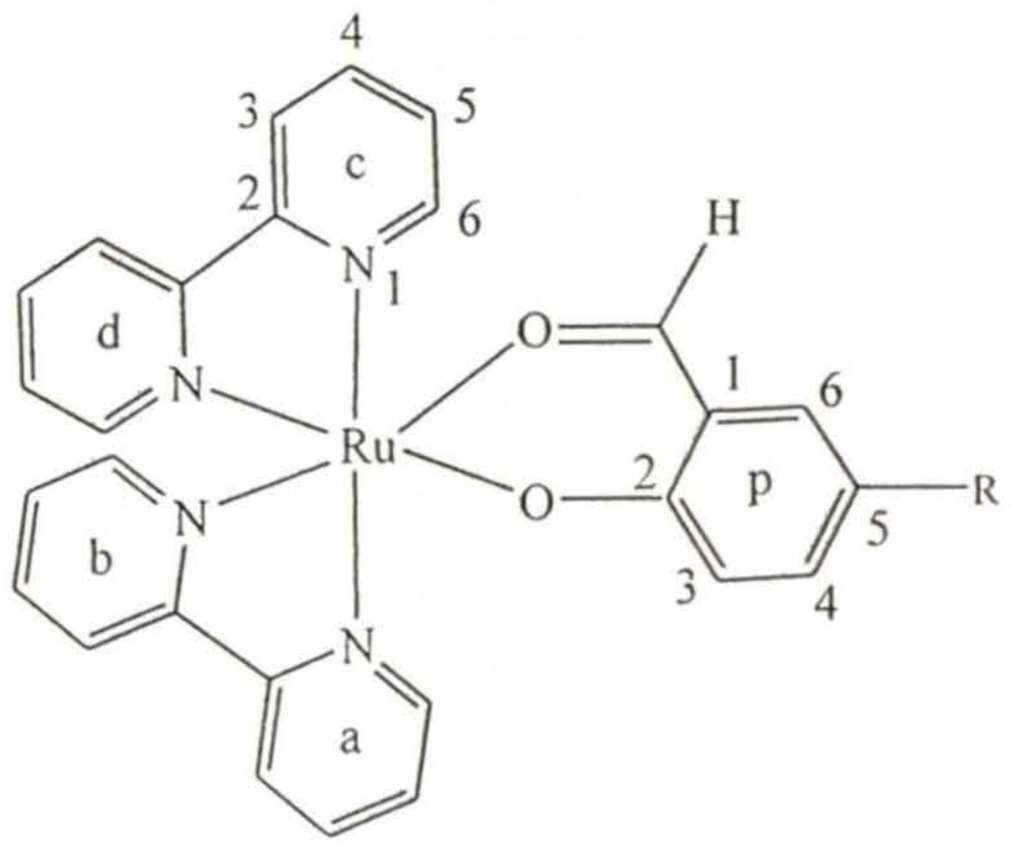

Scheme 1

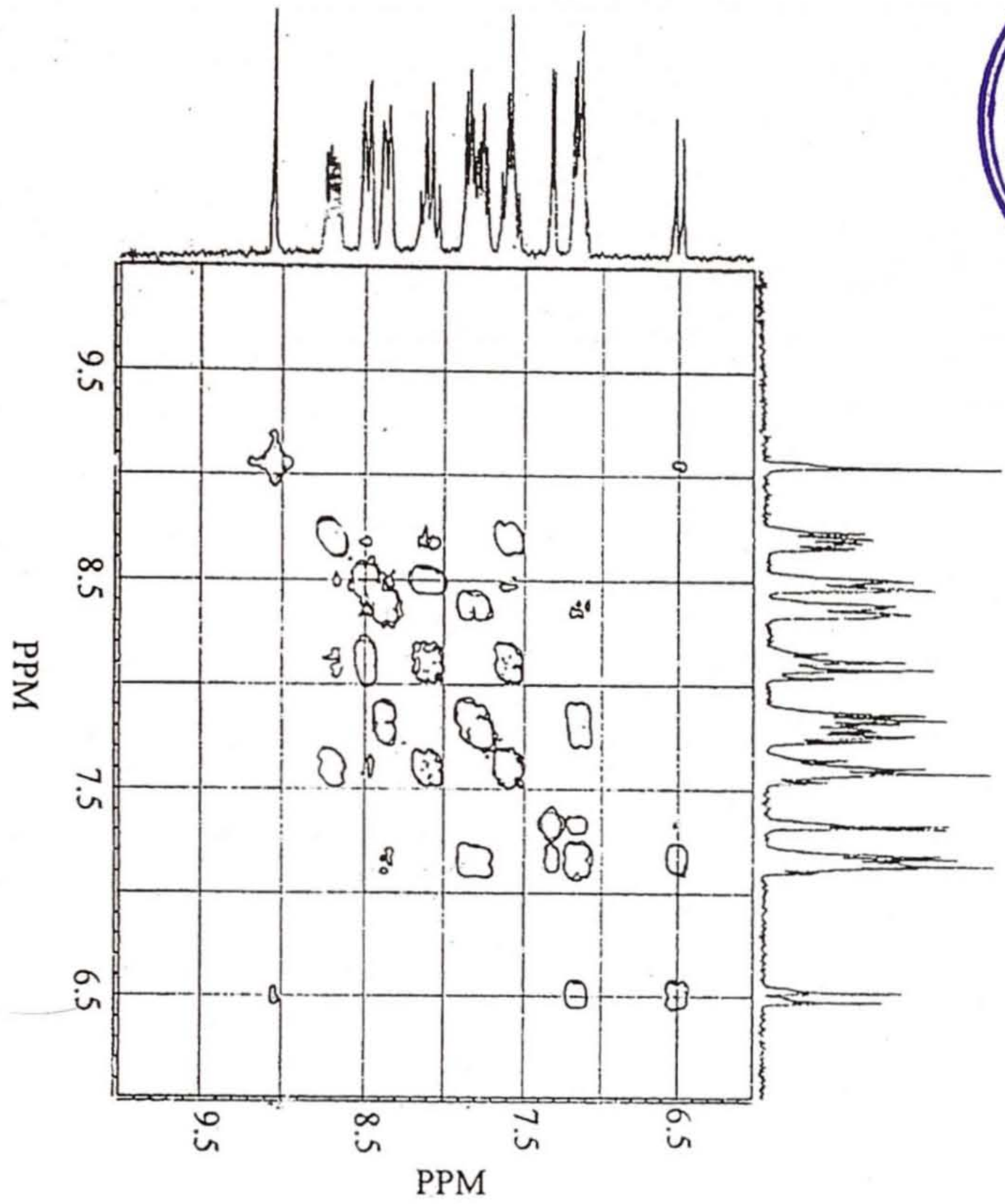

Figure 3.5. ^{1}H - ^{1}H COSY spectrum of $[Ru(bpy)_2(salCl)]PF_6$ in CD_3CN.

3.4.5. Redox properties

Acetonitrile solutions of all the complexes were used to study the redox behavior with the help of cyclic voltammetry. Representative voltammograms are shown in Figure 3.6 and the potential data are provided in Table 3.7. The complexes display the Ru(III)-Ru(II) couple in the potential range 0.61-0.84 V (vs. Ag/AgCl) with a peak-to-peak separation of 70-80 mV and essentially

identical anodic and cathodic peak current. The one electron stoichiometry of this response is confirmed for each complex by comparison of peak currents with known one electron redox processes under identical conditions.[22] The potential of this response is sensitive to R. It decreases with increasing electron releasing nature of the substituent. Thus as the electron density on the phenolate-O decreases Ru(II) to Ru(III) oxidation becomes more difficult. When these potentials are plotted against the Hammett substituent constants (σ_p)[23] a linear correlation is observed (Figure 3.7). At a more anodic potential, two more irreversible oxidations are displayed by $[Ru(bpy)_2(salOMe)]PF_6$. On the other

Table 3.7. Cyclic voltammetric data[a,b] in acetonitrile at 298 K

Complex	$E_{1/2}$ (V) (ΔE_p (mV))	E_{pa} (V)	$E_{1/2}$ (V) (ΔE_p (mV))
1	0.61 (70)	1.45, 1.81	-1.64[c], -1.90[c]
2	0.65 (70)	1.75	-1.47 (60), -1.68 (100)
3	0.68 (80)	1.84	-1.45[c], -1.68 (90)
4	0.73 (70)	1.85	-1.67[c], -1.87[c]
5	0.84 (80)	-	-1.55[c], -1.74[c]

[a] E_{pa}, anodic peak potential; E_{pc}, cathodic peak potential; $E_{1/2} = (E_{pa} + E_{pc})/2$; $\Delta E_p = E_{pa} - E_{pc}$. [b] Scan rate is 100 mVs^{-1}. [c] E_{pc} values.

hand, there is no such oxidation response for $[Ru(bpy)_2(salNO_2)]PF_6$. Rest three complexes display only one irreversible oxidation response (Table 3.7). The anodic peak currents of these responses are comparable with that of the preceding Ru(III)-Ru(II) couple. Similar two monoelectronic irreversible oxidations after

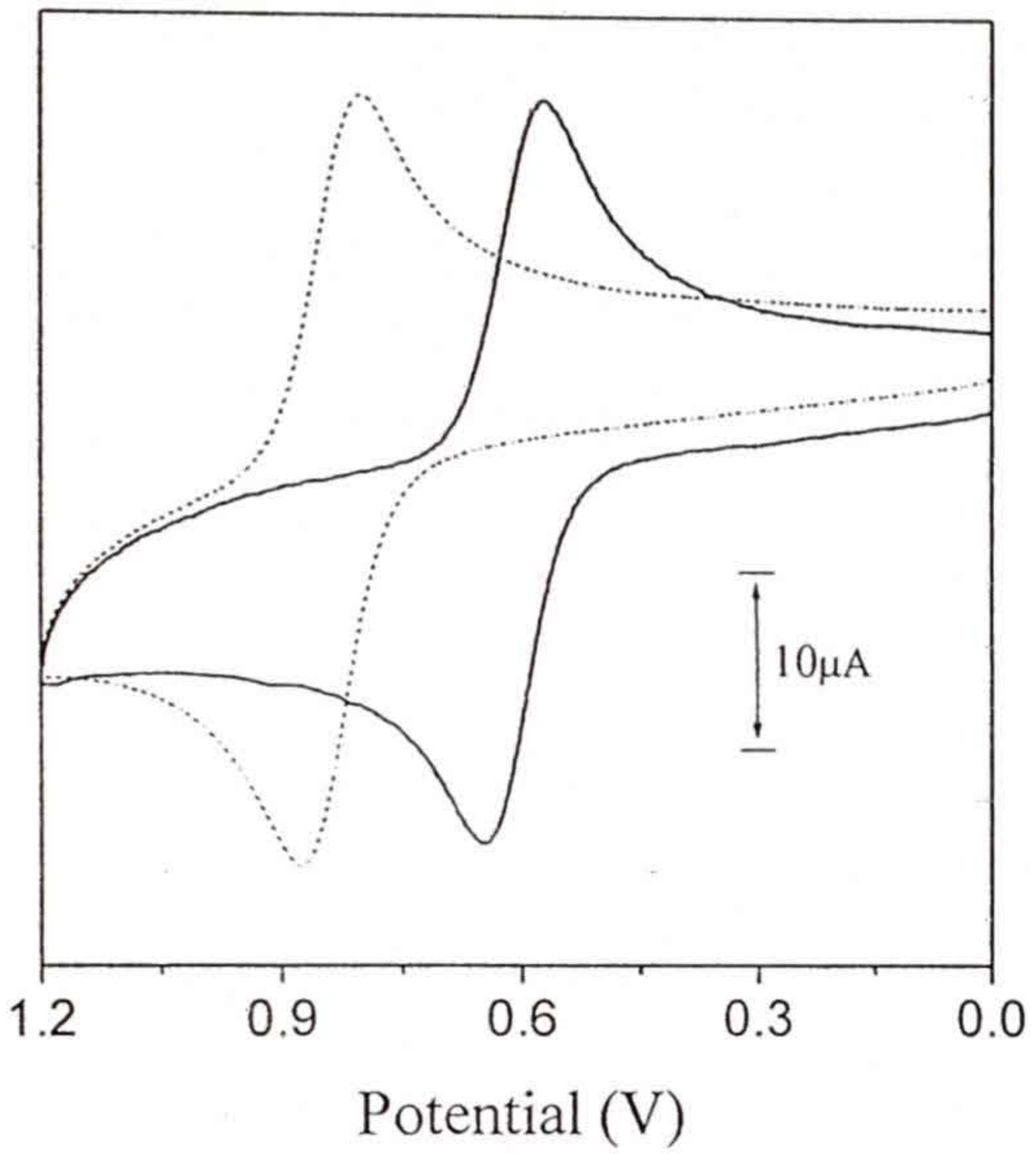

Figure 3.6. Cyclic voltammograms (scan rate 100 mVs^{-1}) of $[Ru(bpy)_2(salOMe)]PF_6$ (——) and $[Ru(bpy)_2(salNO_2)]PF_6$ (·····) in CH_3CN.

the reversible Ru(II) to Ru(III) oxidation as observed for $[Ru(bpy)_2(salOMe)]PF_6$ are reported for $[Ru(bpy)_2L]$ (L^{2-} is salicylate).[6a] In the latter case, after allowing the highest oxidation on reverse scan a new reversible Ru(III)-Ru(II) couple was observed. On repeated scan the current height of the new couple increases in expense of the original couple. It has been shown for $[Ru(bpy)_2L]$ that the first irreversible response is due to oxidation of salicylate to its semiquinone form and the following one involves oxidation of the semiquinone to an electrophile, which undergoes hydroxylation. The new redox active species has been proposed to be a complex of $\{Ru(bpy)_2\}$ with 4-hydroxysalicylate semiquinone. Considering the

similarity of oxidation responses observed for the present series of complexes with that for $[Ru(bpy)_2L]$, we assign the first irreversible response to one electron

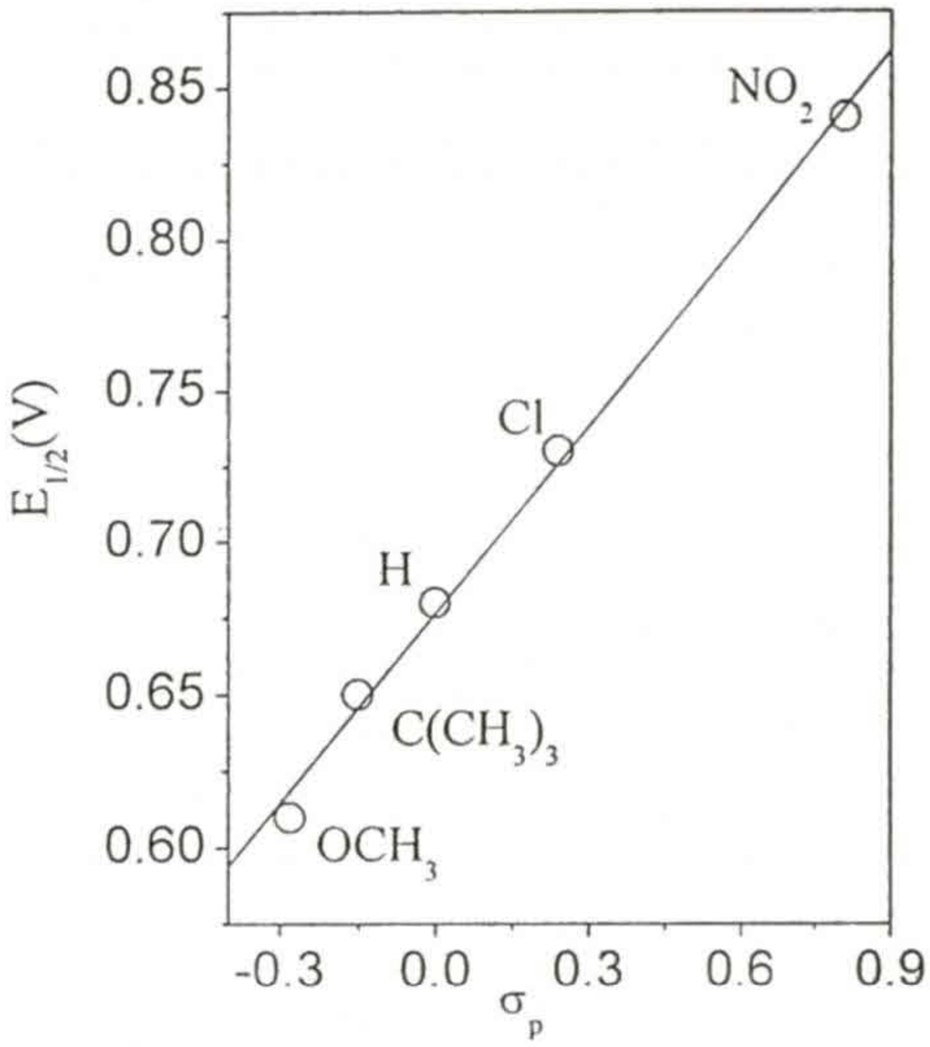

Figure 3.7. Correlation between the $E_{1/2}$ values for Ru(III)-Ru(II) couple and the Hammett substituent constants. The straight line represents a linear least-squares fit.

oxidation of $salR^-$ (R = OMe, H, ^tBu and Cl) to semiquinone form. The second oxidation observed for only the complex with $salOMe^-$ is possibly due to further one electron oxidation of its semiquinone form to a cationic species. The observation of two irreversible oxidation responses when R in $salR^-$ is an electron releasing group (OMe), no such response when R is an electron withdrawing group (NO_2) and one irreversible oxidation for the other three complexes having R (^tBu, H, Cl) of intermediate electronic character is consistent with the above assignment. Cyclic voltammograms of the five complexes do not show any

change during repeated scans from 0 - 2 V. Thus there is no chemical transformation of any of the complexes in the cyclic voltammetric time scale after the oxidation of the $salR^-$ ligand as observed for the salicylate complex.[6a] All the complexes display two successive quasi-reversible to irreversible reduction responses in the potential range -1.45 to -1.90 V (Table 3.7). Such successive reductions at similar potentials for $\{Ru(bpy)_2\}^{2+}$ complexes with other bidentate chelating ligands are assigned to one electron reduction of each of the two bpy ligands.[4b,d,5c,7]

3.4.6. Description of structures

In the solid state, molecular structures of two complexes $[Ru(bpy)_2(salH)]PF_6$ and $[Ru(bpy)_2(salCl)]PF_6$, have been determined by X-ray crystallography. The structures of the cations are depicted in Figures 3.8 and 3.9. Selected bond parameters are listed in Table 3.8. Both the complexes are pseudo-octahedral. The metal ion is chelated by two bipyridine and one $salR^-$ (R = H and Cl) ligands. The bipyridine chelate bite angles (79.20(16)-79.58(16)°) are very similar and unexceptional.[4b,d,6a,24] The bite angle (92.22(14)°) for the six-membered $salH^-$ chelate ring is little larger than that (90.61(14)°) for the chelate ring formed by $salCl^-$. The bipyridine ligands in both complexes are essentially planar. The inter-ring torsion angles are within 2.9(3)-4.9(2)°. In $[Ru(bpy)_2(salH)]^+$, the $\{Ru(salH)\}$ fragment is planar (mean deviation 0.006 Å). On the other hand, the $salCl^-$ ligand in $[Ru(bpy)_2(salCl)]^+$ is satisfactorily planar (mean deviation 0.02 Å) but the metal ion is displaced from this plane by 0.272(3) Å. Thus the six-membered chelate ring is folded along the O, O line with a fold angle 9.7(2)°. Similar folding has been observed for complexes with Schiff bases derived from salicylaldehyde.[22] The Ru-N bond lengths in these two complexes are in the range 2.025(4)-2.054(4) Å. In each complex, the $Ru\text{-}N_{axial}$ (Ru-N2 and Ru-N4) bond lengths are relatively longer than the $Ru\text{-}N_{equatorial}$ (Ru-N1 and Ru-

N3) bond lengths (Table 3.8). Similar long Ru-N_{axial} and short Ru-$N_{equatorial}$ distances are reported for other $[Ru^{II}(bpy)_2L]^{0/+}$ complexes where L is an asymmetric bidentate chelating ligand.[4b,d,6a] An interesting observation in the structure of $[Ru(bpy)_2(salH)]^+$ is that the Ru-O1 and the Ru-O2 bond lengths are essentially same. The former is 2.058(3) Å and the latter is 2.060(3) Å. Thus both phenolate-O and keto-O bind the metal ion in practically equal strength.

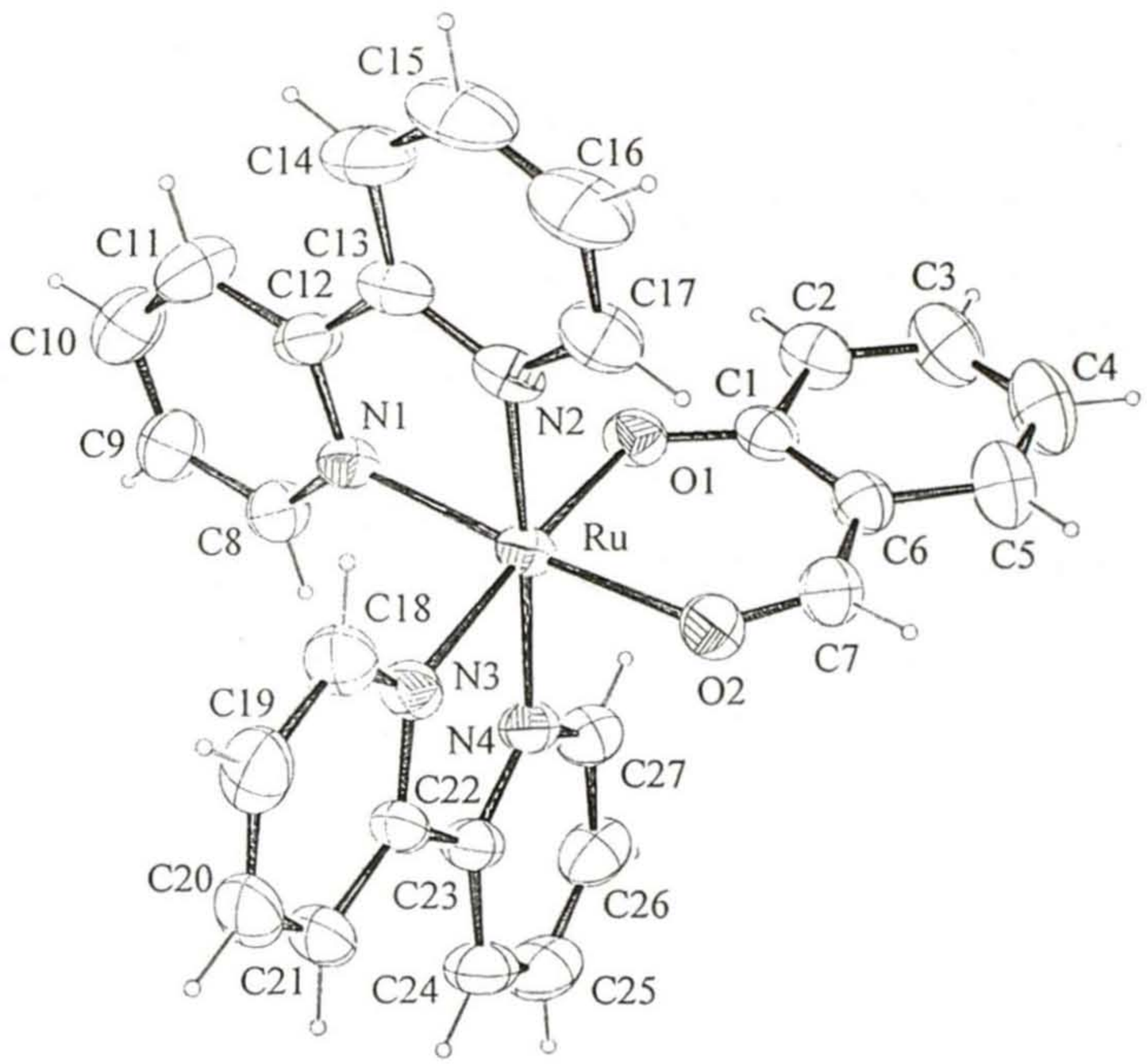

Figure 3.8. Structure of $[Ru(bpy)_2(salH)]^+$ showing the 30% probability thermal ellipsoids for the non-hydrogen atoms and the atom-labeling scheme.

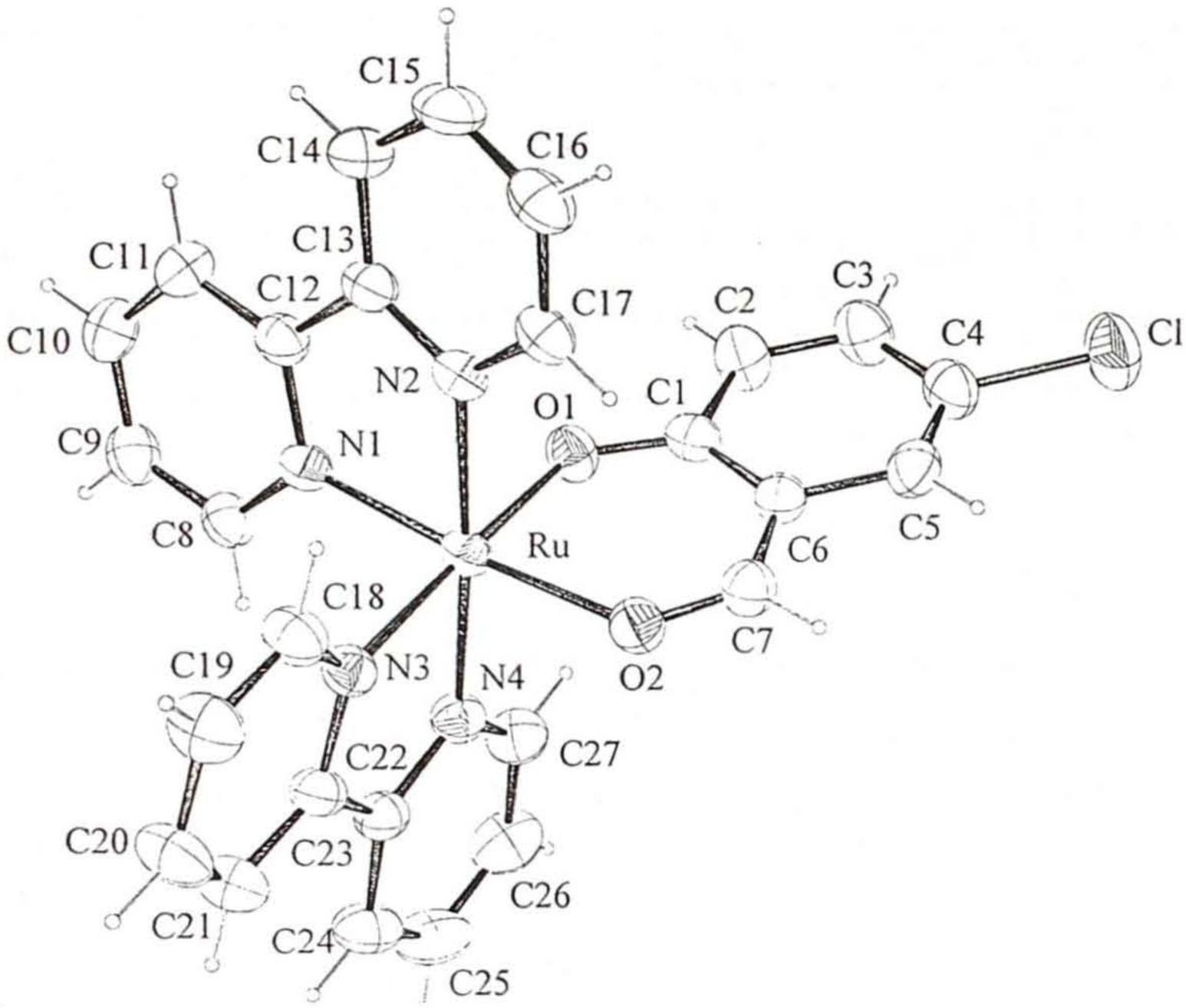

Figure 3.9. Structure of $[Ru(bpy)_2(salCl)]^+$ with the atom-labeling scheme. All non-hydrogen atoms are represented by their 30% probability thermal ellipsoids.

However, the Ru-O1 bond length is expected to be shorter than the Ru-O2 bond length as the phenolate-O is a better σ-donor than the keto-O. Authentic Ru(II) to phenolate-O bond distance is scarce. The Ru-O and C-O bond lengths reported for a Ru(II) catecholate complex are 2.026(5) and 1.342(9) Å, respectively.[25] The C1-O1 bond length (1.302(6) Å) in $[Ru(bpy)_2(salH)]^+$ is significantly shorter than that in the catecholate complex. Further scrutiny of the individual bond lengths (Table 3.8) in $salH^-$ moiety reveals the following trends. The value of C6-C7

bond length is considerably shorter than the ideal single bond value[26] of 1.54 Å. In the ring, C1-C2, C3-C4, C5-C6 and C6-C1 bond lengths are noticeably longer than the C2-C3 and C4-C5 bond lengths (Table 3.8). Ideally all these six bond lengths should have been identical. The above trends and the same Ru-O1 and Ru-O2 bond lengths suggest that the negative charge of $salH^-$ is not localized

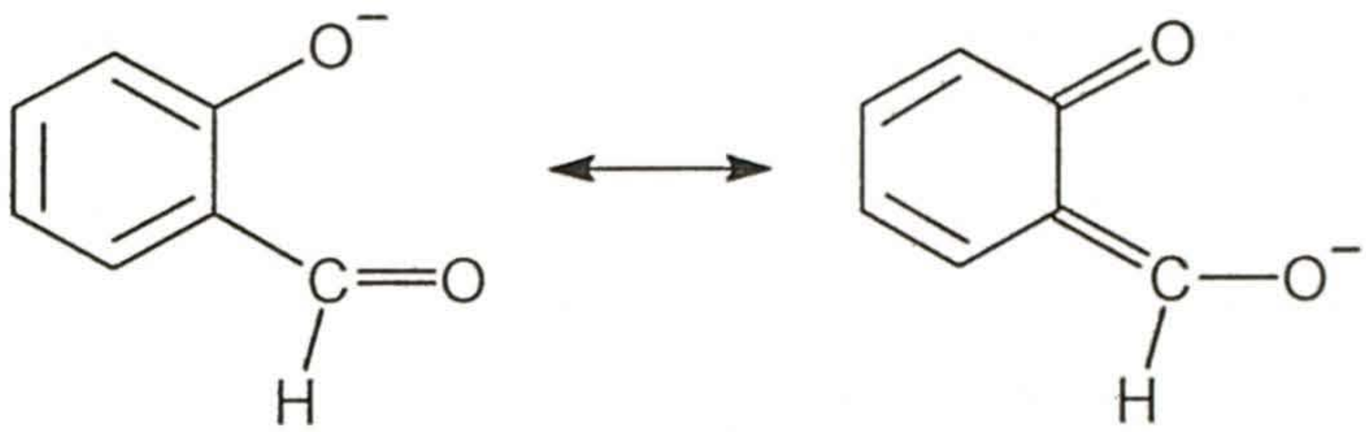

Scheme 2

exclusively on the phenolate-O. Delocalization of the charge can be envisaged through a resonating quinonoid structure as shown in scheme 2. Thus Ru-O1 and Ru-O2 bond lengths associated with the $salH^-$ fragment reflects the average of the two possible resonating structures in solid state. The lengthening of the C7-O2 bond length (1.249(6) Å) from the ideal C=O bond length (1.20 Å) is likely to be not only due to metal coordination by the keto-O but also due to the resonance. In the case of $[Ru(bpy)_2(salCl)]^+$, the same trends (Table 3.8) as noted for $[Ru(bpy)_2(salH)]^+$ are observed. Thus a similar resonance is also present in $salCl^-$. However, here the difference between the Ru-O1 (2.052(3) Å) and the Ru-O2 (2.067(4) Å) bond lengths though statistically insignificant is relatively more prominent. A possible reason may be the presence of the electron withdrawing substituent in the ring, which in principle can hinder the effective delocalization of the negative charge.

Table 3.8. Selected bond distances (Å) and angles (deg.)

$[Ru(bpy)_2(salH)]PF_6 \cdot CH_2Cl_2$			
Ru-O(1)	2.058(3)	Ru-N(2)	2.047(4)
Ru-O(2)	2.060(3)	Ru-N(3)	2.025(4)
Ru-N(1)	2.035(4)	Ru-N(4)	2.053(4)
C(1)-C(2)	1.417(7)	C(1)-C(6)	1.427(7)
C(2)-C(3)	1.353(9)	C(6)-C(7)	1.420(7)
C(3)-C(4)	1.393(10)	C(7)-O(2)	1.249(6)
C(4)-C(5)	1.357(10)	C(1)-O(1)	1.302(6)
C(5)-C(6)	1.417(8)		
N(1)-Ru-N(2)	79.58(16)	N(2)-Ru-O(2)	94.64(15)
N(1)-Ru-N(3)	92.67(15)	N(3)-Ru-N(4)	79.48(16)
N(1)-Ru-N(4)	99.06(14)	N(3)-Ru-O(1)	173.03(15)
N(1)-Ru-O(1)	87.63(14)	N(3)-Ru-O(2)	88.19(14)
N(1)-Ru-O(2)	174.22(14)	N(4)-Ru-O(1)	93.59(15)
N(2)-Ru-N(3)	96.58(15)	N(4)-Ru-O(2)	86.72(14)
N(2)-Ru-N(4)	175.80(15)	O(1)-Ru-O(2)	92.22(14)
N(2)-Ru-O(1)	90.33(14)		
$[Ru(bpy)_2(salCl)]PF_6 \cdot (CH_3)_2CO$			
Ru-O(1)	2.052(3)	Ru-N(2)	2.054(4)
Ru-O(2)	2.067(4)	Ru-N(3)	2.034(4)
Ru-N(1)	2.028(4)	Ru-N(4)	2.039(4)
C(1)-C(2)	1.420(7)	C(1)-C(6)	1.423(7)
C(2)-C(3)	1.363(8)	C(6)-C(7)	1.401(7)
C(3)-C(4)	1.398(9)	C(7)-O(2)	1.246(6)
C(4)-C(5)	1.326(8)	C(1)-O(1)	1.300(6)
C(5)-C(6)	1.440(7)		
N(1)-Ru-N(2)	79.24(16)	N(2)-Ru-O(2)	95.71(16)
N(1)-Ru-N(3)	91.94(16)	N(3)-Ru-N(4)	79.20(16)
N(1)-Ru-N(4)	97.04(16)	N(3)-Ru-O(1)	174.39(15)
N(1)-Ru-O(1)	87.52(15)	N(3)-Ru-O(2)	90.40(15)
N(1)-Ru-O(2)	174.72(14)	N(4)-Ru-O(1)	95.33(16)
N(2)-Ru-N(3)	99.37(16)	N(4)-Ru-O(2)	88.04(16)
N(2)-Ru-N(4)	176.01(17)	O(1)-Ru-O(2)	90.61(14)
N(2)-Ru-O(1)	86.02(15)		

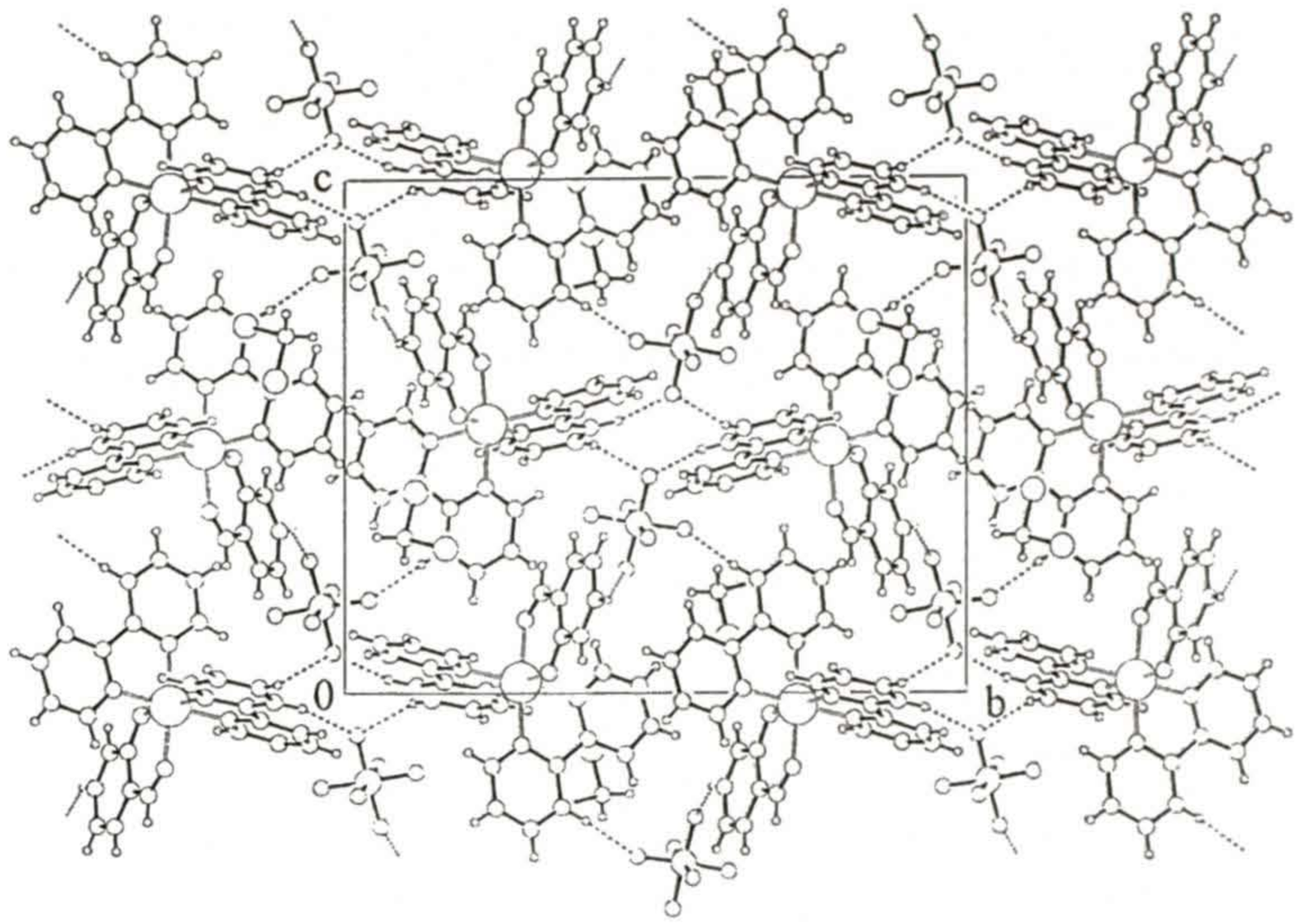

Figure 3.10. Two dimensional network of $[Ru(bpy)_2(salH)]PF_6$ formed *via* C-H····F hydrogen bonding.

In these two structures, we did not find any strong hydrogen bonding interactions. However, there are several weak hydrogen bonding interactions between C-H of bipyridine rings and F atoms of PF_6^- moiety.[27] In each case, these hydrogen bonding interaction form two dimensional network in the crystal lattice as shown in Figures 3.10 and 3.11. There is also one C-H···O interaction[28] between C-H of a bipyridine ring and acetone present in $[Ru(bpy)_2(salCl)]^+$. The H···F distances and C-H···F angles are within 2.37 – 2.52 Å and 126 – 160°, respectively. Whereas for C-H···O hydrogen bonding H···O distance and C-H···O angle are 2.57 Å and 134°, respectively.

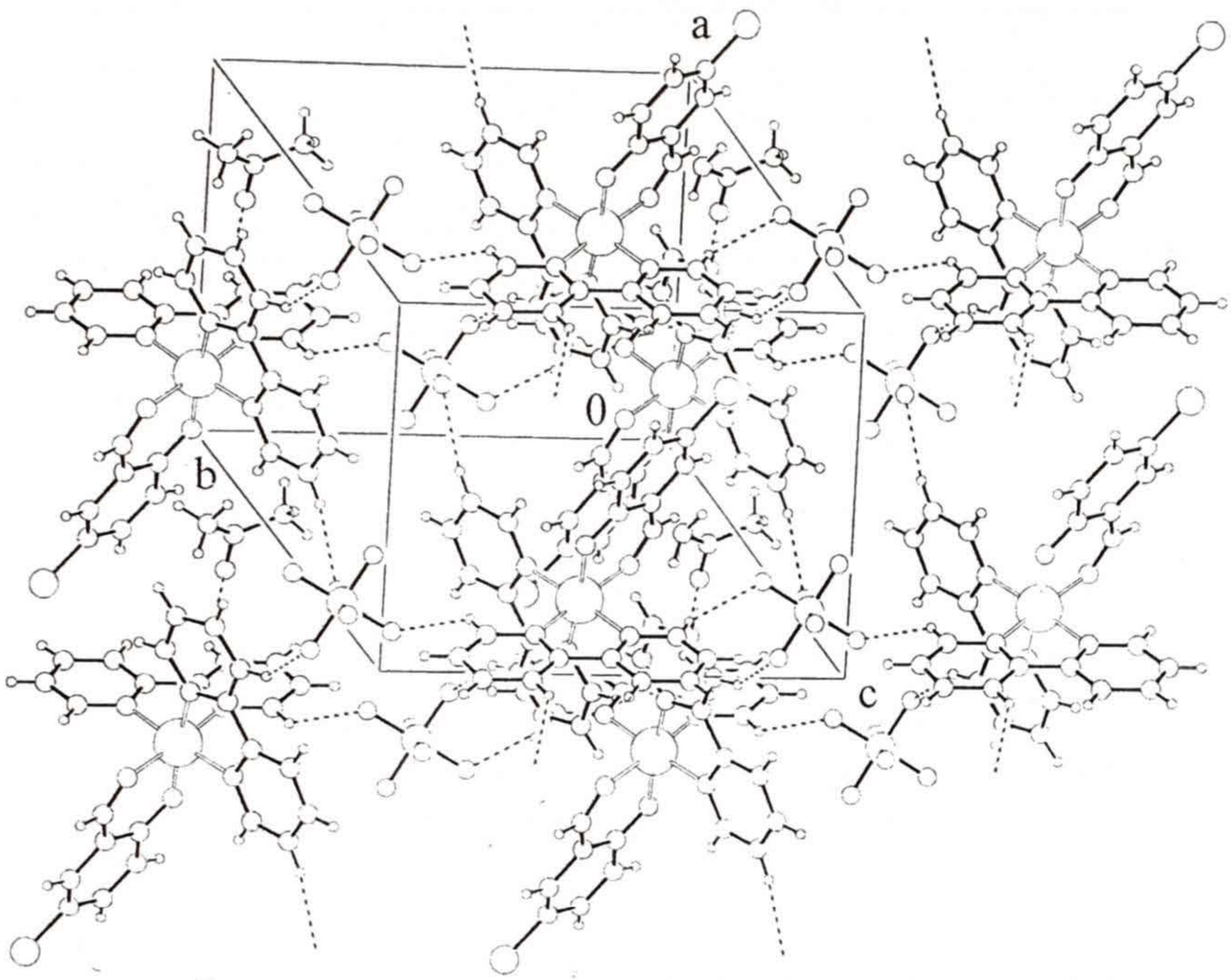

Figure 3.11. Two dimensional network of $[Ru(bpy)_2(salCl)]PF_6 \cdot (CH_3)_2CO$ formed *via* C-H····F hydrogen bonding.

3.5. Conclusion

Though our aim was to prepare diazine bridged dinuclear ruthenium(II) complexes from *cis*-$[Ru(bpy)_2Cl_2] \cdot 2H_2O$ and H_2salhnR but we have succeeded only in isolating mixed-ligand complexes of type $[Ru^{II}(bpy)_2(salR)]^+$ where $salR^-$ represents deprotonated salicylaldehyde or its 5-substituted derivatives. Hydrolysis at -C=N- moieties of H_2salhnR in each case leads to the formation of these mononuclear complexes.

The same complexes were synthesized from methanolic media by reacting *cis*-$[Ru(bpy)_2Cl_2]\cdot 2H_2O$, HsalR, and NaOH in 1:1:1 mole ratio. All the complexes show low energy electronic bands primarily due to the metal-to-bpy charge transfer. Solid state structures of two complexes have been determined. The Ru-O and the intraligand ($salR^-$) bond lengths suggest that the negative charge of the $salR^-$ ligand is delocalized between the phenolate-O and the keto-O through a quinonoid structure. The complexes are redox active and display reversible Ru(III)- Ru(II) couples with a systematic shift of potentials due to the electronic nature of the substituent.

3.6. References

1. (a) E. A. Seddon, K. R. Seddon, *The Chemistry of Ruthenium*, Elsevier, New York 1984. (b) K. R. Seddon, *Coord. Chem. Rev.*, **1985**, *67*, 171. (c) G. Wilkinson, R. D. Gillard, J. A. McCleverty, *Comprehensive Coordination Chemistry*, Pergamon, Oxford 1987, Vol. 4, p. 279. (d) W. -T. Wong, *Coord. Chem. Rev.*, **1994**, *131*, 45. (e) S. -M. Lee, W. -T. Wong, *Coord. Chem. Rev.*, **1997**, *164*, 415.
2. (a) B. K. Ghosh, A. Chakravorty, *Coord. Chem. Rev.*, **1989**, *95*, 239. (b) A. B. P. Lever, *Inorg. Chem.*, **1990**, *29*, 1271. (c) S. I. Gorelsky, E. S. Dodsworth, A. B. P. Lever, A. A. Vlcek, *Coord. Chem. Rev.*, **1998**, *174*, 469.
3. (a) T. J. Meyer, *Pure Appl. Chem.*, **1986**, *58*, 1193. (b) A. Juris, V. Balzani, F. Barigelletti, S. Campagna, P. Belser, A. von Zelewsky, *Coord. Chem. Rev.*, **1988**, *84*, 85. (c) K. Kalyanasundaram, *Photochemistry of Polypyridine and Porphyrin Complexes*, Academic Press, London 1992. (d) A. B. P. Lever, H. Masui, R. A. Metcalfe, D. J. Stufkens, E. S. Dodsworth, P. R. Auburn, *Coord. Chem. Rev.*, **1993**, *125*, 317. (e) J. -P. Sauvage, J. -P. Collin, J. -C. Chambron, S. Guillerez, C. Coudret, V. Balzani, F. Barigelletti, L. De Cola,

L. Flamigni, *Chem. Rev.*, **1994**, *94*, 993. (f) V. Balzani, A. Juris, M. Venturi, S. Campagna, S. Serroni, *Chem. Rev.*, **1996**, *96*, 759. (g) L. De Cola, P. Belser, *Coord. Chem. Rev.*, **1998**, *177*, 301. (h) K. Szaciowski, W. Macyk, G. Stochel, Z. Stasicka, S. Sostero, O. Traverso, *Coord. Chem. Rev.*, **2000**, *208*, 277. (i) M. Osawa, M. Hoshino, Y. Wakatsuki, *Angew. Chem., Int. Ed.*, **2001**, *40*, 3472. (j) H. Dürr, S. Bossmann, *Acc. Chem. Res.*, **2001**, *34*, 905. (k) C. A. Bignozzi, R. Argazzi, C. Chiorboli, S. Roffia, F. Scandola, *Coord. Chem. Rev.*, **1991**, *111*, 261.

4. (a) N. Bag, G. K. Lahiri, S. Bhattacharya, L. R. Falvello, A. Chakravorty, *Inorg. Chem.*, **1988**, *27*, 4396. (b) B. M. Holligan, J. C. Jeffery, M. K. Norgett, E. Schatz, M. D. Ward, *J. Chem. Soc., Dalton Trans.*, **1992**, 3345. (c) S. Choudhury, A. K. Deb, S. Goswami, *J. Chem. Soc., Dalton Trans.*, **1994**, 1305. (d) S. Chakraborty, M. G. Walawalkar, G. K. Lahiri, *J. Chem. Soc., Dalton Trans.*, **2000**, 2875.
5. (a) P. Belser, A. von Zelewsky, M. Zehnder, *Inorg. Chem.*, **1981**, *20*, 3098. (b) H. Masui, A. B. P. Lever, P. R. Auburn, *Inorg. Chem.*, **1991**, *30*, 2402. (c) H. Masui, A. B. P. Lever, E. S. Dodsworth, *Inorg. Chem.*, **1993**, *32*, 258. (d) F. Hartl, T. L. Snoeck, D. J. Stufkens, A. B. P. Lever, *Inorg. Chem.*, **1995**, *34*, 3887. (e) A. B. P. Lever, S. I. Gorelsky, *Coord. Chem. Rev.*, **2000**, *208*, 153.
6. (a). V. R. L. Constantino, H. E. Toma, L. F. C. de Oliveira, F. N. Rein, R. C. Rocha, D. de Oliveira Silva, *J. Chem. Soc., Dalton Trans.*, **1999**, 1735. (b) R. Samanta, B. Mondal, P. Munshi, G. K Lahiri, *J. Chem. Soc., Dalton Trans.*, **2001**, 1827. (c) D. P. Rillema, G. Allen, T. J. Meyer, D. Conrad, *Inorg. Chem.*, **1983**, *22*, 1617. (d) O. Ishitani, P. S. White, T. J. Meyer, *Inorg. Chem.*, **1996**, *35*, 2167. (e) A. Jurie, L. Prodi, A. Harriman, R. Ziessel, M. Hissler, A. El-ghayoury, F. Wu, E. C. Riesgo, R. P. Thummel, *Inorg. Chem.*, **2000**, *39*, 3590. (f) F. Wu, R. P. Thummel, *Inorg. Chim. Acta*, **2002**, *327*, 26.

(g) T. Hirao, K. Iida, *Chem. Commun.*, **2001**, 431. (h) L. H. Uppadine, M. G. B. Drew, P. D. Beer, *Chem. Commun.*, **2001**, 291.

7. (a) R. Alsfasser, R. van Eldik, *Inorg. Chem.*, **1996**, *35*, 628. (b) M. D. Ward, *Inorg. Chem.*, **1996**, *35*, 1712. (c) R. N. Mukherjee, A. Chakravorty, *J. Chem. Soc., Dalton Trans.*, **1983**, 2197.
8. (a) V. Balzani, A. Juris, M. Venturi, S. Campagna, S. Seroni, *Chem. Rev.*, **1996**, *96*, 759. (b) A. Harriman, R. Ziessel, *Chem. Commun.*, **1996**, 1707. (c) M. D. Ward, *Chem. Soc. Rev.*, **1995**, 121. (d) D. Gust, T. A. Moore, L. Moore, *Acc. Chem. Res.*, **1993**, *115*, 5975. (e) B. O'Regan, M. Gratzel, *Nature*, **1991**, *353*, 738. (f) V. Balzani, L. De Cola, Eds. *Supramolecular Chemistry;* Kluwer: Dordrecht, The Netherlands, 1992. (g) V. Balzani, F. Scandola, *Supramolecular Photochemistry;* Horwood: Chichester, UK., 1991.
9. B. P. Sullivan, D. J. Salmon, T. J. Meyer, *Inorg. Chem.*, **1978**, *17*, 3334.
10. D. T. Sawyer, J. L. Roberts, Jr., *Experimental Electrochemistry for Chemists*, Wiley, New York 1974, p. 208.
11. w, weak; m, medium; s, strong; vs, very strong.
12. A. C. T. North, D. C. Philips, F. S. Mathews, *Acta Crystallogr.*, **1968**, *A24*, 351.
13. L. J. Farrugia, *J. Appl. Crystallogr.*, **1999**, *32*, 837.
14. *XTAL3.4 User's Manual*, S. R. Hall, G. S. D. King, J. M. Stewart (eds), University of Western Australia, Perth 1995.
15. J. Riebenspies, Q & D Crystallographic Program Package, Texas A & M University, College Station, Texas 1989.
16. G. M. Sheldrick, SHELX-97, Structure Determination Software, University of Göttingen, Göttingen, Germany 1997.
17. (a) A. L. Spek, Platon, *Molecular Graphics Software*, University of Glasgow, UK, 2001. (b) L. J. Farrugia, *Ortep-3 for Windows*, *Version 1.074*, University of Glasgow, UK, 2002.

18. W. J. Geary, *Coord. Chem. Rev.*, **1971**, *7*, 81.
19. K. Nakamoto, *Infrared and Raman Spectra of Inorganic and Coordination Compounds*, John Wiley and Sons, New York 1986, p. 154 & 257.
20. G. M. Brown, T. R. Weaver, F. R. Keene, T. J. Meyer, *Inorg. Chem.*, **1976**, *15*, 190.
21. *Handbook of Proton NMR Spectra and Data*, Academic Press, Tokyo 1985, Vol. 2, p. 216, 263.
22. (a) S. K. Chandra, P. Basu, D. Ray, S. Pal, A. Chakravorty, *Inorg. Chem.*, **1990**, *29*, 2443. (b) J. Saroja, V. Manivannan, P. Chakraborty, S. Pal, *Inorg. Chem.*, **1995**, *34*, 3099. (c) S. N. Pal, S. Pal, *Inorg. Chem.*, **2001**, *40*, 4807.
23. J. March, *Advanced Organic Chemistry*, 4th Ed., Wiley, New York 1992, p. 280.
24. (a) D. P. Rillema, D. S. Jones, H. A. Levy, *J. Chem. Soc., Chem. Commun.*, **1979**, 849. (b) P. Passaniti, W. R. Browne, F. C. Lynch, D. Hughes, N. Nieuwenhuyzen, P. James, M. Maestri, J. G. Vos. *J. Chem. Soc., Dalton Trans.*, **2002**, 1740. (c) T. Togano, H. Kuroda, N. Nagao, Y. Maekawa, H. Nishimura, F. S. Howell, M. Mukaida, *Inorg. Chim. Acta*, **1992**, *196*, 57. (d) M. Mukaida, Y. Sato, H. Kato, M. Mori, D. Ooyama, H. Nagao, F. S. Howell, *Bull. Chem. Soc. Jpn.*, **2000**, *73*, 85. (e) M. Ruben, S. Rau, A. Skirl, K. Krause, H. Gorls, D. Walther, J. G. Vos, *Inorg. Chim. Acta*, **2000**, *303*, 206.
25. N. Bag, A. Pramanik, G. K. Lahiri, A. Chakravorty, *Inorg. Chem.*, **1992**, *31*, 40.
26. J. E. Huheey, E. A. Keiter, R. L. Keiter, *Inorganic Chemistry Principles of Structure and Reactivity*, 4th Ed., Addison-Wesley, Reading, Massachusetts 1993, p. A-30.
27. (a) V. R. Thalladi, H. -C. Weiss, D. Bläser, R. Boese, A. Nangia, G. R. Desiraju, *J. Am. Chem. Soc.*, **1998**, *120*, 8702. (b) L. Simoni, J. P. Glusker,

Struct. Chem., **1994**, *5*, 383. (c) H. C. Weiss, R. Boese, H. L. Smith, M. M. Haley, *Chem. Commun.*, **1997**, 2403.

28. (a) G. R. Desiraju, *Acc. Chem. Res.*, **1996**, *29*, 441. (b) S. N. Pal, K. R. Radhika, S. Pal, *Z. Anorg. Allg. Chem.*, **2001**, *627*, 1631. (c) G. R. Desiraju, *Angew. Chem., Int. Ed.*, **1995**, *34*, 2328. (d) T. Steiner, *Chem. Commun.*, **1997**, 727. (e) M. G. Davidson, A. E. Goeta, J. A. K. Howard, S. Lamb, S. A. Mason, *New J. Chem.*, **2000**, *24*, 477. (f) N. R. Sangeetha, S. Pal, *Polyhedron*, **2000**, *19*, 1593. (g) D. Braga, F. Grepioni, G. R. Desiraju, *Chem. Rev.*, **1998**, *98*, 1375. (h) J. -M. Lehn, *Angew. Chem., Int. Ed.*, **1990**, *29*, 1304. (i) P. N. W. Baxter, J. -M. Lehn, B. O. Kneisel, D. Fenske, *Angew. Chem., Int. Ed.*, **1997**, *36*, 1978.

CHAPTER 4

Ruthenium(II) Complexes with Imine-N, Pyridine-N and Amide-O Coordinating Schiff Bases*

4.1. Abstract

A series of ruthenium(II) complexes of general formula $[RuL_2]$ with the pyridine-N, the imine-N and the amide-O donor N-(aroyl)-N'-(picolinylidene)hydrazines (HL) has been synthesized. The ligands differ on the substituent at the *para* position of the aroyl fragment. The complexes have been characterized by analytical, ^1H NMR, electronic absorption spectroscopy and cyclic voltammetry. X-ray structures of representative complexes have been determined. The lowest energy MLCT ($Ru(d\pi) \rightarrow L(\pi^*)$) transitions for these complexes are observed at essentially identical wavelength (544 ± 1 nm). The complexes display a metal centered oxidation and a ligand-centered reduction in the potential ranges 0.44 to 0.59 V and -1.49 to -1.35 V (vs. Ag/AgCl), respectively. The differences in the metal and ligand redox potentials ($\Delta E_{1/2}$) are practically same (1.94 ± 0.01 V) for all the complexes. The identical MLCT band positions and the same $\Delta E_{1/2}$ values suggest that in this series of complexes, the energy gap between the metal-$d\pi$ and the ligand-π^* levels is constant. The effective pK_a values of the species obtained by protonation of the coordinated amide functionalities in one of the complexes have been evaluated by spectrophotometric titration. The corresponding diprotonated species has been characterized by X-ray crystallography.

*This work has been published in *J. Chem. Soc., Dalton Trans.*, **2002**, 2102.

4.2. Introduction

In the last two chapters, we have studied the complexation behavior of H_2salhnR with $[Ru(PPh_3)_3Cl_2]$ and *cis*-$[Ru(bpy)_2Cl_2]$. With $[Ru(PPh_3)_3Cl_2]$ this Schiff base system forms dinuclear ruthenium(III) species. Whereas with *cis*-$[Ru(bpy)_2Cl_2]$, H_2salhnR affords mononuclear ruthenium(II) species $[Ru(bpy)_2(salR)]^+$ (where $salR^-$ is 5-substituted deprotonated salicylaldehyde generated by the hydrolysis of H_2salhnR).

In this chapter, we have studied the ruthenium(II) chemistry with tridentate N-(aroyl)-N'-(picolinylidene)hydrazines (HL) (Figure 4.1). In deprotonated state, these Schiff bases can coordinate ruthenium(II) *via* the pyridine-N, the imine-N and the amide-O atoms and form neutral *bis*-chelates.

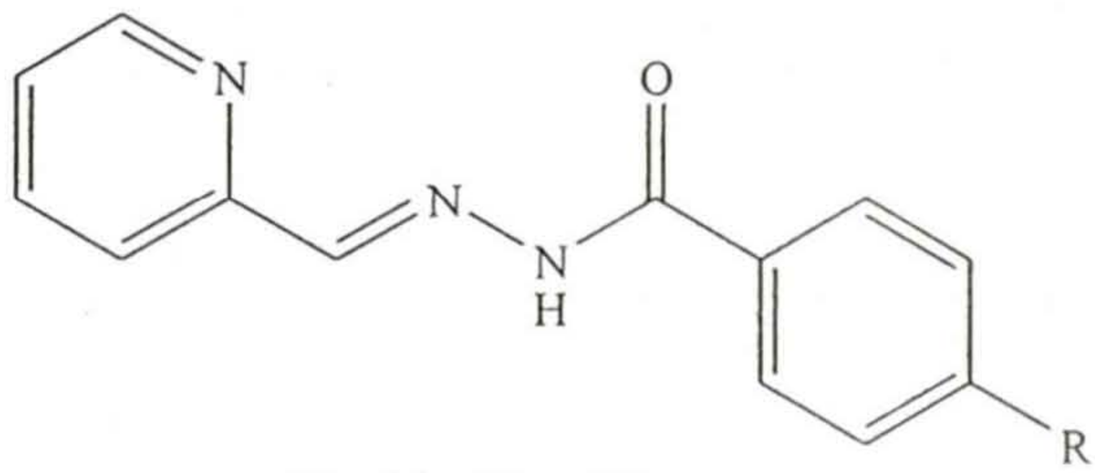

Hpabh (R = H)
Hpach (R = Cl)
Hpath (R = Me)
Hpamh (R = OMe)
Hpadh (R = NMe_2)

Figure 4.1

Complexes of ruthenium(II) with α,α'-diimine ligands particularly bipyridine[1] and its derivatives are most extensively studied for their redox, photophysical and photochemical properties that are determined by the availability of low lying π* orbitals of the coordinated ligands and hence a low energy metal-to-ligand charge transfer excited state. These properties have led to increased

utilization of such ruthenium complexes in the studies on artificial photosynthesis,[2] photomolecular devices[3] and protein and DNA structures and electron transfer in them.[4] Due to such wide range of applications there is a continuing quest for new ruthenium(II) complexes with different ligands containing the α,α'-diimine fragment[5,6] or with derivatives of polypyridine ligands.[7] The primary goal is to improve their efficiency in the above mentioned applications by modification of the coordinated ligands.

The reasons for the choice of N-(aroyl)-N'-(picolinylidene)hydrazines (HL) to study ruthenium chemistry are as follows. Like 2,2'-bipyridine they also contain the α,α'-diimine fragment, which is π-acidic and can form a five-membered chelate ring with metal ions. The third coordinating center, the O-atom of the deprotonated amide functionality is predominantly σ-basic, which is opposite in character compared to the diimine fragment. The σ-basicity of this coordinating atom can be varied by using different substituents at the *para* position of the aroyl moiety. Thus the electron transfer properties of the complexes can be tuned by this variation. In addition to the above, this ligand system provides the scope of studying the effect of coordinated amide protonation state on the physical properties of the complex. Herein, we describe the synthesis and characterization of a new series of ruthenium(II) complexes with the above ligand system. X-ray structures of representative complexes have been determined. In solutions, electron transfer and spectral properties, and protonation behavior of the coordinated amide have been investigated.

4.3. Experimental Section

4.3.1. Materials

cis-[$Ru(dmso)_4Cl_2$] was prepared by following a reported procedure.[8] The Schiff bases were obtained in 80-90% yield by the condensation of one mole of picolinaldehyde with one mole of the corresponding aroylhydrazine in methanol.[9] Acetonitrile used for electrochemical and spectral studies was purified and dried according to a reported method.[10] All other chemicals and solvents used were of analytical grade available commercially and were used without further purification.

4.3.2. Physical measurements

All the physical measurements were performed as described in the previous chapters.

4.3.3. Synthesis of complexes

The complexes, [$Ru(padh)_2$] (**1**), [$Ru(pamh)_2$] (**2**), [$Ru(path)_2$] (**3**), [$Ru(pabh)_2$] (**4**), and [$Ru(pach)_2$] (**5**), reported in this chapter were synthesized by the same general procedure in similar yields. Details are therefore given for a representative case.

[$Ru(pabh)_2$] (4)

To a yellow solution of Hpabh (101 mg, 0.45 mmol) and NaOH (18 mg, 0.45 mmol) in methanol (30 ml) was added solid *cis*-[$Ru(dmso)_4Cl_2$] (108 mg, 0.22 mmol). The mixture was refluxed for 12 h and then cooled to room temperature. The brown solid precipitated was collected by filtration, washed with ice-cold methanol and dried in vacuum. The purification of the complex was

performed on a neutral aluminium oxide column. The first moving purple band was eluted with acetone-dichloromethane-hexane (1:5:5) mixture. This was collected and evaporated. The solid thus obtained was recrystallized from a mixture of dichloromethane-hexane (1:1). Yield: 50 mg (41%).

Selected IR bands[11] *(cm^{-1})*: 1593(m), 1471(s), 1452(s), 1413(s), 1361(s), 1140(m), 1049(m), 814(m), 702(s), 542(w).

Selected IR bands[11] (cm^{-1}) for the other four complexes are as follows:

*$[Ru(padh)_2]$ **(1)**:* 1604(vs), 1531(w), 1437(w), 1352(vs), 1188(s), 1047(m), 943(m), 823(m), 758(m), 621(w), 547(w).

*$[Ru(pamh)_2]$ **(2)**:* 1604(s), 1516(m), 1440(s), 1365(s), 1250(s), 1167(s), 1049(s), 912(w), 839(m), 756(m), 628(w), 549(w).

*$[Ru(path)_2]$ **(3)**:* 1606(m), 1469(m), 1427(s), 1361(s), 1286(m), 1174(m), 1138(m), 1047(m), 914(m), 833(m), 744(s), 547(w), 482(w).

*$[Ru(pach)_2]$ **(5)**:* 1593(m), 1466(s), 1433(s), 1361(s), 1282(m), 1209(m), 1140(m), 1084(w), 1053(m), 1008(m), 916(m), 843(m), 746(s), 572(s), 482(w).

4.3.4. Spectrophotometric titration

In a typical titration, a 3 ml aliquot of a stock solution of $[Ru(pabh)_2]$ in acetonitrile (3.66×10^{-5} M, prepared by dissolving 2.01 mg (3.66 μmol) of $[Ru(pabh)_2]$ in 10 ml of acetonitrile and then diluting 1 ml of this solution to 10 ml by adding the same solvent) was taken in an airtight cuvette. Protonation of $[Ru(pabh)_2]$ was performed by addition of aliquots (2 μL) of an acetonitrile solution of CF_3SO_3H (5.65×10^{-3} M, prepared by dissolving 0.5 ml (5.65 mmol) in 10 ml of acetonitrile and then diluting 0.1 ml of this solution to 10 ml by adding the same solvent) with a gastight syringe. Protonation was considered complete when no significant change of the electronic spectrum was observed by further addition of CF_3SO_3H solution.

4.3.5. Single crystal X-ray structure determination

Single crystals of $[Ru(path)_2]$ (**3**) and $[Ru(pabh)_2]$ (**4**) were grown by slow evaporation of CH_2Cl_2-hexane (1:1) solutions. Slow evaporation of a CH_3CN-toluene (1:1) solution of $[Ru(pabh)_2]$ (**4**) and $HClO_4$ (1:2.5 mole ratio) in air at room temperature produced the single crystals of $[Ru(Hpabh)_2(CH_3CN)_2](ClO_4)_2 \cdot H_2O$ (**6**). The data were collected on an Enraf-Nonius Mach-3 single crystal diffractometer using graphite monochromated Mo Kα radiation (λ = 0.71073 Å) by ω-scan method at room temperature (298 K). Unit cell parameters were determined by the least-squares fit of machine-centered 25 reflections. In each case, the stability of the crystal was monitored by measuring the intensities of three check reflections after every 1.5 h during the data collection. No decay was observed in any case. The data were corrected for Lorentz-polarization effects. An empirical absorption correction was applied on the data sets based on Ψ-scans.[12] The structures were solved by direct methods and refined by full-matrix least-squares on F^2. All the three complexes crystallize in the $P2_1/n$ space group. In each case, the asymmetric unit contains a single molecule of the complex. In the case of $[Ru(path)_2]$, the tolyl ring (C22-C27, Figure 4.11) of one of the ligands is disordered. The ring plane has two orientations. Three C-atoms (C22, C25 and C28) are common to both planes. Each of the other four C-atoms (C23, C24, C26 and C27) is found at two positions and refined with half occupancy. The oxygen of the water molecule in $[Ru(Hpabh)_2(CH_3CN)_2](ClO_4)_2 \cdot H_2O$ (**6**) was located at two sites and each was refined with half occupancy. For $[Ru(path)_2]$ (**3**) and $[Ru(pabh)_2]$ (**4**) all the non-hydrogen atoms and for $[Ru(Hpabh)_2(CH_3CN)_2](ClO_4)_2 \cdot H_2O$ (**6**) except the disordered water oxygen, all other non-hydrogen atoms were refined anisotropically. Hydrogen atoms were added at calculated positions by using riding model for structure factor calculation, but not refined. Calculations were done using the programs of WinGX[13] for data reduction and absorption correction, and SHELX-97 programs[14] for structure solution and refinement. ORTEX6a[15a] and Platon programs[15b] were used for molecular graphics. Significant crystal data are summarized in Table 4.1.

Table 4.1. Crystal and structure refinement data for $[Ru(path)_2]$ (**3**), $[Ru(pabh)_2]$ (**4**), and $[Ru(Hpabh)_2(CH_3CN)_2](ClO_4)_2 \cdot H_2O$ (**6**)

Complex	**3**	**4**	**6**
Chemical formula	$C_{28}H_{24}N_6O_2Ru$	$C_{26}H_{20}N_6O_2Ru$	$C_{30}H_{30}N_8O_{11}Cl_2Ru$
Formula weight	577.60	549.55	850.59
Space group	Monoclinic, $P2_1/n$	Monoclinic, $P2_1/n$	Monoclinic, $P2_1/n$
a, Å	8.7422(17)	9.5802(14)	10.750(2)
b, Å	8.6826(19)	23.874(3)	27.396(5)
c, Å	33.738(5)	10.3378(12)	13.087(2)
β, deg.	94.986(15)	105.102(13)	95.054(16)
V, Å^3	2551.2(8)	2282.8(5)	3839.3(12)
Z	4	4	4
ρ_{calcd}, g cm^{-3}	1.504	1.599	1.472
μ, mm^{-1}	0.652	0.724	0.612
Reflections collected/ Unique	4822/4492	4133/4014	6875/6707
Reflections $I > 2\sigma(I)$ /parameters	2882/372	2893/316	4251/470
R1,[a] wR2[b] $[I>2\sigma(I)]$	0.0518, 0.1079	0.0389, 0.0660	0.0705, 0.1912
R1,[a] wR2[b] (all data)	0.1021, 0.1258	0.0716, 0.0754	0.1176, 0.2231
Goodness-of-fit[c] on F^2	1.047	1.03	1.025
$\Delta\rho_{max/min}$ e Å^{-3}	0.88, -0.66	0.29, -0.30	1.25, -0.93

[a] $R1 = \sum||F_o| - |F_c||/\sum|F_o|$. [b] $wR2 = \{\sum[(F_o^2 - F_c^2)^2]/\sum[w(F_o^2)^2]\}^{1/2}$.

[c] $GOF = \{\sum[w(F_o^2 - F_c^2)^2]/(n - p)\}^{1/2}$ where 'n' is the number of reflections and 'p' is the number of parameters refined; $w = 1/[\sigma^2(F_o^2) + (aP)^2 + bP]$ where a = 0.0513 and b = 2.7435 for **3**; a = 0.0269 and b = 1.3055 for **4**; a = 0.1121 and b = 14.1446 for **6**.

Table 4.2. Atomic coordinates (x 10^4) and equivalent isotropic displacement parameters[a] (Å^2 x 10^3) for [Ru(path)$_2$]

Atom	x	y	z	U(eq)
Ru	6953(1)	656(1)	1236(1)	40(1)
O(1)	8006(4)	-1521(4)	1304(1)	42(1)
O(2)	8848(4)	1547(5)	965(1)	50(1)
N(1)	6200(6)	2750(5)	1419(1)	47(1)
N(2)	7635(5)	585(6)	1805(1)	39(1)
N(3)	8369(5)	-709(6)	1959(1)	42(1)
N(4)	4829(5)	-219(6)	1249(1)	48(1)
N(5)	6248(6)	699(7)	669(1)	55(1)
N(6)	7196(6)	1264(7)	397(2)	67(2)
C(1)	5424(8)	3841(8)	1204(2)	61(2)
C(2)	4905(10)	5150(9)	1377(2)	80(2)
C(3)	5204(9)	5372(8)	1779(2)	76(2)
C(4)	6010(8)	4303(7)	1998(2)	58(2)
C(5)	6509(7)	2984(7)	1815(2)	46(1)
C(6)	7332(7)	1760(7)	2024(2)	48(2)
C(7)	8497(6)	-1708(6)	1670(2)	39(1)
C(8)	9271(6)	-3186(7)	1779(2)	42(1)
C(9)	10048(7)	-3438(7)	2148(2)	54(2)
C(10)	10779(8)	-4809(8)	2237(2)	63(2)
C(11)	10771(7)	-5979(7)	1965(2)	61(2)
C(12)	10008(7)	-5737(8)	1595(2)	64(2)
C(13)	9277(7)	-4362(8)	1501(2)	52(2)
C(14)	11569(10)	-7485(8)	2055(3)	95(3)
C(15)	4097(7)	-644(7)	1562(2)	51(2)
C(16)	2610(8)	-1179(8)	1532(2)	66(2)
C(17)	1843(9)	-1279(11)	1167(3)	95(3)
C(18)	2579(10)	-907(14)	847(3)	127(4)
C(19)	4034(8)	-338(10)	888(2)	73(2)
C(20)	4892(8)	192(12)	567(2)	97(3)
C(21)	8508(7)	1661(7)	587(2)	51(2)

C(22)	9711(8)	2278(8)	347(2)	54(2)
C(23)	10710(3)	3390(2)	495(7)	87(7)
C(24)	11890(3)	3920(3)	268(8)	101(9)
C(26)	11188(17)	2120(2)	-237(4)	65(4)
C(27)	9991(16)	1559(16)	-11(4)	54(3)
C(23')	11160(2)	2500(2)	497(6)	58(5)
C(24')	12320(2)	2970(2)	272(7)	72(6)
C(26')	10447(18)	3290(2)	-281(4)	71(4)
C(27')	9280(17)	2828(19)	-53(4)	66(4)
C(25)	12027(9)	3349(11)	-117(2)	76(2)
C(28)	13265(10)	3878(11)	-359(3)	111(3)

[a] U(eq) is defined as one third of the trace of the orthogonalized Uij tensor.

Table 4.3. Atomic coordinates (x 10^4) and equivalent isotropic displacement parameters[a] ($Å^2$ x 10^3) for $[Ru(pabh)_2]$

Atom	x	y	z	U(eq)
Ru	6521(1)	995(1)	8659(1)	35(1)
O(1)	4644(3)	1338(1)	9113(3)	44(1)
O(2)	7988(3)	1412(1)	10251(3)	41(1)
N(1)	8078(3)	944(1)	7647(3)	37(1)
N(2)	5856(3)	1568(1)	7279(3)	36(1)
N(3)	4586(3)	1853(1)	7198(3)	41(1)
N(4)	5299(3)	335(1)	7741(3)	38(1)
N(5)	7280(3)	389(1)	9926(3)	36(1)
N(6)	8451(4)	494(1)	11006(3)	41(1)
C(1)	9259(4)	624(2)	7885(4)	46(1)
C(2)	10224(5)	633(2)	7107(5)	54(1)
C(3)	10016(4)	996(2)	6054(4)	56(1)
C(4)	8823(5)	1348(2)	5812(4)	48(1)
C(5)	7869(4)	1318(2)	6599(4)	39(1)
C(6)	6604(4)	1655(2)	6420(4)	42(1)
C(7)	4056(4)	1697(2)	8200(4)	39(1)
C(8)	2659(4)	1962(2)	8232(4)	42(1)

C(9)	1983(4)	2336(2)	7224(4)	53(1)
C(10)	668(5)	2571(2)	7232(6)	65(1)
C(11)	21(5)	2434(2)	8199(6)	73(2)
C(12)	657(6)	2068(2)	9188(6)	69(2)
C(13)	1995(5)	1830(2)	9226(5)	55(1)
C(14)	4224(5)	327(2)	6614(4)	52(1)
C(15)	3438(5)	-144(2)	6147(5)	63(1)
C(16)	3740(5)	-630(2)	6874(4)	59(1)
C(17)	4826(5)	-637(2)	8037(4)	49(1)
C(18)	5603(4)	-154(2)	8465(4)	41(1)
C(19)	6753(4)	-113(2)	9661(4)	42(1)
C(20)	8719(4)	1038(2)	11050(4)	40(1)
C(21)	10002(4)	1227(2)	12115(4)	41(1)
C(22)	11186(5)	874(2)	12572(4)	54(1)
C(23)	12386(5)	1057(2)	13500(4)	60(1)
C(24)	12440(5)	1586(2)	14025(4)	60(1)
C(25)	11287(5)	1939(2)	13570(5)	66(1)
C(26)	10089(5)	1762(2)	12611(4)	56(1)

[a] U(eq) is defined as one third of the trace of the orthogonalized Uij tensor.

Table 4.4. Atomic coordinates.(x 10^4) and equivalent isotropic displacement parameters[a] ($Å^2$ x 10^3) for $[Ru(Hpabh)_2(CH_3CN)_2](ClO_4)_2 \cdot H_2O$

Atom	x	y	z	U(eq)
Ru	7496(1)	1906(1)	6546(1)	41(1)
Cl(1)	7126(3)	557(1)	3597(3)	95(1)
Cl(2)	12545(2)	1871(1)	6586(2)	63(1)
O(1)	9861(8)	2055(3)	3619(7)	126(3)
O(2)	6951(11)	1622(4)	9947(6)	167(5)
O(3)	7393(8)	991(3)	3100(7)	118(3)
O(4)	7577(9)	620(3)	4660(7)	125(3)
O(5)	5783(9)	503(4)	3514(10)	165(5)
O(6)	7712(11)	155(3)	3206(8)	143(4)
O(7)	11558(9)	1626(4)	6902(9)	147(4)

O(8)	12200(13)	2063(5)	5655(8)	188(6)
O(9)	12857(13)	2231(5)	7265(9)	204(7)
O(10)	13594(11)	1627(6)	6534(15)	252(9)
O(11)	4040(2)	4332(10)	6140(2)	178(9)
O(11A)	620(3)¯	-451(13)	9890(3)	248(14)
N(1)	6404(5)	2441(2)	5864(4)	44(1)
N(2)	8136(6)	1943(2)	5118(5)	50(2)
N(3)	9020(6)	1622(3)	4799(5)	59(2)
N(4)	8681(5)	2439(2)	7172(5)	47(2)
N(5)	6891(6)	1989(2)	7983(5)	45(2)
N(6)	5970(6)	1711(3)	8362(5)	56(2)
N(7)	6226(6)	1380(2)	6079(5)	53(2)
N(8)	8678(6)	1355(2)	7042(5)	52(2)
C(1)	5417(7)	2653(3)	6237(7)	58(2)
C(2)	4743(8)	3023(3)	5711(7)	65(2)
C(3)	5095(9)	3176(4)	4804(8)	77(3)
C(4)	6109(9)	2954(4)	4380(7)	72(3)
C(5)	6731(7)	2581(3)	4937(6)	52(2)
C(6)	7706(7)	2301(3)	4539(6)	53(2)
C(7)	9808(8)	1679(3)	4070(6)	56(2)
C(8)	10616(7)	1266(3)	3899(6)	57(2)
C(9)	10677(12)	858(5)	4483(10)	105(4)
C(10)	11452(12)	458(5)	4246(13)	122(5)
C(11)	12196(13)	516(7)	3476(14)	130(6)
C(12)	12180(17)	946(8)	2905(16)	160(8)
C(13)	11372(12)	1303(5)	3119(10)	106(4)
C(14)	9635(7)	2653(3)	6763(7)	56(2)
C(15)	10311(9)	3027(4)	7239(9)	77(3)
C(16)	9992(10)	3199(4)	8186(9)	84(3)
C(17)	9035(10)	2970(3)	8623(7)	73(3)
C(18)	8397(8)	2596(3)	8124(6)	53(2)
C(19)	7405(7)	2332(3)	8533(6)	54(2)
C(20)	6058(10)	1526(4)	9332(8)	87(3)
C(21)	5079(11)	1186(4)	9567(9)	98(4)

C(22)	5270(13)	932(5)	10514(10)	122(5)
C(23)	4380(18)	614(5)	10836(13)	152(7)
C(24)	3233(19)	575(9)	10149(19)	271(17)
C(25)	3176(19)	785(10)	9350(2)	540(4)
C(26)	4106(14)	1092(8)	9061(15)	310(2)
C(27)	5539(9)	1077(4)	5886(8)	69(3)
C(28)	4628(12)	685(5)	5640(11)	128(5)
C(29)	9323(8)	1032(4)	7227(7)	65(2)
C(30)	10133(12)	617(4)	7433(11)	120(5)

[a] U(eq) is defined as one third of the trace of the orthogonalized Uij tensor.

4.4. Results and discussion

4.4.1. Synthesis and some properties

The dark brown complexes were synthesized in good yields by reacting *cis*-$[Ru(dmso)_4Cl_2]$, HL and NaOH in 1:2:2 mole ratio in boiling methanol. In each case, the complex was precipitated from the reaction mixture. However, chromatographic purification was necessary on a neutral aluminium oxide column. Elemental analysis data (Table 4.5) are satisfactory with the molecular formula $[RuL_2]$ (L^- = $pach^-$, $pabh^-$, $path^-$, $pamh^-$ and $padh^-$). All the complexes are electrically non-conducting in CH_3CN solutions. They are diamagnetic and NMR active. Thus the metal ions in these complexes are in +2 oxidation state and low-spin in character.

Table 4.5. Elemental analysis data[a]

Complex	C(%)	H(%)	N(%)
$[Ru(padh)_2]$	56.41 (56.68)	4.69 (4.76)	17.50 (17.62)
$[Ru(pamh)_2]$	54.95 (55.17)	3.86 (3.97)	13.64 (13.79)
$[Ru(path)_2]$	58.06 (58.22)	4.31 (4.19)	14.39 (14.55)
$[Ru(pabh)_2]$	56.70 (56.82)	3.74 (3.67)	15.14 (15.29)
$[Ru(pach)_2]$	50.13 (50.49)	2.84 (2.93)	13.31 (13.59)

[a] Calculated values are given in parentheses.

4.4.2. Infrared spectral properties

In the infrared spectra, none of the complexes displays the characteristic bands associated with the N-H and C=O bonds of the amide functionality[16]

present in the free Schiff bases. Thus in each complex the amide functionality is deprotonated and exists in the enolate form. A medium to strong band observed in the range 1593-1605 cm^{-1} is possibly due to the conjugate C=N-N=C fragment[17] of the coordinated ligand.

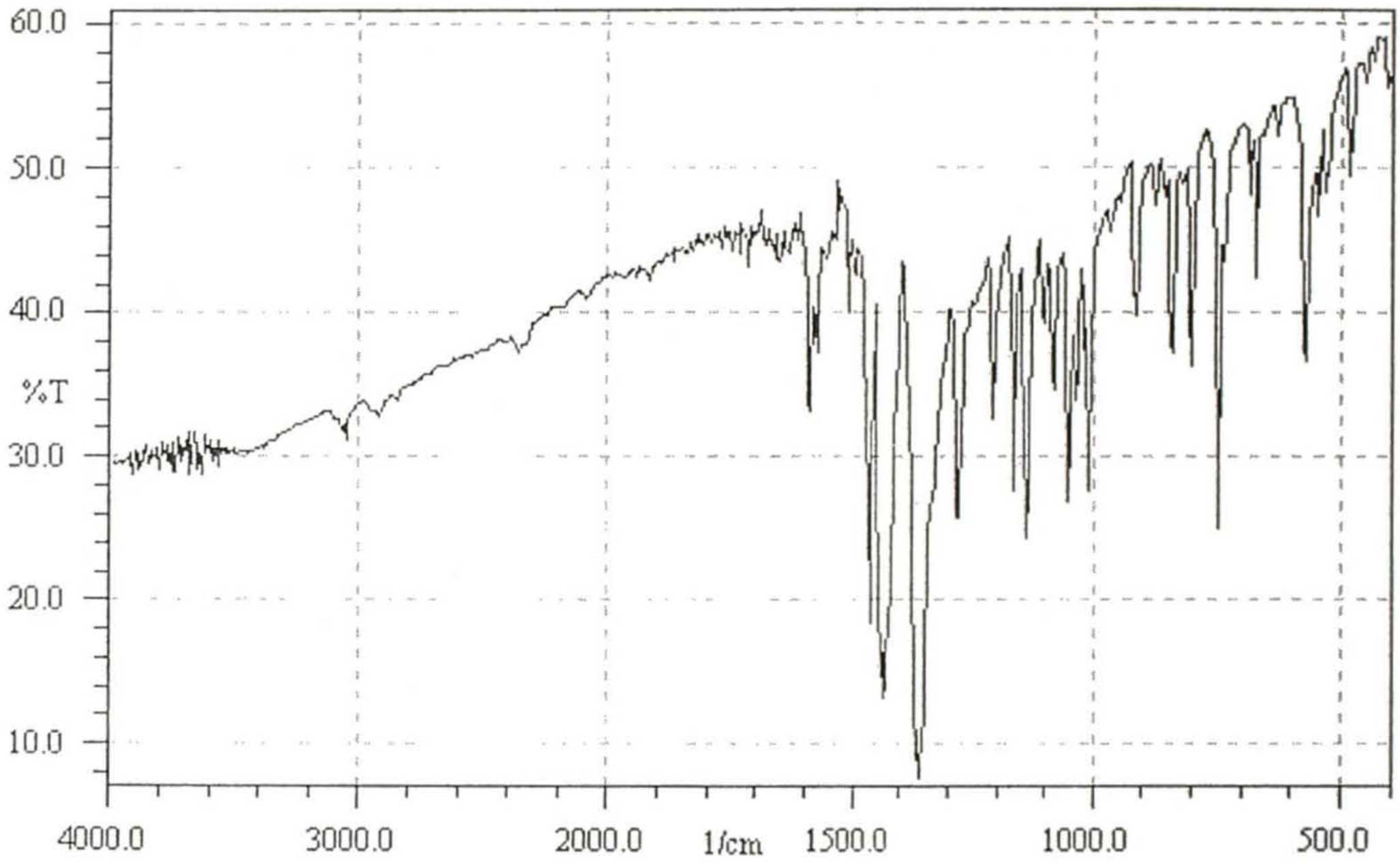

Figure 4.2. Infrared spectrum of $[Ru(pach)_2]$ in KBr disc.

4.4.3. NMR spectral properties

The proton NMR spectra of all the five complexes clearly suggest that in solutions both ligands in each complex are magnetically equivalent. The azomethine hydrogen appears as a singlet in the range 8.75-8.89 δ. An interesting observation is that as the electron donating ability of the substituent on the aroyl

moiety of the ligand increases the signal corresponding to the azomethine proton displays a high-field shift. For the three complexes, $[Ru(padh)_2]$, $[Ru(pamh)_2]$ and $[Ru(path)_2]$ the methyl protons of the substituent on the aroyl fragment of the ligands are observed as singlet at 2.98, 3.81 and 2.36 δ, respectively. Aromatic protons resonate in the range 6.58-8.13. H6 in all spectra (Table 4.6) appears as doublet and H4 as multiplet. In $[Ru(pabh)_2]$, H10 and H14 appear as multiplet, whereas these two protons appear as doublet in other four complexes. H11/H13 and H3/H5 appear as muliplet in $[Ru(pabh)_2]$ and $[Ru(pach)_2]$. In other three complexes, these four protons appear in two sets as doublets (Table 4.6). H11 and H13 appear in up field region compared to the H3 and H5. This is possibly due to the electron releasing nature of the substituents.

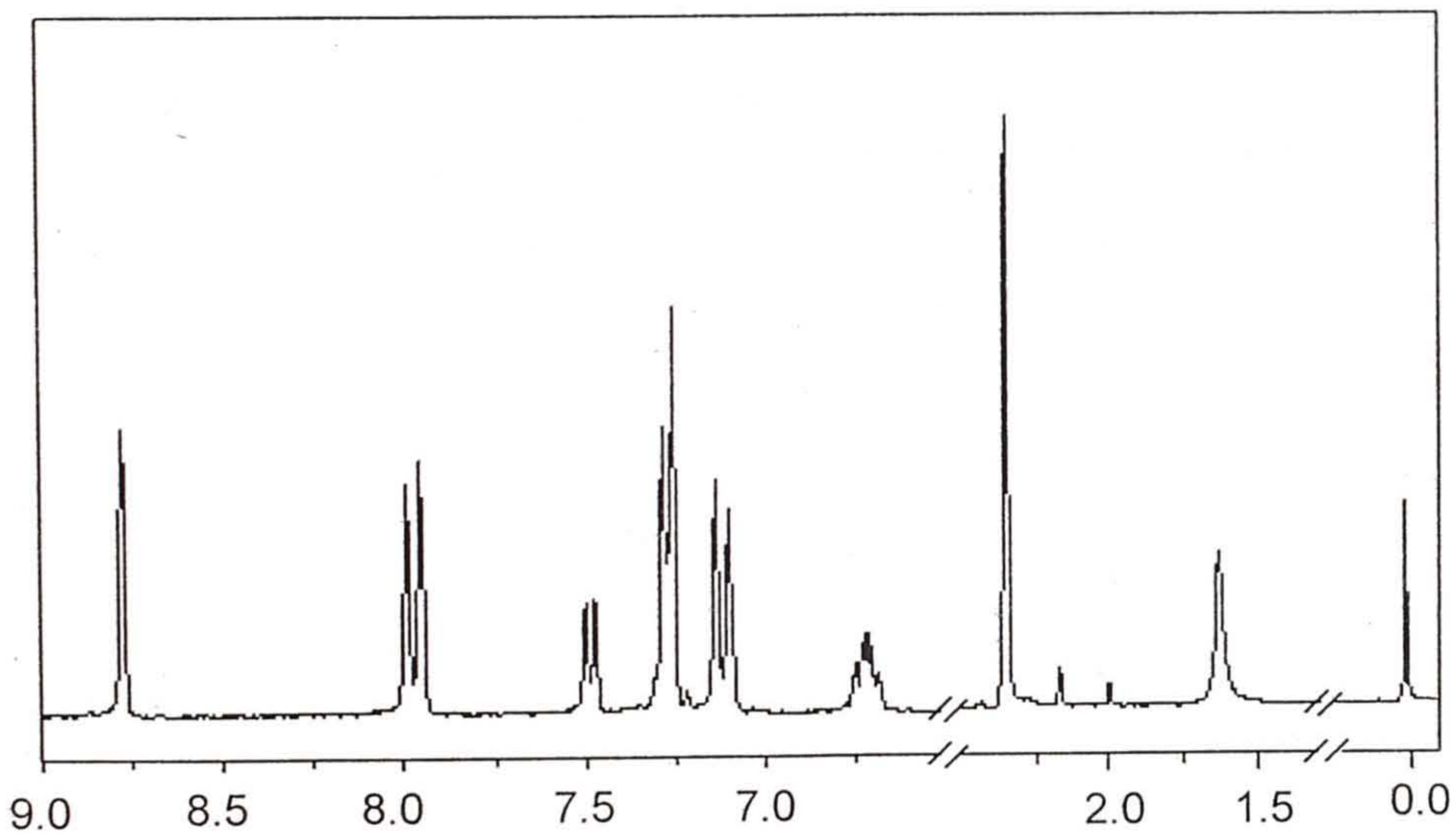

Figure 4.3. ^1H NMR spectrum of $[Ru(path)_2]$ in $CDCl_3$ solution.

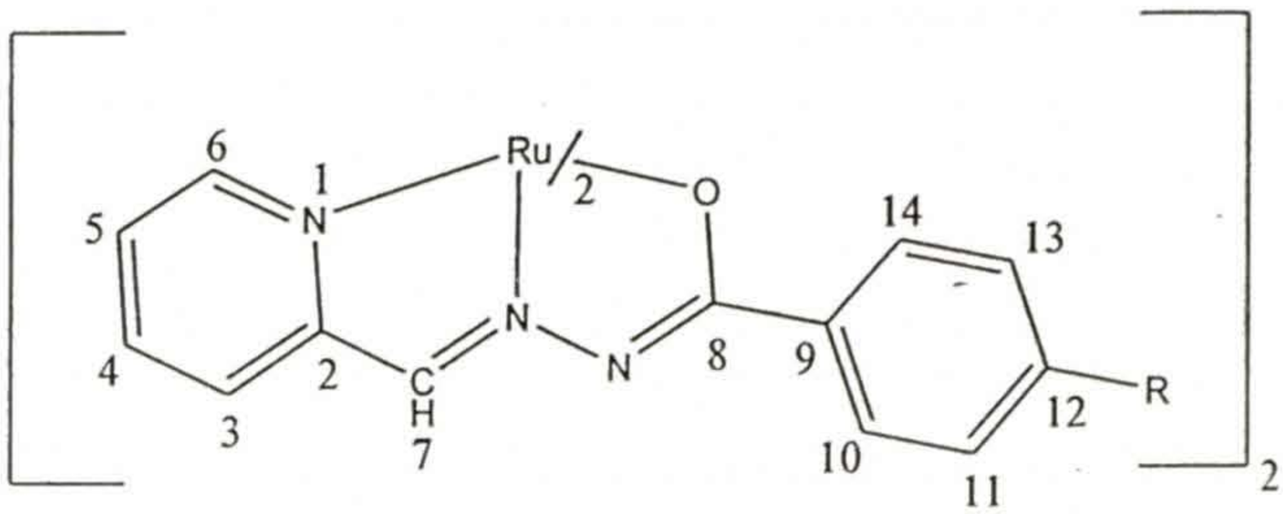

[Ru(padh)$_2$] R = NMe_2
[Ru(pamh)$_2$] R = OMe
[Ru(path)$_2$] R = CH_3
[Ru(pabh)$_2$] R = H
[Ru(pach)$_2$] R = Cl

Table 4.6. ^{1}H NMR spectral data[a] (δ) (J (Hz)) in $CDCl_3$

Complex	H7	H10/H14	H6	H11/H13 & H3/H5	H4	Methyl protons
[Ru(padh)$_2$]	8.75 s	7.97 - 8.02 d (6)	7.47 d (6)	6.60 d (12) (H11/H13); 7.21 - 7.26 m (H3/H5)	6.64 - 6.70 m	2.98 s -NMe_2
[Ru(pamh)$_2$]	8.78 s	8.05 d (8)	7.48 d (6)	6.82 d (8) (H11/H13); 7.27 d (6) (H3/H5)	6.69 - 6.76 m	3.81 s -OMe
[Ru(path)$_2$]	8.78 s	7.97 d (8)	7.49 d (8)	7.12 d (8) (H11/H13); 7.27 d (6) (H3/H5)	6.68 - 6.76 m	2.36 s -CH_3
[Ru(pabh)$_2$]	8.80 s	8.06 - 8.13 m	7.50 d (6)	7.26 - 7.37 m	6.70 - 6.78 m	
[Ru(pach)$_2$]	8.89 s	8.01 d (8)	7.47 d (4)	7.26 - 7.34 m	6.74 - 6.81 m	

s, singlet; d, doublet; t, triplet; m, multiplet

4.4.4. Electronic spectral properties

The electronic absorption spectral data for the complexes are collected in Table 4.7. The spectral profiles are very similar. All the complexes display the lowest energy band at 544 ± 1 nm with absorption coefficients in the order of 10^4 M^{-1} cm^{-1}. In each case, a shoulder in the range 486-492 nm follows this band. These bands are assigned to metal-to-ligand (Ru(dπ) → L(π*)) charge transfer transitions (MLCT). Broad mutiple MLCT bands for this type of complexes are not unusual considering the possibility of several acceptor levels of different

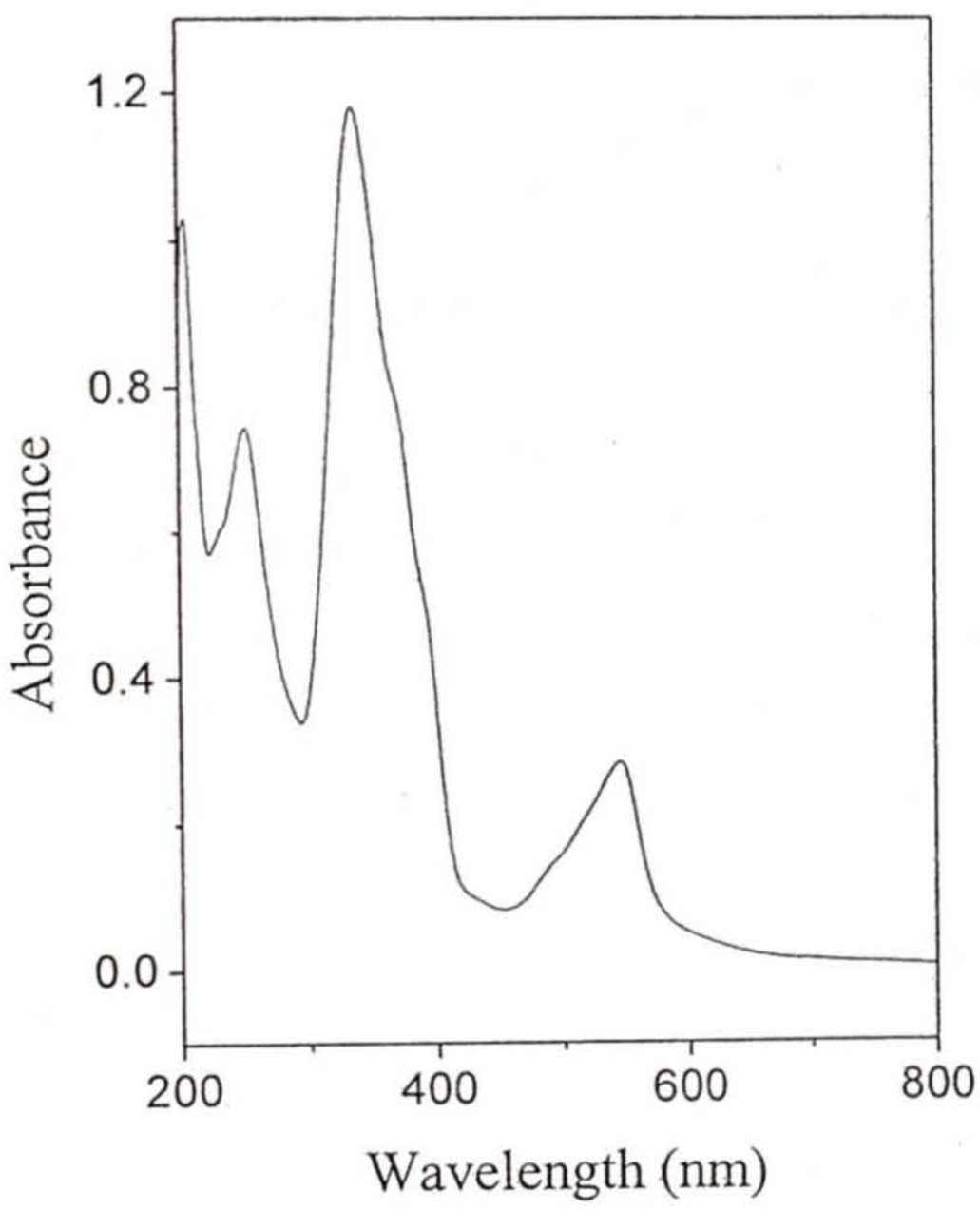

Figure 4.4. Electronic spectrum of $[Ru(pabh)_2]$ in acetonitrile.

energies being available.[5,18] This spectral profile in the visible region is strikingly similar to those of tris(diimino) complexes of ruthenium(II) ($[RuL_3]^{2+}$ where L is

2,2'-bipyridine or aryl(2-pyridylmethylene)amine).[5] It is interesting to note that the present series of complexes display the lowest energy MLCT band at a much longer wavelength compared to that displayed by the above mentioned $[RuL_3]^{2+}$ species (454 nm when L = 2,2'-bipyridine and 480 nm when L = aryl(2-pyridylmethylene)amine). At higher energy the complexes display two very intense bands in the ranges 335-407 nm and 251-282 nm. The former is preceded by several shoulders (Table 4.7). The first intense absorption shows a high-energy shift as the substituent on the aroyl moiety becomes more electron withdrawing.

The main spectral features for the complexes in the higher energy range are very similar with those of the corresponding free Schiff bases. In general for

Table 4.7. Electronic spectral data[a]

Complex	λ_{max} (nm) (ε (M^{-1} cm^{-1}))
$[Ru(padh)_2]$	545 (9791), 492[b] (6447), 407 (61402), 282 (27262)
$[Ru(pamh)_2]$	543 (15713), 486[b] (7892), 437[b] (5388), 396[b] (41964), 373[b] (62810), 348 (71965), 272[b] (29968), 246 (35144)
$[Ru(path)_2]$	544 (11474), 489[b] (5853), 433[b] (3966), 395[b] (23603), 371[b] (36694), 340 (50440), 256 (28012)
$[Ru(pabh)_2]$	544 (11410), 486[b] (5020), 431[b] (3590), 394[b] (17585), 370[b] (28467), 335 (43253), 251 (27269)
$[Ru(pach)_2]$	545 (9790), 487[b] (5063), 433[b] (3440), 396[b] (16890), 373[b] (27950), 337 (47070), 257 (28560)

[a] In CH_3CN solutions. [b] Shoulder.

each complex these bands are at longer wavelengths compared to the band positions displayed by the corresponding free Schiff base. The Schiff bases display a weak band (ε, 396-1222 M^{-1} cm^{-1}) in the range 375-412 nm followed by two intense peaks in the ranges 299-335 nm and 211-245 nm. The first two absorptions display a high-energy shift with the increasing electron withdrawing nature of the substituent on the aroyl moiety. Thus except the lowest energy absorptions the other higher energy absorptions observed for the complexes are assigned to the intraligand transitions.

4.4.5. Redox properties

Electron transfer properties of all the complexes have been studied by cyclic voltammetry in acetonitrile solutions (0.1 M TBAP). The potential data are listed in Table 4.8 and representative cyclic voltammograms are illustrated in Figure 4.5. Each complex displays a metal centered oxidation response and a ligand centered reduction response on the anodic and cathodic side of the Ag/AgCl electrode, respectively. The one electron stoichiometry of these responses is established by coulometry. The oxidation response is assigned to the couple (**1**) and the reduction response is assigned to the couple (**2**) (Figure 4.5). The potentials for both couples are sensitive to the polar effect of the substituent on the aroyl moiety of the ligand. For each couple the potential gradually decreases as the substituent becomes more and more electron releasing. These

$$[Ru^{III}L_2]^+ + e^- \rightleftharpoons [Ru^{II}L_2] \qquad (1)$$

$$[Ru^{II}L_2] + e^- \rightleftharpoons [Ru^{II}L(L^{\bullet})]^- \qquad (2)$$

plots of $E_{1/2}$ against the Hammett substituent constants (σ_p)[19] are satisfactorily linear (Figure 4.6). The effect of substituent on the potential ($E_{1/2}$(Ru)) of couple

Table 4.8. Cyclic voltammetric data[a]

Complex	Metal-centered oxidation $E_{1/2}$/V (ΔE_p/mV)	Ligand-based reduction $E_{1/2}$/V (ΔE_p/mV)
$[Ru(padh)_2]$	0.44 (70)	-1.49 (70)
$[Ru(pamh)_2]$	0.52 (80)	-1.42 (70)
$[Ru(path)_2]$	0.54 (70)	-1.40 (80)
$[Ru(pabh)_2]$	0.56 (70)	-1.38 (70)
$[Ru(pach)_2]$	0.59 (70)	-1.35 (70)

[a] $E_{1/2} = (E_{pa} + E_{pc})/2$, where E_{pa} and E_{pc} are anodic and cathodic peak potentials, respectively; $\Delta E_p = E_{pa} - E_{pc}$; scan rate 100 mVs^{-1}.

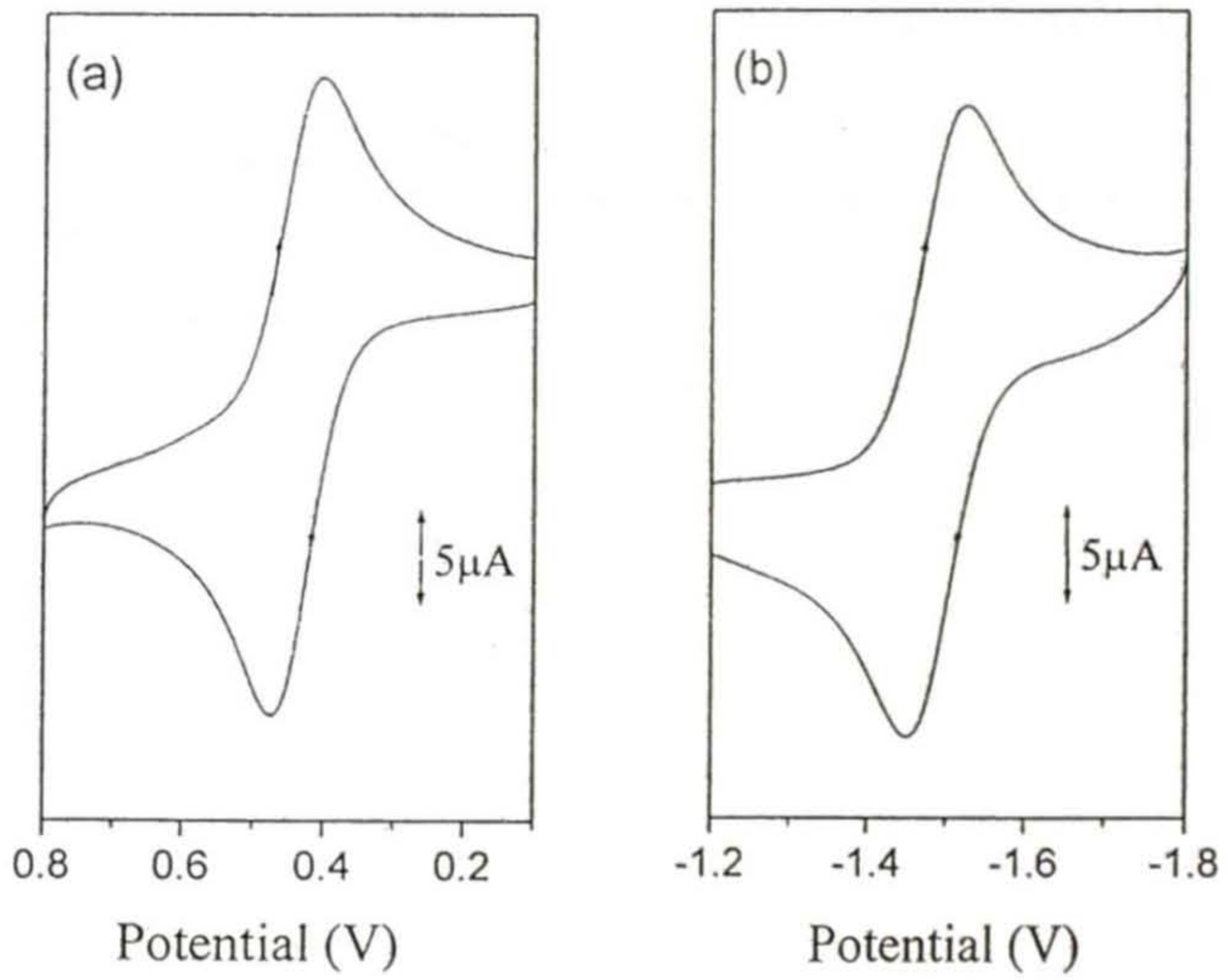

Figure 4.5. Cyclic voltammograms (scan rate 100 mVs^{-1}) of $[Ru(padh)_2]$ in acetonitrile (0.1 M TBAP) at a glassy carbon working electrode at 298 K.

(**1**) and on that ($E_{1/2}$(L)) of couple (**2**) is same within experimental error (Table 4.8). As a consequence the value of $\Delta E_{1/2}$ ($E_{1/2}$(Ru) – $E_{1/2}$(L)) is essentially identical (1.94 ± 0.01 V) for all the complexes (Table 4.8). In additon, the $E_{1/2}$(Ru) is linearly correlated with $E_{1/2}$(L) (Figure 4.7) with a slope very close to unity (1.09(6)). A possible rational for these observations is as follows:

An electron withdrawing group on the aroyl fragment of the ligand decreases σ-donor capability of the O-atom of the deprotonated amide functionality and hence increases the effective nuclear charge on the ruthenium center. As a result the energy of the metal-dπ orbitals and that of the ligand-π* orbitals are lowered.[20] The ensuing metal-dπ to ligand-π* backbonding

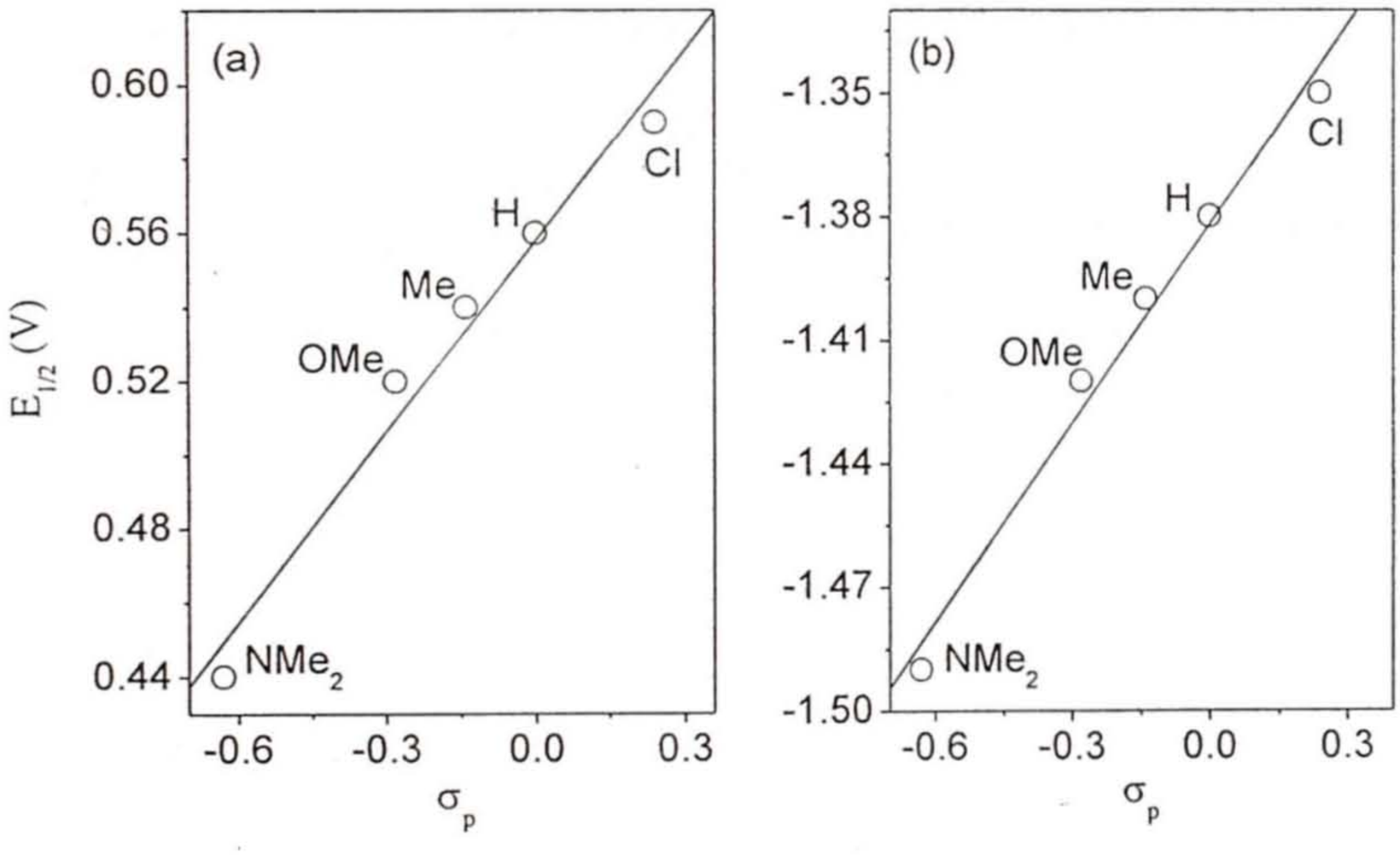

Figure 4.6. Correlations between the (a) $E_{1/2}$ values of the metal oxidation and Hammett substituent constants, (b) $E_{1/2}$ values of the ligand reduction and Hammett substituent constants. The straight line in each plot represents a linear least-squares fit.

further stabilizes the metal-dπ orbitals, however, destabilizes the ligand-π* orbitals. The $\Delta E_{1/2}$ values and the slope of the straight line obtained by plotting $E_{1/2}$(Ru) against $E_{1/2}$(L) reflect the extent of changes in the metal-dπ and the ligand-π* levels.[21] In the present series of complexes, the very similar values of $\Delta E_{1/2}$ and a slope very close to unity suggest that the net perturbations in the metal-dπ and the ligand-π* levels are same due to the polar effect of the substituent on the aroyl fragment of the ligand. This is also substantiated by essentially identical lowest energy band positions (544 ± 1 nm) observed in the electronic spectra of these complexes (*vide supra*) due to MLCT transitions that involve excitation of electron from metal-dπ to ligand-π* level.

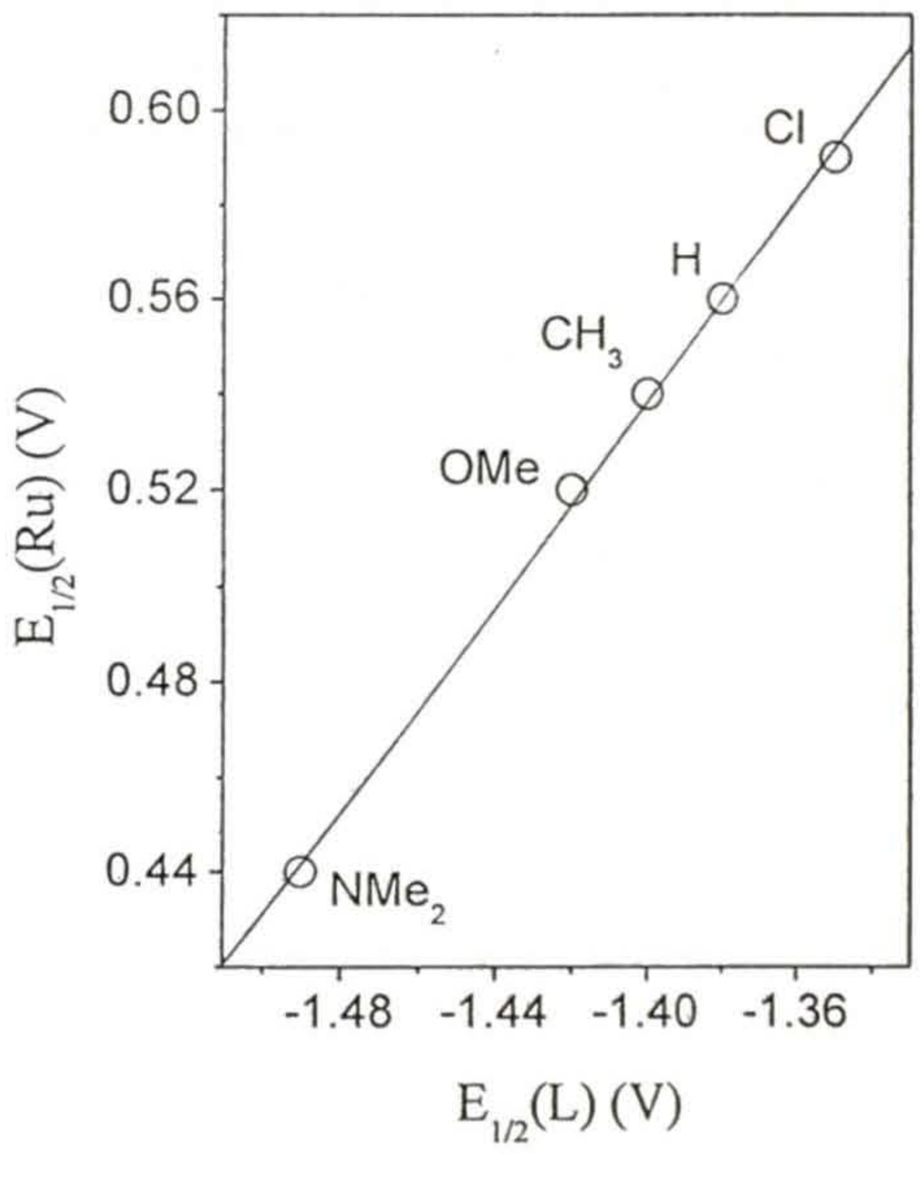

Figure 4.7. Correlation between $E_{1/2}$ (Ru) and $E_{1/2}$ (L) values. The straight line represents a linear least-squares fit.

4.4.6. Protonation behavior of [Ru(pabh)$_2$]

Protonation behavior of the coordinated amide functionalities in [Ru(pabh)$_2$] has been studied by spectrophotometric titration using acetonitrile solutions of the complex and CF_3SO_3H. With the progressive addition of the acid, the absorptions are blue-shifted (Figures 4.8 and 4.9). The interesting aspect of the titration is that the extent of change in the spectral profile gradually decreases and when the complex to acid mole ratio becomes about 1:1.1 it becomes minimum. Figure 4.8(a) depicts the shift of band positions through five isobestic points in this part of the titration. These isobestic points are at 509, 421, 319, 276, and 241 nm. However, continued addition of the acid causes further

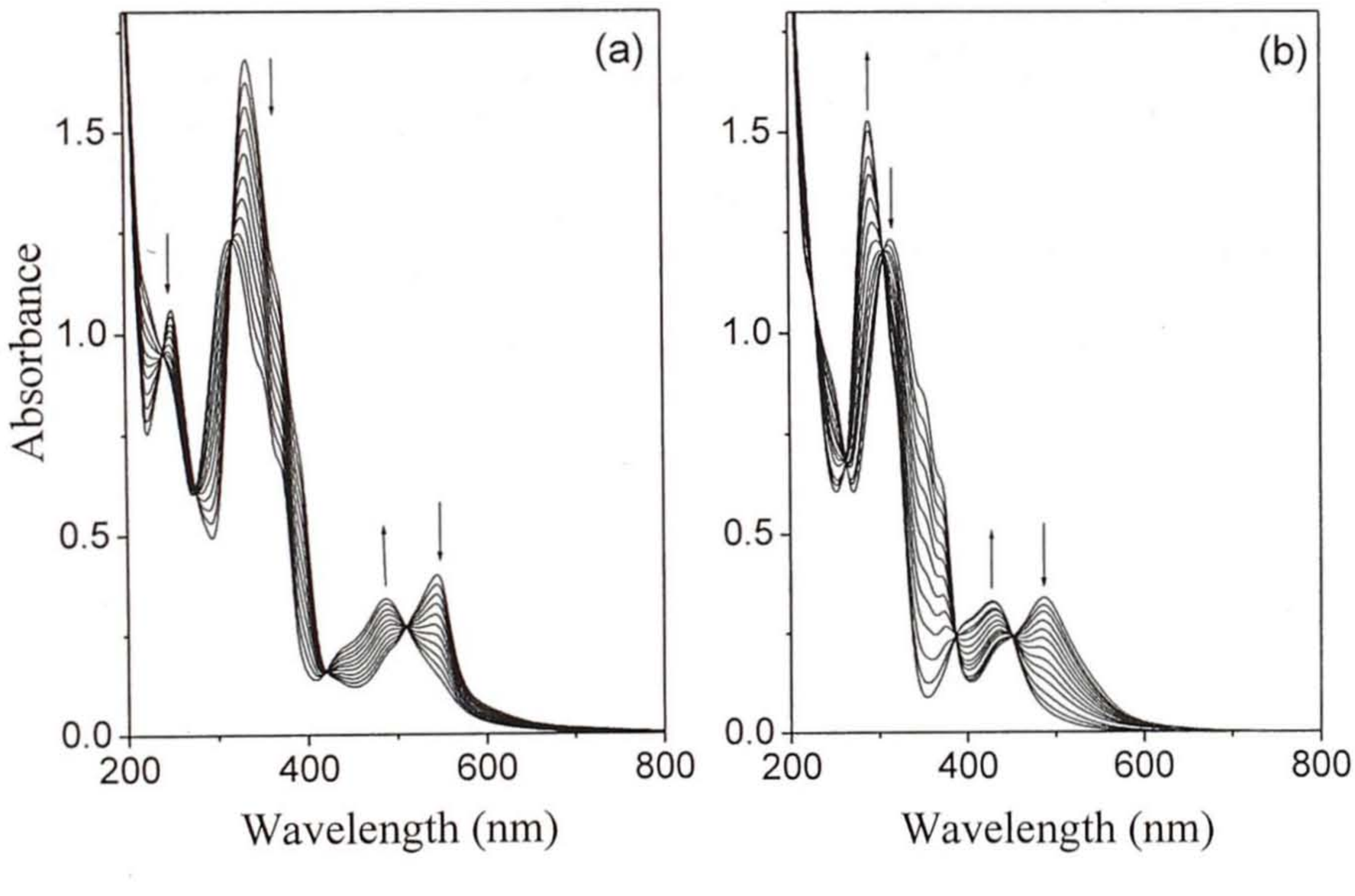

Figure 4.8. Spectrophotometric titration of [Ru(pabh)$_2$] in acetonitrile with CF_3SO_3H. (a) First segment of the titration. (b) Second segment of the titration.

shift of band positions to higher energy through a different set of five isobestic points (at 451, 387, 307, 263, and 228 nm) and at about 1:2.4 complex to acid mole ratio the spectral profile becomes constant (Figure 4.8b). The observation of two sets of isobestic points clearly suggest two sequential protonation of the pair of metal coordinated amide functionalities present in the complex.

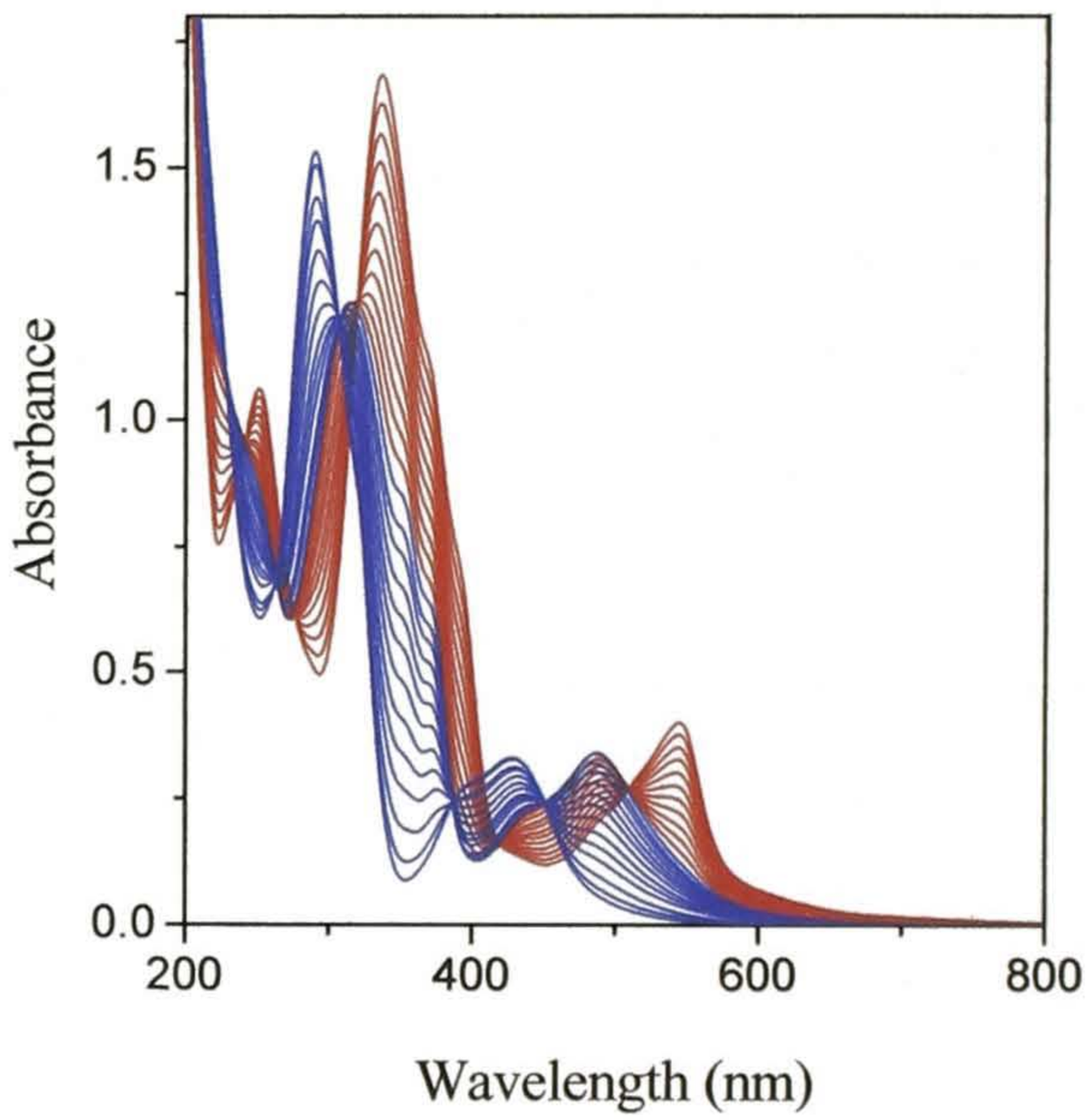

Figure 4.9. First (red) and second (blue) segments of titration.

Quantitative reversibility of this protonation behavior was confirmed by spectrophotometric back-titration with $(C_2H_5)_3N$. The effective pK_{ai} (i = 1 and 2) values were determined from the two segments (Figure 4.8(a) for pK_{a2} and Figure 4.8(b) for pK_{a1}) of the spectrophotometric titration using equations 3, 4 and 5.[22]

The value of $K_a(CF_3SO_3H)$ in acetonitrile was obtained from ref. 23. The change in absorbance at 486.5 nm and that at 544 nm were used to calculate K_{c1} and K_{c2},

$$K_{ai} = K_a(CF_3SO_3H)/K_{ci} \quad (3)$$

$$K_{c1} = [complexH_2^{2+}][CF_3SO_3^-]/[complexH^+][CF_3SO_3H] \quad (4)$$

$$K_{c2} = [complexH^+][CF_3SO_3^-]/[complex][CF_3SO_3H] \quad (5)$$

respectively. The values of pK_{a1} and pK_{a2} thus obtained are 6.85(5) and 7.44(9), respectively. The large pK_a value (~15)[24] of free amide functionality in organic compounds suggest that the -C(=O)NH- proton is very weakly acidic. It is interesting to note that although in the diprotonated species ($complexH_2^{2+}$), and possibly in the monoprotonated species ($complexH^+$), the amide functionalities are not bound to the metal ion (*vide infra*) still the acidity of the amide proton increases by ~8 orders of magnitude. A combination of several reasons could be responsible for the increase of the acidity. One of the possible reasons is as follows. The electron deficiency of the N-atom adjacent to the protonated amide N-atom arising out of the formers coordination to the Ru(II) center is partially compensated by the free amide moiety. As a consequence the N-center in the amide functionality becomes less basic and hence the attached proton becomes more acidic. In some ruthenium(II) complexes with Schiff bases derived from phenylhydrazine and 2- hydroxybenzaldehydes, a similar increase in acidity of the N-H proton due to metal coordination to the adjacent N-atom has been noted.[25]

4.4.7. Structures of $[Ru(pabh)_2]$ and $[Ru(path)_2]$

The molecular structures of $[Ru(pabh)_2]$ and $[Ru(path)_2]$ are illustrated in Figures 4.10 and 4.11, respectively. The selected bond parameters associated with the metal ions are listed in Table 4.9. In each complex, the metal ion is in distorted octahedral N_4O_2 coordination sphere assembled *via* the meridionally

spanning pyridine-N, imine-N and deprotonated amide-O donor tridentate ligands. The N-N, N-C and C-O distances in the =N-N=C(O^-)- fragments of the coordinated ligands in both complexes are in the range 1.374(6)-1.384(4) Å, 1.310(7)-1.323(5) Å and 1.281(6)-1.292(4) Å, respectively. These distances are consistent with the enolate form of the amide functionalities in each complex.[8] In these complexes, the average chelate bite angles in the five-membered rings formed by the pyridine-N and the imine-N are slightly larger than that in the five - membered rings formed by the amide-O and the imine-N. The former is 79.03° and 79.25° and the latter is 76.44° and 76.5° for [Ru(pabh)$_2$] and [Ru(path)$_2$],

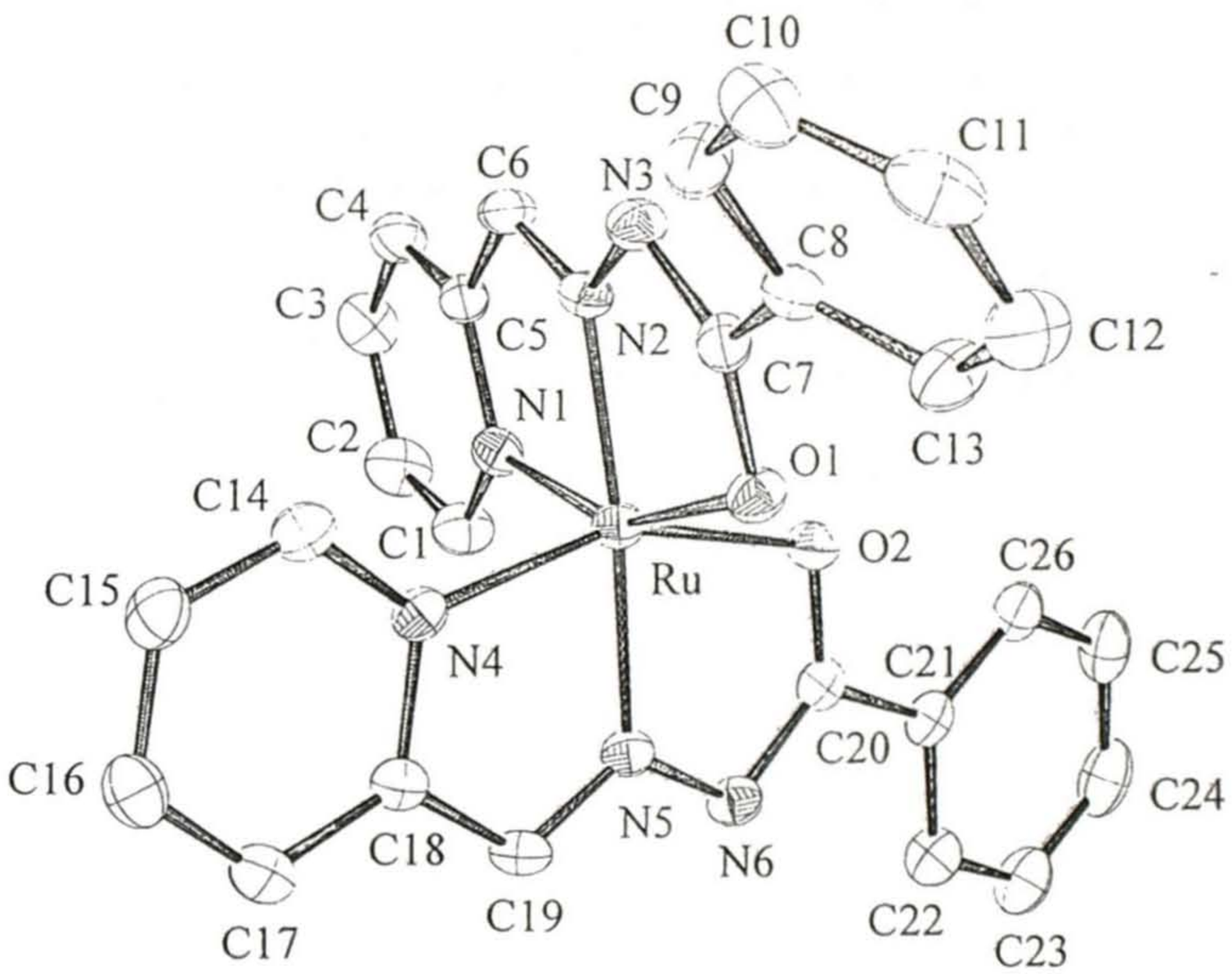

Figure 4.10. Structure of [Ru(pabh)$_2$] with the atom-labeling scheme. All atoms are represented by their 25% probability thermal ellipsoids. Hydrogen atoms are omitted for clarity.

respectively. The Ru(II)-N(pyridine) bond lengths are within the range reported for Ru(II) complexes having the same coordinating atom.[7,26] The Ru(II)-N(imine) bond lengths are comparable with those reported earlier.[6] However, the Ru(II)-N(pyridine) bond lengths (2.010(5)-2.042(3) Å) are significantly longer than the Ru(II)-N(imine) bond lengths (1.957(5)-1.962(4) Å). Most probably this

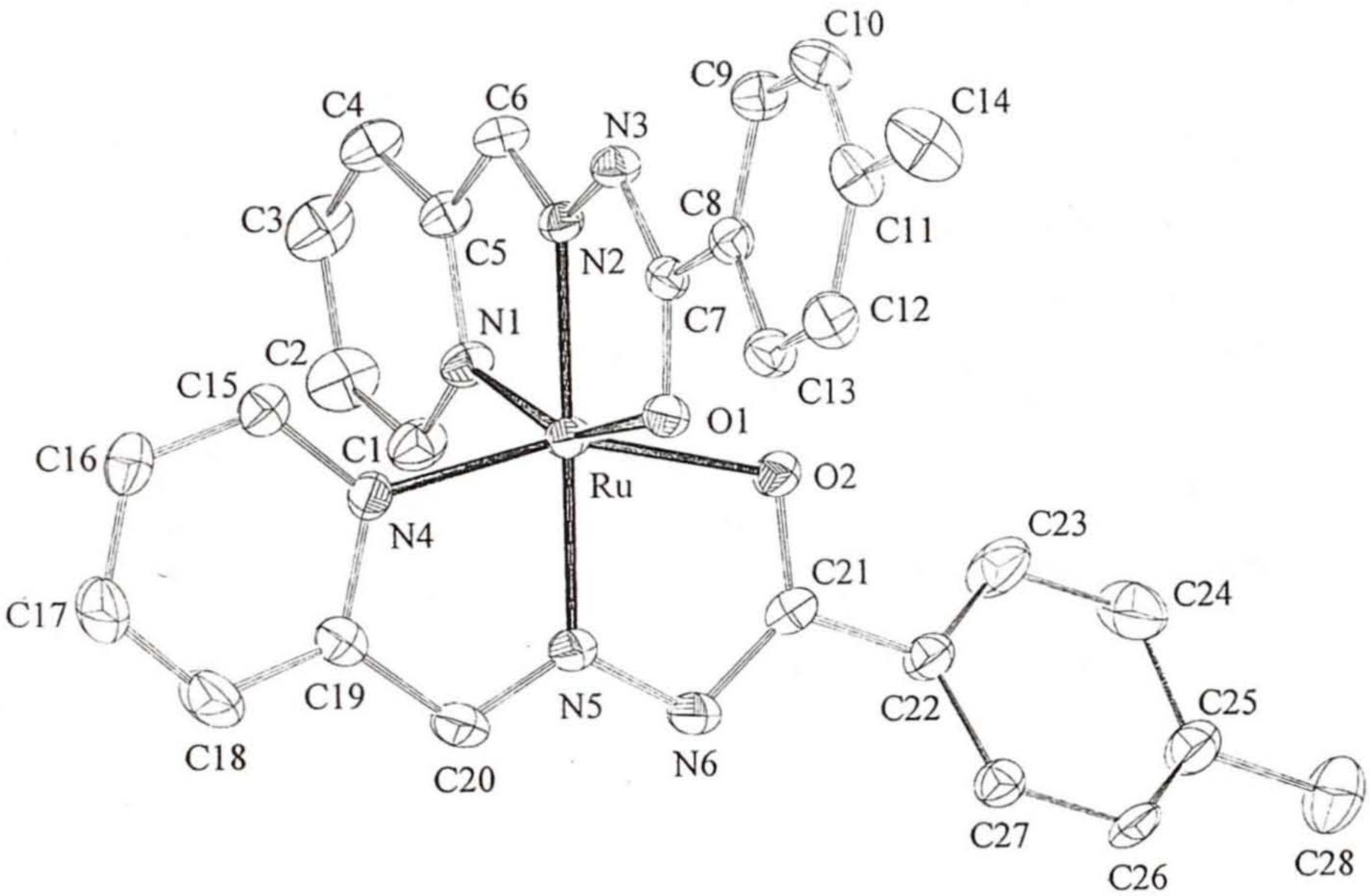

Figure 4.11. Structure of [Ru(path)$_2$] showing the 25% probability thermal ellipsoids and the atom-labeling scheme. For clarity, hydrogen atoms are omitted and only one of the two orientations of the disordered tolyl ring (C22-C27) is shown.

Table 4.9. Selected bond distances (Å) and angles (deg.) for $[Ru(pabh)_2]$ and $[Ru(path)_2]$

	$[Ru(pabh)_2]$	$[Ru(path)_2]$
Ru-N(1)	2.037(3)	2.047(5)
Ru-N(2)	1.960(3)	1.962(4)
Ru-N(4)	2.042(3)	2.010(5)
Ru-N(5)	1.958(3)	1.957(5)
Ru-O(1)	2.137(3)	2.106(4)
Ru-O(2)	2.115(3)	2.108(4)
N(1)-Ru-N(2)	79.03(13)	79.11(19)
N(1)-Ru-N(4)	97.09(13)	90.4(2)
N(1)-Ru-N(5)	96.08(13)	101.3(2)
N(1)-Ru-O(1)	155.01(11)	155.90(17)
N(1)-Ru-O(2)	89.99(11)	95.17(18)
N(2)-Ru-N(4)	99.31(13)	99.75(19)
N(2)-Ru-N(5)	174.65(13)	179.1(2)
N(2)-Ru-O(1)	76.09(12)	76.79(17)
N(2)-Ru-O(2)	105.18(11)	104.65(17)
N(4)-Ru-N(5)	79.03(13)	79.4(2)
N(4)-Ru-O(1)	89.17(12)	93.09(17)
N(4)-Ru-O(2)	155.39(11)	155.58(17)
N(5)-Ru-O(1)	108.87(11)	102.8(2)
N(5)-Ru-O(2)	76.80(12)	76.20(18)
O(1)-Ru-O(2)	94.29(10)	91.41(15)

difference is mainly due to the rigidity of the tridentate ligand.[27] Better π-backbonding in the Ru(II)-N(imine) bond compared to that in the Ru(II)-N(pyridine) bond[28] may also be partially responsible for this difference. The Ru(II)-O(amide) bond lengths in $[Ru(pabh)_2]$ are longer than those in $[Ru(path)_2]$. This is most likely due to better Ru(II)-O σ-bonding in the latter compared to that in the former. This difference in the σ-bond strength can be rationalized considering the presence of electron releasing methyl group at the *para* position of the aroyl fragment in $path^-$.

In the crystal lattice, both complex molecules display self-assembly *via* weak intermolecular hydrogen bonding. In $[Ru(pabh)_2]$ intermolecular C-H···O[29]

.

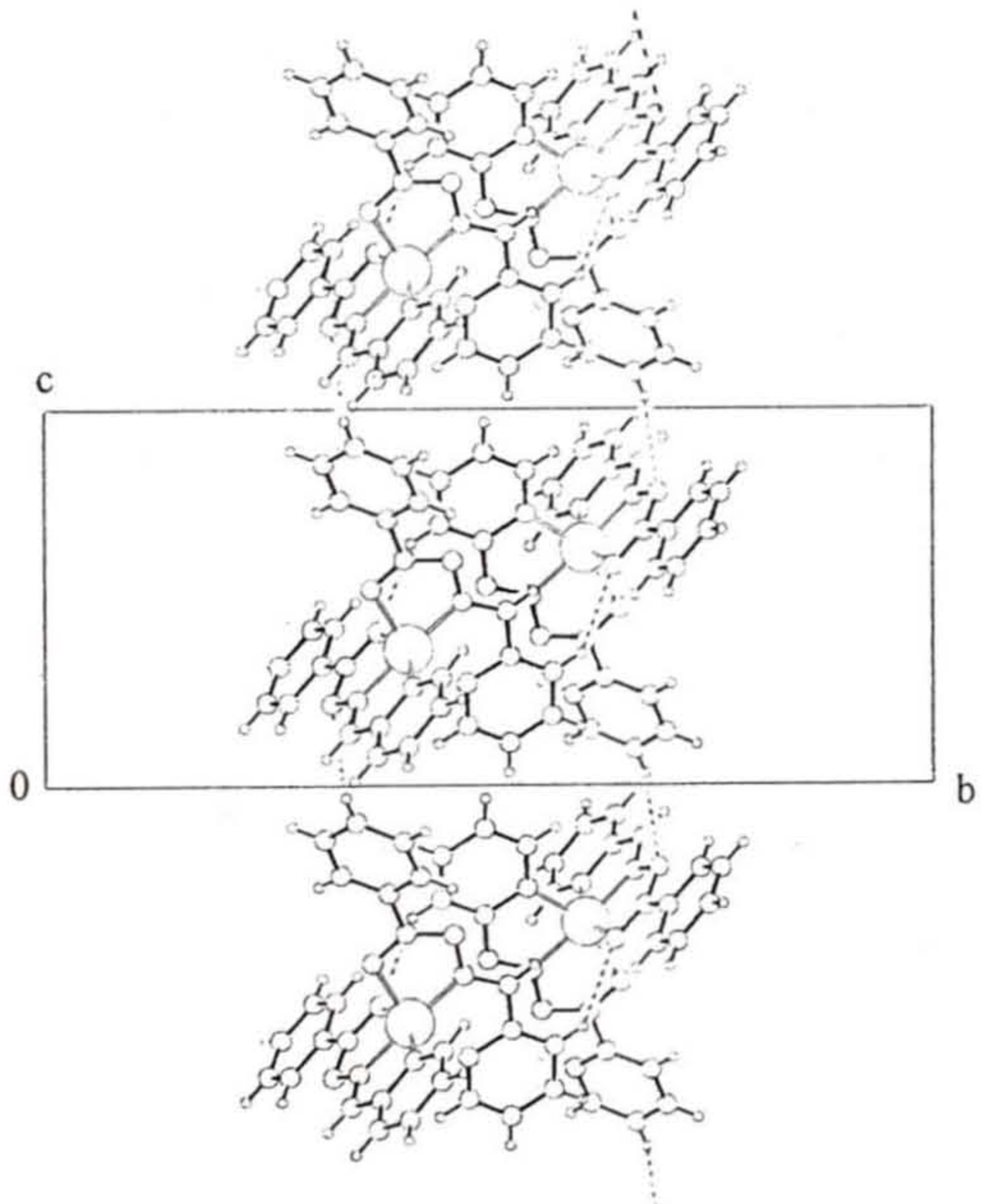

Figure 4.12. One-dimensional arrangement of $[Ru(pabh)_2]$ molecules.

and C-H···N[30] interactions help to form a one-dimensional chain of the complex molecules (Figure 4.12), whereas for [Ru(path)$_2$], the same interactions leads to a two dimensional network of the molecules (Figure 4.13). All the C-H···O hydrogen bonding involves the aromatic protons and coordinated amide oxygens. In [Ru(path)$_2$], both the coordinated amide oxygen atoms are involved in hydrogen bonding but in [Ru(pabh)$_2$] only one amide oxygen is hydrogen bonded. C-H···N hydrogen bonding involves the aromatic protons and one of the amide nitrogens. Another amide nitrogen (N6) in each of the two structures is not involved in such type of hydrogen bonding. The hydrogen bonding distances and angles (Table 4.10) are within the acceptable range.[29,30]

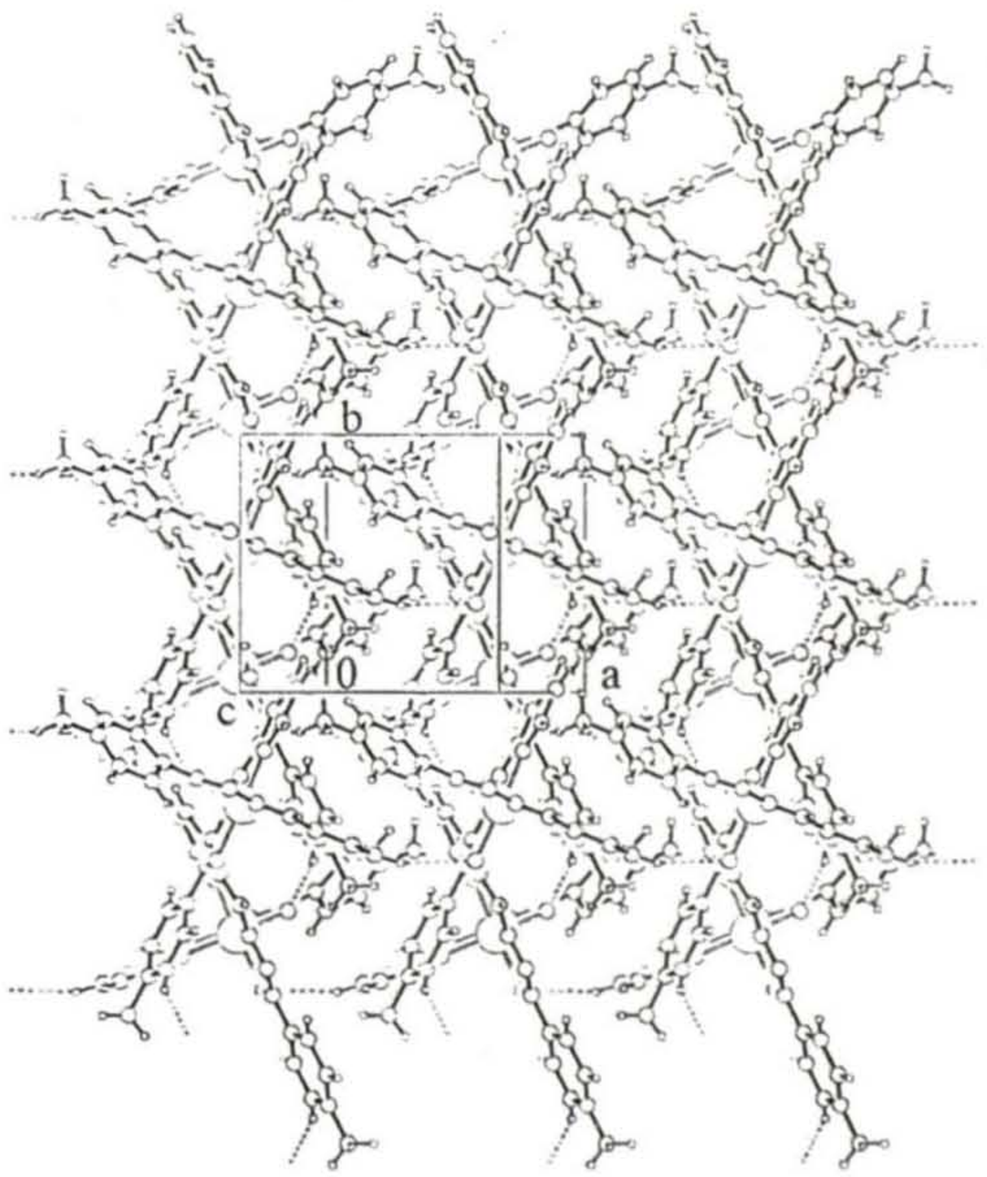

Figure 4.13. Two dimensional network of [Ru(path)$_2$].

Table 4.10. Hydrogen bonding parameters

	H···A (Å)	D···A (Å)	D-H···A (°)
[Ru(pabh)$_2$]			
C17 - H17···O1#1	2.53	3.31	141.50
C24 - H24···N3#2	2.60	3.44	150.29
[Ru(path)$_2$]			
C4 - H4···N3#3	2.60	3.52	168.43
C12 - H12···O2#4	2.40	3.28	156.55
C17 - H17···O1#5	2.57	3.43	153.65

A = acceptor. D = donor. #1 = 1-x, -y, 2-z. #2 = 1+x, y, 1+z.
#3 = 1.5-x, 0.5+y, 0.5-z. #4 = x, -1+y, z. #5 = -1+x, y, z.

4.4.8. Isolation and characterization of the diprotonated complex

We are unable to grow X-ray quality crystals of $CF_3SO_3^-$ salts of the monoprotonated and diprotonated species. However, slow evaportaion of an acetonitrile solution of [Ru(pabh)$_2$] and $HClO_4$ (1:2.5 mole ratio) produces a light brown crystalline material. X-ray structure determination (*vide infra*) of this material reveals the protonation of both amide functionalities in [Ru(pabh)$_2$]. This diprotonated complex crystallizes as [Ru(Hpabh)$_2$(CH_3CN)$_2$](ClO_4)$_2$·H_2O. A similar approach to obtain the crystals of the ClO_4^- salt of the monoprotonated species failed. The diprotonated complex [Ru(Hpabh)$_2$(CH_3CN)$_2$](ClO_4)$_2$·H_2O starts loosing solvent immediately after isolation and become light brown amorphous solid. The exact nature of this amorphous solid is not clear at present. Infrared spectrum does not indicate the presence of the acetonitrile molecules. The perchlorate ions display a strong and broad peak at ~1100 cm^{-1} and a sharp peak at ~620 cm^{-1}. A broad peak centered at ~3440 cm^{-1} and a sharp peak at

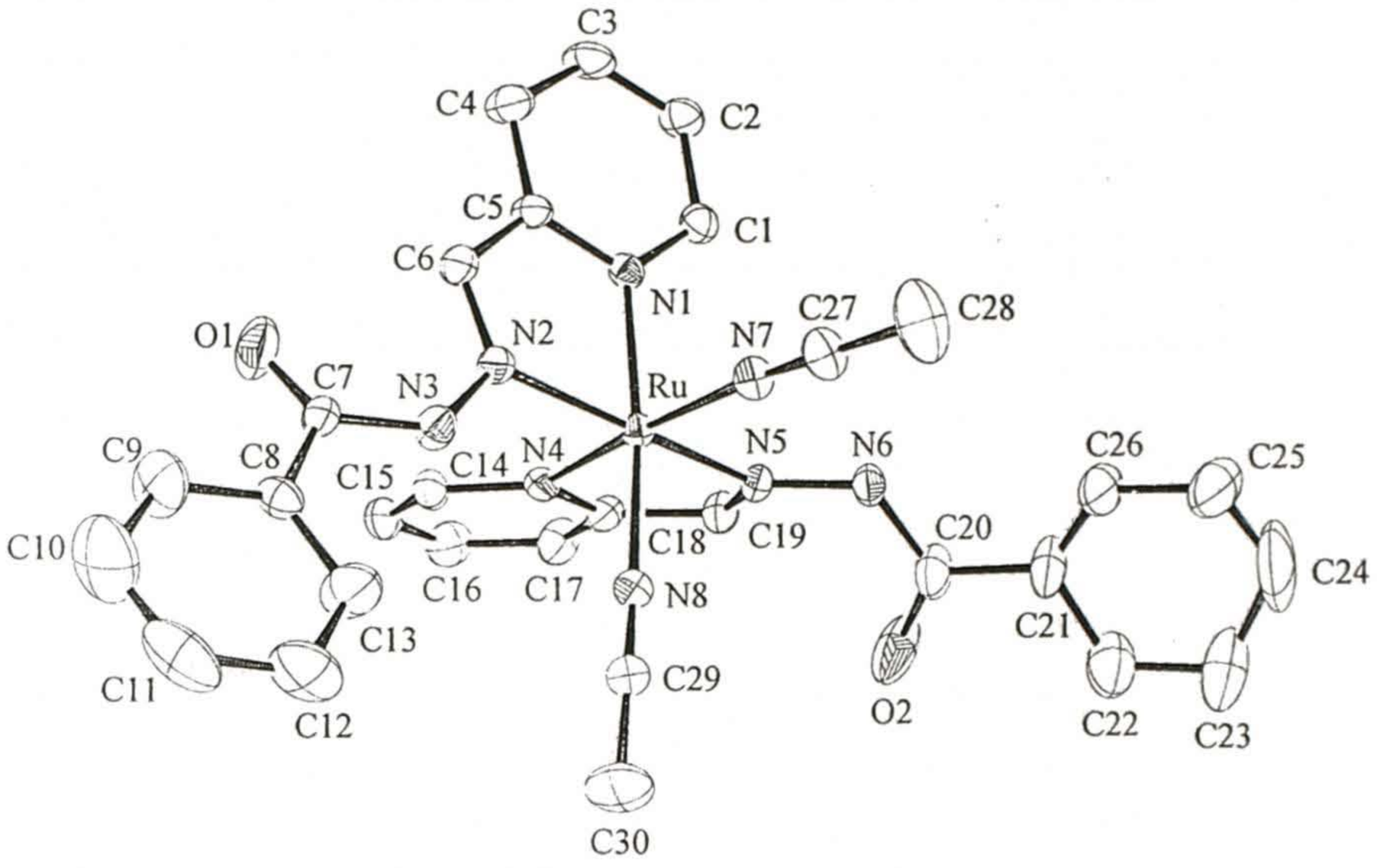

Figure 4.14. Structure of the cation in $[Ru(Hpabh)_2(CH_3CN)_2](ClO_4)_2 \cdot H_2O$ showing the 20% probability thermal ellipsoids and the atom-labeling scheme. Hydrogen atoms are omitted for clarity.

2924 cm^{-1} are likely to be associated with the water molecule and amide N-H stretches, respectively. The strong peak observed at 1682 cm^{-1} is possibly due to the amide C=O moiety. Because of the solvent loss problem the solution properties of the crystalline complex were studied by dissolving it in acetonitrile within 5 min. after isolation of the crystals and the concentration was calculated assuming the molecular formula, $[Ru(Hpabh)_2(CH_3CN)_2](ClO_4)_2 \cdot H_2O$ as found in the X-ray structure determination. In acetonitrile, the complex behaves as 1:2 electrolyte. The molar conductivity value is 263 Ω^{-1} cm^2 mol^{-1}. The electronic spectrum in acetonitrile solution displays a peak at 429 nm (ε, 7500 M^{-1} cm^{-1}) followed by two shoulders (393 and 323 nm) and another peak at 290 nm

(ε, 34,200 M^{-1} cm^{-1}). This spectral profile is identical with that obtained from the mixture of [Ru(pabh)$_2$] and CF_3SO_3H (1:2.4 mole ratio) in acetonitrile (Figure 4.8(b)). The ^1H NMR spectrum in CD_3CN displays the N-H proton at 10.53 δ and the =C-H proton at 9.69 δ. The aromatic protons are observed in the range 7.62-8.04 δ. Thus in solution both the Hpabh ligands of [Ru(Hpabh)$_2$(CH_3CN)$_2$](ClO_4)$_2$·H_2O are magnetically equivalent. The structure of the complex cation in [Ru(Hpabh)$_2$(CH_3CN)$_2$](ClO_4)$_2$·H_2O is illustrated in Figure 4.14. The selected bond parameters associated with the Ru(II) center are given in Table 4.11. The metal center in [Ru(Hpabh)$_2$(CH_3CN)$_2$](ClO_4)$_2$·H_2O is in distorted octahedral N_6 coordination sphere. Each of the two Hpabh ligands act as bidentate ligand and coordinates the metal ion through the pyridine-N and

Table 4.11. Selected bond distances (Å) and angles (deg.) for [Ru(Hpabh)$_2$(CH_3CN)$_2$](ClO_4)$_2$·H_2O

Ru-N(1)	2.036(6)	Ru-N(2)	2.050(6)
Ru-N(4)	2.059(6)	Ru-N(5)	2.055(6)
Ru-N(7)	2.042(7)	Ru-N(8)	2.042(7)
N(1)-Ru-N(2)	78.0(2)	N(1)-Ru-N(4)	88.7(2)
N(1)-Ru-N(5)	96.0(2)	N(1)-Ru-N(7)	91.8(3)
N(1)-Ru-N(8)	172.3(2)	N(2)-Ru-N(4)	94.7(3)
N(2)-Ru-N(5)	170.8(2)	N(2)-Ru-N(7)	91.8(3)
N(2)-Ru-N(8)	94.4(3)	N(4)-Ru-N(5)	78.0(2)
N(4)-Ru-N(7)	173.5(3)	N(4)-Ru-N(8)	93.0(2)
N(5)-Ru-N(7)	95.5(3)	N(5)-Ru-N(8)	91.7(3)
N(7)-Ru-N(8)	87.4(3)		

the imine-N atoms forming a five membered chelate ring. Two acetonitrile-N atoms occupy the remaining two mutually *cis* coordination sites. The N-N, N-C and C-O bond lengths in the =N-NH-C(=O)- fragments of the two coordinated ligands are 1.386(8), 1.375(8); 1.340(10), 1.363(10); and 1.191(11), 1.226(12) Å, respectively. Comparison of these bond lengths with the corresponding bond lengths in $[Ru(pabh)_2]$ clearly indicate that the amide fragments in $[Ru(Hpabh)_2(CH_3CN)_2](ClO_4)_2 \cdot H_2O$ are protonated. Thus when the amide functionalities in $[Ru(pabh)_2]$ get protonated the Ru(II)-O(amide) bonds are dissociated and the N-atoms of two acetonitrile molecules coordinate the metal ion at the same two sites. The Ru(II)-N(pyridine) bond lengths (2.036(6) and 2.059(6) Å) are essentially identical with those in $[Ru(pabh)_2]$. However, the Ru(II)-N(imine) distances (2.050(6) and 2.055(6) Å) are significantly longer than those (1.960(3) and 1.958(3) Å) in $[Ru(pabh)_2]$. As mentioned before the rigidity of the $pabh^-$ ligands in $[Ru(pabh)_2]$ arising from its tridentate binding mode and the imine-N being the middle coordinating atom are likely to be the reasons for the shorter Ru(II)-N(imine) bond lengths in $[Ru(pabh)_2]$ compared to those in $[Ru(Hpabh)_2(CH_3CN)_2](ClO_4)_2 \cdot H_2O$. The Ru(II)-N(acetonitrile) bond lengths are unexceptional.[31]

The molecules of **6** forms a two dimensional network through the intermolecular N-H···O and C-H···O hydrogen bonding. H···A distances and D - H···A angles (A = acceptor; D = donor) are in the ranges 2.41 to 2.59 Å and 128.17 to 165.98°, respectively (Table 4.12). Between the two uncoordinated amide oxygens, O1 is involved in hydrogen bonding with aromatic C-H moiety, whereas O2 remains free. Both the perchlorate moieties are extensively involved in hydrogen bonding with aldehydic C-H, methyl C-H, aromatic C-H, and amide N-H protons. These hydrogen bonding interactions involving both the cation and anion in **6** form the two dimensional network (Figure 4.15).

Table 4.12. Hydrogen bonding parameters

	H···A (Å)	D···A (Å)	D – H···A (°)
N(6) - H(6)···O(10)#1	2.5152	3.3560	165.98
C(1) - H(1)···O(1)#2	2.5825	3.3202	136.59
C(4) - H(4)···O(7)#3	2.5927	3.5083	168.23
C(6) - H(6)···O(9)#3	2.4140	3.2633	151.78
C(10) - H(10)···O(4)#4	2.5439	3.4049	154.09
C(19) - H(19)···O(8)	2.4188	3.2567	149.84
C(28) - H(28B)···O(5)#1	2.4925	3.1768	128.17

A = acceptor, D = donor, #1 = -1/2+x, 1/2-y, -1/2+z.

#2 = -1/2+x, 1/2-y, 1/2+z. #3 = x, y, -1+z. #4 = 3/2-x, 1/2+y, 1/2-z.

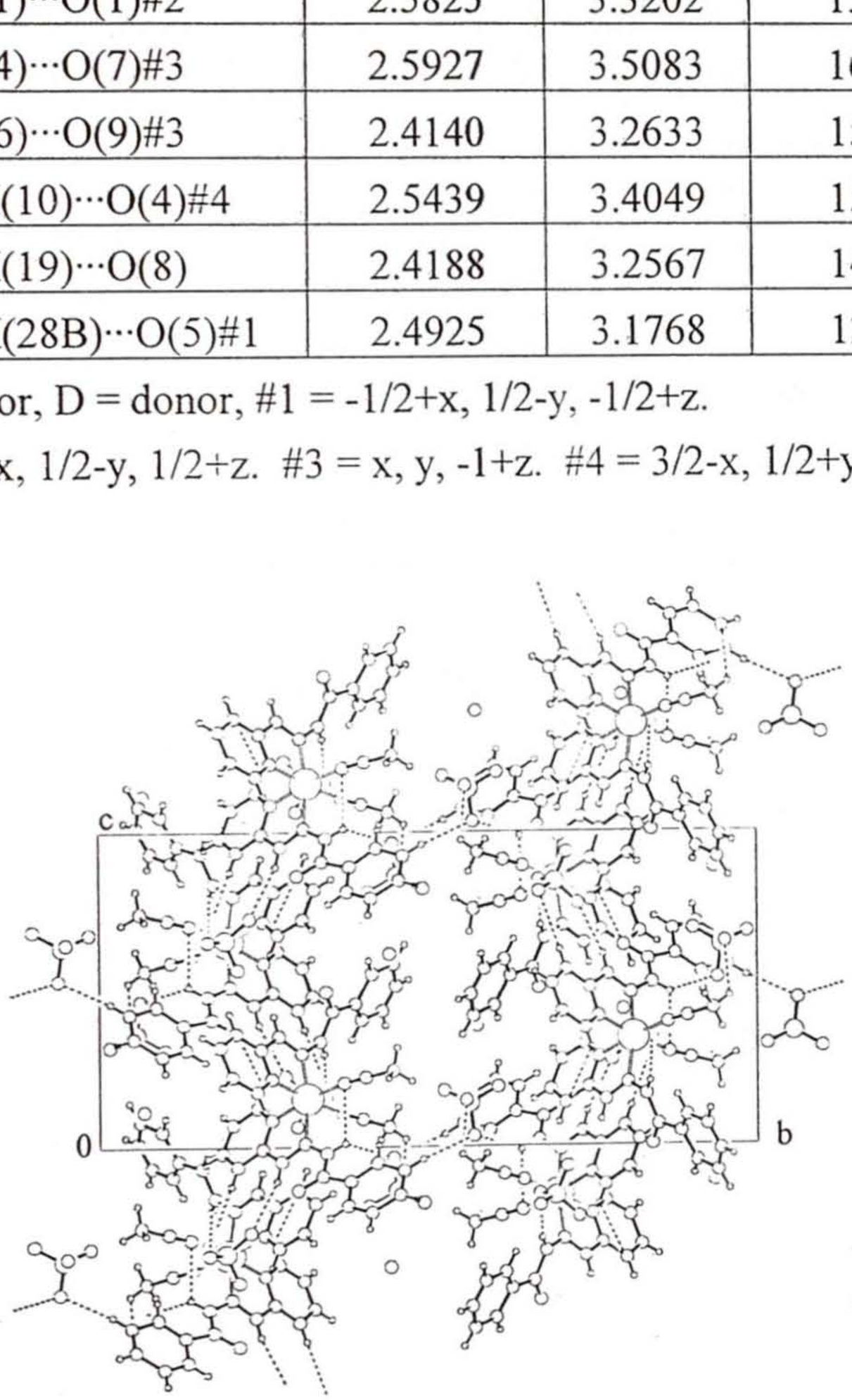

Figure 4.15. Two dimensional network of $[Ru(Hpabh)_2](ClO_4)_2 \cdot H_2O$.

4.5. Conclusion

In this chapter, a new series of mononuclear ruthenium(II) complexes with N,N,O-donor N-(aroyl)-N'-(picolinylidene)hydrazines has been described. It has been demonstrated that the polar effect of the substituent on the ligand affects the energies of the metal-dπ and the ligand-π* levels. However, the energy difference between them remains constant in all the complexes. The coordinated amide functionalities can be reversibly protonated and deprotonated. The X-ray structure reveals that in the diprotonated species the ligands act as bidenate N,N-donor and the ruthenium(II) center prefers two acetonitrile-N atoms instead of the oxygen atoms of the protonated amide functionalities in the coordination sphere.

4.6. References

1. (a) E. A. Seddon, K. R. Seddon, *The Chemistry of Ruthenium*, Elsevier, Amsterdam, 1984. (b) K. R. Seddon, *Coord. Chem. Rev.*, **1985**, *67*, 171. (c) A. Juris, V. Balzani, F. Barigelletti, S. Campagna, P. Belser, A. V. Zelewsky, *Coord. Chem. Rev.*, **1988**, *84*, 85. (d) B. K. Ghosh, A. Chakravorty, *Coord. Chem. Rev.*, **1989**, *95*, 239. (e) W. T. Wong, *Coord. Chem. Rev.*, **1994**, *131*, 45. (f) K. Kalyanasundaram, M. S. Lakeeruddin, M. K. Lakeeruddin, *Coord. Chem. Rev.*, **1994**, *132*, 259. (g) S. M. Lee, W. T. Wong, *Coord. Chem. Rev.*, **1997**, *164*, 415. (h) S. I. Gorelsky, E. S. Dodsworth, A. B. P. Lever, A. A. Vlcek, *Coord. Chem. Rev.*, **1998**, *174*, 469.
2. (a) M. Calvin, *J. Membrane Sci.*, **1987**, *33*, 137. (b) L. Sun, L. Hammarström, B. Åkermark, S. Styring, *Chem. Soc. Rev.*, **2001**, *30*, 36.
3. (a) P. D. Beer, *Acc. Chem. Res.*, **1998**, *31*, 71. (b) J. P. Sauvage, J. P. Collin, J. C. Cambron, S. Guillerez, C. Coudret, V. Balzani, F. Barigelletti, L. De Cola, L. Flamingni, *Chem. Rev.*, **1994**, *94*, 933. (b) V. Balzani, A. Juris, M. Venturi, S. Campagna, S. Serroni, *Chem. Rev.*, **1996**, *96*, 759.

4. (a) H. B. Gray, J. R. Winkler, *Annu. Rev. Biochem.*, **1996**, *65*, 537. (b) J. K. Barton, in *Bioinorganic Chemistry*, ed. I. Bartini, H. B. Gray, S. J. Lippard, J. Valentine, University Science Books, Mill Valley, 1994, p. 455. (c) N. Sardesai, S. C. Lin, K. Zimmermann, J. K. Barton, *Bioconjugate Chem.*, **1995**, *6*, 302. (d) P. Lincoln, E. Tuite, B. Nordén, *J. Am. Chem. Soc.*, **1997**, *119*, 1454.
5. S. Choudhury, A. K. Deb, S. Goswami, *J. Chem. Soc., Dalton Trans.*, **1994**, 1305.
6. A. K. Das, S. M. Peng, S. Bhattacharya, *Polyhedron*, **2001**, *20*, 327.
7. (a) M. Ziegler, V. Monney, H. Stoeckli-Evans, A. V. Zelewsky, I. Sasaki, G. Dupic, J. C. Daran, G. G. A. Balavoine, *J. Chem. Soc., Dalton Trans.*, **1999**, 667. (b) J. E. Collins, J. J. S. Lamba, J. C. Love, J. E. McAlvin, C. Ng, B. P. Peters, X. Wu, C. L. Fraser, *Inorg. Chem.*, **1999**, *38*, 2020. (c) B. Geisser, A. Ponce, R. Alsfasser, *Inorg. Chem.*, **1999**, *38*, 2030. (d) A. Juris, L. Prodi, A. Harriman, R. Ziessel, M. Hissler, A. El-ghayoury, F. Wu, E. C. Riesgo, R. P. Thummel, *Inorg. Chem.*, **2000**, *39*, 3590. (e) X. Zhou, D. S. Tyson, F. N. Castellano, *Angew. Chem., Int. Ed.*, **2000**, *39*, 4301. (f) L. H. Uppadine, M. G. B. Drew, P. D. Beer, *Chem. Commun.*, **2001**, 291. (g) H. Chao, G. Yang, G. Q. Xue, H. Li, H. Zang, I. D. Williams, L. N. Ji, X. M. Chen, X. Y. Li, *J. Chem. Soc., Dalton Trans.*, **2001**, 1326.
8. I. P. Evans, A. Spencer, G. Wilkinson, *J. Chem. Soc., Dalton Trans.*, **1973**, 204.
9. (a) N. R. Sangeetha, S. N. Pal, S. Pal, *Polyhedron*, **2000**, *19*, 2713. (b) S. N. Pal, K. R. Radhika, S. Pal, *Z. Anorg. Allg. Chem.*, **2001**, *627*, 1631. (c) N. R. Sangeetha, S. N. Pal, C. E. Anson, A. K. Powell, S. Pal, *Inorg. Chem. Commun.*, **2000**, *3*, 415.
10. D. T. Sawyer, J. L. Roberts Jr., in *Experimental Electrochemistry for Chemists*, Wiley, New York, 1974, p. 208.

11. w, weak; m, medium; s, strong;. vs, very strong.
12. A. C. T. North, D. C. Philips, F. S. Mathews, *Acta Crystallogr., Sect. A*, **1968**, *24*, 351.
13. L. J. Farrugia, *J. Appl. Crystallogr.*, **1999**, *32*, 837.
14. G. M. Sheldrick, *SHELX-97 Structure Determination Software*, University of Göttingen, Göttingen, Germany, 1997.
15. (a) P. McArdle, *J. Appl. Crystallogr.*, **1995**, *28*, 65. (b) A. L. Spek, Platon, *Molecular Graphics Software*, University of Glasgow, UK, 2001.
16. (a) R. M. Silverstein, F. X. Webster, in *Spectrometric Identification of Organic Compounds*, Wiley, New York, 6th edn., 1998, p. 101. (b) K. Nakamoto, in *Infrared and Raman Spectra of Inorganic and Coordination Compounds*, Wiley, New York, 4th edn., 1986, p. 242.
17. S. N. Pal, S. Pal, *Inorg. Chem.*, **2001**, *40*, 4807.
18. G. M. Brown, T. R. Weaver, F. R. Keene, T. J. Meyer, *Inorg. Chem.*, **1982**, *21*, 3967.
19. J. March, in *Advanced Organic Chemistry*, Wiley, New York, 4th edn., 1998, p. 280.
20. D. P. Rillema, G. Allen, T. J. Meyer, D. Conrad, *Inorg. Chem.*, **1983**, *22*, 1617.
21. C. M. Elliott, E. J. Hershenhart, *J. Am. Chem. Soc.*, **1982**, *104*, 7519.
22. C. E. Dubé, D. W. Wright, S. Pal, P. J. Bonitatebus Jr., W. H. Armstrong, *J. Am. Chem. Soc.*, **1998**, *120*, 3704.
23. K. Izutsu, in *Acid-Base Dissociation Constants in Dipolar Aprotic Solvents*, Blackwell, Oxford, 1990, p. 28.
24. D. D. Perrin, B. Dempsey, E. P. Serjeant, in pK_a *Prediction for Organic Acids and Bases*, Chapman and Hall, London, New York, 1981.

25. B. Mondal, S. Chakraborty, P. Munshi, M. G. Walawalkar, G. K. Lahiri, *J. Chem. Soc., Dalton Trans.*, **2000**, 2327.
26. S. Baitalik, U. Flörke, K. Nag, *Inorg. Chem.*, **1999**, *38*, 3296.
27. G. D. Storrier, S. B. Colbran, D. C. Craig, *J. Chem. Soc., Dalton Trans.*, **1997**, 3011.
28. (a) N. R. Sangeetha, S. Pal, *Polyhedron*, **2000**, *19*, 1593. (b) S. N. Pal, J. Pushparaju, N. R. Sangeetha, S. Pal, *Trans. Met. Chem.*, **2000**, *25*, 529.
29. (a) G. R. Desiraju, *Acc. Chem. Res.*, **1996**, *29*, 441. (b) G. R. Desiraju, *Angew. Chem., Int. Ed.*, **1995**, *34*, 2328. (c) T. Steiner., *Chem. Commun.*, **1997**, 727. (d) M. G. Davidson, A. E. Goeta, J. A. K. Howard, S. Lamb, S. A. Mason, *New J. Chem.*, **2000**, *24*, 477. (e) N. R. Sangeetha, S. Pal, *Polyhedron*, **2000**, *19*, 1593. (f) D. Braga, F. Grepioni, G. R. Desiraju, *Chem. Rev.*, **1998**, *98*, 1375. (g) J. -M. Lehn, *Angew. Chem., Int. Ed.*, **1990**, *29*, 1304. (h) P. N. W. Baxter, J. -M. Lehn, B. O. Kneisel, D. Fenske, *Angew. Chem., Int. Ed.*, **1997**, *36*, 1978.
30. (a) M. Ohkita, T. Suzuki, K. Nakatani, T. Tsuji, *Chem. Commun.*, **2001**, 1454. (b) R. Taylor, O. Kennard, *J. Am. Chem. Soc.*, **1982**, *104*, 5063. (c) D. S. Reddy, B. S. Goud, K. Panneerselvam, G. R. Desiraju, *J. Chem. Soc., Chem. Commun.*, **1993**, 663. (d) D. S. Reddy, D. C. Craig, G. R. Desiraju, *J. Am. Chem. Soc.*, **1996**, *118*, 4090. (e) F. A. Cotton, L. M. Daniels, G. R. Jordan, IV, C. A. Murillo, *Chem. Commun.*, **1997**, 1673. (f) M. Mascal, *Chem. Commun.*, **1998**, 303. (g) A. N. M. M. Rahman, R. Bishop, D. C. Craig, M. L. Scodder, *Chem. Commun.*, **1999**, 2389. (h) T. Steiner, G. R. Desiraju, *Chem. Commun.*, **1998**, 891.
31. P. Braunstein, Y. Chauvin, J. Nahring, Y. Dusausoy, D. Bayeul, A. Tiripicchio, F. Ugozzoli, *J. Chem. Soc., Dalton Trans.*, **1995**, 851.

CHAPTER 5

Mononuclear Ruthenium(III) Complexes with a Phenolate-O, Imine-N and Amide-O Coordinating Ligand*

5.1. Abstract

The reaction of *cis*-[Ru(dmso)$_4$Cl$_2$], N-(acetyl)-N'-(salicylidene)hydrazine (H_2acs), and KOH (in 1:2:2 mole ratio) in methanol under aerobic condition produces a ruthenium(III) complex, [Ru(acs)(Hacs)]·H_2O. Addition of one mole equivalent of $HClO_4$ to this complex in methanol affords [Ru(Hacs)$_2$]ClO_4. On the other hand, reaction of one mole equivalent of KOH with [Ru(acs)(Hacs)]·H_2O in methanol produces K[Ru(acs)$_2$]. All the three complexes have been characterized by elemental analyses, magnetic, spectroscopic, and electrochemical techniques. In solutions, except [Ru(acs)(Hacs)]·H_2O, the other two complexes are 1:1 electrolytic in nature. Solid state magnetic moments (at 298 K) of the complexes are in the range 1.91–2.15 μ_B. These values reflect a S = ½ spin state and hence low-spin ruthenium(III) in each complex. X-ray structures of [Ru(acs)(Hacs)]·H_2O and tetraphenylphosphonium salt of [Ru(acs)$_2$]$^-$ have been determined. In both complexes, the ligands bind the metal ion meridionally through the phenolate-O, the imine-N and the amide-O atoms. In [Ru(acs)(Hacs)]·H_2O, the amide functionality of one of the ligands is protonated and in [PPh_4][Ru(acs)$_2$], amide functionalities of both ligands are deprotonated. Electronic spectra of the complexes display ligand-to-metal charge transfer bands in the range 626–699 nm. Cyclic voltammetry reveals a Ru(III) → Ru(IV) oxidation in the potential range 0.56–0.84 V (vs. SCE) for these complexes. The charge transfer band positions and the oxidation potentials are

*This work has been accepted for publication in *Eur. J. Inorg. Chem.*

significantly influenced by the protonation state of the O-coordinating amide functionality present in each ligand. The pK_a values of the coordinated amide functionalities have been determined by spectrophotometric titration.

5.2. Introduction

In the previous chapter, we have described a series of mononuclear ruthenium(II) complexes with Schiff bases obtained from substituted hydrazines and picolinaldehyde. In these complexes, the ligands bind ruthenium(II) center through the pyridine-N, the imine-N, and the deprotonated amide-O. The neutral ruthenium(II) complexes display interesting redox, spectral and protonation behavior of amide functionalities. In this chapter, we have explored the coordination chemistry of ruthenium with a similar kind of Schiff base N-(acetyl)-N'-(salicylidene)hydrazine (H_2acs, 2 H represent the dissociable phenolic and amide protons (Figure 5.1)). In deprotonated state (acs^{2-}), this Schiff base can coordinate a metal ion *via* the phenolate-O, the imine-N, and the deprotonated amide-O atoms forming a six- and a five-membered chelate ring. This type of coordination mode by this and similar ligands are known.[1] The reasons for the choice of this Schiff base are as follows. It contains high oxidation state promoting[2] phenolic hydroxy and amide functionalities. The O-coordinating amide functionality provides the rare opportunity of studying the influence of amide protonation state on the coordination geometry and physical properties of the complex, which is not easy

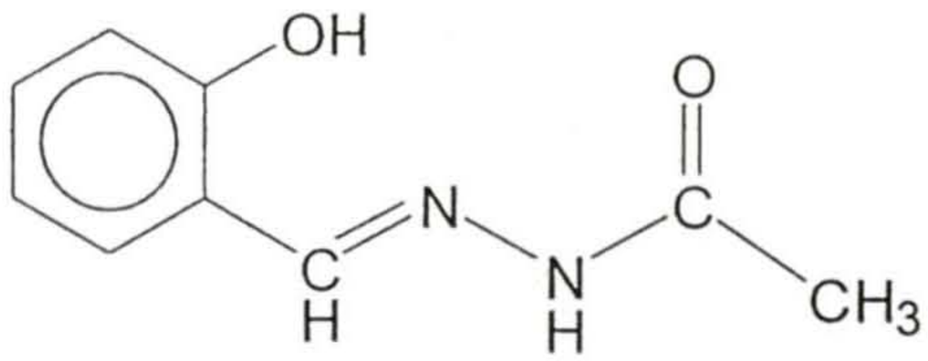

H_2acs

Figure 5.1

for amide-N coordinated species. Herein, we describe three new ruthenium(III) bis-chelates with H_2acs. These complexes differ only in the protonation state of the coordinated amide functionalities. Solid state molecular structures of two of them determined by X-ray crystallography have been reported. In solution, dependence of the spectral and the redox features on the amide protonation state has been scrutinized.

5.3. Experimental Section

5.3.1. Materials

The Schiff base H_2acs[1a] and *cis*-[Ru(dmso)$_4$]Cl$_2$[3] were prepared by following reported procedures. All other chemicals and solvents were of analytical grade available commercially and were used as received.

5.3.2. Physical measurements

All the physical measurements were performed as described in the preceding chapters.

5.3.3. Synthesis of the ruthenium complexes

[Ru(acs)(Hacs)]·H_2O

Solid *cis*-[Ru(dmso)$_4$Cl$_2$] (242 mg, 0.5 mmol) was added to a methanol solution (40 ml) of H_2acs (178 mg, 1 mmol) and KOH (56 mg, 1 mmol). The mixture was heated under reflux for 8 h. The hot brown solution was cooled to room temperature and left in air for 5 h. The color of the solution changed to green and the complex was precipitated as a dark green solid. It was collected by filtration, washed with methanol followed by ether and finally dried in air. The

yield was 95 mg (40%). Single crystals suitable for X-ray structure determination were obtained by storing the filtrate at 5° C for about 3-4 days.

Selected IR bands[4] *(cm^{-1}):* 3427(m), 1597(s), 1521(vs), 1467(w), 1435(vs), 1379(m), 1323(vs), 1267(vs), 1192(s), 1149(m), 1033(w), 943(m), 898(m) 748(vs).

$[Ru(Hacs)_2]ClO_4$

A methanol solution (10 ml) of 70% aqueous $HClO_4$ (0.2 ml) was prepared. To a suspension of $[Ru(acs)(Hacs)]\cdot H_2O$ (118 mg, 0.25 mmol) in 25 ml methanol, 1 ml of the above $HClO_4$ solution was added and the mixture was magnetically stirred in air. Initially a clear green solution was obtained and after about ½ h a green solid separated. The complex thus obtained was collected by filtration, washed with ether and dried in air. The isolated yield was 70 mg (49%).

Selected IR bands[4] *(cm^{-1})*: 3205(m), 3067(m), 2710(w), 1599(s), 1550(vs), 1429(s), 1381(s), 1273(vs), 1194(s), 1107(vs), 997(m), 902(w), 767(s), 621(m).

$K[Ru(acs)_2]$

$[Ru(acs)(Hacs)]\cdot H_2O$ (150 mg, 0.32 mmol) was taken in 50 ml of methanol and 18 mg (0.32 mmol) of KOH was added to the suspension. The mixture was magnetically stirred in air for 6 h. The green solution thus obtained was filtered to remove any unreacted starting complex and the filtrate was evaporated to about ~4-5 ml in vacuum. The green solid obtained was collected by filtration, washed with ether and dried in air. The yield obtained by this procedure was 120 mg (76%).

Selected IR bands[4] *(cm^{-1})*: 1595(m), 1520(vs), 1433(s), 1388(m), 1363(m), 1317(vs), 1197(m), 943(m), 748(s).

5.3.4. Spectrophotometric titration

In a typical titration, a 3 ml aliquot of a stock solution of $K[Ru(acs)_2]$ in acetonitrile (3.74×10^{-5} M, prepared by dissolving 1.84 mg (3.74 μmol) of $K[Ru(acs)_2]$ in 10 ml of acetonitrile and then diluting 1 ml of this solution to 10 ml by adding the same solvent) was taken in an air-tight cuvette. Protonation of $K[Ru(acs)_2]$ was performed by addition of aliquots (1 μl) of an acetonitrile solution of CF_3SO_3H (1.13×10^{-2} M, prepared by dissolving 0.5 ml (5.65 mmol) in 10 ml of acetonitrile and then diluting 0.2 ml of this solution to 10 ml by adding the same solvent) with a gas-tight syringe. Protonation was considered complete when no significant change of the electronic spectrum was observed by further addition of CF_3SO_3H solution. The effective pK_{ai} (i = 1 and 2) values were determined from the two segments (Figure 5.6a for pK_{a2} and Figure 5.6b for pK_{a1}) of the spectrophotometric titration curves using the equations 1, 2 and 3.[5,6] The value of $K_a(CF_3SO_3H)$ in acetonitrile[7] used to calculate the pK_{ai} values is 2.512×10^{-3}. The change in absorbance at 364 nm and that at 340 nm were used to calculate K_{c1} and K_{c2}, respectively.

$$K_{ai} = K_a(CF_3SO_3H)/K_{ci} \quad (1)$$

$$K_{c1} = [Ru(Hacs)_2^+][CF_3SO_3^-]/[Ru(acs)(Hacs)][CF_3SO_3H] \quad (2)$$

$$K_{c2} = [Ru(acs)(Hacs)][CF_3SO_3^-]/[Ru(acs)_2^-][CF_3SO_3H] \quad (3)$$

5.3.5. Single crystal X-ray structure determination

X-ray data for crystals of both $[Ru(acs)(Hacs)]\cdot H_2O$ and $[PPh_4][Ru(acs)_2]\cdot C_6H_5CH_3$ were collected on an Enraf-Nonius Mach-3 single crystal diffractometer using graphite monochromated Mo-$K\alpha$ radiation (λ = 0.71073 Å) by ω-scan method at 298 K. In each case, unit cell parameters were determined by least-squares fit of 25 reflections having 2θ values in the range 10-22°. Intensities of 3 check reflections were measured after every 1.5 h during the data collection to monitor the crystal stability. In both cases, there was no

significant change in the intensities of the check reflections. Empirical absorption corrections were applied to both data sets based on the ψ-scans.[8] The structures were solved by direct methods and refined on F^2 by full-matrix least-squares procedures. In each case, the asymmetric unit contains one molecule of the complex and one solvent molecule. All non-hydrogen atoms having full occupancy were refined using anisotropic thermal parameters. For both molecules the methyl group H-atoms and the aromatic H-atoms were placed geometrically by using a riding model. In the case of $[Ru(acs)(Hacs)]\cdot H_2O$, H-atoms attached to the water oxygen atom and the amide nitrogen atom were located in a difference map. For both structures all the H-atoms were included in the structure factor calculation at idealized positions [with U_{iso}(methyl-H) = $1.5U_{eq}$(C), U_{iso}(aromatic-H) = $1.2U_{eq}$(C), U_{iso}(water-H) = $1.5U_{eq}$(O), and U_{iso}(amide-H) = $1.2U_{eq}$(N)], but not refined. The programs of WinGX[9] were used for data reduction and absorption correction. Structure solution and refinement were performed with the SHELX-97 programs.[10] The Ortex6a[11] and Platon[12] packages were used for molecular graphics. Selected crystal and refinement data are listed in Table 5.1. The supplementary crystallographic data for the structures reported in this work have been deposited with the Cambridge Crystallographic Data Centre (CCDC). The deposition numbers are CCDC-208845 and -208846 for $[Ru(acs)(Hacs)]\cdot H_2O$ and $[PPh_4][Ru(acs)_2]\cdot C_6H_5CH_3$, respectively.

Table 5.1. Crystal and structure refinement data for $[Ru(acs)(Hacs)]\cdot H_2O$ (**1**) and $[PPh_4][Ru(acs)_2]\cdot C_6H_5CH_3$ (**2**)

Compound	**1**	**2**
Empirical formula	$RuC_{18}H_{19}N_4O_5$	$RuPC_{49}H_{44}N_4O_4$
Crystal size, mm	0.50 x 0.48 x 0.24	0.49 x 0.24 x 0.16
Formula weight	472.44	884.92
Space group	Monoclinic, C2/c	Triclinic, P –1
a, Å	10.789(3)	11.910(3)
b, Å	19.872(2)	13.437(3)
c, Å	8.768(2)	15.227(7)
α, deg.	90	91.93(3)
β, deg.	103.46(3)	109.650(19)
γ, deg.	90	106.50(3)
V, Å^3	1828.2(7)	2177.7(12)
Z	4	2
$\rho_{calcd.}$ g cm^{-3}	1.716	1.350
μ, mm^{-1}	0.897	0.445
Reflections collected/unique	4178/4020	7617/7617
Reflections [$I > 2\sigma(I)$]/parameters	3267/131	3819/535
R1,[a] wR2[b] [$I > 2\sigma(I)$]	0.0545, 0.1394	0.0840, 0.1913
R1, wR2 (all data)	0.0690, 0.1559	0.1797, 0.2474
Goodness-of-fit[c] on F^2	1.083	1.022
$\Delta\rho_{max/min}$ e Å^{-3}	1.487, -1.989	0.850, -0.361

[a] $R1 = \sum||F_o| - |F_c||/\sum|F_o|$. [b] $wR2 = \{\sum[(F_o^2 - F_c^2)^2]/\sum[w(F_o^2)^2]\}^{1/2}$.

[c] $GOF = \{\sum[w(F_o^2 - F_c^2)^2]/(n - p)\}^{1/2}$ where 'n' is the number of reflections and 'p' is the number of parameters refined; $w = 1/[\sigma^2(F_o^2) + (aP)^2 + bP]$ where a = 0.1001 and b = 0.6487 for **1**; a = 0.1199 and b = 0.1847 for **2**.

Table 5.2. Atomic coordinates (x 10^4) and equivalent isotropic displacement parameters[a] ($Å^2$ x 10^3) for $[Ru(acs)(Hacs)]\cdot H_2O$

Atom	x	y	z	U(eq)
Ru	0	2191(1)	2500	36(1)
O(1)	20(2)	1525(1)	855(3)	45(1)
O(2)	-321(2)	2954(1)	3958(3)	46(1)
O(3)	-5000	2775(2)	2500	116(3)
N(1)	-1888(2)	2199(1)	2079(3)	39(1)
N(2)	-2395(3)	2689(1)	2904(3)	42(1)
C(1)	-991(3)	1164(1)	163(3)	41(1)
C(2)	-767(4)	654(2)	-844(4)	53(1)
C(3)	-1728(4)	233(2)	-1610(5)	61(1)
C(4)	-2951(4)	315(2)	-1432(5)	60(1)
C(5)	-3215(3)	824(2)	-494(4)	53(1)
C(6)	-2251(3)	1261(2)	326(3)	42(1)
C(7)	-2659(3)	1783(2)	1221(3)	42(1)
C(8)	-1515(3)	3046(2)	3845(3)	42(1)
C(9)	-1918(4)	3579(2)	4814(4)	53(1)

[a] U(eq) is defined as one third of the trace of the orthogonalized Uij tensor.

Table 5.3. Atomic coordinates (x 10^4) and equivalent isotropic displacement parameters[a] ($Å^2$ x 10^3) for $[PPh_4][Ru(acs)_2]\cdot C_6H_5CH_3$

Atom	x	y	z	U(eq)
Ru	921(1)	8868(1)	3138(1)	60(1)
P	3427(2)	3542(2)	3115(2)	54(1)
O(1)	1091(6)	7515(5)	3518(5)	72(2)
O(2)	478(6)	10161(5)	2711(5)	72(2)
O(3)	1300(6)	8637(5)	1995(5)	78(2)
O(4)	764(6)	9263(5)	4376(4)	65(2)
N(1)	-919(8)	8282(8)	2327(5)	75(2)
N(2)	-1527(7)	8998(7)	1878(5)	68(2)

N(3)	2714(6)	9607(5)	3938(5)	51(2)
N(4)	2930(7)	10016(6)	4862(5)	60(2)
C(1)	156(10)	6635(8)	3215(7)	67(3)
C(2)	400(12)	5732(10)	3555(9)	94(4)
C(3)	-437(18)	4794(13)	3275(13)	137(6)
C(4)	-1652(18)	4607(13)	2624(15)	162(8)
C(5)	-1958(13)	5470(12)	2272(10)	127(5)
C(6)	-1057(9)	6532(8)	2585(8)	70(3)
C(7)	-1564(10)	7369(10)	2129(7)	76(3)
C(8)	-676(10)	9934(8)	2155(7)	68(3)
C(9)	-1147(13)	10809(9)	1733(9)	107(4)
C(10)	2460(9)	8937(7)	1981(7)	57(2)
C(11)	2567(11)	8728(8)	1110(8)	79(3)
C(12)	3697(13)	9028(10)	982(9)	96(4)
C(13)	4790(11)	9534(9)	1754(10)	93(4)
C(14)	4703(10)	9756(8)	2594(8)	76(3)
C(15)	3583(8)	9483(6)	2749(6)	50(2)
C(16)	3656(8)	9786(6)	3674(6)	55(2)
C(17)	1868(9)	9770(7)	5000(7)	62(2)
C(18)	1900(10)	10126(9)	5958(7)	87(3)
C(19)	3918(8)	4909(7)	3011(6)	55(2)
C(20)	5161(10)	5441(8)	3107(7)	75(3)
C(21)	5528(13)	6480(9)	3027(9)	98(4)
C(22)	4641(15)	6994(9)	2858(8)	94(4)
C(23)	3436(14)	6505(9)	2765(8)	92(4)
C(24)	3082(11)	5459(7)	2851(7)	73(3)
C(25)	4759(9)	3087(7)	3607(7)	61(3)
C(26)	5137(10)	2888(7)	4519(7)	73(3)
C(27)	6181(12)	2547(8)	4866(9)	86(4)
C(28)	6834(11)	2418(8)	4326(11)	91(4)
C(29)	6477(12)	2603(9)	3447(11)	99(4)
C(30)	5450(11)	2960(9)	3041(8)	84(3)
C(31)	2554(9)	3354(7)	3877(6)	61(2)
C(32)	2627(10)	4164(8)	4512(7)	73(3)
C(33)	1932(12)	3972(11)	5087(8)	94(4)
C(34)	1185(12)	2961(13)	5041(9)	94(4)

C(35)	1149(11)	2159(10)	4454(9)	90(4)
C(36)	1802(10)	2343(8)	3864(8)	77(3)
C(37)	2496(8)	2785(6)	1973(6)	49(2)
C(38)	1838(10)	3203(8)	1244(7)	69(3)
C(39)	1177(10)	2623(9)	376(7)	72(3)
C(40)	1081(10)	1612(9)	220(7)	73(3)
C(41)	1692(12)	1162(9)	947(8)	94(4)
C(42)	2416(11)	1744(8)	1827(7)	78(3)
C(43)	-900(2)	4142(18)	-587(19)	166(10)
C(44)	-840(2)	4378(19)	304(19)	147(7)
C(45)	60(3)	5257(19)	868(15)	153(8)
C(46)	-1680(4)	3610(4)	690(3)	210(2)
C(47)	-4310(2)	4700(2)	-486(16)	204(13)
C(48)	-5000(2)	3970(14)	-86(16)	280(2)
C(49)	-5710(2)	4260(2)	374(18)	220(15)
C(50)	-5010(6)	2850(2)	-160(4)	320(4)

[a] U(eq) is defined as one third of the trace of the orthogonalized Uij tensor.

5.4. Results and Discussion

5.4.1. Syntheses and characterization of the complexes

The neutral complex [Ru(acs)(Hacs)] was isolated from methanolic medium by reacting *cis*-[$Ru(dmso)_4Cl_2$], H_2acs and KOH in 1:2:2 mole ratio under aerobic condition. The monohydrate of the complex precipitates from the reaction mixture as a green solid in reasonable yield. The aerial oxygen is the most likely oxidizing agent in the oxidation of the metal ion during the formation of the complex. If stoichiometrically required mole ratio (1:2:3) is taken the amount of the precipitated complex is significantly low. However, the potassium salt of the anionic complex $[Ru(acs)_2]^-$ can be recovered from the filtrate. The dissociation of the phenolic-OH proton may happen in absence of a strong base like OH^-. Most likely for this reason 1:2:2 mole ratio gives better yield of the neutral complex and for stoichiometric mole ratio formation of $[Ru(acs)_2]^-$ has been noticed. A more convenient and clean method for the synthesis of $K[Ru(acs)_2]$ is the treatment of $[Ru(acs)(Hacs)]\cdot H_2O$ with one mole equivalent of KOH in methanol. By using a similar approach the perchlorate salt of the cationic complex $[Ru(Hacs)_2]^+$ can be prepared by reacting $[Ru(acs)(Hacs)]\cdot H_2O$ and $HClO_4$ in 1:1 mole ratio in methanol. The elemental analysis data (Table 5.4) for all the three complexes are satisfactory with the proposed molecular formulae.

Table 5.4. Elemental analysis [a], and magnetic moment[b] data

Complex	%C	%H	%N	μ_{eff}/μ_B
$[Ru(acs)(Hacs)]\cdot H_2O$	45.53 (45.76)	3.87 (4.05)	11.63 (11.86)	1.91
$[Ru(Hacs)_2]ClO_4$	38.61 (38.96)	3.42 (3.27)	9.85 (10.10)	2.15
$K[Ru(acs)_2]$	43.58 (43.90)	3.13 (3.27)	11.04 (11.37)	2.01

[a] Calculated values are in parentheses, [b] In powder phase at 298 K.

Molar conductivity values (Table 5.5) of the complexes in solutions are consistent with the neutral character of $[Ru(acs)(Hacs)]\cdot H_2O$ and 1:1 electrolytic nature[13] of both $K[Ru(acs)_2]$ and $[Ru(Hacs)_2]ClO_4$. The solid-state magnetic moments (Table 5.4) of these complexes at 298 K are in the range 1.91–2.15 μ_B. Thus in each complex, the ruthenium center is in +3 oxidation state and low-spin in character.

5.4.2. Infrared spectral properties

The infrared spectra of $[Ru(acs)(Hacs)]\cdot H_2O$ and $[Ru(Hacs)_2]ClO_4$ display multiple peaks in the range 2710–3206 cm^{-1}. These peaks are most likely associated with the N-H group of the protonated amide functionalities in these complexes.[14a] On the other hand, absence of any such peak in this region of the spectrum of $K[Ru(acs)_2]$ confirms deprotonation of amide functionalities in both ligands. In addition to the above mentioned peaks, $[Ru(acs)(Hacs)]\cdot H_2O$ displays a broad peak centered at 3427 cm^{-1} ascribable to the lattice water.[14b] All the three complexes display three medium to strong peaks at ~1597, ~1550 and ~1520 cm^{-1}. These peaks are possibly due to the metal coordinated azomethine and protonated/deprotonated amide functionalities of the ligands.[1,5,14a] The presence of perchlorate ion in $[Ru(Hacs)_2]ClO_4$ is indicated by a broad and strong peak at ~1100 cm^{-1} and a sharp peak at ~620 cm^{-1}. A representative spectrum is shown in Figure 5.2.

5.4.3. Electronic spectral properties

The electronic spectral data of the complexes in acetonitrile solutions are listed in Table 5.5. The spectral profiles are quite similar. In the visible region, the major features displayed by the complexes are a band in the range 626-699 nm and a shoulder within 487-504 nm (Table 5.5). These absorptions are assigned to

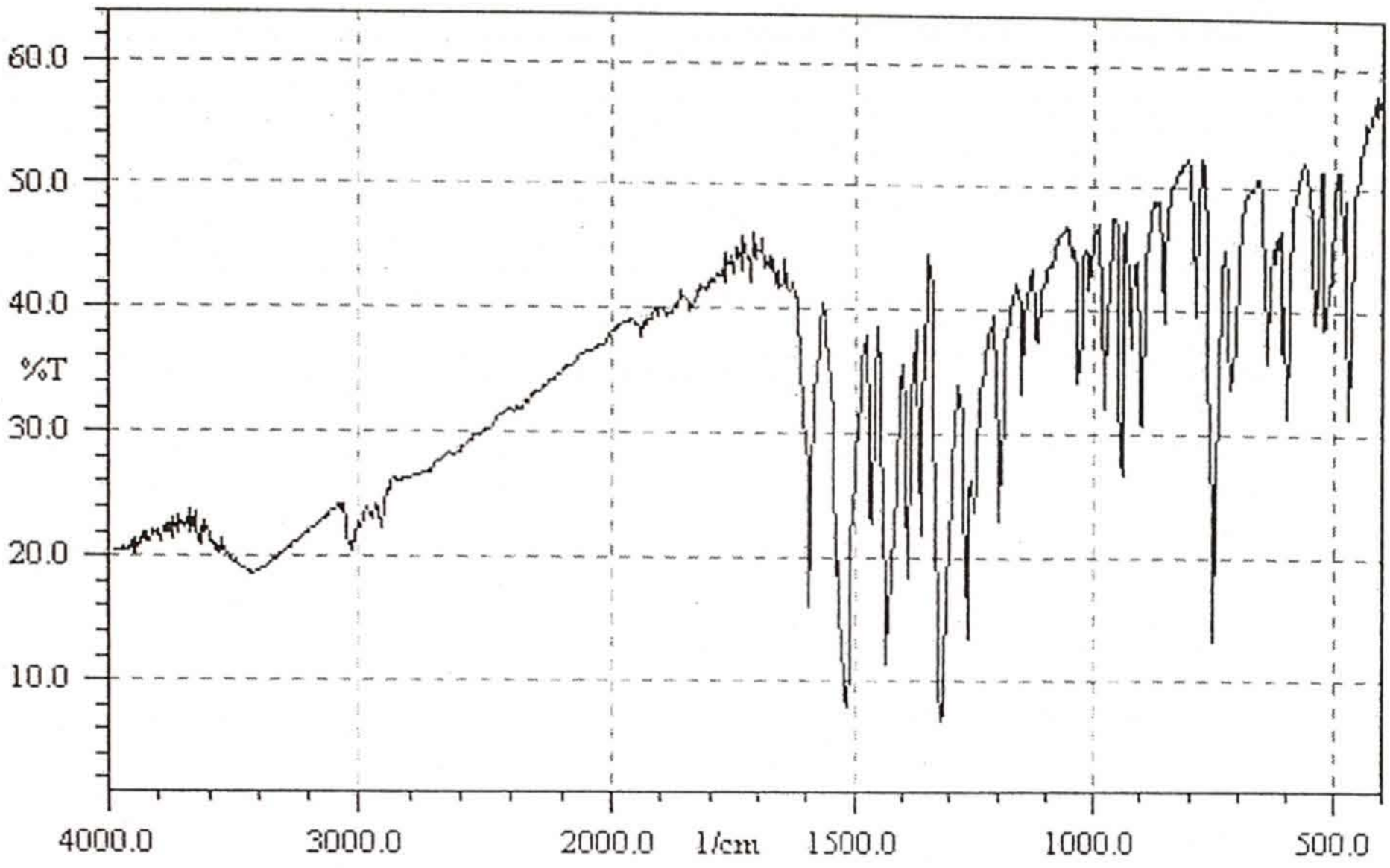

Figure 5.2. Infrared spectrum of $K[Ru(acs)_2]$ in KBr disc.

Table 5.5. Molar conductivity, and electronic spectral[a] data

Complex	Λ_M (Ω^{-1} cm^2 mol^{-1})	λ_{max} (nm) (ε (10^3 M^{-1} cm^{-1}))
$[Ru(acs)(Hacs)]\cdot H_2O$	15[b]	630 (1.1), 504[c] (1.2), 375 (15.4), 343 (15.5), 271[c] (19.6)
$[Ru(Hacs)_2]ClO_4$	117[d]	699 (2.0), 496[c] (1.1), 365 (13.6) 267 (18.6), 235 (26.1)
$K[Ru(acs)_2]$	138[d]	626 (0.7), 487[c] (1.2), 380 (14.7), 342 (16.4), 282[c] (15.6), 241 (28.3)

[a] In CH_3CN solution. [b]In $HCON(CH_3)_2$-CH_3CN (1:4). solution. [c]Shoulder. [d] In CH_3CN solution.

the phenolate-pπ to the metal-dπ charge transfer transitions.[15] Interestingly $[Ru(Hacs)_2]ClO_4$, where both the amide functionalities of the ligands are protonated, display the first band (Figure 5.3) at the lowest energy (699 nm) whereas the completely deprotonated species $K[Ru(acs)_2]$ display the same at highest energy (626 nm). This shift of the band position suggests that due to the protonation of the O-coordinating amide functionalities of the two ligands the

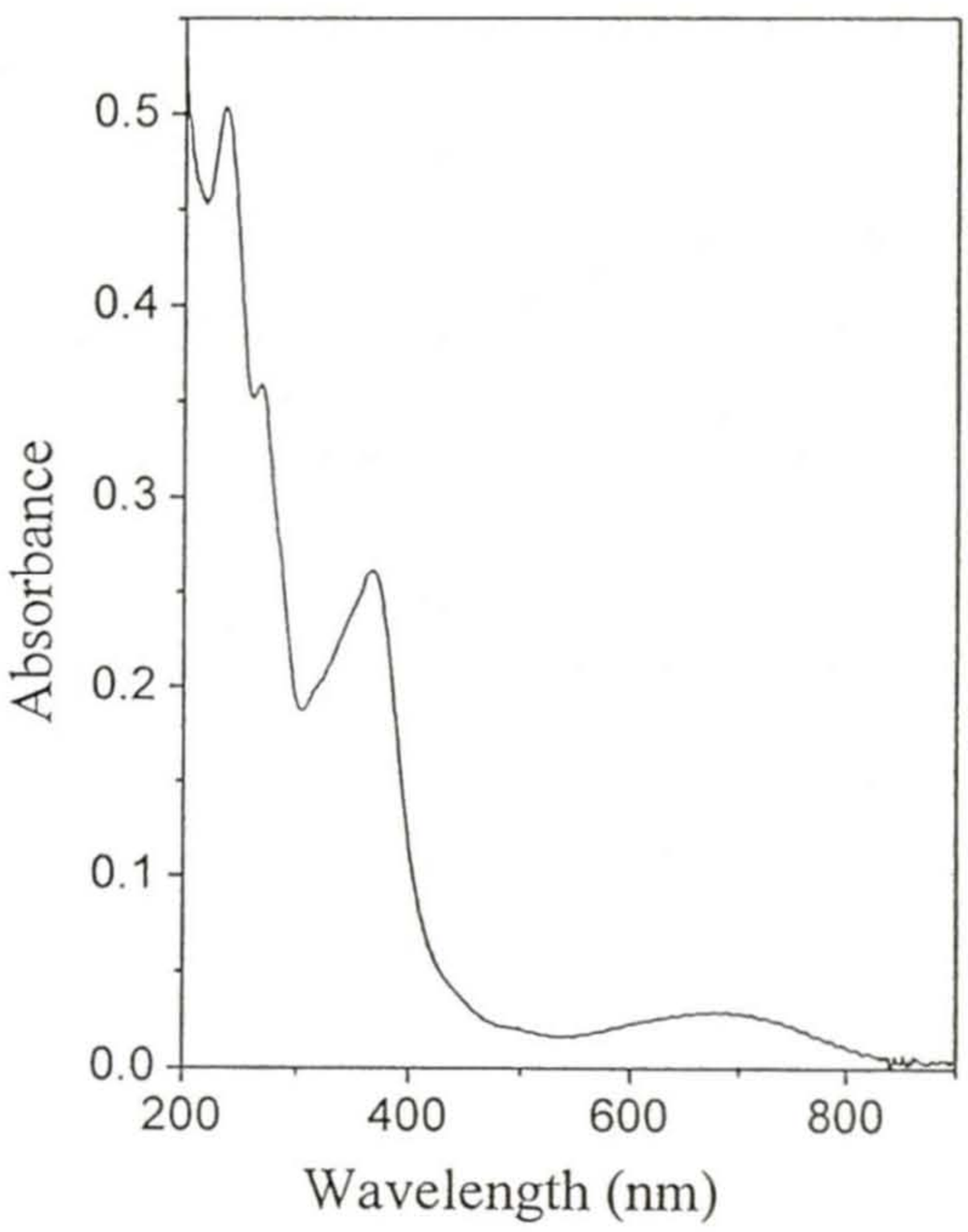

Figure 5.3. Electronic spectrum of $[Ru(Hacs)_2]ClO_4$ in acetonitrile.

energy gap between the phenolate-pπ and the metal-dπ levels is significantly decreased. The band position of the neutral complex [Ru(acs)(Hacs)], where only one amide functionality is protonated, shows the same trend but to a much smaller

extent. The strong absorptions (Table 5.5) observed in the ultraviolet region of the spectra are most likely due to transitions involving only ligand orbitals.

5.4.4. EPR spectral properties

The EPR spectra of the complexes in frozen (103 K) methanol-toluene (1:1) solutions are very similar. A representative spectrum is shown in Figure 5.4. Each of them displays three distinct signals (Table 5.6) indicating the distortion of the N_2O_4 coordination sphere around the metal center from octahedral symmetry. The distortion can be measured in terms of axial (Δ) and rhombic (V) components. The axial distortion (Δ) splits t_2 into 'a' and 'e' and the rhombic component again splits 'e' into nondegenerate components (Figure 5.4). In addition to Δ and V, spin-orbit coupling also influences the extent of energy gaps between these levels. Thus two ligand field transitions of energies ΔE_1 and ΔE_2 ($\Delta E_1 < \Delta E_2$) are possible within these three levels. The distortion parameters and the transition energies have been quantitated using the observed g values and the

Table 5.6. EPR g-values,[a] calculated distortion parameters and near-IR transitions[b]

Complex	g_1	g_2	g_3	Δ/λ	V/λ	$\Delta E_1/\lambda$	$\Delta E_2/\lambda$
[Ru(acs)(Hacs)]	2.186	2.133	1.876	4.849	-0.935	4.377	5.659
$[Ru(Hacs)_2]ClO_4$	2.166	2.114	1.888	5.069	-1.064	4.540	5.921
$K[Ru(acs)_2]$	2.208	2.161	1.854	4.492	-0.670	4.125	5.225

[a] In 1:1 methanol-toluene at 103 K. [b] The calculations are based on spin-orbit coupling constant $\lambda = 1000\ cm^{-1}$.

g tensor theory of low-spin d^5 complexes.[16] The results are collected in Table 5.6. The distortion parameters suggest that the axial component is significantly larger than the rhombic component in each of the three complexes. The ΔE_1 and ΔE_2 transitions are expected to occur in the range 4100–4600 and 5200–6000 cm^{-1} (Table 5.6), respectively. No absorption was detected in either of the above

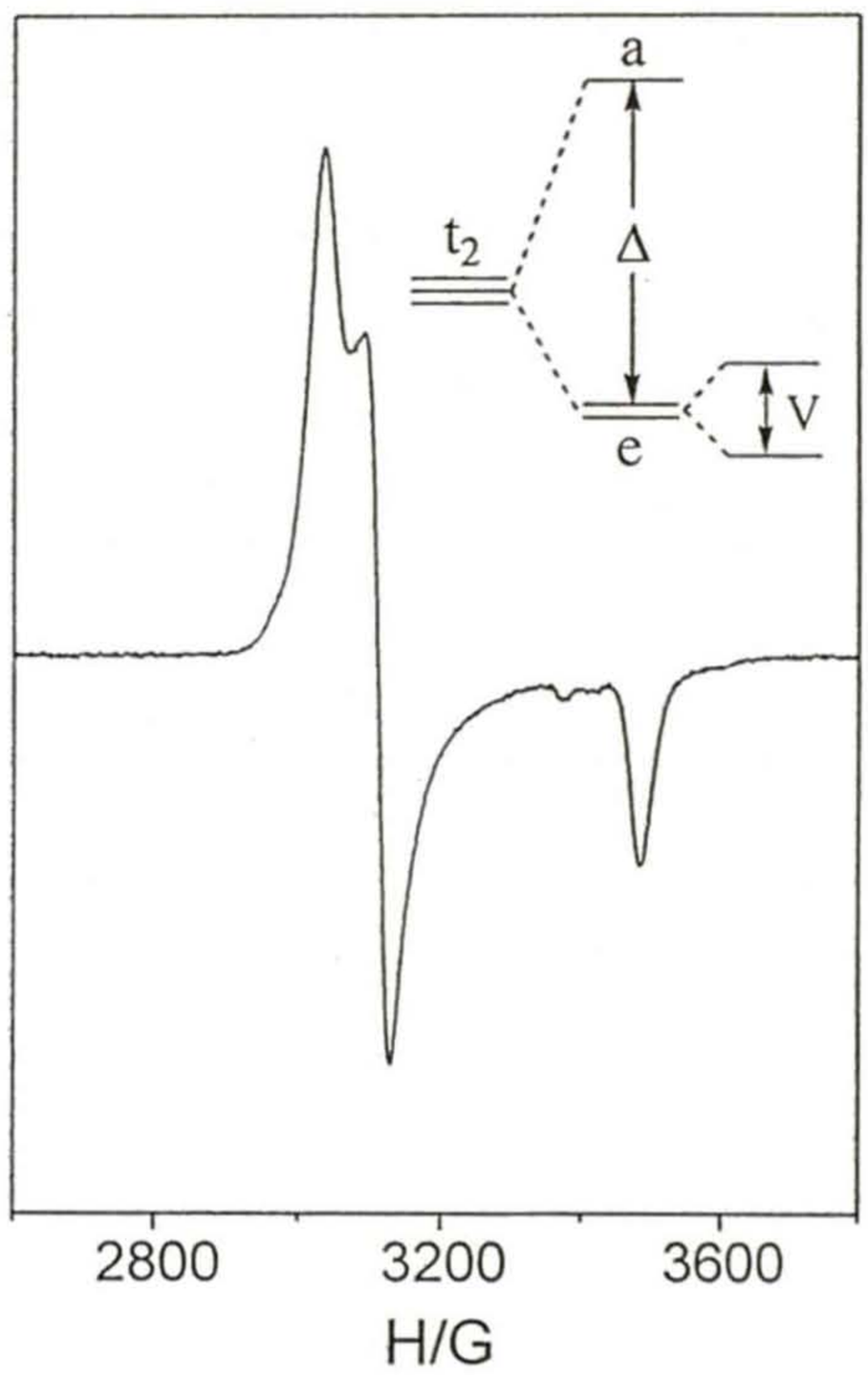

Figure 5.4. EPR spectrum of $[Ru(Hacs)_2]ClO_4$ in frozen (103 K) methanol-toluene (1:1) solution and t_2 splitting pattern.

two regions due to non-transparency of the solvent. Similar EPR spectral profiles and the comparable values of the distortion parameters calculated from the EPR

data indicate that the nature and extent of distortions from the octahedral geometry are not very different in these complexes. Thus there is no significant change in the distortion pattern of the N_2O_4 coordination sphere around the low spin ruthenium(III) center due to protonation or deprotonation of the amide functionalities of the ligands. A few years ago we reported a similar series of three high-spin iron(III) complexes with enolate-O, imine-N, and amide-O donor deprotonated acetylacetone benzoylhydrazone. It may be noted that unlike the present series of complexes the variation of the protonation state of the amide functionalities changes the distortion pattern from rhombic to near-axial in the iron(III) complexes.[1b]

5.4.5. Electrochemical properties

Electron transfer properties of the complexes in acetonitrile-dimethylformamide (9:1) solutions (0.1 M TBAP) have been investigated with the help of cyclic voltammetry. Each of the three complexes displays an oxidation response on the anodic side of SCE (Figure 5.5). The one-electron stoichiometry for these oxidation processes is ascertained by comparing the current heights with known one electron redox processes under identical conditions.[5,17a] The potential for the anionic complex, $[Ru(acs)_2]^-$, is the lowest ($E_{1/2}$ = 0.56 V and ΔE_p = 70 mV)[18] and that for the cationic complex, $[Ru(Hacs)_2]^+$, is the highest ($E_{1/2}$ = 0.84 V and ΔE_p = 150 mV). The potential ($E_{1/2}$ = 0.76 V and ΔE_p = 240 mV) for the neutral complex, [Ru(acs)(Hacs)], is in between the above two values. The free Schiff base (H_2acs) shows an irreversible oxidation with comparatively much higher current at +1.38 V under identical conditions. Thus the oxidation responses observed for the complexes are assigned to the Ru(III) → Ru(IV) process. The trend in the $E_{1/2}$ values indicates that the oxidation of the metal center in the anionic complex where the amide functionality of each of the two ligands is deprotonated is most favorable and that in the cationic complex where

the amide functionalities are protonated is most difficult. This behavior is likely to be primarily due to the electrostatic reasons.

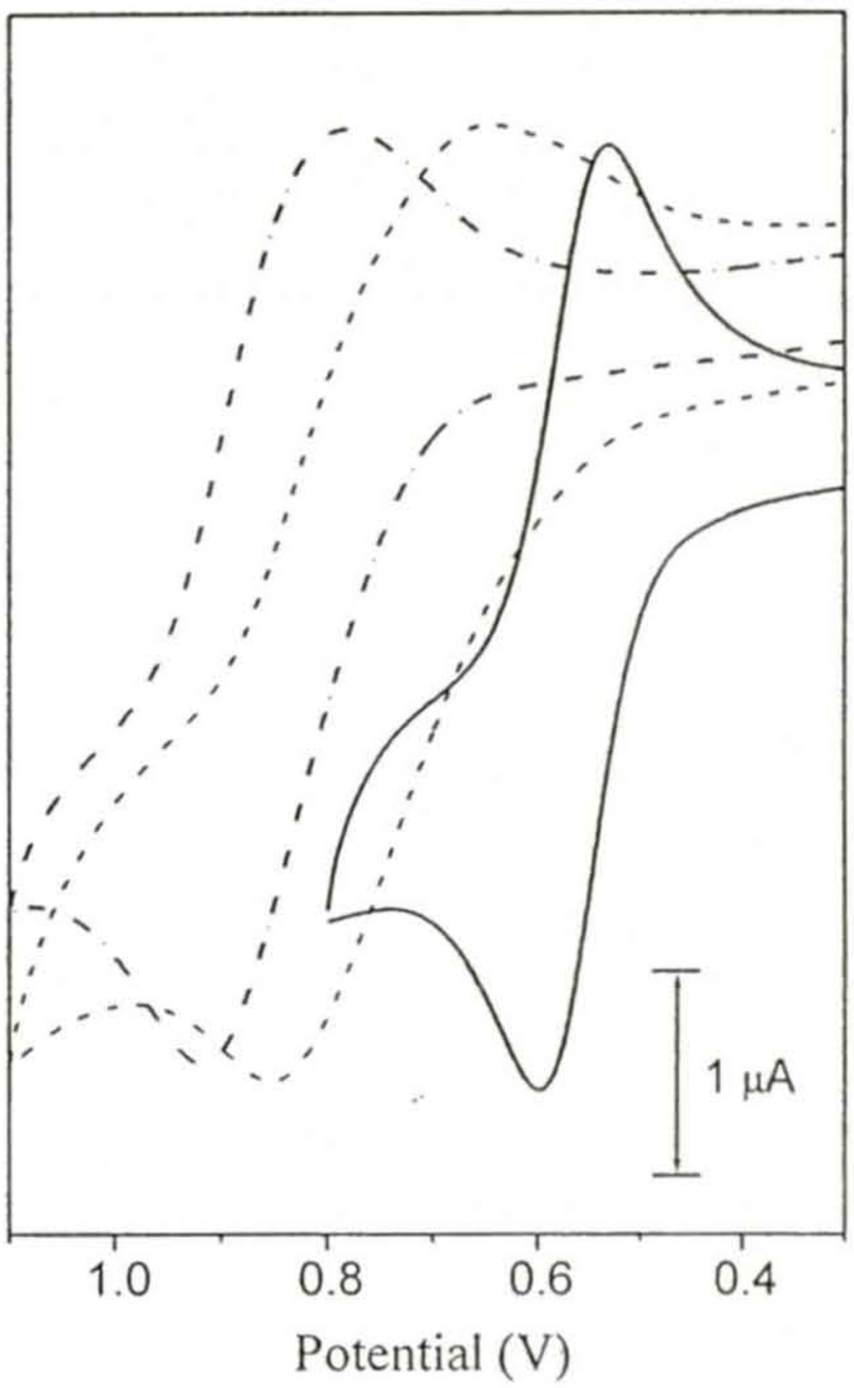

Figure 5.5. Cyclic voltammograms of $K[Ru(acs)_2]$ (——), $[Ru(acs)(Hacs)]\cdot H_2O$ (-----), and $[Ru(Hacs)_2]ClO_4$ (–·–·–) in acetonitrile-dimethylformamide (9:1) solutions (0.1 M TBAP) at scan rates of 50 mV s^{-1}.

On the cathodic side of the SCE, both $K[Ru(acs)_2]$ and $[Ru(acs)(Hacs)]$ display a reduction response. The $E_{1/2}$ values are –1.11 V (ΔE_p = 80 mV) and –1.13 V (ΔE_p = 80 mV), respectively. In both cases, the anodic (i_{pa}) and cathodic (i_{pc}) peak currents are very similar and comparable with the current heights observed for the Ru(III) → Ru(IV) processes. On the other hand,

$[Ru(Hacs)_2]ClO_4$ displays three reduction responses at $E_{1/2}$ = –0.20 V (ΔE_p = 100 mV), E_{pc} = –0.90 and –1.63 V. For the highest potential reduction i_{pc} is much larger than the i_{pa}. However, the i_{pc} is comparable to that of the Ru(III) → Ru(IV) process. This first reduction response of $[Ru(Hacs)_2]ClO_4$ and the reduction responses observed for [Ru(acs)(Hacs)] and $K[Ru(acs)_2]$ may be assigned to the Ru(III) → Ru(II) process and the differences in the potential values can be rationalized considering the electrostatic effect. However, the trend in the reduction potential values is significantly different than that of the oxidation potential values. The reduction potentials observed for $K[Ru(acs)_2]$ (–1.11 V) and [Ru(acs)(Hacs)] (–1.13 V) are very similar and much lower than the first reduction potential (–0.20 V) observed for $[Ru(Hacs)_2]ClO_4$. Whereas the Ru(III) → Ru(IV) potentials are observed in comparatively much narrow range (0.56–0.84 V). Under identical conditions, free perchloric acid shows a reduction response ($E_{1/2}$ = –0.25 V, ΔE_p = 100 mV). This voltammogram is very similar to that of the first reduction displayed by $[Ru(Hacs)_2]ClO_4$. The free Schiff base (H_2acs) under the same conditions displays a reduction response. E_{pc} and E_{pa} values for this reduction response are –1.37 and –0.96 V, respectively. Considering all the above the reductions displayed by the present series of complexes cannot be assigned to the Ru(III) → Ru(II) process unambiguously.

5.4.6. Protonation and deprotonation of coordinated amide

Spectrophotometric titrations have been performed using acetonitrile solutions of $K[Ru(acs)_2]$ and CF_3SO_3H to study the protonation behavior of the coordinated amide functionalities in the complex. With the progressive addition of the acid the change of spectral profiles is characteristic of successive protonation of the two amide functionalities present in the two ligands of $K[Ru(acs)_2]$.[5,19] The initial change in the spectral profile gradually decreases and becomes minimum when the complex to acid mole ratio reaches 1:1.2. At this

stage the spectral profile is akin to that of the neutral complex [Ru(acs)(Hacs)] indicating the protonation of the first ligand amide functionality. In this portion of the titration, the shift of band positions occurs through eight isobestic points (455, 378, 361, 284, 250, 242, 222, and 207 nm) (Figure 5.6a). Continued addition of the acid causes a further shift of band positions through another set of five isobestic points (584, 344, 374, 299, and 263 nm) (Figure 5.6b). The spectral profile becomes constant and similar to that of the $[Ru(Hacs)_2]^+$ at about 1:2.6 complex to acid mole ratio. Quantitative reversibility of this protonation behavior was confirmed by spectrophotometric back-titration with triethylamine. The values of pK_{a1} and pK_{a2} determined from the two segments of the titration are 6.64(4) and 7.19(1), respectively. These values are much lower than the pK_a (~15) of free amide functionality in organic compounds.[20] This difference in the pK_a values is likely to be due to a combination of several factors. Among various possibilities one readily apparent is as follows. The electron deficiency at the imine-N adjacent to the amide-N arising out of coordination of the former to the metal center being compensated by the amide functionality and thereby contributing to the increase of the amide N-H acidity.[5,21] Interestingly the pK_a values determined in this work are very similar with those [pK_{a1} = 6.85(5) and pK_{a2} = 7.44(9)] determined for the ruthenium(II) complex, $[RuL_2]$, where HL is N-(benzoyl)-N'-(picolinylidene)hydrazine.[5] It seems there is no effect of the difference in the oxidation states (+3 and +2) of the metal ion on the acidities of the ligand amide functionalities. However, there are two very distinct dissimilarities between the two systems. In the ruthenium(II) complex, after protonation the amide functionalities are no longer bound to the metal center, which is not the case for the present complexes of acs^{2-} and $Hacs^-$ (*vide supra*). The ligand (L^-) is pyridine-N, imine-N, and deprotonated amide-O donor, whereas acs^{2-} is phenolate-O, imine-N, and deprotonated amide-O donor.

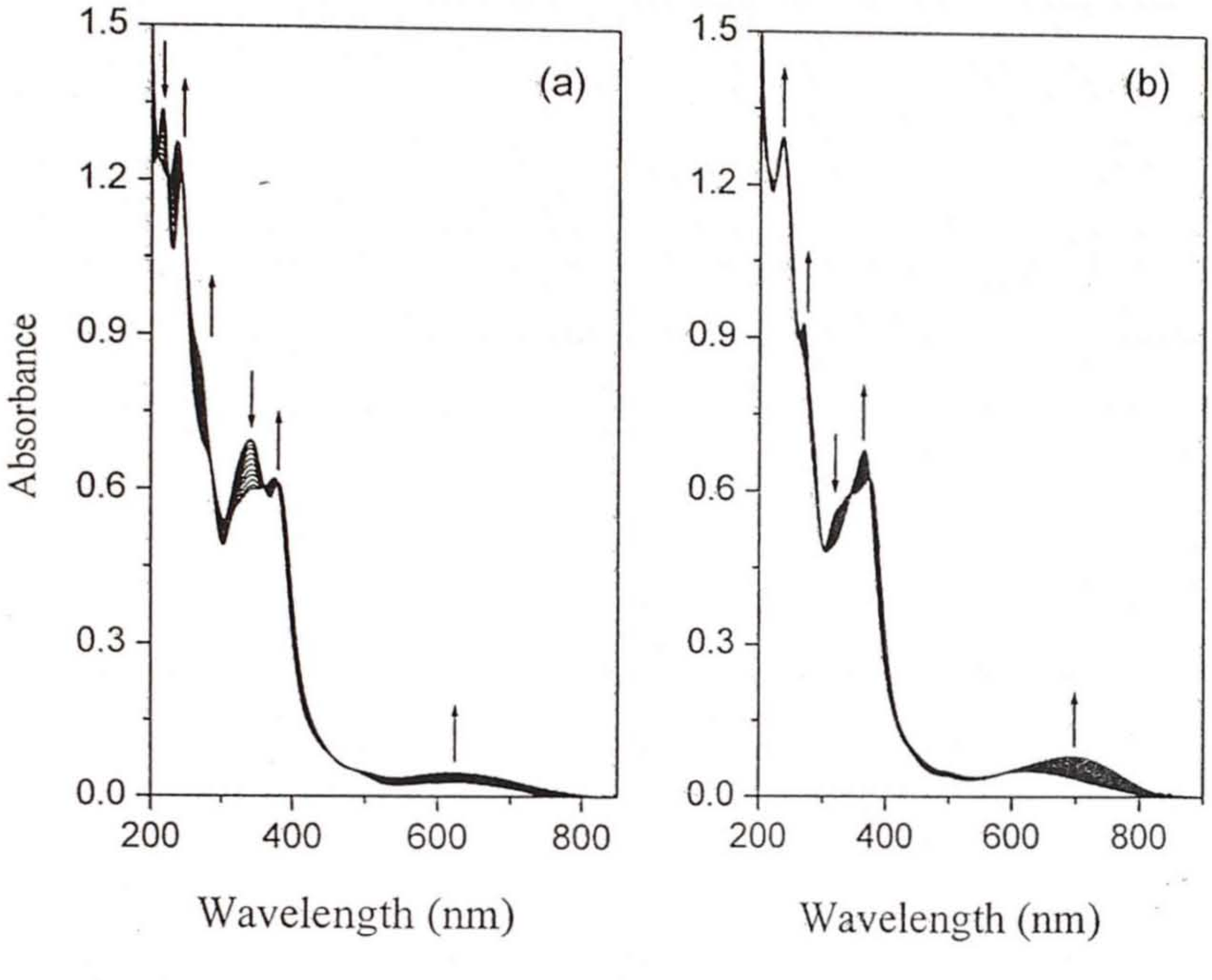

Figure 5.6. Spectrophotometric titration of $K[Ru(acs)_2]$ in acetonitrile with CF_3SO_3H. (a) First segment and (b) second segment of the titration.

Perhaps these dissimilarities offset the effect of oxidation state on the acidity of ligand amide functionalities and similar pK_a values are observed for both systems.

5.4.7. Description of structures

The solid state molecular structure of $[Ru(acs)(Hacs)]\cdot H_2O$ has been determined by X-ray crystallography. The complex crystallizes in the C2/c space group. The structure of the complex molecule is depicted in Figure 5.7. The bond parameters associated with the metal center are listed in Table 5.7. Each ligand binds the metal ion meridionally through the phenolate-O, the imine-N, and the amide-O atoms forming a six- and a five-membered chelate ring. Two

ligands are related by a crystallographically imposed two-fold axis of symmetry passing through Ru and bisecting the angles O1–Ru–O1' and O2–Ru–O2' (Figure 5.7). The presence of this two-fold axis of symmetry indicates that two ligands

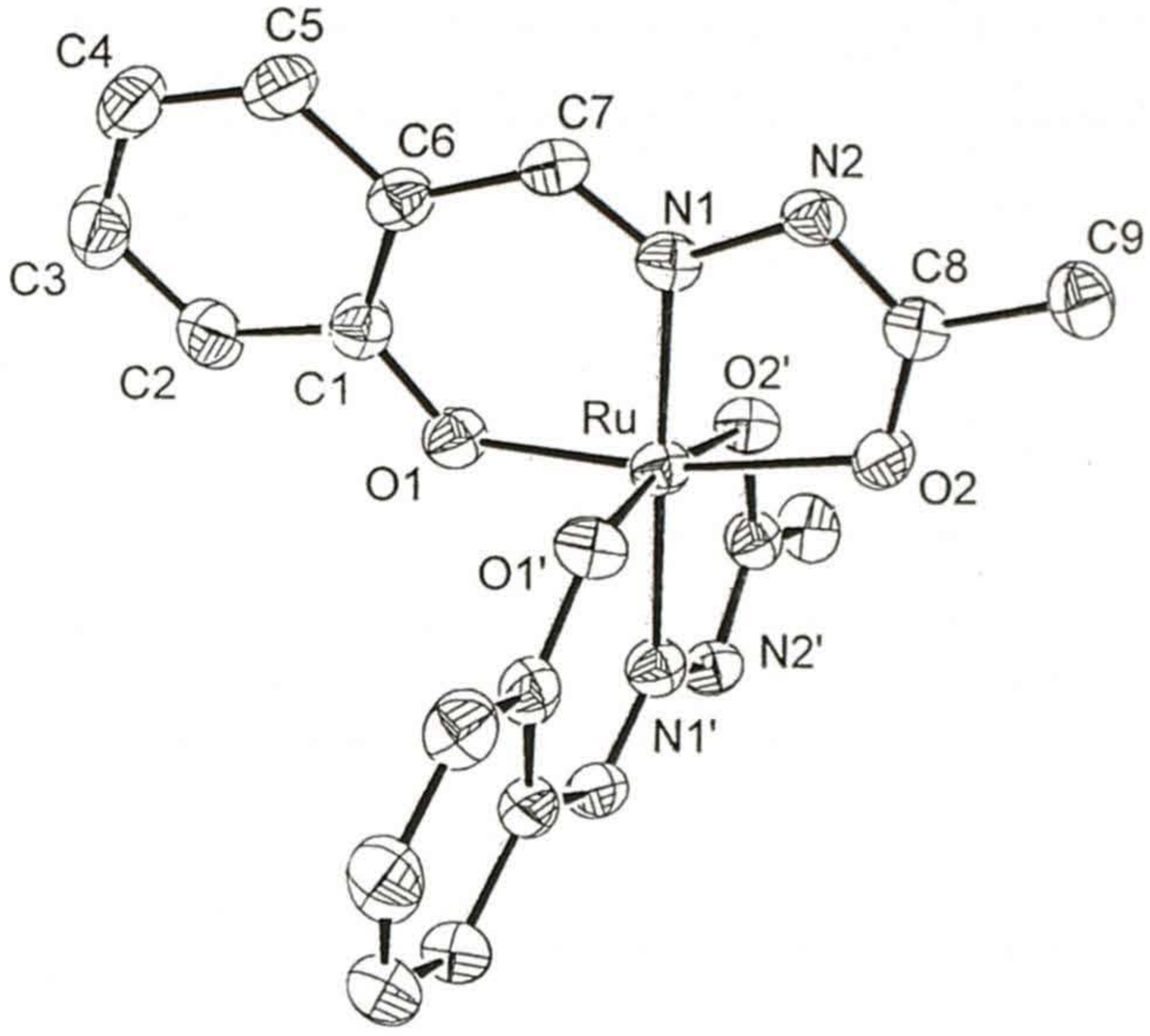

Figure 5.7. The structure of [Ru(acs)(Hacs)] showing the 35% probability thermal ellipsoids and the atom-labeling scheme. Hydrogen atoms are omitted for clarity.

are crystallographically equivalent. This could also indicate that both ligands are chemically equivalent. Taking into account the neutral character of the complex, this will be possible if the oxidation state of the metal center is +2 and the ligands are monoanionic ($Hacs^-$). Considering the more acidic character of the phenolic-OH the amide functionality in each ligand has to be protonated. The second possibility is that the oxidation state of the metal center is +4 and the ligands are

dianionic (acs^{2-}). However, the physical properties (*vide supra*) of the complexes clearly suggest +3 oxidation state of the metal ion in all the complexes. In addition, the observed (Table 5.7) Ru-O(phenolate) and Ru-N(imine) distances are comparable to the distances reported for Ru(III) complexes with ligands that provide the deprotonated salcylaldimine or similar moiety for metal ion binding.[17] The significantly shorter Ru-O(amide) distance compared to the distances observed in ruthenium(II) complexes[5] containing the same coordinating atom is also consistent with the +3 oxidation state of the metal ion. Thus the two ligands

Table 5.7. Selected bond lengths (Å), and angles (deg.) for $[Ru(acs)(Hacs)]\cdot H_2O$

Ru-O(1)	1.961(2)	Ru-O(1)'	1.961(2)
Ru-N(1)	1.983(3)	Ru-N(1)'	1.983(3)
Ru-O(2)	2.063(2)	Ru-O(2)'	2.063(2)
O(1)-Ru-O(1)'	95.12(14)	O(1)-Ru-O(2)	169.57(9)
O(1)-Ru-O(2)'	90.46(11)	O(1)-Ru-N(1)	93.16(9)
O(1)-Ru-N(1)'	87.45(9)	O(1)'-Ru-O(2)	90.46(11)
O(1)'-Ru-O(2)'	169.57(9)	O(1)'-Ru-N(1)	87.45(9)
O(1)'-Ru-N(1)'	93.16(9)	O(2)-Ru-O(2)'	85.45(14)
O(2)-Ru-N(1)	78.27(10)	O(2)-Ru-N(1)'	101.06(9)
O(2)'-Ru-N(1)	101.06(9)	O(2)'-Ru-N(1)'	78.27(10)
N(1)-Ru-N(1)'	179.11(13)		

Symmetry transformation used to generate equivalent atoms: -x, y, -z+1/2.

are not chemically equivalent and one of them is dianionic (acs^{2-}) and the other one is monoanionic ($Hacs^{-}$). The origin of the crystallographic equivalence of the two ligands is therefore due to either a static disorder resulting from the crystallographic superposition of an equal number of $Hacs^{-}$ and acs^{2-}, or a dynamic disorder due to rapid (on the crystallographic time scale) H-atom transfer between the two amide-N centres. Rapid H-atom transfer in solid state is highly unlikely to occur and hence the observed crystallographic equivalence of the two ligands can be attributed solely to a static disorder. The lattice water molecule is also similarly disordered and the O-atom sits at a special position with half occupancy. The distance (2.754 Å) between the amide-N atom (N2) and the water O-atom suggests N-H···O hydrogen bonding interaction. Due to disorder

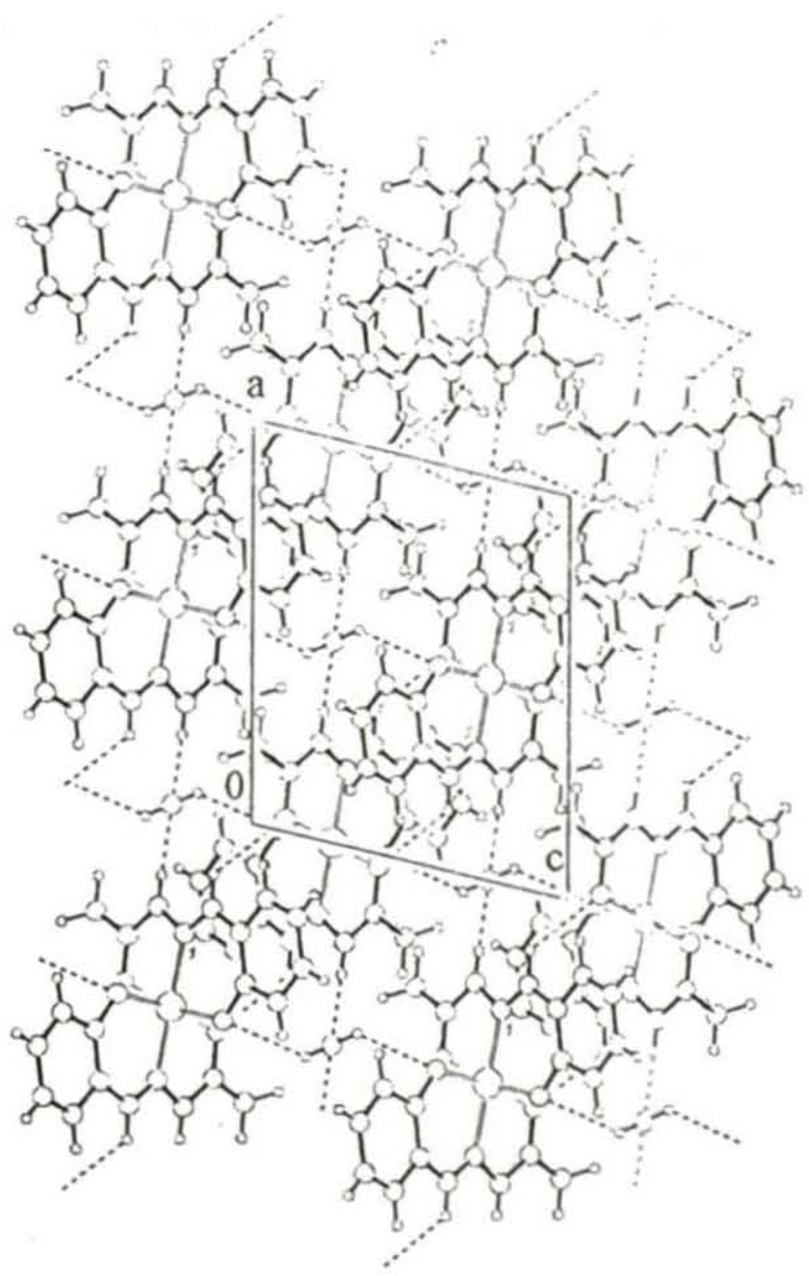

Figure 5.8. Two-dimensional network of $[Ru(acs)(Hacs)]\cdot H_2O$ along *b* axis.

amide-N atoms of both ligands show the same interaction. In the crystal lattice, a one-dimensional chain of alternating complex molecule and water molecule is formed *via* this hydrogen bonding. The water hydrogen atoms are also involved in inter-chain weak H-bonding interactions with the amide-O and phenolate-O atoms (O-H···O distances are 3.370 and 3.250 Å, respectively) forming a two-dimensional network of $[Ru(acs)(Hacs)]\cdot H_2O$ in the crystal lattice (Figure 5.8).

We were unable to grow X-ray quality single crystals of $K[Ru(acs)_2]$. However, the tetraphenylphosphonium salt of $[Ru(acs)_2]^-$ crystallizes in the P-1 space group. Single crystals of $[PPh_4][Ru(acs)_2]$ were obtained by the reaction of $K[Ru(acs)_2]$ and PPh_4Cl in acetonitrile followed by addition of toluene and slow

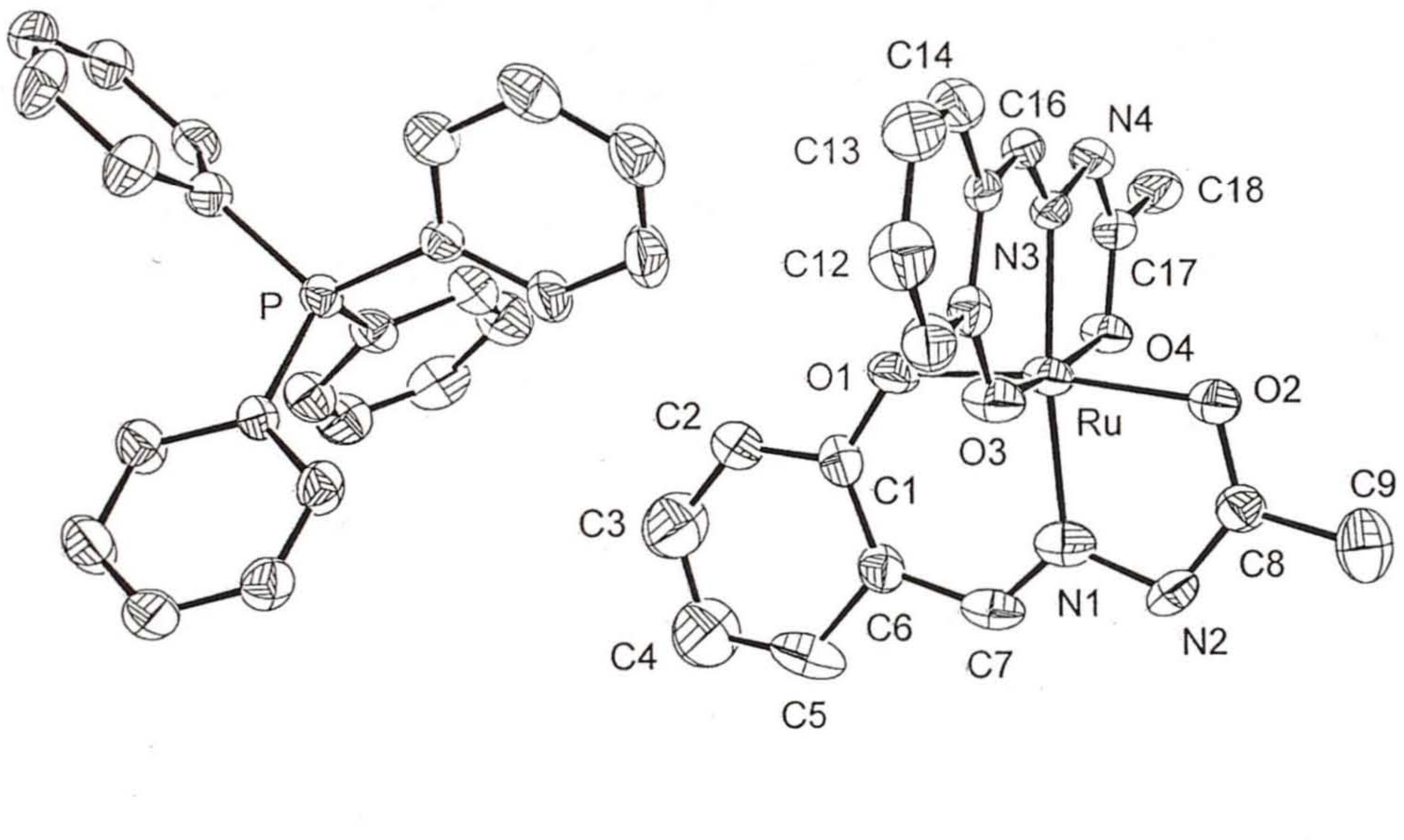

Figure 5.9. Structure of $[PPh_4][Ru(acs)_2]$ showing 25% probability thermal ellipsoids and the atom-labeling scheme. The labeling of the carbon atoms in $[PPh_4]^+$ and H-atoms are not shown for clarity.

evaporation of the mixture in air. The asymmetric unit contains a PPh_4^+ cation, a complex anion $[Ru(acs)_2]^-$, and a toluene molecule that has been located at two sites. The structure of $[PPh_4][Ru(acs)_2]$ is shown in Figure 5.9 and selected bond parameters involving the metal center are collected in Table 5.8. As in the previous structure the ligands bind the metal ion meridionally. The Ru-O(amide), Ru-O(phenolate) and Ru-N(imine) distances are typical for a ruthenium(III) species.[5,17] These distances clearly indicate that there is essentially no difference with respect to the binding strength of the two ligands. The dianionic nature of both ligands and hence the single negative charge on the complex and the +3 oxidation state of the metal ion are further confirmed by the presence of the

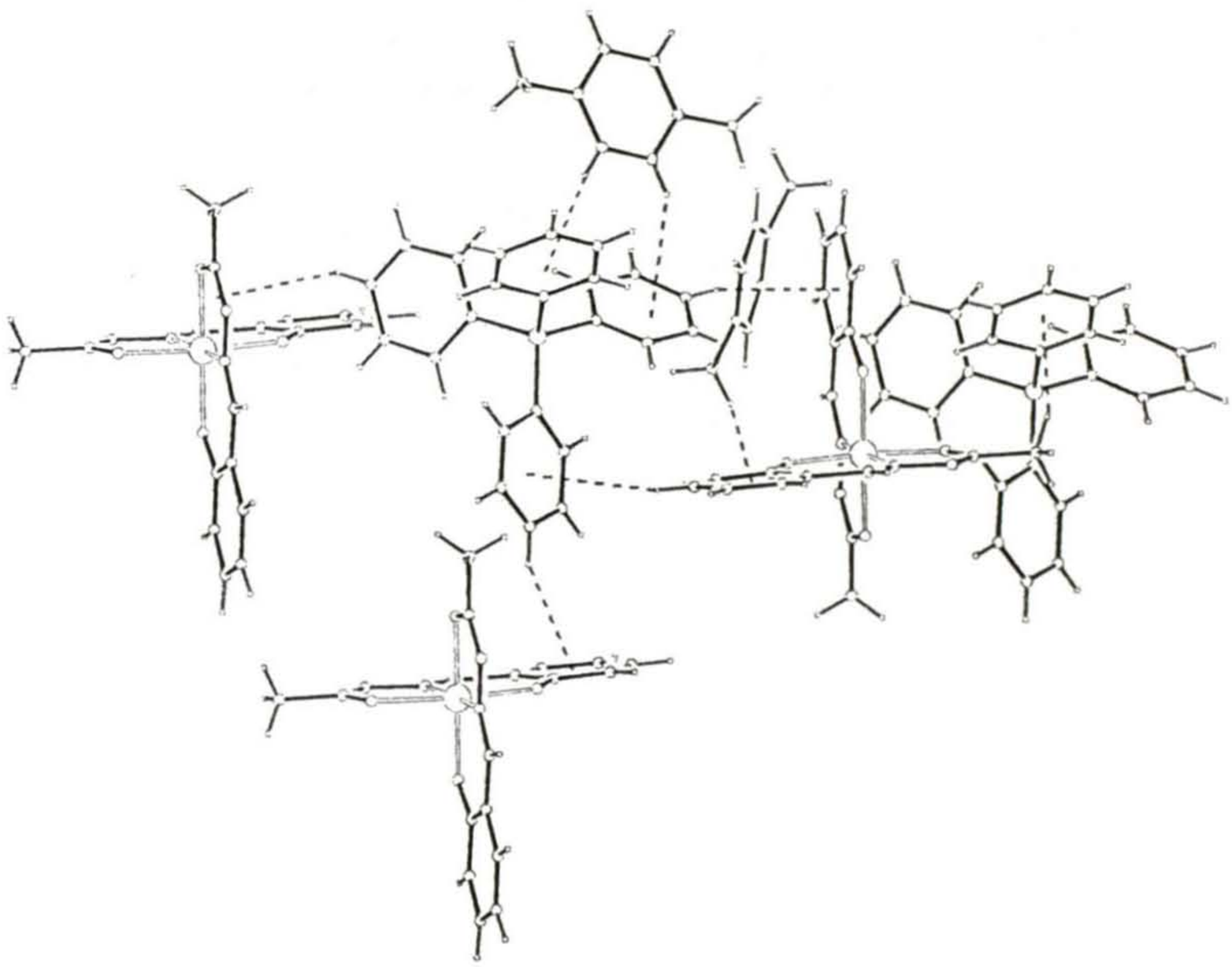

Figure 5.10. Various C–H···π interactions in the crystal lattice of $[PPh_4][Ru(acs)_2]\cdot C_6H_5CH_3$.

PPh_4^+ ion. The bond parameters of the cation are unexceptional.[22] As in $[Ru(acs)(Hacs)]\cdot H_2O$, there is no good conventional hydrogen-bond acceptors or donors in $[PPh_4][Ru(acs)_2]\cdot C_6H_5CH_3$. However, this species also forms a two-dimensional network in the crystal lattice *via* several C–H···π interactions.[23] The H···centroid distances and the C-H···centroid angles are within 2.742–3.177 Å and 134.98–169.48°, respectively. The ligand methyl group C-H, aromatic C-H from the ligand and the phenyl groups of the cation are involved in these interactions with the π-electrons of the toluene, PPh_4^+ phenyl groups, ligand phenolate ring and the chelate rings. Few of these interactions are depicted in Figure 5.10.

Table 5.8. Selected bond lengths (Å) and angles (deg.) for $[PPh_4][Ru(acs)_2]\cdot C_6H_5CH_3$

Ru-O(1)	1.971(7)	Ru-O(2)	2.021(7)
Ru-O(3)	1.975(7)	Ru-O(4)	2.024(6)
Ru-N(1)	2.020(9)	Ru-N(3)	1.999(7)
O(1)-Ru-O(2)	171.7(3)	O(1)-Ru-O(3)	92.5(3)
O(1)-Ru-O(4)	90.4(3)	O(1)-Ru-N(1)	95.2(3)
O(1)-Ru-N(3)	90.9(3)	O(2)-Ru-O(3)	90.4(3)
O(2)-Ru-O(4)	87.7(3)	O(2)-Ru-N(1)	77.1(3)
O(2)-Ru-N(3)	96.6(3)	O(3)-Ru-O(4)	172.1(3)
O(3)-Ru-N(1)	87.8(3)	O(3)-Ru-N(3)	93.9(3)
O(4)-Ru-N(1)	99.3(3)	O(4)-Ru-N(3)	78.7(3)
N(1)-Ru-N(3)	173.6(4)		

5.5. Conclusion

Syntheses and physical properties of three new ruthenium(III) complexes with N-(acetyl)-N'-(salicylidene)hydrazine (H_2acs) have been described. The *bis* complexes vary in the protonation state of amide functionality of the ligands. The crystal structures of [Ru(acs)(Hacs)] and $[Ru(acs)_2]^-$ reveal the meridionally spanning phenolate-O, imine-N and amide-O coordinating mode of both $Hacs^-$ and acs^{2-}. In frozen solutions, all the three complexes display the typical rhombic EPR spectra for low-spin ruthenium(III) species indicating no significant variation in the distortion pattern from octahedral symmetry of the N_2O_4 coordination spheres around the metal center due to protonation or deprotonation of the amide functionalities. However, the potentials of the Ru(III) → Ru(IV) oxidation are markedly affected by the protonation state of the amide functionalities. Reversible protonation and deprotonation of the O-coordinating amide functionalities present in the ligands have been demonstrated.

5.6. References

1. (a) S. C. Chan, L. L. Koh, P. -H. Leung, J. D. Ranford, K. Y. Sim, *Inorg. Chim. Acta*, **1995**, *236*, 101. (b) N. R. Sangeetha, C. K. Pal, P. Ghosh, S. Pal, *J. Chem. Soc., Dalton Trans.*, **1996**, 3293. (c) S. P. Rath, S. Mondal, A. Chakravorty, *Inorg. Chim. Acta*, **1997**, *263*, 247. (d) N. R. Sangeetha, S. Pal, *Bull. Chem. Soc. Jpn.*, **2000**, *73*, 357. (d) M. R. Maurya, S. Khurana, C. Schulzke, D. Rehder, *Eur. J. Inorg. Chem.*, **2001**, 779.
2. (a) D. W. Margerum, *Pure Appl. Chem.*, **1983**, *55*, 23. (b) K. L. Kotska, B. G. Fox, M. P. Hendrich, T. J. Collins, C. E. Pickard, L. J. Wright, E. Münck, *J. Am. Chem. Soc.*, **1993**, *115*, 6746. (c) M. Mikuriya, D. Jie, Y. Kakuta, T. Tokii, *Bull. Chem. Soc. Jpn.*, **1993**, *66*, 1132.

3. I. P. Evans, A. Spencer, G. Wilkinson, *J. Chem. Soc., Dalton Trans.*, **1973**, 204.
4. w, weak; m, medium; s, strong; vs, very strong.
5. S. N. Pal, S. Pal, *J. Chem. Soc., Dalton Trans.*, **2002**, 2102.
6. C. E. Dubé, D. W. Wright, S. Pal, P. J. Bonitatebus, Jr., W. H. Armstrong, *J. Am. Chem. Soc.*, **1998**, *120*, 3704.
7. K. Izutsu, *Acid-Base Dissociation Constants in Dipolar Aprotic Solvents*, Blackwell, Oxford, **1990**, p. 28.
8. A. C. T. North, D. C. Philips, F. S. Mathews, *Acta Crystallogr., Sect. A*, **1968**, *24*, 351.
9. L. J. Farrugia, *J. Appl. Crystallogr.*, **1999**, *32*, 837.
10. G. M. Sheldrick, *SHELX-97, Programs for Structure Determination and Refinement*, University of Göttingen, Göttingen. Germany.
11. P. McArdle, *J. Appl. Crystallogr.*, **1995**, *28*, 65.
12. A. L. Spek, *Platon, Molecular Graphics Software*, University of Glasgow, UK, 2001.
13. W. J. Geary, *Coord. Chem. Rev.*, **1971**, *7*, 81.
14. (a) R. M. Silverstein, F. X. Webster, *Spectrometric Identification of Organic Compounds*, Wiley, New York, **1998**, 6th ed., p 101. (b) K. Nakamoto, *Infrared and Raman Spectra of Inorganic and Coordination Compounds*, Wiley, New York, **1986**, 4th ed., p 228.
15. F. Basuli, A. K. Das, G. Mostafa, S.-M. Peng, S. Bhattacharya, *Polyhedron*, **2000**, *19*, 1663.
16. (a) B. Bleany, M. C. M. O'Brien, *Proc. Phys. Soc. London, Sect. B*, **1956**, *69*, 1216. (b) J. S. Griffith, *The Theory of Transition Metal Ions*, Cambridge University Press, London, **1961**, p. 364. (c) S. Bhattacharya, A. Chakravorty, *Proc. Indian Acad. Sci., (Chem. Sci.)*, **1985**, *95*, 159.

17. (a) S. N. Pal, S. Pal, *Inorg. Chem.*, **2001**, *40*, 4807. (b) A. K. Das, S. -M. Peng, S. Bhattacharya, *J. Chem. Soc., Dalton Trans.*, **2000**, 181. (c) B. Mondal, S. Chakraborty, P. Munshi, M. G. Walawalkar, G. K. Lahiri, *J. Chem. Soc., Dalton Trans.*, **2000**, 2327. (d) K. Nakajima, Y. Ando, H. Mano, M. Kojima, *Inorg. Chim. Acta*, **1998**, *274*, 184. (e) S. Pattanayak, K. Pramanik, N. Bag, P. Ghosh, A. Chakravorty, *Polyhedron*, **1997**, *16*, 2951.

18. $E_{1/2} = (E_{pa} + E_{pc})/2$, $\Delta E_p = E_{pa} - E_{pc}$, where E_{pa} and E_{pc} are anodic and cathodic peak potentials. Scan rate is 50 mVs^{-1}.

19. (a) C. Long, J. G. Vos, *Inorg. Chim. Acta*, **1984**, *89*, 125. (b) S. Baitalik, U. Flörke, K. Nag, *Inorg. Chem.*, **1999**, *38*, 3296.

20. D. D. Perrin, B. Dempsey, E. P. Serjeant, *pK_a Prediction for Organic Acids and Bases*, Chapman and Hall, London and New York, **1981**.

21. B. Mondal, S. Chakraborty, P. Munshi, M. G. Walawalkar, G. K. Lahiri, *J. Chem. Soc., Dalton Trans.*, **2000**, 2327.

22. H. Miyasaka, H. -C. Chang, K. Mochizuki, S. Kitagawa, *Inorg. Chem.*, **2001**, *40*, 3544.

23. (a) M. Nishio, Y. Umezawa, M. Hirota, Y. Takeuchi, *Tetrahedron*, **1995**, *51*, 8665. (b) K. S. B. Hancock, J. W. Steed, *Chem. Commun.*, **1998**, 1409. (c) K. Biradha, M. J. Zaworotko, *J. Am. Chem. Soc.*, **1998**, *120*, 6431. (c) P. Dastidar, I. Goldberg, *Acta Crystallogr.*, 1996, C52, 1976.

List of Publications

Thesis work

1. A diruthenium(III) complex possessing a diazine and two chloride bridges: synthesis, structure and properties

   Satyanarayan Pal and Samudranil Pal

   Inorg. Chem., **2001**, *40*, 4807-4810.

2. Bis(2,2'-bipyridine)ruthenium(II) complexes with salicylaldehyde and its 5-substituted derivatives - synthesis, structure and properties

   Satyanarayan Pal and Samudranil Pal

   Z. Anorg. Allg. Chem., **2002**, *628*, 2091-2098.

3. Ruthenium(II) complexes containing RuN_4O_2 spheres assembled *via* pyridine-imine-amide coordination. Syntheses, structures, properties and protonation behaviour of coordinated amide

   Satyanarayan Pal and Samudranil Pal

   J. Chem. Soc., Dalton Trans., **2002**, 2102-2108.

4. Ruthenium(III) complexes with a phenolate-O, imine-N, and amide-O coordinating ligand: syntheses, structures, properties and protonation studies of coordinated amide

   Satyanarayan Pal and Samudranil Pal

   Eur. J. Inorg. Chem., in press.

Other Publications

1. A dimeric pervanadyl (VO_2^+) complex with a tridentate Schiff base ligand

   S. N. Pal and S. Pal

   J. Chem. Crystallogr., **2000**, *30*, 329-333.

2. A one-dimensional assembly of copper(II) polyhedra *via* dual use of hydrogen bonding and π- π interaction

   N. R. Sangeetha, S. N. Pal, C. E. Anson, A. K. Powell and S. Pal

   Inorg. Chem. Commun., **2000**, *3*, 415-419.

3. Copper(II) complexes containing a CuN_4O_2 coordination sphere assembled *via* pyridine-imine-amide coordination: synthesis, structure and properties

   S. N. Pal, J. Pushparaju, N. R. Sangeetha and S. Pal

   Trans. Met. Chem., **2000**, *25*, 529-533.

4. Copper(II) activated transformation of azomethine to imidate: synthetic and structural studies

   N. R. Sangeetha, S. N. Pal and S. Pal

   Polyhedron, **2000**, *19*, 2713-2717.

5. Reaction of 2-(phenylazo)aniline with Na_2PdCl_4: formation of a 2-(phenylazo)imino complex of bivalent palladium

   N. Maiti, S. N. Pal and S. Chattopadhyay

   Inorg. Chem., **2001**, *40*, 2204-2205.

6. Silver(I) helicates with 2-(arylazo)pyrimidines. Single crystal X-ray structure of {2-phenylazo)pyrimidine}silver(1) nitrate

   P. K. Santra, U. Ray, S. N. Pal and C. R. Sinha

   Inorg. Chem. Commun., **2001**, *4*, 269-73.

7. [N-(4-chlorobenzoyl)-N'-(picolinylidene)hydrazinato]dioxovanadium(V)

   S. N. Pal and S. Pal

   Acta Crystallogr., **2001**, *C57*, 141-42.

8. Mononuclear pervanadyl (VO_2^+) complexes with tridentate Schiff bases: self-assembling *via* C-H----oxo and π - π interactions

   S. N. Pal, K. R. Radhika and S. Pal

   Z. Anorg. Allg. Chem., **2001**, *627*, 1631-37.

9. A trigonal prismatic Mn(II) complex, $[MnL(H_2O)]^{2+}$, with bis(picolinyl-idenehydrazyl)(2-pyridyl)methane (L). Synthesis, structure and properties

   S. G. Sreerama, S. N. Pal and S. Pal

   Inorg. Chem. Commun., **2001**, *4*, 656-660.

10. trans-(2-Acetylpyridine-κ^2N,O)dichlorobis(dimethyl sulfoxide-κS)ruthenium(II)

    S. N. Pal and S. Pal

    Acta Crystallogr., **2002**, *C58*, m273 - m274.

11. Square-planar nickel(II) complexes with a tridentate Schiff base and monodentate heterocycles: self-assembly to dimeric and one-dimensional array *via* hydrogen bonding

    A. Mukhopadhyay, G. Padmaja, S. N. Pal and S. Pal

    Inorg. Chem. Commun., **2003**, *6*, 381-386.

12. Syntheses, structures and properties of *trans*-dichlororuthenium(II) complexes with N_4-donor Schiff bases

    S. N. Pal and S. Pal

    Polyhedron, **2003**, *22*, 867-873.

13. Structure of a self-assembled chain of water molecules in a crystal host

    S. N. Pal, N. B. Sankaran and A. Samanta

    Angew. Chem., Int. Ed., **2003**, *42*, 1741-1743.

14. A one-dimensional assembly of a square-planar copper(II) complex with alternate short and long Cu...Cu distances. Metal ion spin-exchange *via* π-π interactions

    S. Das, G. P. Muthukumaragopal, S. N. Pal and S. Pal

    New J. Chem., **2003**, *27*, 1102-1107

15. Cobalt(II) and cobalt(III) complexes with N-(aroyl)-N'-(picolinylidene)-hydrazines. Spin crossover in the cobalt(II) complexes

    S. G. Sreerama, D. Shyamraj, S. N. Pal and S. Pal

    Indian J. Chem., Sect. A, in press.